Imperial College London

Bounds on Heat Transport for Internally Heated Convection

Ali Arslan

Supervisors:
Dr. Andrew Wynn
Dr. John Craske
Dr. Giovanni Fantuzzi

Imperial College London
Department of Aeronautics

Thesis is submitted for the degree of Doctor of Philosophy
February 27, 2023

Abstract

Convection of a fluid between parallel plates driven by uniform internal heating is a problem where the asymptotic scaling of the mean vertical convective heat transport $\overline{\langle wT \rangle}$ was largely unknown. This thesis proves upper bounds on $\overline{\langle wT \rangle}$ with respect to the non-dimensional Rayleigh number R. Here R quantifies the destabilising effect of heating compared to the stabilising effect of diffusion. By the background field method, formulated in terms of quadratic auxiliary functionals, linear convex optimisation problems are constructed whose solutions provide upper bounds on $\overline{\langle wT \rangle}$. The numerical optimisation carried out with semidefinite programming guides the mathematical analysis and subsequent proofs.

The quantity $\overline{\langle wT \rangle}$ has different physical implications based on the three thermal boundary conditions studied: perfect conductors, an insulating bottom and perfectly conducting top, and poorly conducting boundaries. In the first setup, $\overline{\langle wT \rangle}$ quantifies the flux of heat out of the top and bottom. Whereas in the latter two cases, $\overline{\langle wT \rangle}$ quantifies the ratio of total heat transport to the mean conductive heat transport. Critical to the proofs is the use of a minimum principle on the temperature. Finally, we also prove bounds in the scenarios of infinite Prandtl numbers and free-slip boundaries.

Copyright Declaration

I hereby declare that this thesis is the product of my own research only and no parts of it has been submitted for another degree. References or quotations from other works are fully acknowledged. When parts of this thesis have been published, this has been clearly indicated and references to the published work has been given.

Ali Arslan

Acknowledgements

I need to start by thanking in turn my supervisors all of whom have encouraged and supported me beyond all expectation. Firstly to Dr Andrew Wynn, who was willing to entertain the tangents I may have gone down, but whose patience and guidance has shown me what it entails to be an applied mathematician. To Dr John Craske for providing advice both in research and science overall. Then, I owe a great many thanks to Dr Giovanni Fantuzzi for time spent helping me in picking up the skills that make up this PhD, especially when it came to numerical work.

I am grateful to the Engineering and Physical Sciences Research Council (EPSRC) funded Centre for Doctoral Training (CDT) in Fluid Dynamics across Scales at Imperial College London for funding this project. I am grateful to have visited the Isaac Newton Institute for the 'Mathematical aspects of turbulence' workshops and in particular to Dr David Goluskin, for sharing insights, data and the basis for all things internally heated convection.

Finally, a series of thanks to those that I met on this journey. My cohort of the Fluids CDT I thank for the many hours spent encouraging me to coauthor a book, my neighbours in room 141 for making the days all the more delightful. Then I am indebted to my friends from UCL, opening their living room to me when need be. Finally, to both the comrades here in London and the Alevis from across the UK and Europe, I am grateful to their support, and for cheering me up especially during the low times that happen in life. Last but not least, to those that are and became family, I hope I can one day earn their unconditional love.

Writing is a way for us to communicate with ourselves, not others. So I apologise in advance. I'm terrible at writing because I have nothing to say to myself. But, these letters will capture something of me that I hope can bring you some warmth. After all, winter is coming. For you and me both.

Contents

List of Figures

List of Tables

Chapter 1

Introduction

The philosophers have only interpreted the world, in many ways;

the point is to change it !

Karl Marx - Thesis on Feuerbach

One of the main interests of 21st-century science are the effect of chaos in nature. The origins of the discovery of chaotic systems go hand in hand with the study of the nonlinear dynamics and chaos in fluids known as turbulence. The effects of turbulence appear across the natural sciences and engineering, aiding in the prediction of geophysical phenomena, the engineering of planes and infrastructure in society. In recent years, the paradigmatic character of research into chaos has been multidisciplinary. All paradigm shifts have come about by not only combining ideas from within research fields but by merging the knowledge acquired from experiments, simulations and rigorous mathematics from across disciplines. Leaps forward in computational architecture make simulations increasingly accessible and yet one is usually unable to span the entire space of possibilities such that mathematically provable statements are highly desirable.

Turbulence and the associated chaotic behaviour of incompressible fluids are notoriously difficult to analyse mathematically. In particular, these systems are described by nonlinear partial differential equations (PDEs) whose states live in an

infinite-dimensional phase space. As such, closed-form solutions are only available in a relatively small number of special cases. As opposed to individual trajectories, the mathematical analysis of fluids involves considering the class of solutions that could exist for a given PDE. While many general results exist to guarantee the existence and uniqueness of large classes of ordinary differential equations, this is not the case for nonlinear PDEs, which most often are treated on a case-by-case basis. The Navier-Stokes equations represent a particularly challenging special case for analysis. The existence of smooth solutions for all times of the 3D Navier-Stokes equations remains unsolved within the millennium prize problems outlined by the Clay mathematical institute.

1.1 Background field method

In contrast to probing the nature of the solutions to the governing equations we can look for rigorous bounds on the time-averaged properties of turbulence. The challenge is in determining the functional dependence of the mean quantities on relevant nondimensional parameters, such as the Reynolds number or the Rayleigh number, which characterise the dynamics of the flow. The governing equations may be discretised and numerical methods used to simulate a flow. However simulations are statistical estimators for the possible state as a finite time or ensemble average and are limited to low Reynolds/Rayleigh numbers in comparison to flows observed in nature. In comparison, bounds can provide rigorous statements about turbulence for values of the control parameters that cannot be probed computationally. In particular, rigorous bounds are sought that come directly from the equations governing the flows without recourse to physically reasonable, but unproven assumptions.

For the case of turbulent convection, one way to study mean quantities rigorously was pioneered by Malkus, Priestley, Howard and Busse [9, 69, 98, 121]. Based on the premise that turbulence might maximise the transport of heat or momentum,

bounds can be obtained using variational techniques. The idea is simple: rather than optimizing the mean quantity of interest like the heat transport over solutions to the flow's governing equations, one optimizes it over a larger set of incompressible flow fields that satisfy only integral constraints in the form of energy and flux balances, which are weaker but more tractable. In particular, the physical intuition behind the work of Howard [69, 70] was to consider static boundary layers which conduct heat. Then, an optimisation is carried out to permit the boundary layers to be as thick as possible while balancing convection and diffusion in the turbulent state. This method of bounding required the construction of intricate flow fields even when assuming horizontally periodic domains.

The optima of the Malkus, Howard and Busse [10, 70, 98] approach are still hard to evaluate, but in the 1990s Doering and Constantin [20, 28–30] demonstrated that conservative one-sided estimates (lower bounds for minima and upper bounds for maxima) can be obtained with a technique referred to as the *background method*. By use of a decomposition idea first introduced by Hopf [67] to extend Leray's weak solutions to bounded domains [95], the background method decomposes a flow variable into a fluctuating component and a steady background field. The background field need only satisfy the boundary conditions and incompressibility but is otherwise arbitrary. This reduces the bounding problem from a variational problem over the state variables into one of constructing a background field of, in most applications, one dimension. It transpires that the quantity of interest can be bounded as a function of the background field, which varies with the system's control parameter, provided a specific quadratic form that depends on it is positive semidefinite. This extra condition is referred to as the *spectral constraint*.

In general, optimizing the background field and other optimisation parameters to produce the best possible bound is a dual problem (in the sense of convex duality) to the Malkus–Howard–Busse approach described above [79–81] and is generally difficult to solve. Suboptimal background fields can usually be constructed using

Table 1.1: A nonexhaustive summary of flows to which the background method has been applied.

Flow	Analysis	Computations
Rayleigh–Bénard convection	[21, 22, 30, 32, 78, 81, 115] [35, 72, 116, 119, 165, 168, 172] [17, 40, 59, 112, 117, 166, 167]	[34, 72, 119, 159, 169] [26, 40, 117, 140, 141],[120]†
Bénard–Marangoni convection	[43, 65]	[44]
Porous-media convection	[31]	[114, 157, 158, 160]
Internally heated convection	[1–3, 57, 89, 97, 164, 166]	[1, 2]
Double-diffusive convection	[4]	none
Horizontal convection	[129]	none
Parallel shear flows	[28, 29, 78, 99, 107] [36, 66, 79, 82, 110]	[47, 92, 108, 109, 120, 137]
Taylor–Couette flow	[18, 27, 56, 88]	[27]
Pressure-driven channel flow	[20, 86]	none
Precessing flow	[77]	none
Flows in unbounded domains	[90, 142]	none

†Computations for Couette flow in [120] imply optimal bounds for Rayleigh–Bénard convection [81, §4].

only elementary calculus and functional inequalities, and often yield useful bounds. For these reasons, the background method has enjoyed tremendous success since its introduction in the 1990s (see Table 1.1 for a non-exhaustive list of flows to which it has been applied) and, to this date, it remains one of the key tools for rigorous flow analysis.

Simple constructions of background fields can, with relative algebraic ease, yield non-trivial bounds on the quantity of interest. The main task for a given flow is to construct background fields that capture the true asymptotic scaling of the system as observed empirically. Taking the canonical case of Rayleigh–Bénard (RB) convection, rigorous bounds have been continuously improved by increasingly sophisticated background field constructions in the finite and infinite Prandtl number cases [111].

Recently, theoretical work has demonstrated that the background method and alternative bounding methodologies [116, 128] can be formulated systematically within a more general framework for bounding infinite-time averages called the *auxiliary functional method* [14, 15, 42]. This method is known to yield sharp bounds for well-posed ordinary and partial differential equations under suitable technical

conditions [126, 144]. The main advantages of this interpretation of the background method [1, 2, 40, 60] as compared to the original formulation of the method by Doering and Constantin [20, 28–30] are that (i) it allows for the consideration of generalized perturbation energies and background fields, (ii) it can be used easily to bound mean quantities not equivalent to the dissipation rate, and (iii) it always reduces the search for a bound to a *convex* variational principle. Additionally, this convex variational principle can be simplified using symmetries and, sometimes, improved by incorporating additional constraints such as maximum/minimum principles. The use of symmetries and especially the incorporation of additional constraints play a pivotal role in the bounds obtained in this thesis.

In the task of constructing background fields, computational methods can be of use. Even though no algorithm can produce rigorous bounds for all possible values of a flow's governing parameters, numerical approximations of the best bound available to the background method can reveal the optimal scaling. If they do not, computations can guide improved analysis. This was recently demonstrated for Bénard–Marangoni convection at infinite Prandtl number [43, 44] and for internally heated convection in this thesis.

Calculating the best upper bound that the background method has to offer requires solving a minimization problem. When these problems are analytically challenging they can be tackled numerically. This issue has historically been addressed using delicate numerical schemes based on continuation and bifurcation analysis [34, 108, 109, 114, 119, 120, 137, 169]. Two simpler alternatives have emerged that do not require continuation and have been applied successfully to a variety of flows. One approach [2, 44, 45, 47, 48, 50, 140, 141] discretizes the minimization problem into a semidefinite program (SDP)—a convex optimization problem where matrices with affine dependence on the optimization variables are constrained to be positive semidefinite. This SDP can then be solved using algorithms with polynomial-time complexity [105, 106, 113, 150, 163]. The other approach [27, 92, 157–159] applies the

steepest gradient method to the saddle-point formulation to derive time-dependent versions of the Euler–Lagrange equations, which can be timestepped until convergence to a stationary solution. This thesis utilises the former strategy.

1.2 Thermal convection

The fundamental physical process studied in this thesis is convection. The term 'convection' was first introduced by William Prout in 1834 though it was after Henri Bénard's experiments on thermal instability in 1900 that Lord Rayleigh paved the way for a theoretical study of RB convection in 1920 [13]. While, mathematical studies are recent convection is of significance by virtue of its prevalence in the physical world.

In nature, on length scales larger than that of humans the preeminent process affecting our lives is that of buoyant convection. Specifically, buoyant convection is the overturning of a fluid due to rising lower density and falling higher density fluid in order to minimise the potential energy in a system. Stable stratification occurs when lower density fluid sits above higher density fluid. In the adverse scenario, where some mechanism can cause lower density fluid to inhabit the space below higher density fluid, instability can occur, and the fluid moves. One mechanism that creates such an instability is the heating of a fluid from below. The motion generated by this convection can lead to turbulence.

Convection causes transport and turbulence from the atmosphere to the oceans and down to the core of the Earth. In the atmosphere, solar radiation is trapped following absorption by gases either directly, after re-emission, or reflection off the planet's surface [145]. Atmospheric convection creates large-scale weather patterns and forces winds that drive surface waves across the planet's bodies of water. Heating of the oceans by the same radiation also causes thermohaline circulation. More precisely, thermal convection occurs as the upper layers of oceans absorb heat, partly

evaporating to change the salinity of the water. Variations in salinity create variations in density generating chemical convection. Both processes combine to drive planetary thermohaline circulation [148].

Another geophysical environment in which convection is critical is the Earth's interior. The liquid outer core generates the magnetic fields protecting life on Earth from the solar wind and cosmic rays. The expansion of the solid inner core generates chemical variations in the outer core. Giving rise to chemical and thermal convection that maintain the planetary dynamo [24, 133]. In addition to the core, convection also plays a role in the Mantle. The bulk of the planet's interior is the Mantle, where convection, albeit on larger timescales, is critical to planetary dynamics. Mantle convection sustains the temperature difference across the liquid outer core, and drives tectonic activity. However, the majority of the heat in the Mantle comes from the radioactive decay of isotopes [5, 103].

Convection of fluids is prevalent across geophysical scales. A key question is how the thermal energy enters the system to create the necessary density variations. The fluid in question could either (i) be heated from the boundaries as in RB convection (ii) be heated from within as in internally heated (IH) convection, or (iii) be heated by a combination of boundary and internal heating. The case (i) for a fluid confined between two parallel plates and horizontally periodic has been well studied and is the canonical setup for convection. Historically RB convection has been extensively studied through experiments, numerical simulations, and mathematical analysis. Instead, this thesis is concerned with cases (ii) and (iii) where heating is driven by an internal heat source and possibly combined with boundary heating.

1.2.1 Internally heated convection

IH convection in a bounded domain between parallel plates is an alternative flow to RB convection and has qualitatively different features. The dynamics of IH convection also apply to flows driven by means other than temperature, such as density variations

due to electromagnetic forces or chemical concentration differences [58]. IH convection therefore warrants study in its own right to enhance the fundamental understanding of buoyancy-driven turbulence, yet has received relatively little attention in comparison with RB convection.

The first theoretical investigation into the linear stability of IH convection came with the seminal work of Roberts in 1967 [124]. The linear stability analysis of IH convection was prompted by the first experiments involving a fluid layer heated internally only a year earlier [146]. The first experiments and numerical simulations were for configurations where the lower boundary is a thermal insulator while the upper boundary is maintained at a constant temperature [6, 16, 134, 139]. The scenario of isothermal boundaries has since been researched in experiments [84] and simulations both in 2D and 3D [57, 61] (see [58] for an extensive review). Two other variations of IH convection that have been the subject of investigation are that of non-uniform IH convection [83, 101, 122, 135, 138] and IH convection within self-gravitating spheres [11, 12, 73, 123, 125].

IH convection is described by the Navier-Stokes equations with forcing due to buoyancy. In writing down a system of PDEs to describe the motion of a fluid driven by internal heating, the Boussinesq approximation is employed [132] . Initially, consider a Newtonian fluid confined between two parallel plates separated by a vertical distance d. The fluid has density ρ and ρ_0 at a reference temperature T_0, dynamic viscosity μ, thermal conductivity k, thermal expansion coefficient α, specific heat capacity c_p, and is heated uniformly at a volumetric rate H. To simplify the discussion we assume that the layer is periodic in the horizontal (x and y) directions with periods $L_x d$ and $L_y d$. The dimensional equations governing the dynamics, where

hats denote dimensional variables, are

$$\hat{\nabla} \cdot \hat{\boldsymbol{u}} = 0\,, \tag{1.2.1a}$$

$$\rho_0 \left(\hat{\partial}_t \hat{\boldsymbol{u}} + \hat{\boldsymbol{u}} \cdot \hat{\nabla} \hat{\boldsymbol{u}}\right) + \hat{\nabla} \hat{p} = \mu \hat{\Delta} \hat{\boldsymbol{u}} - \rho g \mathbf{e}_3\,, \tag{1.2.1b}$$

$$\rho_0\, c_p (\hat{\partial}_t \hat{T} + \hat{\boldsymbol{u}} \cdot \hat{\nabla} \hat{T}) = \hat{\nabla} \cdot (k \hat{\nabla} \hat{T}) + H, \tag{1.2.1c}$$

where $\hat{\boldsymbol{u}} = (\hat{u}, \hat{v}, \hat{w})$ and $\Delta f = \nabla \cdot (\nabla f)$ is the Laplacian operator on f. As part of the Boussinesq approximation the following linear equation of state is assumed

$$\hat{\rho} - \hat{\rho}_0 = \alpha(\hat{T}_0 - \hat{T}). \tag{1.2.2}$$

To make the problem nondimensional the length scale is given by d, the time scale by d^2/κ and the temperature scale by $d^2 H/\kappa\, \rho\, c_p$, where $\kappa = k/\rho\, c_p$ is the thermal diffusivity. Then with (1.2.2) and the assumptions of the Boussinesq approximation, the equations governing the motion of the fluid in the nondimensional domain $\Omega = [0, L_x] \times [0, L_y] \times [0, 1]$ are [58]

$$\nabla \cdot \boldsymbol{u} = 0\,, \tag{1.2.3a}$$

$$\partial_t \boldsymbol{u} + \boldsymbol{u} \cdot \nabla \boldsymbol{u} + \nabla p = Pr \Delta \boldsymbol{u} + Pr R\, T \mathbf{e}_3\,, \tag{1.2.3b}$$

$$\partial_t T + \boldsymbol{u} \cdot \nabla T = \nabla^2 T + 1. \tag{1.2.3c}$$

As a note the nondimensional temperature is in fact a temperature difference from a reference value, while the pressure term coincides with pressure variation for domains of height much less than the characteristic scale height [132]. The dimensionless Prandtl and Rayleigh numbers are defined as

$$Pr := \frac{\nu}{\kappa}, \qquad R := \frac{g \alpha H d^5}{\rho c_p \nu \kappa^2}. \tag{1.2.4}$$

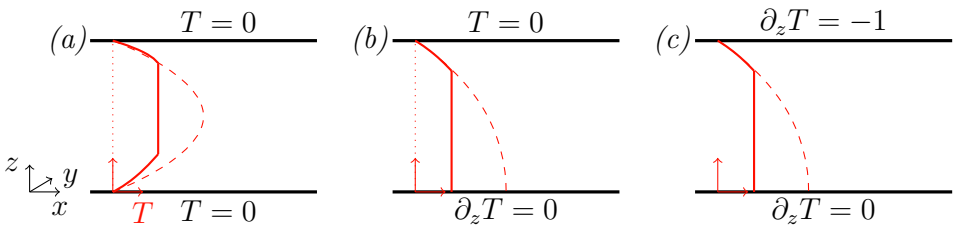

Figure 1.1: IH convection between *(a)* perfect thermal conductors, *(b)* perfectly conducting top and insulating bottom, *(c)* poor thermal conductors. In all panels, IH represents the uniform unit internal heat generation. Red lines denote the conductive temperature profiles (---) and indicative mean temperature profiles in the turbulent regime (—).

The former measures the ratio of momentum and heat diffusivity and is a property of the fluid, while the latter measures the destabilising effect of internal heating compared with the stabilising effect of diffusion and is the control parameter in this thesis.

The possible boundary conditions considered in this thesis for the velocity are no-slip and free-slip, and for the temperature is isothermal, insulating bottom isothermal top and insulating bottom fixed flux at the top. For reference later these are respectively

$$\boldsymbol{u}|_{z=\{0,1\}} = 0, \tag{1.2.5a}$$

$$w|_{z=\{0,1\}} = \partial_z u|_{z=\{0,1\}} = \partial_z v|_{z=\{0,1\}} = 0, \tag{1.2.5b}$$

$$T|_{z=\{0,1\}} = 0, \tag{1.2.5c}$$

$$\partial_z T|_{z=0} = T|_{z=1} = 0, \tag{1.2.5d}$$

$$\partial_z T|_{z=0} = 0, \qquad \partial_z T|_{z=1} = -1. \tag{1.2.5e}$$

The three thermal boundary configurations are sketched in Figure 1.1 with the corresponding conductive temperature profiles and illustrative sketches of the mean temperature profiles in the turbulent regime. Later chapters will refer to the thermal boundary conditions by their physical representations. Specifically, isothermal boundary conditions correspond to perfect thermal conductors, zero flux conditions

to perfect thermal insulators, while a fixed flux condition (as in (1.2.5e)) corresponds to a poor thermal conductor.

In RB convection, due to continuous heat injection at the bottom boundary warm fluid wants to move up while cold fluid moves downwards and the net heating is zero. In contrast for IH convection the net heating is positive everywhere, which given the preferred direction in the system due to gravity, creates a fundamental difference between the bottom (stably stratified) and top (unstably stratified) thermal boundary layers (see Figure 1.1)[63]. Furthermore the asymptotic scaling of the upper bounds on heat transport in RB convection is the same for all thermal boundary conditions. This is not the case for internally heated convection.

1.2.2 Integral relations

Significant insight can be gained into the dynamics of internally heated convection as described by (1.2.3) by relatively simple manipulations. Let $\overline{\langle f \rangle}$ denote the time- and volume-average of some quantity f in Ω. The result of taking $\overline{\langle \boldsymbol{u} \cdot (1.2.3\text{b}) \rangle}$, given either no-slip or free-slip boundaries is that

$$\overline{\langle wT \rangle} = \frac{1}{R} \overline{\langle |\nabla \boldsymbol{u}|^2 \rangle}. \tag{1.2.6}$$

The relation (1.2.6) states that the mean vertical convective heat transport, which converts potential energy into kinetic energy, is equal to the viscous dissipation of the fluid on average. In dimensional units (1.2.6) becomes

$$g\alpha \overline{\left\langle \hat{w}\hat{T} \right\rangle} = \nu \overline{\langle |\nabla \hat{\boldsymbol{u}}|^2 \rangle}, \tag{1.2.7}$$

and the left-hand side of (1.2.7) is the buoyancy flux. Since the viscous dissipation is a non-negative quantity, the implication of (1.2.6) is that $\overline{\langle wT \rangle} \geq 0$. This lower bound is sharp as it is always saturated by pure conduction and this flow state is attracting for R below the energy stability limit. The lower bound need not necessarily be

attained for R above the energy stability limit. In IH convection, unlike RB, the energy and linear stability limits are not equivalent such that subcritical convection can occur for all possible thermal configurations (1.2.5c)-(1.2.5e).

The demonstration of a uniform upper bound on $\overline{\langle wT \rangle}$ is also relatively trivial. Let $\overline{\langle f \rangle_h}$ denote the horizontal time average of f. Then, taking the horizontal time average of (1.2.3c), given impermeable boundaries, integrating in the vertical direction from 0 to z gives

$$\overline{\langle wT \rangle_h} = \overline{\langle \partial_z T \rangle_h} - \overline{\langle \partial_z T|_{z=0} \rangle_h} + z. \tag{1.2.8}$$

This identity can further be integrated in z from 0 to 1 to obtain

$$\overline{\langle wT \rangle} = -\overline{\langle \partial_z T|_{z=0} \rangle_h} + \frac{1}{2}, \qquad \textit{(for (1.2.5c))}, \tag{1.2.9a}$$

$$\overline{\langle wT \rangle} = -\overline{\langle T|_{z=0} \rangle_h} + \frac{1}{2}, \qquad \textit{(for (1.2.5d))}, \tag{1.2.9b}$$

$$\overline{\langle wT \rangle} = \overline{\langle T|_{z=1} \rangle_h} - \overline{\langle T|_{z=0} \rangle_h} - \overline{\langle \partial_z T|_{z=0} \rangle_h} + \frac{1}{2}, \qquad \textit{(for (1.2.5e))}. \tag{1.2.9c}$$

There are three relations in (1.2.9) for the three possible thermal boundary conditions. It is the case that for (1.2.9a) and (1.2.9b) where the upper boundary is isothermal, we can invoke a minimum principle on the temperature (a rigorous statement and proof of which is given in Lemma 2.3.1), which states that $T \geq 0$ within the domain. The implication for (1.2.9a) is that since $T|_{z=0} = 0$, if T is to be non-negative for all $z \in (0, 1)$ then $\partial_z T|_{z=0} \geq 0$. In the case of (1.2.9b) the implication on the minimum principle is that $T|_{z=0} \geq 0$. Both of these inequalities immediately imply that

$$\overline{\langle wT \rangle} \leq \frac{1}{2}. \tag{1.2.10}$$

There is no minimum principle on T for the boundary conditions (1.2.5e), however an upper bound on $\overline{\langle wT \rangle}$ was demonstrated analytically [58] by use of the Poincaré

and Cauchy-Schwarz inequalities to be

$$\overline{\langle wT \rangle} \leq \frac{1}{2} + \frac{1}{\sqrt{3}}. \tag{1.2.11}$$

However, as will be demonstrated in chapter 7, this uniform upper bound can be exactly halved (cf. Theorem 7.1.1).

The parameters that determine the value of $\overline{\langle wT \rangle}$ are R, Pr, the aspect ratio and initial conditions. This thesis aims to answer the question can a nontrivial relation of the form

$$\overline{\langle wT \rangle} \leq \frac{1}{2} - f(R), \tag{1.2.12}$$

be *a priori* determined from the governing equations?

A quantity of interest for which R-dependent bounds exist is $\overline{\langle T \rangle}$, equivalent to the thermal dissipation and can be shown by evaluating $\overline{\langle T \cdot (1.2.3\text{c}) \rangle}$. Specifically

$$\overline{\langle T \rangle} = \overline{\langle |\nabla T|^2 \rangle}, \tag{1.2.13}$$

as with $\overline{\langle wT \rangle}$ clearly $\overline{\langle T \rangle}$ is non-negative. For a physical intuition in dimensional units (1.2.13) states

$$\frac{H}{\rho\, c_p} \overline{\left\langle \hat{T} \right\rangle} = \kappa \overline{\left\langle |\nabla \hat{T}|^2 \right\rangle}, \tag{1.2.14}$$

where the left-hand side is the temperature change due to internal heating and the right-hand side the thermal dissipation. Laboratory experiments [74, 75, 85, 93] and direct numerical simulations [39, 62, 63, 118, 136, 147, 170] indicate that the dimensional mean temperature increases sublinearly with the heating rate, which, in nondimensional terms, implies that $\overline{\langle T \rangle}$ decreases with R. Scaling arguments for Rayleigh-Bénard convection [64] can be applied to the top boundary layer of IH convection [23, 62, 152] and one implication is that $\overline{\langle T \rangle} \sim Pr^{-\frac{1}{3}} R^{-\frac{1}{3}}$ when $Pr \lesssim R^{-\frac{1}{4}}$ and $\overline{\langle T \rangle} \sim R^{-\frac{1}{4}}$ otherwise. The dependence of these predictions on the Rayleigh

number agrees with rigorous lower bounds on $\overline{\langle T \rangle}$ for both finite and infinite Pr [97, 164] up to logarithmic corrections.

It was demonstrated that $\overline{\langle T \rangle} \leq \frac{1}{12}$ for isothermal boundaries while $\overline{\langle T \rangle} \leq \frac{1}{3}$ when the lower boundary is insulating [58, 62]. For all boundary conditions it has been proven that $\overline{\langle T \rangle} \geq cR^{-\frac{1}{3}}$, where c is some constant independent of Pr, the aspect ratio or initial conditions [97]. In the limit of infinite Prandtl number, the lower bound on $\overline{\langle T \rangle}$ was demonstrated to be $\overline{\langle T \rangle} \geq c(R \log R)^{-\frac{1}{4}}$, while if the no-slip boundaries are replaced with free-slip $\overline{\langle T \rangle} \geq cR^{-\frac{5}{17}}$ [164, 166]. Beyond experiments and simulations, rigorous results exist about the scaling behaviour of $\overline{\langle T \rangle}$ with R, however no such results exist for $\overline{\langle wT \rangle}$. There is no *a priori* relation between the quantities $\overline{\langle wT \rangle}$ and $\overline{\langle T \rangle}$ in IH convection. This thesis, for the first time demonstrates that bounds can be proven on $\overline{\langle wT \rangle}$ from the governing equations, without recourse to ad hoc assumptions or heuristic arguments.

The numerical value of $\frac{1}{2}$ for the uniform upper bound on $\overline{\langle wT \rangle}$ emerges from the choice of nondimensionalisation, instead a bound on $\overline{\langle wT \rangle}$ has clear physical implications for any given thermal boundary condition. For isothermal boundaries, the mean conductive heat flux is zero, so no well defined Nusselt number, Nu, exists. Instead, $\overline{\langle wT \rangle}$ is a measure of the asymmetry of the heat leaving the domain due to convection. Indeed, upon computing $\overline{\langle z \cdot (1.2.3\text{c}) \rangle}$ one can show that the horizontally averaged heat fluxes through the top and bottom boundaries, denoted by $\mathcal{F}_T$ and $\mathcal{F}_B$ respectively, can be expressed as

$$\mathcal{F}_T := -\partial_z \overline{\langle T \rangle}_h|_{z=1} = \frac{1}{2} + \overline{\langle wT \rangle}, \tag{1.2.15a}$$

$$\mathcal{F}_B := \quad \partial_z \overline{\langle T \rangle}_h|_{z=0} = \frac{1}{2} - \overline{\langle wT \rangle}. \tag{1.2.15b}$$

Indeed the volume averaged heat flux vertically upwards is given as $\overline{\langle J \rangle} = \overline{\langle wT \rangle}$, re-illustrating that $\overline{\langle wT \rangle}$ represents the role played by the velocity field, driven to motion by internal heating, to transport heat.

When the lower boundary is an insulator, the mean conductive heat flux is positive, and the effects of convection on the enhancement of heat transport in the system can be described using a Nusselt number. This is defined as the ratio of the mean total heat flux to the mean conductive heat flux and can be expressed in terms of $\overline{\langle wT \rangle}$ as

$$Nu = \frac{\overline{\langle J \rangle}}{\overline{\langle J_{\text{cond}} \rangle}} = \frac{\overline{\langle \delta T \rangle_h} + \overline{\langle wT \rangle}}{\overline{\langle \delta T \rangle_h}} = \left(1 - 2\overline{\langle wT \rangle}\right)^{-1}, \tag{1.2.16}$$

where $\overline{\langle J_{\text{cond}} \rangle} = \overline{\langle \delta T \rangle_h} = \overline{\langle T|_{z=0} \rangle_h} - \overline{\langle T|_{z=1} \rangle_h} =$ is the conductive heat flux. That a well defined Nusselt number exists for configurations (1.2.5d) and (1.2.5e) allows for a useful comparison with RB convection.

1.3 Outline

The main aims and objectives of this thesis have been mentioned at relevant places within the introduction and are stated once more here. R-dependent upper bounds on the quantity $\overline{\langle wT \rangle}$ are proven for IH convection by use of the background field method assisted by computational optimisation.

The bounds proven in this thesis are highlighted in Table 1.2. In addition to the analytic bounds, numerical optimisation is carried out for a selection of cases in Table 1.2 to obtain the best bounds within the framework of the background method.

The outline of the thesis is as follows. First, chapter 2 introduces the modern formulation of the background method, stating and proving the minimum principle, and stating the optimisation problem in generality for IH convection. In chapter 3 the boundary conditions considered are no-slip and isothermal ((1.2.5a) & (1.2.5c)) where numerical and analytical bounds are derived with and without utilising the minimum principle, these appear in two publication [2, 89]. Then chapter 4 analyses no-slip insulating bottom and isothermal top boundary conditions, proving bounds numerically and analytically without a minimum principle and an analytical bound when the minimum principle is utilised, the analytical bound appears in the

Table 1.2: A summary of the R-dependent upper bounds on $\overline{\langle wT \rangle}$ proven in this thesis, where any c corresponds to constants independent of R or Pr with the respective values given in the respective sections. For entries where a bound is said to be not known, there is no proven R-dependent bound.

Thermal b.c.	$T\|_{z=1} = 0$ $T\|_{z=0} = 0$	$T\|_{z=1} = 0$ $\partial_z T\|_{z=0} = 0$	$\partial_z T\|_{z=1} = -1$ $\partial_z T\|_{z=0} = 0$
Uniform bound	$\frac{1}{2}$	$\frac{1}{2}$	$\frac{1}{2}\left(\frac{1}{2} + \frac{1}{\sqrt{3}}\right)$
No-slip	$cR^{\frac{1}{5}}$† $\frac{1}{2} - c_1 R^{\frac{1}{5}} \mathrm{e}^{-c_2 R^{\frac{3}{5}}}$	$\frac{1}{2}\left(\frac{1}{2} + \frac{1}{\sqrt{3}}\right) - cR^{-\frac{1}{3}}$† $\frac{1}{2} - c_1 R^{-\frac{1}{5}} \mathrm{e}^{-c_2 R^{\frac{3}{5}}}$	$\frac{1}{2}\left(\frac{1}{2} + \frac{1}{\sqrt{3}}\right) - cR^{-\frac{1}{3}}$
Free-slip	$\frac{1}{2} - cR^{-\frac{40}{29}}$	not known	not known
$Pr = \infty$ **(no-slip)**	$\frac{1}{2} - cR^{-2}$	$\frac{1}{2} - cR^{-4}$	not known
$Pr = \infty$ **(free-slip)**	$\frac{1}{2} - cR^{-\frac{40}{29}}$	not known	not known

†Bounds proven where the minimum principle is not utilised, such that at finite R, $\overline{\langle wT \rangle} > 1/2$ and hence suboptimal relative to the uniform upper bound.

publications [89]. In chapter 5 analytical bounds for the boundary conditions of the previous two chapters are considered when in the limit of infinite Pr, the work appears in the publication [3]. With chapter 6 analytical bounds for isothermal and free-slip boundaries are proven. Afterward, chapter 7 demonstrates numerical and analytical bounds for no-slip boundaries where fixed flux thermal boundary conditions are prescribed, published in [1], before presenting preliminary ideas in chapter 8 where the same boundary conditions are used but with instead non-uniform heating or cooling throughout the domain. Finally, chapter 9 provides concluding remarks on the bounds proven with thoughts for future work and reflections on the scaling laws obtained.

1.4 Notation

As is standard $\mathbb{R}^n$ is the n-dimensional Euclidean space. The real and imaginary parts of complex-valued quantity a are denoted $\mathrm{Re}(a)$ and $\mathrm{Im}(a)$, respectively and

a^* is the complex conjugate of a. Any vector quantity is denoted with lower-case boldface.

Given an open bounded set as $\Omega \subset \mathbb{R}^n$ the compact set $\overline{\Omega}$ is its closure. Give a positive integer q, $C^m(\overline{\Omega}, \mathbb{R}^q)$ is the space of $m-$times continuously differentiable functions mapping $\overline{\Omega}$ to $\mathbb{R}^q$. Given $1 \leq p < \infty$, $L^p(\Omega, \mathbb{R}^q)$ is the usual Lebesgue space of p-integrable vector-valued functions, while $L^\infty(\Omega, \mathbb{R}^q)$ is the space of essentially bounded functions. The standard Lebesgue norms of $\boldsymbol{f} \in L^p(\Omega, \mathbb{R}^q)$ and $\boldsymbol{g} \in L^\infty(\Omega, \mathbb{R}^q)$, denoted by $\|\boldsymbol{f}\|_{L^p(\Omega)}$ unless $\Omega = [0,1]$, then for brevity we write $\|\boldsymbol{f}\|_p$ and $\|\boldsymbol{g}\|_\infty$ which are

$$\|\boldsymbol{f}\|_{L^p(\Omega)} = \left[\int_\Omega \sum_{i=1}^{n} |f_i(\boldsymbol{x})|^p \mathrm{d}^n\boldsymbol{x}\right]^{\frac{1}{p}}, \qquad \|\boldsymbol{g}\|_\infty = \max_{i=1,..,n}\left[\operatorname*{ess\,sup}_{x\in\Omega} g_i(\boldsymbol{x})\right].$$

For $\ell \geq 1$ the ℓ-th derivative of a function $f(x_i)$ is denoted $\partial_{x_i \ldots x_i^{\ell-1}} f$. If $f = f(z)$ then primes are used to denote derivatives (e.g. f'). Let $f = f(\boldsymbol{x}, t)$ be a real-valued function of a time variable $t \in [0, +\infty)$ and working in Cartesian coordinates such that $x_i = (x, y, z) = \boldsymbol{x}$, with $(x, y) \in \mathbb{R}^2$ and $z \in (0, 1)$ and the standard velocity vector $\boldsymbol{u} = (u, v, w)$. Overbars denote infinite time averages, angled brackets denote volume averages while a subscript h denotes a horizontal average. More precisely in $\Omega = [0, L_x] \times [0, L_y] \times [0, 1]$ where L_x is the length scale in x, L_y is the length scale in y then,

$$\langle f \rangle_h := \frac{1}{L_x L_y} \int_0^{L_x} \int_0^{L_y} f(x, y, z, t) \mathrm{d}y \, \mathrm{d}x, \tag{1.4.1a}$$

$$\langle f \rangle := \int_0^1 \langle f \rangle_h \mathrm{d}z, \tag{1.4.1b}$$

$$\overline{\langle f \rangle} := \limsup_{\tau \to \infty} \frac{1}{\tau} \int_0^\tau \langle f \rangle \, \mathrm{d}t. \tag{1.4.1c}$$

Functionals are denoted with calligraphic letters with arguments given in curly brackets. The functional $\mathcal{F}$ acting on u is denoted $\mathcal{F}\{u\}$. The functional derivative

of $\mathcal{F}$ at v is the functional $\frac{\delta \mathcal{F}}{\delta v} : V \to \mathbb{R}$ such that

$$\frac{\delta \mathcal{F}}{\delta v}\{u\} := \lim_{h \to 0} \frac{\mathcal{F}\{v + h\, u\} - \mathcal{F}\{v\}}{h},$$

provided the limit exists and is finite. If V is a Hilbert space and $\frac{\delta \mathcal{F}}{\delta v}$ is a bounded linear functional, then $\frac{\delta \mathcal{F}}{\delta v}$ can be identified with V by the Riesz representation theorem.

Chapter 2

Bounding via auxiliary functionals

Fluid dynamicists are divided into,
hydraulic engineers who observe what cannot be explained,
and mathematicians who explain things that cannot be observed.

Cyril Hinshelwood

This chapter introduces the approach known as the *background method*, by which we prove the results in Table 1.2. A recent extensive review of the method is given in [41], while its connection to other approaches to derive *a priori* estimates in fluid mechanics is given in [14]. We refer to these papers for a general discussion of the background method. Here we focus only on its application to the problem of convection driven by uniform internal heating and, in particular, on the bounding of the nondimensional vertical convective heat flux $\overline{\langle wT \rangle}$. As discussed in chapter 1, this quantity has a different physical meaning depending on the thermal boundary conditions of the particular example considered. Any modifications necessary for the individual cases considered in this thesis are explained at the beginning of the corresponding chapters (see chapters 5 to 7).

2.1 Preliminaries

The aim of this chapter is to formulate optimization problems whose solutions yield *a priori* upper bounds on $\overline{\langle wT \rangle}$, and which are derived by considering necessary conditions that are satisfied by all solutions of the Boussinesq equations. Using the nondimensionalisation from chapter 1, these are

$$\nabla \cdot \boldsymbol{u} = 0, \tag{2.1.1a}$$

$$\partial_t \boldsymbol{u} + \boldsymbol{u} \cdot \nabla \boldsymbol{u} + \nabla p = Pr\, \Delta \boldsymbol{u} + Pr\, R\, T \mathbf{e}_3, \tag{2.1.1b}$$

$$\partial_t T + \boldsymbol{u} \cdot \nabla T = \Delta T + 1, \tag{2.1.1c}$$

for an incompressible fluid between parallel plates occupying the domain $\Omega = [-L_x, L_x] \times [-L_y, L_y] \times [0, 1]$. We remind the reader that the Prandtl number Pr is the ratio of kinematic viscosity and thermal diffusivity, while the Rayleigh number R measures the strength of the thermal forcing compared to diffusion; see (1.2.4) in chapter 1 for more details.

As mentioned in chapter 1, we consider different sets of boundary conditions for the temperature as well as the velocity. For this reason, it is convenient to define various function spaces, each of which encodes a particular choice for the boundary conditions. Let $H^p(\Omega)$ be the usual Sobolev space of square-integrable functions on Ω with square-integrable (weak) pth order derivatives. We introduce two spaces of incompressible velocity fields satisfying the no-slip and free-slip boundary conditions, respectively:

$$\mathcal{U}_1 := \Big\{ \boldsymbol{u} \in H^2(\Omega) \;\Big|\; \nabla \cdot \boldsymbol{u} = 0,\ \boldsymbol{u} \text{ is periodic in } x, y,\ (1.2.5\text{a}) \Big\}, \tag{2.1.2a}$$

$$\mathcal{U}_2 := \Big\{ \boldsymbol{u} \in H^2(\Omega) \;\Big|\; \nabla \cdot \boldsymbol{u} = 0,\ \boldsymbol{u} \text{ is periodic in } x, y,\ (1.2.5\text{b}) \Big\}. \tag{2.1.2b}$$

Similarly, we will use three different temperature spaces, which encode whether the top and bottom boundaries are insulated or isothermal:

$$\mathcal{T}_1 := \left\{ T \in H^1(\Omega) \;\middle|\; T \text{ is periodic in } x, y, \text{ (1.2.5c)} \right\}, \tag{2.1.3a}$$

$$\mathcal{T}_2 := \left\{ T \in H^1(\Omega) \;\middle|\; T \text{ is periodic in } x, y, \text{ (1.2.5d)} \right\}, \tag{2.1.3b}$$

$$\mathcal{T}_3 := \left\{ T \in H^1(\Omega) \;\middle|\; T \text{ is periodic in } x, y, \text{ (1.2.5e)} \right\}. \tag{2.1.3c}$$

Strictly speaking, $\mathcal{T}_3$ is not a linear space but rather an affine space, because it is defined using inhomogenous boundary conditions.

Finally, as we will see in §2.3.1 below, it will sometimes be convenient to restrict our attention to temperature fields that are nonnegative on Ω. For this, we define the sets

$$\mathcal{T}_i^+ = \left\{ T \in \mathcal{T}_i \,\middle|\, T(\boldsymbol{x}) \geq 0 \text{ a.e. } \boldsymbol{x} \in \Omega \right\}, \qquad i \in \{1, 2, 3\}. \tag{2.1.4}$$

2.2 Upper bounds via the auxiliary function method

Having defined the setup, let us now derive an optimisation problem giving an upper bound on $\overline{\langle wT \rangle}$. We start in §2.2.1 with a general strategy based on so called *auxiliary functions*, and then make a particular choice of quadratic auxiliary functions in §2.2.2. This restriction leads to an approach which is equivalent to the background method.

2.2.1 General auxiliary functions

An *a priori* upper bound on $\overline{\langle wT \rangle}$ can be derived with the use of an appropriately chosen functional $\mathcal{V}$. Indeed let $(\boldsymbol{u}(t), T(t))$ be a solution to (2.1.1) satisfying one of the described set of boundary conditions discussed in chapter 1 , i.e., $\boldsymbol{u} \in \mathcal{U}_i$ and $T \in \mathcal{T}_j$ for some i, j. Then, provided that a functional $\mathcal{V} : \mathcal{U}_i \times \mathcal{T}_j \to \mathbb{R}$ remains bounded along solutions of (2.1.1), the fundamental theorem of calculus guarantees

that

$$\overline{\frac{\mathrm{d}}{\mathrm{d}t}\mathcal{V}\{\boldsymbol{u}(t),T(t)\}} = \limsup_{\tau\to\infty}\frac{1}{\tau}\int_0^\tau \frac{\mathrm{d}}{\mathrm{d}t}\mathcal{V}\{\boldsymbol{u}(t),T(t)\}\mathrm{d}t$$
$$= \limsup_{\tau\to\infty}\frac{\mathcal{V}\{\boldsymbol{u}(\tau),T(\tau)\}-\mathcal{V}\{\boldsymbol{u}(0),T(0)\}}{\tau} = 0. \tag{2.2.1}$$

We call $\mathcal{V}$ an *auxiliary functional*.

In the above equation, calculation of the time derivative of $\mathcal{V}\{\boldsymbol{u}(t),T(t)\}$ using the governing equations gives another functional on the relevant velocity and temperature spaces, and we denote this functional $\mathcal{LV}$ (see §2.2.2 for an explicit example). Using this notation and (2.2.1) we can then write

$$\overline{\langle w(t)T(t)\rangle} = \overline{\langle w(t)T(t)\rangle + \mathcal{LV}\{\boldsymbol{u}(t),T(t)\}}. \tag{2.2.2}$$

In other words, we can construct infinitely many quantities that have the same time average as $\langle wT\rangle$.

At this point we consider two key simplifications. First, we estimate the average over time of (2.2.2) from above by the pointwise-in-time maximum of $\langle w(t)T(t)\rangle + \mathcal{LV}\{\boldsymbol{u}(t),T(t)\}$ along the solution of the governing equations in (2.1.1). Then, since such solutions can rarely be explicitly constructed, we estimate this maximum by the maximum value that $\langle wT\rangle + \mathcal{LV}\{\boldsymbol{u},T\}$ can take over *all* velocity and temperature fields inside a set $\mathbb{A}$ for which solutions of (2.1.1) are known to belong, at least for sufficiently large times $t > 0$. Precisely, it is assumed that $\mathbb{A}$ is an absorbing set for the dynamics governed by (2.1.1). It then follows from the above discussion that

$$\overline{\langle w(t)T(t)\rangle} \le \sup_{(\boldsymbol{u},T)\in\mathbb{A}}\{\langle wT\rangle + \mathcal{LV}\{\boldsymbol{u},T\}\}. \tag{2.2.3}$$

Since this argument holds for every functional $\mathcal{V}$ satisfying (2.2.1), we can in principle optimize its choice to arrive at the minmax upper bound

$$\overline{\langle w(t)T(t)\rangle} \leq \inf_{\mathcal{V}} \sup_{(\boldsymbol{u},T)\in\mathbb{A}} \{\langle wT\rangle + \mathcal{L}\mathcal{V}\{\boldsymbol{u},T\}\}. \tag{2.2.4}$$

It is reasonable to wonder how conservative the estimates we have performed to derive this last inequality are. It turns out that optimizing $\mathcal{V}$ can yield *sharp* bounds for well-posed ODEs and PDEs with compact absorbing sets $\mathbb{A}$ [126, 144]. Solving the minmax problem (2.2.4), however, is generally a very hard task. For this reason, in this thesis we restrict the attention to a tractable but suboptimal family of quadratic functionals $\mathcal{V}$.

2.2.2 A family of quadratic auxiliary functions

A tractable family of functionals $\mathcal{V}$ was implicitly introduced by Doering and Constantin in a series of papers [19, 28–30]. The analysis in these works uses quadratic functionals $\mathcal{V}$ of the form

$$\mathcal{V}\{\boldsymbol{u},T\} := \left\langle \frac{\alpha}{2R\,Pr}|\boldsymbol{u}|^2 + \frac{\beta}{2}\left|T - \frac{\varphi(z)}{\beta}\right|^2 \right\rangle, \tag{2.2.5}$$

where α and β are tunable non-negative numbers and $\varphi(z)$ is a tunable function satisfying the same boundary conditions as the temperature at the top and bottom boundaries. The parameters α and β, often referred to as the *balance parameters*, determine the relative weight of a term proportional to the kinetic energy $|\boldsymbol{u}|^2$ and a term similar to a "thermal energy" measured with respect to a *background temperature field* $\varphi(z)/\beta$. For simplicity, we will abuse the established terminology and simply refer to $\varphi(z)$ as the *background field*. The goal throughout this thesis will be to choose α, β and $\varphi(z)$ to ensure that the right-hand side of (2.2.4) is finite and, ideally, as small as possible. These choices, of course, will depend on the boundary conditions imposed on $\boldsymbol{u}$ and T, and on the parameters R and Pr.

The first step to evaluate the bound in (2.2.4) with $\mathcal{V}$ in (2.2.5) for given choices of α, β and $\varphi(z)$ is to calculate the Lie derivative of $\mathcal{V}$ over solutions of the governing equations (2.1.1), which we previously denoted as $\mathcal{LV}$. When T, and consequently $\varphi(z)$, satisfies the boundary conditions in (1.2.5c) or (1.2.5d) (i.e., $T \in \mathcal{T}_1$ or $T \in \mathcal{T}_2$), one finds after appropriate application of integration by parts in (2.2.5) that

$$\mathcal{LV}\{\boldsymbol{u}, T\} = -\left\langle \frac{\alpha}{R}|\nabla \boldsymbol{u}|^2 + \beta|\nabla T|^2 - (\alpha - \varphi'(z))wT \right\rangle - \langle (\beta z - \varphi'(z))\partial_z T + \varphi(z) \rangle . \quad (2.2.6)$$

When $T \in \mathcal{T}_3$, instead, it is more convenient to work with perturbations ϑ from the conductive temperature profile $-\frac{1}{2}z^2 + \frac{1}{6}$, rather than with the full temperature T. The calculation is analogous and the result will be given in chapter 7, which is the only place where the boundary conditions in (1.2.5e) are studied.

Returning to the case in which either $T \in \mathcal{T}_1$ or $T \in \mathcal{T}_2$, and using (2.2.6), the upper bound in (2.2.4) becomes

$$\overline{\langle w(t)T(t)\rangle} \leq \inf_{\alpha,\beta,\varphi(z)} \sup_{(\boldsymbol{u},T)\in\mathbb{A}} \Big\{ -\left\langle \frac{\alpha}{R}|\nabla \boldsymbol{u}|^2 + \beta|\nabla T|^2 - (\alpha + 1 - \varphi'(z))wT \right\rangle - \langle (\beta z - \varphi'(z))\partial_z T + \varphi(z) \rangle \Big\}. \quad (2.2.7)$$

The right-hand side can be rewritten as the equivalent constrained minimization problem

$$\inf_{U,\alpha,\beta,\varphi(z)} \Big\{ U \mid \mathcal{S}\{\boldsymbol{u}, T\} \geq 0 \quad \forall (\boldsymbol{u}, T) \in \mathbb{A} \Big\}, \quad (2.2.8)$$

where

$$\mathcal{S}\{\boldsymbol{u}, T\} := \left\langle \frac{\alpha}{R}|\nabla \boldsymbol{u}|^2 + \beta|\nabla T|^2 - (\alpha + 1 - \varphi'(z))wT \right\rangle + \langle (\beta z - \varphi'(z))\partial_z T + \varphi(z) \rangle + U. \quad (2.2.9)$$

This minimization problem (2.2.8) is still challenging to solve in general, and its solution depends crucially on the choice of absorbing set $\mathbb{A}$. In the next section, we will consider two particular choices of absorbing set. The first is to consider all velocity and temperature fields satisfying the incompressibility and boundary conditions, i.e., $\mathbb{A} = \mathcal{U}_i \times \mathcal{T}_j$ for choices of $i, j \in \{1, 2\}$. The second choice will appeal to a "minimum principle" to restrict the attention to nonnegative temperature fields, i.e., we set $\mathbb{A} = \mathcal{U}_i \times \mathcal{T}_j^+$.

2.3 An improved optimization problem

In this section initially we assume that $\mathbb{A} = \mathcal{U}_i \times \mathcal{T}_j$ for $i, j \in \{1, 2\}$. It is not *a priori* clear that parameters $(U, \varphi(z), \alpha, \beta)$ exist for which the optimisation problem in (2.2.8) is feasible. However, observing the structure of $\mathcal{S}$ in (2.2.9), a necessary condition is that the parameters $(\alpha, \beta, \varphi(z))$ are chosen such that the quadratic part of $\mathcal{S}$ is positive semidefinite since $\mathbb{A}$ is a linear space. This necessary condition is typically referred to as a *spectral constraint*.

Definition 2.3.1 (Spectral Constraint)**.** The parameters $(\alpha, \beta, \varphi(z))$ is said to satisfy the spectral constraint if

$$\left\langle \frac{\alpha}{R}|\nabla \boldsymbol{u}|^2 + \beta|\nabla T|^2 - (\alpha + 1 - \varphi'(z))wT \right\rangle \geq 0, \quad \forall (\boldsymbol{u}, T) \in \mathbb{A}. \tag{2.3.1}$$

For sufficiently small R when $\boldsymbol{u} = 0$ and since β is non-negative the condition (2.3.1) can be satisfied when $\varphi(z)$ is the conductive temperature profile. In fact, when $\varphi(z)$ is the conductive temperature profile (2.2.9) is exactly the energy stability condition, and the flow is known to be stable at sufficiently small $R > 0$ [58]. Then, intuitively it can be expected that above energy stability the positive $|\nabla \boldsymbol{u}|^2$ remains sufficiently large to control the indefinite term proportional to wT.

The optimization problem (2.2.8) remains difficult to solve and can be further simplified. Let us define

$$\varphi(z) := \tau(z) + z - 1. \tag{2.3.2}$$

Where $\tau(z)$ appears, we will, with slight abuse of notation, also refer to it as the background field. For clarity the boundary conditions on $\tau(z)$ are that if $\mathbb{A} = \mathcal{U}_i \times \mathcal{T}_1$ defined in (2.1.3a) then

$$\tau(0) = 1, \quad \tau(1) = 0, \tag{2.3.3}$$

whereas if $\mathbb{A} = \mathcal{U}_i \times \mathcal{T}_2$ defined by (2.1.3b) then

$$\tau'(0) = -1, \quad \tau(1) = 0. \tag{2.3.4}$$

The functional $\mathcal{S}$ in (2.2.9) after substituting (2.3.2) becomes

$$\begin{aligned}\mathcal{S}\{\boldsymbol{u}, T\} := \Big\langle \frac{\alpha}{R}|\nabla \boldsymbol{u}|^2 + \beta|\nabla T|^2 - (\alpha - \tau'(z))wT \Big\rangle \\ + \langle (\beta z - \tau'(z) - 1)\partial_z T + \tau(z) \rangle + U - \frac{1}{2}.\end{aligned} \tag{2.3.5}$$

In §2.4 below we will make use of (2.3.5) to derive explicit expressions for the extremal values of U (and the best upper bound on $\overline{\langle wT \rangle}$) given optimisation parameters $(\alpha, \beta, \tau(z))$ which satisfy the spectral constraint. Before doing this, we will first analyse the case where additional information on the positivity of the temperature can be used to improve the eventual bound on $\overline{\langle wT \rangle}$.

2.3.1 Utilising the minimum principle

One common strategy when using the background method has been in searching for additional pieces of information that can improve the asymptotic behaviour of the bounds. As discussed in chapter 1, the uniform upper bound $\overline{\langle wT \rangle} \leq \frac{1}{2}$ (in the cases that $T \in \mathcal{T}_i$ for $i \in \{1, 2\}$) follows from the fact that a minimum principle for T holds.

Interestingly, it turns out the optimisation problem (2.2.8) can also be improved by utilising this additional piece of information. To use this fact, we assume that $\mathbb{A}$ in (2.2.8) is of the form $\mathbb{A} = \mathcal{U}_i \times \mathcal{T}_j^+$ for $i, j = \{1, 2\}$ which corresponds to only enforcing the constraint in (2.2.8) for temperature fields that are non-negative.

We will demonstrate that the search over a smaller set can give an improved bound on $\overline{\langle wT \rangle}$. As discussed in chapter 1, for all configurations of uniform internally heated convection where the upper boundary is a perfect thermal conductor, there exists a minimum principle on T. We now prove this result. To do so it is convenient to define the negative parts of T as

$$T_-(\boldsymbol{x}, t) := \max\{-T(\boldsymbol{x}, t), 0\}. \tag{2.3.6}$$

That a minimum principle holds follows if we can show that T_- vanishes for sufficiently large times.

Lemma 2.3.1 (Minimum principle)**.** *Suppose T solves the heat equation* (1.2.3c)*, where $\boldsymbol{u}$ satisfies $\nabla \cdot \boldsymbol{u} = 0$ and $\boldsymbol{u} \cdot \mathbf{n} = 0$ and the boundary condition $T|_{z=1} = 0$. Then*

$$\left\langle T_-(t)^2 \right\rangle \leq \left\langle T_-(0)^2 \right\rangle e^{-\mu t}, \tag{2.3.7}$$

for some $\mu > 0$. In particular if $T(\boldsymbol{x}, 0) > 0$ then $T(\boldsymbol{x}, t) \geq 0$ for all $t > 0$.

Proof. The proof is analogous to arguments for Rayleigh–Bénard convection [52, Lemma 2.1]. With the negative part of T given by (2.3.6), T_- is nonnegative on the fluid's domain Ω. Multiplying the advection-diffusion equation (1.2.3c) by T_- and integrating by parts over the domain using the boundary conditions and incompressibility yields

$$\frac{1}{2}\frac{\mathrm{d}}{\mathrm{d}t}\left\langle T_-^2 \right\rangle = -\left\langle \nabla T_-^2 \right\rangle - \left\langle T_- \right\rangle. \tag{2.3.8}$$

Since T_- vanishes at the top boundary, it follows from the Poincaré inequality that $\langle \nabla T_-^2 \rangle \geq \mu \langle T_-^2 \rangle$ for some constant $\mu > 0$. Moreover since $\langle T_- \rangle \geq 0$, then it follows from (2.3.8) that

$$\frac{1}{2}\frac{\mathrm{d}}{\mathrm{d}t}\langle T_-^2 \rangle \leq -\mu \langle T_-^2 \rangle . \tag{2.3.9}$$

Gronwall's lemma [33] then yields

$$\langle T_-(t)^2 \rangle \leq \langle T_-(0)^2 \rangle \, \mathrm{e}^{-\mu t}, \tag{2.3.10}$$

so T_- tends to zero in $L^2(\Omega)$ at least exponentially quickly. This implies that $T(\boldsymbol{x}, t) \geq 0$ almost everywhere on the global attractor and that $T(\boldsymbol{x}, t)$ is nonnegative at all times if it is so at $t = 0$. □

Remark 2.3.1. This result says that $T \geq 0$ on the global attractor for all initial temperature fields that are non-negative and therefore on trajectories of interest when trying to maximize $\overline{\langle wT \rangle}$.

By choosing a restricted space $\mathbb{A} = \mathcal{U}_i \times \mathcal{T}_j^+$ in (2.2.8) we can enforce the minimum principle Lemma 2.3.1 when solving the optimisation problem to bound $\overline{\langle wT \rangle}$. To actually solve the optimization problem (2.2.8) with this restricted choice of $\mathbb{A}$, it will be useful to introduce the notion of a positive linear functional. A functional $\mathcal{B} : \mathcal{T}_j \to \mathbb{R}$ is said to be *positive* if $\mathcal{B}\{T\} \geq 0$ whenever $T \in \mathcal{T}_j^+$. To make use of the notion of $\mathcal{B}\{T\}$ note that if $\mathcal{B}$ is positive and the constraint

$$\mathcal{S}\{\boldsymbol{u}, T\} \geq \mathcal{B}\{T\}, \qquad \forall (\boldsymbol{u}, T) \in \mathcal{U}_i \times \mathcal{T}_j, \tag{2.3.11}$$

holds, then $\mathcal{S}\{\boldsymbol{u}, T\} \geq 0$ for any $(\boldsymbol{u}, T) \in \mathbb{A} = \mathcal{U}_i \times \mathcal{T}_j^+$. In other words, checking feasibility of (2.2.8) for such a restricted choice of $\mathbb{A}$ can be performed using a positive linear functional $\mathcal{B}$ and imposing the constraint (2.3.11).

Furthermore, (2.3.11) is less restrictive than the constraint $\mathcal{S}\{\boldsymbol{u}, T\} \geq 0$ since $\mathcal{B}$ is not necessarily positive for $T \in \mathcal{T}_j \backslash \mathcal{T}_j^+$. Consequently whenever the minimum

principle applies, we have that

$$\overline{\langle wT \rangle} \leq \inf_{\substack{\mathcal{B}\{T\} \\ U,\alpha,\beta,\tau(z)}} \{U \,|\, \mathcal{S}\{\boldsymbol{u},T\} \geq \mathcal{B}\{T\},\ \forall (\boldsymbol{u},T) \in \mathcal{U}_i \times \mathcal{T}_j\} \tag{2.3.12}$$

$$\leq \inf_{U,\alpha,\beta,\tau(z)} \{U \,|\, \mathcal{S}\{\boldsymbol{u},T\} \geq 0,\ \forall (\boldsymbol{u},T) \in \mathcal{U}_i \times \mathcal{T}_j\}. \tag{2.3.13}$$

Enforcing (2.3.12) in principle improves the bound that can be placed on $\overline{\langle wT \rangle}$.

The following result gives a convenient form of a positive functional $\mathcal{B}$ sufficient to prove the results in Table 1.2, the proof of which is given in appendix A. A more technical argument can be used to demonstrate that we need not take any other $\mathcal{B}$ to demonstrate the desired results, based on a convex duality argument [3].

Lemma 2.3.2. *Let $\lambda : (0,1) \to \mathbb{R}$ be a square-integrable function. The bounded linear functional $\mathcal{B} : \mathcal{T}_j \to \mathbb{R}$ for $j \in \{1,2\}$ given by*

$$\mathcal{B}\{T\} = -\langle \lambda(z) \partial_z T \rangle - \lambda(0) \langle T|_{z=0} \rangle_h, \tag{2.3.14}$$

is positive if and only if $\lambda(z)$ is nondecreasing.

If λ were differentiable, one could integrate the right hand side of (2.3.14) by parts to obtain

$$\mathcal{B}\{T\} = \langle \lambda'(z) T \rangle \ , \tag{2.3.15}$$

which is positive for any $T \in \mathcal{T}_j^+$ and any nondecreasing λ. Consequently, λ' can be viewed as a standard Lagrange multiplier for the condition $T(\boldsymbol{x}) \geq 0$. Working with (2.3.14) simply removes the differentiability requirement from λ. In this thesis we will often refer to λ as the Lagrange multiplier enforcing positivity.

Given Lemma 2.3.2 the optimisation problem exploiting the non-negativity of temperature fields can be rewritten by substituting (2.3.14) into (2.3.12) to obtain

$$\overline{\langle wT\rangle} \leq \inf_{U,\tau(z),\lambda(z),\alpha,\beta} \Big\{ U \mid \mathcal{S}\{\boldsymbol{u},T\} + \langle \lambda(z)\partial_z T\rangle + \lambda(0)\langle T|_{z=0}\rangle_h \geq 0 \\ \forall\, (\boldsymbol{u},T) \in \mathcal{U}_i \times \mathcal{T}_j \Big\}. \quad (2.3.16)$$

The optimisation problem to be solved will be (2.3.16), in all instances where the upper boundary is isothermal. In this case the functional $\mathcal{S}\{\boldsymbol{u},T\}+\langle\lambda(z)\partial_z T\rangle+\lambda(0)\langle T|_{z=0}\rangle_h$ after rearranging becomes

$$\Big\langle \frac{\alpha}{R}|\nabla \boldsymbol{u}|^2 + \beta|\nabla T|^2 - (\alpha - \tau'(z))wT \Big\rangle \\ + \langle(\beta z - \tau'(z) + \lambda(z))\partial_z T + \tau(z)\rangle + U - \frac{1}{2} + (\lambda(0)+1)\langle T|_{z=0}\rangle_h. \quad (2.3.17)$$

This thesis is concerned with solving optimisation problems for bounding $\overline{\langle wT\rangle}$ with numerical techniques to guide mathematical proofs. This task can be simplified by exploiting the horizontal periodicity of $\boldsymbol{u}$ and T. We next demonstrate how periodicity can be used to obtain explicit expressions for the upper bounds.

2.4 Explicit bound for the minimization problem

The problem (2.3.16) applies for the thermal boundary conditions of (1.2.5c) and (1.2.5d) in which the upper boundary is isothermal. We now present explicit expressions for the upper bounds on $\overline{\langle wT\rangle}$ with respect to β, $\tau(z)$ and $\lambda(z)$. It will be demonstrated that without making a choice of background profile, α does not appear in the explicit expression of the upper bound. The two different expressions in the proposition below are for $T \in \mathcal{T}_1$ and $T \in \mathcal{T}_2$ respectively.

Proposition 2.4.1. *(i) (Isothermal boundary conditions) Suppose that* $(\alpha, \beta, \varphi(z))$ *satisfy the spectral constraint of definition 2.3.1, with* $\mathbb{A} = \mathcal{U}_i \times \mathcal{T}_1$ *for* $i \in \{1, 2\}$*. Let* $\varphi(z) = \tau(z) + z - 1$ *where* $\tau(z)$ *has boundary conditions* (2.3.3) *and let* $\lambda : [0, 1] \to \mathbb{R}$ *be such that* $\langle \lambda \rangle = -1$*. Then*

$$\overline{\langle wT \rangle} \leq \frac{1}{2} + \left\langle \frac{1}{4\beta} \left| \beta \left(z - \frac{1}{2} \right) - \tau'(z) + \lambda(z) \right|^2 - \tau(z) \right\rangle, \tag{2.4.1}$$

for any solution $(\boldsymbol{u}, T)$ *to* (2.1.1) *satisfying* $(\boldsymbol{u}, T) \in \mathcal{U}_i \times \mathcal{T}_1$*.*

(ii) (Insulating lower boundary) Suppose that $(\alpha, \beta, \varphi(z))$ *satisfy the spectral constraint of definition 2.3.1, with* $\mathbb{A} = \mathcal{U}_i \times \mathcal{T}_2$ *for* $i \in \{1, 2\}$*. Let* $\varphi(z) = \tau(z) + z - 1$ *where* $\tau(z)$ *has boundary conditions* (2.3.4) *and let* $\lambda : [0, 1] \to \mathbb{R}$ *be such that* $\lambda(0) = -1$*. Then*

$$\overline{\langle wT \rangle} \leq \frac{1}{2} + \left\langle \frac{1}{4\beta} \left| \beta z - \tau'(z) + \lambda(z) \right|^2 - \tau(z) \right\rangle, \tag{2.4.2}$$

for any solution $(\boldsymbol{u}, T)$ *to* (2.1.1) *satisfying* $(\boldsymbol{u}, T) \in \mathcal{U}_i \times \mathcal{T}_2$*.*

Proof. The proposition will be proven by appealing to the optimization problem (2.3.16) and, in particular, making use of the horizontal periodicity of $\boldsymbol{u}$ and T to simplify it. This initial manipulation is common to the proof of parts (i) and (ii) of the proposition.

By periodicity of $\boldsymbol{u}$ and T in x and y we can take the following Fourier decomposition

$$\begin{bmatrix} T(x, y, z) \\ \boldsymbol{u}(x, y, z) \end{bmatrix} = \sum_{\boldsymbol{k}} \begin{bmatrix} \hat{T}_{\boldsymbol{k}}(z) \\ \hat{\boldsymbol{u}}_{\boldsymbol{k}}(z) \end{bmatrix} \mathrm{e}^{i(k_x x + k_y y)}. \tag{2.4.3}$$

The sum is over wavevectors $\boldsymbol{k} = (k_x, k_y)$ compatible with the horizontal periods L_x and L_y. We denote the magnitude of each wavevector by $k = \sqrt{k_x^2 + k_y^2}$. The complex-valued Fourier amplitudes satisfy the complex-conjugate relations $\hat{\boldsymbol{u}}_{-\boldsymbol{k}} = \hat{\boldsymbol{u}}_{\boldsymbol{k}}^*$ and $\hat{T}_{-\boldsymbol{k}} = \hat{T}_{\boldsymbol{k}}^*$, as well as the boundary conditions in (1.2.5c) in the case of (i) or

(1.2.5d) in the case of (ii). After inserting the Fourier expansions (2.4.3) into (2.3.17) and applying Young's inequality and using the incompressibility condition to write the horizontal Fourier amplitudes $\hat{u}_{\boldsymbol{k}}$ and $\hat{v}_{\boldsymbol{k}}$ in terms of $\hat{w}_{\boldsymbol{k}}$, the functional $\mathcal{S}\{\boldsymbol{u}, T\} + \langle\lambda(z)\partial_z T\rangle + \lambda(0)\langle T|_{z=0}\rangle_h$ can be estimated from below, remembering that $\hat{w}_0 = 0$ and dropping positive $\hat{u}_k^2$ and $\hat{v}_k^2$ for all $\boldsymbol{k}$ terms, as

$$\mathcal{S}\{\boldsymbol{u}, T\} + \langle\lambda(z)\partial_z T\rangle + \lambda(0)\langle T|_{z=0}\rangle_h \geq \mathcal{S}_0\{\hat{T}_0\} + \sum_{\boldsymbol{k}} \mathcal{S}_{\boldsymbol{k}}\{\hat{w}_{\boldsymbol{k}}, \hat{T}_{\boldsymbol{k}}\}, \tag{2.4.4}$$

where

$$\mathcal{S}_0\{\hat{T}_0\} := \left\langle \beta|\hat{T}_0'|^2 + (\beta z - \tau'(z) + \lambda(z))\hat{T}_0' + \tau(z)\right\rangle + U - \frac{1}{2} + (\lambda(0)+1)\langle T|_{z=0}\rangle_h, \tag{2.4.5}$$

and

$$\mathcal{S}_{\boldsymbol{k}}\{\hat{w}_{\boldsymbol{k}}, \hat{T}_{\boldsymbol{k}}\} := \left\langle \frac{\alpha}{R}\left(\frac{1}{k^2}\left|\hat{w}_{\boldsymbol{k}}''\right|^2 + 2\left|\hat{w}_{\boldsymbol{k}}'\right|^2 + k^2\left|\hat{w}_{\boldsymbol{k}}\right|^2\right)\right.$$
$$\left. +\beta|\hat{T}_{\boldsymbol{k}}'|^2 + \beta k^2|\hat{T}_{\boldsymbol{k}}|^2 - (\alpha - \tau'(z))\hat{w}_{\boldsymbol{k}}\hat{T}_{\boldsymbol{k}}^*\right\rangle. \tag{2.4.6}$$

For both parts of the proposition, the bound U on $\overline{\langle wT\rangle}$ is obtained by minimising over $\alpha, \beta, \tau(z)$ and $\lambda(z)$ under the constraint that the left hand side of (2.4.4) is non-negative. The lower bound in (2.4.4) implies that this constraint can be satisfied if we impose the stronger condition that the two terms on the right hand side of (2.4.4) are individually non-negative. For both parts (i) and (ii) the assumption that the spectral constraint (2.3.1) is satisfied implies that $\mathcal{S}_k \geq 0$ for any $\boldsymbol{k} \neq 0$. Checking constraint feasibility and identifying the optimal U is then reduced to considering whether $\mathcal{S}_0 \geq 0$. We now consider parts (i) and (ii) separately.

Proof of (i): In the case of the isothermal boundary conditions (1.2.5c) where $\hat{T}_0(0) = 0$ which implies that

$$\mathcal{S}_0\{\hat{T}_0\} := \left\langle \beta|\hat{T}_0'|^2 + (\beta z - \tau'(z) + \lambda(z))\hat{T}_0' + \tau(z)\right\rangle + U - \frac{1}{2}. \tag{2.4.7}$$

The smallest U for which $\mathcal{S}_0$ is nonnegative for any admissible $\hat{T}_0$ is therefore

$$U = \frac{1}{2} + \sup_{\substack{\hat{T}_0(1)=0,\\ \hat{T}_0(0)=0}} \left\{ -\left\langle \beta|\hat{T}_0'|^2 + (\beta z - \tau'(z) + \lambda(z))\hat{T}_0' + \tau(z) \right\rangle \right\}. \tag{2.4.8}$$

The optimising temperature field in (2.4.8) can be found by solving the Euler-Lagrange equations for $\hat{T}_0$ subject to the boundary conditions on $\tau(z)$ in (2.3.3), $\hat{T}_0(0) = \hat{T}_0(1) = 0$ and using the assumption $\langle\lambda\rangle = -1$ gives

$$\hat{T}_0'(z) = \frac{\tau'(z) - \lambda(z)}{2\beta} - \frac{z}{2} + \frac{1}{4}. \tag{2.4.9}$$

Substituting (2.4.9) into (2.4.8) and rearranging gives the desired bound on $\overline{\langle wT\rangle}$.

Proof of (ii): By assumption that $\lambda(0) = -1$ the expression (2.4.5) is given by (2.4.7) even in the case where the lower boundary is insulating. In this case the smallest U for which $\mathcal{S}_0$ is nonnegative for any admissible $\hat{T}_0$ is therefore

$$U = \frac{1}{2} + \sup_{\substack{\hat{T}_0(1)=0,\\ \hat{T}_0'(0)=0}} \left\{ -\left\langle \beta|\hat{T}_0'|^2 + (\beta z - \tau'(z) + \lambda(z))\hat{T}_0' + \tau(z) \right\rangle \right\}. \tag{2.4.10}$$

The optimising temperature field in (2.4.8) can be found by solving the Euler-Lagrange equations with the boundary conditions on $\tau(z)$ (2.3.4) and $\hat{T}_0'(0) = \hat{T}_0(1) = 0$, to obtain

$$\hat{T}_0'(z) = \frac{\tau'(z) - \lambda(z)}{2\beta} - \frac{z}{2}. \tag{2.4.11}$$

Substituting (2.4.11) into (2.4.10) and rearranging gives the desired bound on $\overline{\langle wT\rangle}$.

□

Remark 2.4.1. Velocity and temperature fields with a single nonzero Fourier mode are admissible in the optimization problem (2.2.8), so the right-hand side of (2.4.4) is nonnegative if and only if each term is nonnegative. Moreover, the real and imaginary parts of the Fourier amplitudes $\hat{w}_{\boldsymbol{k}}$ and $\hat{T}_{\boldsymbol{k}}$ give identical and independent

contributions to $\mathcal{S}_{\boldsymbol{k}}$, meaning that we may assume them to be real without loss of generality.

Remark 2.4.2. We may replace the minimization problem in (2.3.16) with

$$\begin{aligned} \inf_{U,\tau(z),\lambda(z),\alpha,\beta} \quad & U \\ \text{subject to} \quad & \mathcal{S}_0\{\hat{T}_0\} \geq 0 \qquad \forall \hat{T}_0 \in \mathcal{T}_j, \quad j \in \{1,2\}, \\ & \mathcal{S}_{\boldsymbol{k}}\{\hat{w}_{\boldsymbol{k}}, \hat{T}_{\boldsymbol{k}}\} \geq 0 \quad \forall (\hat{w}_{\boldsymbol{k}}, \hat{T}_{\boldsymbol{k}}) \in \mathbb{A}, \quad \forall \boldsymbol{k} \neq 0. \end{aligned} \tag{2.4.12}$$

Any choice of U, $\tau(z)$, $\lambda(z)$, α and β satisfying the constraints yields a rigorous upper bound on the mean vertical convective heat flux $\overline{\langle wT \rangle}$.

Remark 2.4.3. If as an initial attempt, an upper bound is sought without utilising the minimum principle, the optimisation problem is given by (2.3.13). The problem (2.3.12) can be relaxed to (2.3.13) with the choice $\lambda = -1$ throughout the domain.

Remark 2.4.4. For $T \in \mathcal{T}_1$, the uniform upper bound $\overline{\langle wT \rangle} \leq \frac{1}{2}$ can be recovered within our approach by taking $\alpha = 0$, $\tau = 0$, $\varphi = z - 1$ and letting $\beta \to 0$. The auxiliary functional in (2.2.5) becomes

$$\mathcal{V}\{\boldsymbol{u}, T\} = \langle (1-z)T \rangle \,, \tag{2.4.13}$$

which corresponds to the flow's potential energy measured with respect to the upper boundary. Whereas for $T \in \mathcal{T}_2$ even when using (2.4.13) the uniform upper bound requires the use of the minimum principle.

2.5 Discussion

The final section of this chapter is dedicated to a discussion on the application of the background method presented. A number of the steps taken in constructing an optimisation problem to bound $\overline{\langle wT \rangle}$ could have been generalised. The reasons why such generalisations were not used will be explained, in addition to means of

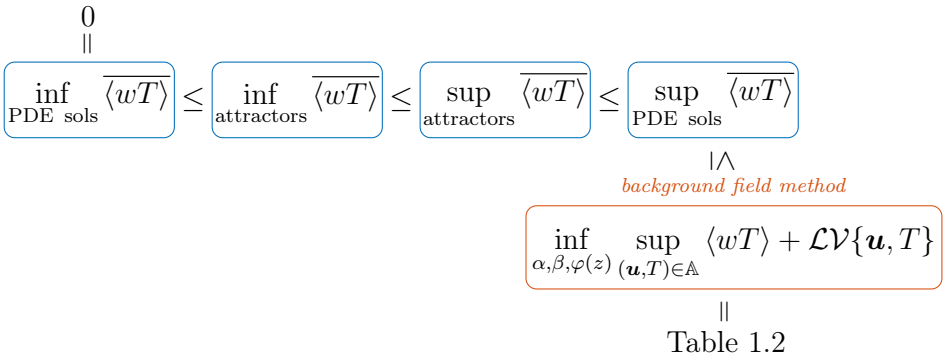

Figure 2.1: Illustrative diagram of the hierarchy for the analysis of the asymptotic behaviour of $\overline{\langle wT\rangle}$ in IH convection. The leftmost blue rectangle is the minimum over all solutions to (2.1.1). This is bounded from above by the min. and then max. over the attractors of (2.1.1) in the turbulent state. Both of which are bounded from above by the maximum over all possible solutions to (2.1.1). The final inequality, in a red rectangle, is the relaxation to the background field method, where one minimises over optimsiation parameters and maximises over $(\boldsymbol{u},T)\in\mathbb{A}$ where $\mathcal{LV}$ is the Lie derivative of the functional $\mathcal{V}$ in (2.2.5) over (2.1.1).

supplementing the analysis for variations of the problem of uniform internally heated convection.

In the context of proving upper bounds, Figure 2.1 shows the hierarchy of bounds for $\overline{\langle wT\rangle}$ and where the background method lies in these ideas. Furthest left in the figure is the minimisation of $\overline{\langle wT\rangle}$ over all solutions, which is zero since this is equal to the value achieved by the steady conductive solution. This is bounded from above by the minimum then maximum over the attractor/s of (2.1.1) in the turbulent state. All of which is bounded from above by the maximum over all solutions to (2.1.1). The final blue rectangle is a difficult problem to solve and can be simplified by expanding the maximisation to be over divergence free velocity fields, satisfying an energy relation and (2.1.1c). This is the *optimal wall-to-wall transport method*. However the relaxation we make from the final blue rectangle is the background field method as outlined in this chapter. The optimisation is a minmax problem over tunable balance parameters and background fields and for an appropriately defined set $\mathbb{A}$ for the velocity and temperature field. However, there are particular choices in the background method approach outlined in the previous sections which we now discuss.

The first possible generalisation is in the quadratic functional (2.2.5). One could imagine replacing the $|\boldsymbol{u}|^2$ with a more general term of the form $|\boldsymbol{u}-\boldsymbol{\psi}(\boldsymbol{x})|^2$, where $\boldsymbol{\psi}$ can be viewed as background velocity field. To understand why we do not use such a field $\boldsymbol{\psi}$ in our analysis we can observe that the Boussinesq equations (2.1.1) are invariant under horizontal translations and under the "flow reversal" operation

$$\begin{pmatrix} \boldsymbol{u}(\mathbf{x},t) \\ T(\mathbf{x},t) \\ p(\mathbf{x},t) \end{pmatrix} \mapsto \begin{pmatrix} G\boldsymbol{u}(G\boldsymbol{x},t) \\ T(G\boldsymbol{x},t) \\ p(G\boldsymbol{x},t) \end{pmatrix}, \qquad G = \begin{pmatrix} -1 & 0 & 0 \\ 0 & -1 & 0 \\ 0 & 0 & 1 \end{pmatrix}. \tag{2.5.1}$$

Any bound which can be proven with a given $\mathcal{V}$ can also be proven with a $\mathcal{V}$ that is invariant under G. For (2.2.5) to be invariant under horizontal translations the background fields $\boldsymbol{\psi}$ and φ must depend only on the vertical coordinate z. Since $\boldsymbol{\psi}$ must be incompressible we have $\boldsymbol{\psi} = (\psi_1(z), \psi_2(z), 0)$. Invariance under the transformation in (2.5.1) requires $\boldsymbol{\psi}(\boldsymbol{x}) = G\boldsymbol{\psi}(G\boldsymbol{x})$, i.e., $\psi_1(z) = -\psi_1(z)$ and $\psi_2(z) = -\psi_2(z)$. This can be true only if $\boldsymbol{\psi} = 0$, demonstrating that the generalized background velocity field may be taken to vanish identically.

Secondly, within the quadratic auxiliary functional (2.2.5) there is no wT term. It is known that when applying the background method to double-diffusive convection, a cross term is necessary to prove any bound at all [4]. Consequently, it is natural to ask if a wT term in (2.2.5) could also assist and improve the bounds we are able to prove in this thesis. It can be demonstrated that for Rayleigh–Bénard convection a cross-term does not help when trying to bound the mean vertical convective heat flux with the background field method [41]. If instead a poloidal and toroidal decomposition is carried out for Rayleigh–Bénard convection then bounds can be proven while enforcing additional constraints on the admissible flow states for a different flow quantity to the Nusselt number [141].

In chapter 5 and chapter 6 bounds on $\overline{\langle wT \rangle}$ are proven with a background method that is augmented with additional information. While the two class of problems addressed in those chapters constitute different flows, of infinite Prandtl number convection and free-slip convection in two or three-dimensions, it is nevertheless interesting that additional information is incorporated into the method. In the case of infinite Prandtl number convection, the functional (2.2.5) is changed to reflect the new governing equations and a pointwise relation between the velocity and temperature are utilised to prove qualitatively different bounds on $\overline{\langle wT \rangle}$ for all R. In the case of free-slip boundaries, the functional in (2.2.5) is altered and the background method utilises information available in the vorticity equation for two dimensions, or in a pseudo-vorticity in three dimensions.

One final comment is that for Rayleigh–Bénard convection, the balance parameters α and β can be taken to be independent of the Rayleigh and Prandtl numbers without worsening the dependence on the Rayleigh number of the bound on the convective heat transport. One major difference when bounding $\overline{\langle wT \rangle}$ for internally heated convection is that, as we shall demonstrate in this thesis, careful choices of R-dependent balance parameters can lead to bounds with a better asymptotic behaviour for large R.

Chapter 3

Perfectly conducting boundaries

Begin with the simplest examples.
The art of doing mathematics consists in finding that special case which contains all the germs of generality.

David Hilbert

To investigate heat transport due solely to convection driven by internal heating, the natural boundary conditions to take are that of isothermal boundaries held at the same temperature. Without loss of generality we choose the boundary temperature to be zero. All the results in §3.2 and §3.3.1 appear in publication [2], whereas §3.3.2 appears in [89]. The physical correspondence of this boundary condition is to perfect thermal conductors. Heat generated within the domain drives convection which determines the heat loss out of the top and bottom boundaries. As discussed in the introduction, in this boundary configuration $\overline{\langle wT \rangle}$ is a measure of the vertical asymmetry of heat transport due to convection and is related to the heat fluxes through the top and bottom by the exact relations

$$\mathcal{F}_T = \frac{1}{2} + \overline{\langle wT \rangle}, \qquad \mathcal{F}_B = \frac{1}{2} - \overline{\langle wT \rangle}. \tag{3.0.1}$$

A Nusselt-like quantity can be defined in this configuration by considering the qualitative behaviour of the mean temperature $\overline{\langle T \rangle}$. The average outward conduction

above and below the plane over which $\overline{\langle T\rangle_h}$ is maximised is equal to $2\overline{\langle T\rangle_h}$ [62]. If one assumes that at high R the temperature field is well mixed, then $\overline{\langle T\rangle}$ scales in the same way as the maximum of $\overline{\langle T\rangle_h}$. The ratio of the total (predominantly convective) heat flux to the conductive heat flux is therefore $1/(2\overline{\langle T\rangle_h}) \sim 1/\overline{\langle T\rangle}$. It is for this reason that all prior analysis was carried out on $\overline{\langle T\rangle}$. As there is no *a priori* relation between $\overline{\langle T\rangle}$ and $\overline{\langle wT\rangle}$, upper bounds on $\overline{\langle wT\rangle}$ were not known prior to this thesis.

In this chapter we first setup up the problem in §3.1, before demonstrating numerically the optimal bounds for the $\overline{\langle wT\rangle}$ initially without and then with a minimum principle enforced §3.2 and §3.3 respectively. In each subsection inspired by the numerical results we prove two theorems.

3.1 Setup

The kinematic and thermal boundary conditions considered in this chapter are

$$\boldsymbol{u}|_{z=\{0,1\}} = 0, \tag{3.1.1a}$$

$$T|_{z=\{0,1\}} = 0, \tag{3.1.1b}$$

where $u \in \mathcal{U}_1$ and $T \in \mathcal{T}_1$ as defined in (2.1.2).

For any value of R and Pr, the Boussinesq equations for uniform internally heated convection (1.2.3a–c) admit the steady solution, $\boldsymbol{u} = \boldsymbol{0}$, $T = \frac{1}{2}z(1-z)$, which represents a purely conductive state. This solution is attracting for any values of the horizontal periods L_x and L_y when $R < 26\,926$ [58] and is linearly unstable when R is larger than a critical threshold $R_L \approx 37\,325$ [25], the exact value of which depends on the horizontal periods. Sustained convection ensues in this regime, but has also been observed at subcritical Rayleigh numbers [147]. Our goal is to characterize the mean vertical convective heat flux through the layer, $\overline{\langle wT\rangle}$, as a function of R. We prove the following two theorems.

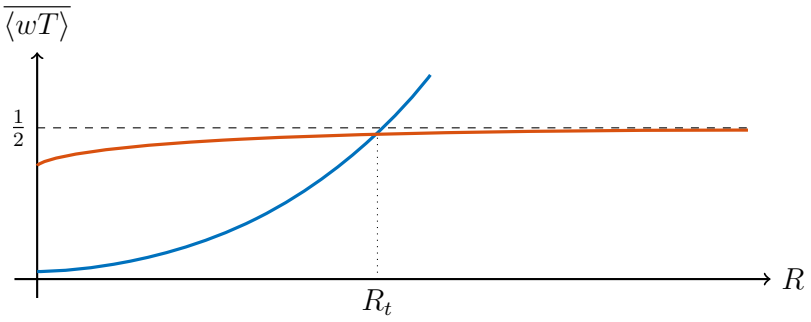

Figure 3.1: Representative plots of the three analytical upper bounds on $\overline{\langle wT \rangle}$, first the uniform in R upper bound of $\frac{1}{2}$ (---), then the bound proven in Theorem 3.1.1 (—) and finally the bound proven in Theorem 3.1.2 (—). R_t denotes the Rayleigh number above which Theorem 3.1.2 becomes the best provable upper bound on $\overline{\langle wT \rangle}$

Theorem 3.1.1 (Isothermal)**.** *Suppose that* $\boldsymbol{u}$ *and* T *solve* (1.2.3) *subject to the no-slip isothermal boundary conditions in* (3.1.1)*. For all sufficiently large* $R > 0$

$$\overline{\langle wT \rangle} \leq cR^{\frac{1}{5}}. \tag{3.1.2}$$

Remark 3.1.1. It is shown in §3.2.2 that the theorem holds with $c = 2^{-4}$.

Upper bounds on $\overline{\langle wT \rangle}$ imply bounds on the heat flux out of the top and bottom boundaries.

Corollary 3.1.1. *For all sufficiently large* R

$$\mathcal{F}_T \leq \frac{1}{2} + cR^{\frac{1}{5}} \quad \textit{and} \quad \mathcal{F}_B \geq \frac{1}{2} - cR^{\frac{1}{5}}. \tag{3.1.3}$$

The bound in Theorem 3.1.1 is derived without the minimum principle (Lemma 2.3.1). Enforcing this additional information leads to an improved bound at large R values, which asymptotes to $\frac{1}{2}$ from below. Figure 3.1 shows representative plots of the three bounds, the horizontal dashed line denoting the previously known uniform in R upper bound, while the two curves show the upper bounds proven in this chapter. There is a R_t above which for all R, the bound enforcing the minimum principle is the best available result. More precisely, in §3.3.2 we prove the following theorem.

Theorem 3.1.2 (Isothermal enforcing $T \geq 0$)**.** *Suppose that* $\boldsymbol{u}$ *and* T *solve* (1.2.3) *subject to the boundary conditions* (3.1.1)*. There exist constants* $c_1, c_2 > 0$ *such that for all sufficiently large* $R > 0$*,*

$$\overline{\langle wT \rangle} \leq \frac{1}{2} - c_1 R^{\frac{1}{5}} \exp\left(-c_2 R^{\frac{3}{5}}\right). \tag{3.1.4}$$

Remark 3.1.2. It is shown in §3.3.2 that the theorem holds with $c_1 = 2^{-3}3^{\frac{7}{5}}$ and $c_2 = 2^{-2}3^{\frac{11}{5}}$ for any $R > 4$.

Corollary 3.1.2. *For all sufficiently large* R*,*

$$\mathcal{F}_T \leq 1 - c_1 R^{\frac{1}{5}} \exp\left(-c_2 R^{\frac{3}{5}}\right) \quad \textit{and} \quad \mathcal{F}_B \geq c_2 R^{\frac{1}{5}} \exp\left(-c_2 R^{\frac{3}{5}}\right). \tag{3.1.5}$$

3.2 Optimal bounds at low R

Initially we ignore the minimum principle for the temperature field, so the analysis can be seen as a "classical" application of the background method. In §3.3, instead, we improve the analysis by taking the minimum principle into account through a Lagrange multiplier.

In this section we take $\lambda = -1$ in (2.4.1). For the case of equal and isothermal boundaries, the upper bound on $\overline{\langle wT \rangle}$ follows from solving (2.3.16) with $\lambda = -1$. The expression for $\mathcal{S}\{\boldsymbol{u}, T\}$ becomes

$$\mathcal{S}\{\boldsymbol{u}, T\} = \left\langle \frac{\alpha}{R}|\nabla \boldsymbol{u}|^2 + \beta|\nabla T|^2 - (\alpha - \tau'(z))wT + (\beta z - \tau'(z) - 1)\partial_z T + \tau(z) \right\rangle + U - \frac{1}{2}. \tag{3.2.1}$$

The best upper bound U on $\overline{\langle wT \rangle}$ that can be proven with the approach described in chapter 2 is

$$\overline{\langle wT \rangle} \leq \inf_{U,\tau(z),\alpha,\beta} \{U : \mathcal{S}\{\boldsymbol{u}, T\} \geq 0 \; \forall (\boldsymbol{u}, T) \in \mathbb{A}\}, \tag{3.2.2}$$

where $\mathbb{A} = \mathcal{U}_1 \times \mathcal{T}_1$. The right-hand side of (3.2.2) is a linear optimisation problem because the optimisation variables, U, $\tau(z)$, α and β, enter the constraint $\mathcal{S}\{\boldsymbol{u}, T\} \geq 0$ and the cost U linearly. If the spectral constraint from definition 2.3.1 is satisfied for the boundary conditions of (3.1.1), then it is possible to bound $\overline{\langle wT \rangle}$ from above in terms of the optimisation parameters.

Finally, the explicit expression for the bound on $\overline{\langle wT \rangle}$ from (2.4.1), becomes

$$\overline{\langle wT \rangle} \leq U(\alpha, \beta, \tau) := \frac{1}{2} + \left\langle \frac{1}{4\beta} \left| \beta(z - \tfrac{1}{2}) - \tau'(z) - 1 \right|^2 - \tau(z) \right\rangle. \tag{3.2.3}$$

The proof of the explicit upper bounds on $\overline{\langle wT \rangle}$ from (2.4.1) passes the variables $(\boldsymbol{u}, T)$ into Fourier space where by incompressibility the boundary conditions are

$$\hat{w}_{\boldsymbol{k}}(0) = \hat{w}'_{\boldsymbol{k}}(0) = \hat{w}_{\boldsymbol{k}}(1) = \hat{w}'_{\boldsymbol{k}}(1) = 0, \tag{3.2.4a}$$

$$\hat{T}_{\boldsymbol{k}}(0) = \hat{T}_{\boldsymbol{k}}(1) = 0. \tag{3.2.4b}$$

For computational ease and to prove the bounds on $\overline{\langle wT \rangle}$ in §3.2.2 & §3.3.2 we utilise a stronger version of the spectral constraint $\mathcal{S}_{\boldsymbol{k}} \geq 0$ where $\mathcal{S}_{\boldsymbol{k}}$ is given in (2.4.6) (with a comparison presented in appendix D). Given the boundary conditions on $\hat{w}_{\boldsymbol{k}}$ (3.2.4), we have the interpolation inequality

$$\left\langle \frac{|\hat{w}''_{\boldsymbol{k}}|^2}{k^2} + k^2 |\hat{w}_{\boldsymbol{k}}|^2 \right\rangle \geq \left\langle 2|\hat{w}'_{\boldsymbol{k}}|^2 \right\rangle. \tag{3.2.5}$$

By use of (3.2.5) we can estimate (2.4.6) from below. This implies that for all $\hat{w}, \hat{T}$ subject to (3.2.4)

$$\mathcal{S}_{\boldsymbol{k}} \geq \tilde{\mathcal{S}}\{\hat{w}, \hat{T}\} := \left\langle \frac{4\alpha}{R} |\hat{w}'|^2 + \beta |\hat{T}'|^2 - (\alpha - \tau'(z))\hat{w}\hat{T} \right\rangle , \tag{3.2.6}$$

then the constraint $\tilde{\mathcal{S}} \geq 0$ is sufficient to enforce $\mathcal{S}_{\boldsymbol{k}} \geq 0$. Since this condition is independent of k we drop the subscript to ease notation for the rest of this chapter.

The optimisation problem for the bound on $\overline{\langle wT \rangle}$ can then be stated as,

$$\begin{aligned} \inf_{U,\tau(z),\alpha,\beta} \quad & U \\ \text{subject to} \quad & \mathcal{S}_0\{\hat{T}_0\} \geq 0 \quad \forall \hat{T}_0 : (3.2.4\text{b}), \\ & \tilde{\mathcal{S}}\{\hat{w}, \hat{T}\} \geq 0 \quad \forall \hat{w}, \hat{T} : (3.2.4a,b). \end{aligned} \tag{3.2.7}$$

While the estimate $\mathcal{S}_{\boldsymbol{k}} \geq \tilde{\mathcal{S}}$ simplifies analysis and computations, it worsens the optimal bound on $\overline{\langle wT \rangle}$ that can be proved. However, this worsening is only quantitative, while the scaling with R remains unchanged. Also, considering the simplified spectral constraint $\tilde{\mathcal{S}} \geq 0$ allows for significant computational savings when optimizing bounds numerically, because it removes the need to consider a large set of wavenumbers and improves the implementation of simple piecewise-linear basis functions (appendix C). This allows for discretization of (3.2.7) and its generalization (3.3.3) derived in §3.3 below on very fine meshes, which is essential to resolve sharp boundary layers in τ accurately.

3.2.1 Numerically optimal bounds

The best upper bounds on $\overline{\langle wT \rangle}$ implied by problem (3.2.7) can be approximated numerically at any fixed Rayleigh number either by deriving and solving the corresponding nonlinear Euler–Lagrange equations [120, 158, 159], or by discretising it into a semidefinite programme (SDP) [44, 46, 47, 140, 141]. Here, we choose the

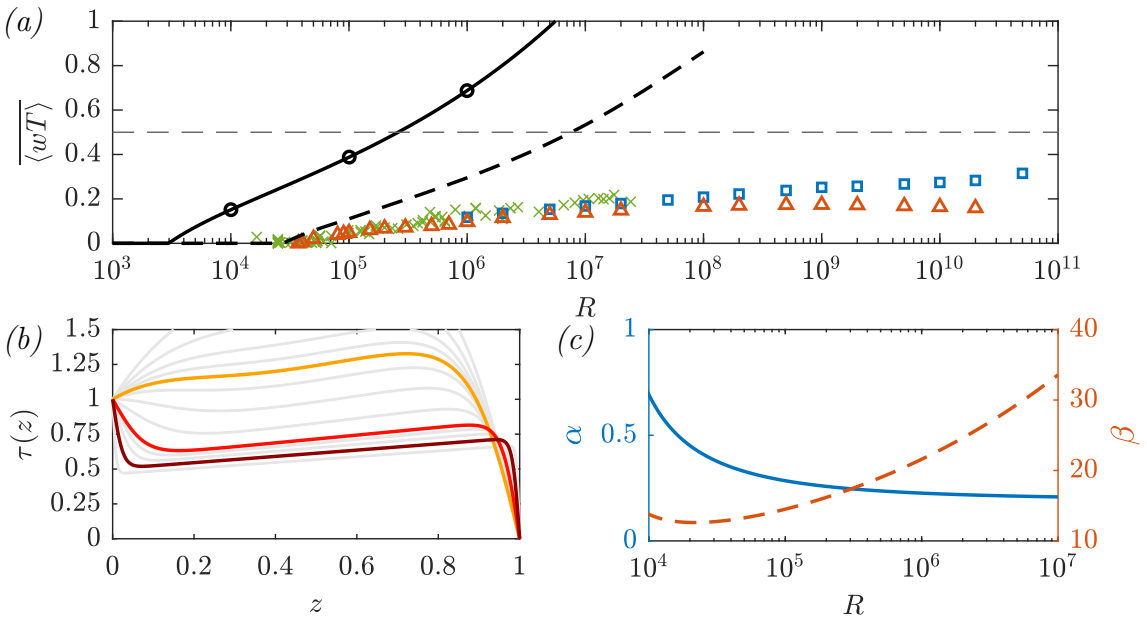

Figure 3.2: *(a)* Optimal bounds on $\overline{\langle wT \rangle}$ obtained by solving the wavenumber-dependent problem (2.4.12) with horizontal periods $L_x = L_y = 2$ (- - -) and the simplified problem (3.2.7) (—). Also plotted are experiments by [85] (×), 2D DNSs by [62] (△) and 3D DNSs by [63] (■). Circles mark values of R at which optimal profiles $\tau(z)$ are plotted in panel *(b)*. The dashed horizontal line (- - -) is the uniform bound $\overline{\langle wT \rangle} \leq 1/2$. *(b)* Optimal profiles $\tau(z)$ at $R = 10^4$ (—), 10^5 (—) and 10^6 (—). *(c)* Optimal balance parameters α (—, left axis) and β (- - -, right axis) as a function of R.

latter approach because it preserves the linearity of (3.2.7); details of our numerical implementation are summarised in Appendix C. Numerically optimal solutions to (3.2.7) for $10^3 \leq R \leq 10^7$ are presented in §3.2.1, while suboptimal but analytical bounds are proved in §3.2.2.

Figure 3.2 compares the numerically optimal upper bounds U on the mean vertical heat transfer $\overline{\langle wT \rangle}$ to experimental [85] and DNS data [62, 63]. The bounds were calculated by solving the minimization problem (3.2.7) for a fluid layer with horizontal periods $L_x = L_y = 2$, and with the simplified problem (3.2.7), which is independent of wavevectors and, therefore, of L_x and L_y. As expected, the bounds obtained with (2.4.12) are zero when the Rayleigh number is smaller than the energy stability limit $R_E \approx 29\,723$, which differs slightly from the value 26 927 [58] due to our choice of horizontal periods. They then increase monotonically with R, showing the same qualitative behaviour as the bounds computed with the simplified problem (3.2.7),

which reach the value of $\frac{1}{2}$ at $R = 259\,032$. Both sets of results exceed the uniform upper bound $\overline{\langle wT \rangle} \leq \frac{1}{2}$ for sufficiently large Rayleigh numbers.

Numerically optimal profiles of $\tau(z)$ for the simplified bounding problem (3.2.7) at selected Rayleigh numbers and the variation of the optimal balance parameters α and β with R are illustrated in Figures 3.2*(b)* and 3.2*(c)* respectively. As expected from the structure of the indefinite term $(a - \tau'(z))\hat{w}\hat{T}$ of the functional $\tilde{\mathcal{S}}$, the derivative τ' in the bulk of the domain approaches the value of α as R is raised and leads to the formation of two boundary layers. Moreover, the asymmetry of the boundary layers reflects qualitatively the asymmetry of the IH convection problem we are studying, which is characterized by a stable thermal stratification near the bottom boundary ($z = 0$) and an unstable one near the top ($z = 1$). However, note that while τ is related to the background temperature field, it is not a physical quantity and need not behave nor scale like the mean temperature in turbulent convection.

Other insightful observations can be made by considering the critical temperature fields $\hat{T}_0$, which minimize the functional $\mathcal{S}_0\{\hat{T}_0\}$ for the optimal choice of τ, α, β and U. These critical temperatures can be recovered upon integrating (2.4.9) with boundary conditions $\hat{T}_0 = 0$, and are plotted in Figure 3.3 for a selection of Rayleigh numbers. As one might expect, when R is sufficiently small such that $U = 0$, $\hat{T}_0 = \frac{1}{2}z(1 - z)$ coincides with the conductive temperature profile. With the onset of convection and increasing R, boundary layers form at $z = 0$ and $z = 1$ and the maximum of $|\hat{T}_0|$ decreases. The profiles are also consistent with the uniform rigorous bound $\overline{\langle T \rangle} \leq \frac{1}{12}$ [58]. However, for sufficiently high Rayleigh numbers they are evidently not related to the horizontal and infinite-time averages of the physical temperature field, because they become negative near $z = 0$. Interestingly, as shown in Figure 3.3*(d)&(e)*, this unphysical behaviour first occurs away from the boundary at $R = 256\,269$, while the numerical upper bound on $\overline{\langle wT \rangle}$ reaches the value of $\frac{1}{2}$ only at $259\,032$, when $\hat{T}_0'(0) = 0$. The latter is not surprising because the identity $\overline{T}'(0) = \frac{1}{2} - \overline{\langle T \rangle}$, derived

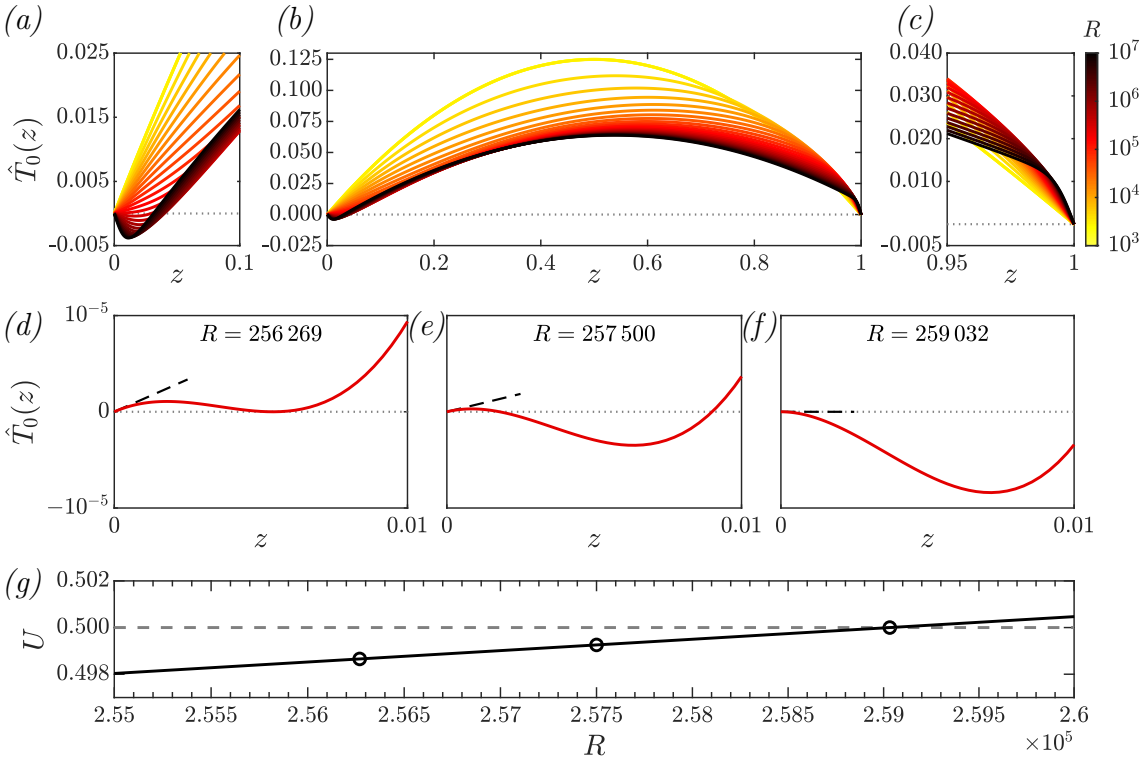

Figure 3.3: *Top*: Critical temperature $\hat{T}_0(z)$ recovered using (2.4.9). Colors indicate the Rayleigh number. Panels *(a)* and *(c)* show details of the boundary layers. *Middle*: Detailed view of $\hat{T}_0$ for $R = 256\,269$, $257\,500$, and $259\,032$. Dashed lines (- - -) are tangent to $\hat{T}_0$ at $z = 0$. In *(d)*, $\hat{T}_0$ is nonnegative and has minimum of zero inside the layer. In *(e)*, $\hat{T}_0$ is initially positive but has a negative minimum. In *(f)*, $\hat{T}_0'(0) = 0$ and there is no positive initial layer. *Bottom*: Upper bounds U on $\overline{\langle wT \rangle}$. Circles mark the values of Ra considered in *(d–f)* and $U = 1/2$ at $R = 259\,032$.

from (3.0.1) upon recognizing that $\mathcal{F}_B = \overline{T}'(0)$, implies that an upper bound of $\frac{1}{2}$ on $\overline{\langle wT \rangle}$ is equivalent to a zero lower bound on $\overline{T}'(0)$, which is obtained when $\hat{T}_0'(0)$ vanishes. It is therefore clear that the bounding problems (2.4.12) and (3.2.7) fail to improve the uniform bound $\overline{\langle wT \rangle} \leq \frac{1}{2}$ [62] at large R due to a violation of the minimum principle for the temperature, which was not taken into account when formulating them.

3.2.2 Analytical bound

The numerical results in the previous section demonstrate that optimising $\tau(z)$, α and β cannot improve the uniform bound $\overline{\langle wT \rangle} \leq \frac{1}{2}$ at arbitrarily large R. Nevertheless, it is possible to derive better bounds analytically over a finite range of Rayleigh numbers by considering piecewise-linear profiles $\tau(z)$ with two boundary layers, such as the one sketched in Figure 3.4. Even though the numerically optimal profiles in Figure 3.2 show no symmetry with respect to the vertical midpoint $z = \frac{1}{2}$, we impose anti-symmetry and take

$$\tau(z) = \begin{cases} 1 - \left(\dfrac{\alpha + 1}{2\delta} - \alpha \right) z, & 0 \leq z \leq \delta \\ \alpha z + \dfrac{1}{2}(1 - \alpha), & \delta \leq z \leq 1 - \delta \\ \left(\dfrac{\alpha + 1}{2\delta} - \alpha \right) (1 - z), & 1 - \delta \leq z \leq 1, \end{cases} \tag{3.2.8}$$

where δ is a boundary layer width to be specified later. This considerably simplifies the algebra, at the cost of a quantitatively (but not qualitatively) worse bound on $\overline{\langle wT \rangle}$. Our goal is to determine values for δ, α and β such that $\tau(z)$ satisfies the constraints in the reduced optimisation problem (3.2.7), while trying to minimise its objective function. A R dependent variation of the parameters follows from enforcing the spectral constraint.

We begin by finding a simple sufficient condition that ensures $\tilde{\mathcal{S}} \geq 0$ (3.2.6).

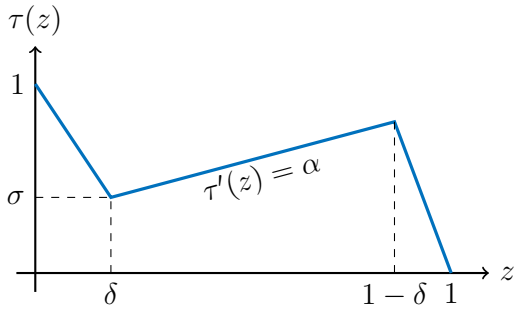

Figure 3.4: General piecewise-linear $\tau(z)$, parametrized by the boundary layer widths δ and ε, the bulk slope α and the boundary layer height σ. In our proof, we set $\varepsilon = \delta$ and $\sigma = \frac{1}{2} - \alpha\left(\frac{1}{2} - \delta\right)$ to obtain a profile that is anti-symmetric with respect to $z = 1/2$.

Lemma 3.2.1 (Sufficient condition for spectral constraint)**.** *Let $\tau(z)$ be given by* (3.2.8)*. Suppose that*

$$\delta = \frac{8\sqrt{\alpha\beta}}{(\alpha+1)\sqrt{R}}. \tag{3.2.9}$$

Then the spectral constraint $\tilde{\mathcal{S}} \geq 0$ in (3.2.6)*, is satisfied.*

Proof. Given $\tau(z)$ from (3.2.8) where $\tau'(z) = \alpha$ for $z \in (\delta, 1-\delta)$, then the sign-indefinite term in (3.2.6) is

$$\left\langle (\alpha - \tau'(z))\hat{w}_{\boldsymbol{k}}\hat{T}_{\boldsymbol{k}} \right\rangle = \int_{[0,\delta]\cup[1-\delta]} (\alpha - \tau'(z))\hat{w}_{\boldsymbol{k}}\hat{T}_{\boldsymbol{k}}\,\mathrm{d}z. \tag{3.2.10}$$

To estimate the integral over $[0, \delta]$, we apply the fundamental theorem of calculus, the boundary conditions (3.2.4) and the Cauchy–Schwarz inequality to obtain the estimates

$$\hat{w}_{\boldsymbol{k}}(z) = \int_0^z \hat{w}'_{\boldsymbol{k}}(\xi)\,\mathrm{d}\xi \leq \sqrt{z}\,\|\hat{w}'_{\boldsymbol{k}}\|_2, \tag{3.2.11a}$$

$$\hat{T}_{\boldsymbol{k}}(z) \leq \sqrt{z}\,\|\hat{T}'_{\boldsymbol{k}}\|_2. \tag{3.2.11b}$$

Due to the choice of $\tau(z)$, $\alpha - \tau'$ is the same in both boundary layers and estimates analogous to (3.2.11) hold at the upper boundary where $1 - z$ replaces z. We pick

up a factor of 2 and using the estimates (3.2.11), the sign-indefinite term becomes

$$\begin{aligned} 2\int_0^\delta (\alpha-\tau'(z))|\hat{w}_{\boldsymbol{k}}\hat{T}_{\boldsymbol{k}}|\mathrm{d}z &\leq 2\|\alpha-\tau'(z)\|_{L^\infty(0,\delta)}\int_0^\delta |\hat{w}_{\boldsymbol{k}}|\,|\hat{T}_{\boldsymbol{k}}|\,\mathrm{d}z \\ &\leq 2\|\alpha-\tau'(z)\|_{L^\infty(0,\delta)}\int_0^\delta z\,\mathrm{d}z\|\hat{w}'_{\boldsymbol{k}}\|_2\|\hat{T}'_{\boldsymbol{k}}\|_2 \\ &= \delta^2\|\alpha-\tau'(z)\|_{L^\infty(0,\delta)}\|\hat{w}'_{\boldsymbol{k}}\|_2\|\hat{T}'_{\boldsymbol{k}}\|_2. \end{aligned} \tag{3.2.12}$$

Substituting this estimate into $\tilde{\mathcal{S}}$ given by (3.2.6) yields

$$\tilde{\mathcal{S}} \geq \frac{4\alpha}{R}\|\hat{w}'_{\boldsymbol{k}}\|_2^2 - \delta^2\|\alpha-\tau'(z)\|_{L^\infty(0,\delta)}\|\hat{w}'_{\boldsymbol{k}}\|_2\|\hat{T}'_{\boldsymbol{k}}\|_2 + \beta\|\hat{T}'_{\boldsymbol{k}}\|_2^2. \tag{3.2.13}$$

The right-hand side of the last inequality is a homogeneous quadratic form in the variables $\|\hat{w}'_{\boldsymbol{k}}\|_2$ and $\|\hat{T}'_{\boldsymbol{k}}\|_2$, which is nonnegative if the discriminant is nonpositive. When τ is as in (3.2.8), the condition for positivity is

$$\delta^2(\alpha+1)^2 \leq \frac{64\alpha\beta}{R}, \tag{3.2.14}$$

which holds for δ in (3.2.9). □

Proof of Theorem 3.1.1

For any choice of α, β and δ satisfying the assumptions of Lemma 3.2.1, substituting $\tau(z)$ (3.2.8) into (3.2.3), gives an explicit bound on $\overline{\langle wT\rangle}$ in terms of the parameters. We have that

$$\begin{aligned} \overline{\langle wT\rangle} &\leq \frac{1}{2} + \left\langle \frac{1}{4\beta}\left|\beta(z-\tfrac{1}{2}) - \tau'(z) - 1\right|^2 - \tau(z)\right\rangle \\ &= \frac{\beta}{48} + \frac{(\alpha+1)^2}{8\beta\delta} - \frac{(\alpha+1)^2}{4\beta}. \end{aligned} \tag{3.2.15}$$

Setting δ according as (3.2.9), gives

$$\overline{\langle wT \rangle} = \frac{\beta}{48} + \frac{(\alpha+1)^3\sqrt{R}}{64\sqrt{\alpha\beta^3}} - \frac{(\alpha+1)^2}{4\beta} \tag{3.2.16}$$

$$\leq \frac{\beta}{48} + \frac{(\alpha+1)^3\sqrt{R}}{64\sqrt{\alpha\beta^3}}. \tag{3.2.17}$$

The values of α and β minimising the right-hand side of (3.2.17) solve

$$\frac{\sqrt{R}}{128\sqrt{\alpha^3\beta^3}}(\alpha+1)^2(5\alpha-1) = 0, \tag{3.2.18a}$$

$$1 - \frac{9(\alpha+1)^3\sqrt{R}}{8\sqrt{\alpha\beta^5}} = 0, \tag{3.2.18b}$$

and can be found explicitly as

$$\alpha = \frac{1}{5} \qquad \text{and} \qquad \beta = \frac{9}{5}R^{\frac{1}{5}}. \tag{3.2.19}$$

Substituting these values into (3.2.17) results in

$$\overline{\langle wT \rangle} \leq 2^{-4}R^{\frac{1}{5}}\,. \tag{3.2.20}$$

This proves Theorem 3.1.1.

Remark 3.2.1. The bound in (3.2.20) plotted as a solid line in Figure 3.5, is smaller than the uniform bound of $\frac{1}{2}$ up to $R = 2^{15} = 32\,768$, which is approximately 1.22 times larger than the energy stability threshold.

Remark 3.2.2. The right-hand side of (3.2.16) can be optimised numerically for α and β. This gives an improved bound as compared to the fully analytic result shown with the dot dashed blue line in Figure 3.5.

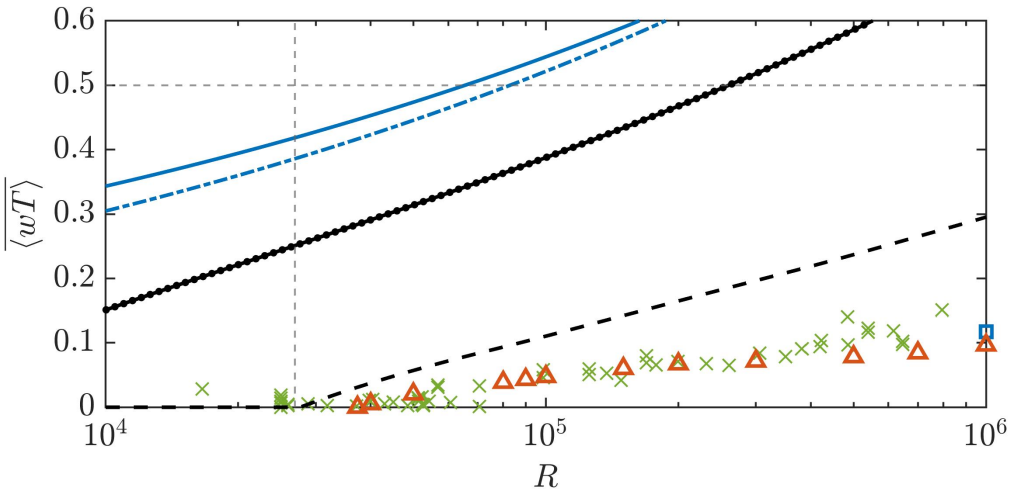

Figure 3.5: Comparison between the semi-analytical bounds computed with (3.2.16) and (3.2.18*a*,*b*) (-·-), the explicit bound (3.2.20) (—), the numerically optimal bounds obtained in §3.2.1 with (2.4.12) (- - -, $L_x = L_y = 2$) and with (3.2.7) (•), and experimental and DNS data (see Figure 3.2 for a key of the symbols). A dashed vertical line (- - -) indicates the smallest energy stability threshold, $R \approx 26\,926$, while a dashed horizontal line (- - -) indicates the uniform upper bound $\overline{\langle wT \rangle} \leq \frac{1}{2}$.

3.3 Bounds utilising the minimum principle

The upper bounding principle derived in §3.2 can be improved by imposing the minimum principle from Lemma 2.3.1, which guarantees that temperature fields solving the Boussinesq equations (1.2.3*a*–*c*) are nonnegative in the domain Ω at large time.

The major variation from §3.2 is that we optimise over $\lambda(z)$ instead of fixing $\lambda = -1$. The explicit expression for the bound given by Proposition 2.4.1 is

$$\overline{\langle wT \rangle} \leq U := \tfrac{1}{2} + \left\langle \tfrac{1}{4\beta} \left| \beta(z - \tfrac{1}{2}) - \tau'(z) + \lambda(z) \right|^2 - \tau(z) \right\rangle, \tag{3.3.1}$$

with the normalisation condition ,

$$\langle \lambda(z) \rangle = \tau(1) - \tau(0) = -1. \tag{3.3.2}$$

The optimisation problem to be solved both numerically and analytically in this section is

$$\begin{aligned} \inf_{U,\alpha,\beta,\tau(z),\lambda(z)} \quad & U \\ \text{subject to} \quad & \mathcal{S}_0\{\hat{T}_0\} + \left\langle \lambda(z)\hat{T}_0'(z) \right\rangle \geq 0 \qquad \forall\, \hat{T}_0 : \hat{T}_0(0) = 0 = \hat{T}_0(1), \\ & \tilde{\mathcal{S}}\{\hat{w}, \hat{T}\} \geq 0 \qquad \forall \hat{w}, \hat{T} : (3.2.4a,b), \\ & \lambda(z) \text{ nondecreasing and } \langle \lambda \rangle = -1. \end{aligned} \tag{3.3.3}$$

If one does not simplify the spectral constraints, one obtains a very similar problem where $\tilde{\mathcal{S}}$ is replaced by the $\boldsymbol{k}$-dependent functional appearing in (2.4.12). This problem gives a quantitative but not qualitative improvement to the bound on $\overline{\langle wT \rangle}$ but has a higher computational complexity than (3.3.3).

The analysis and computations of §3.2 demonstrate that if one wants to improve on the uniform bound $\overline{\langle wT \rangle} \leq \frac{1}{2}$ at large R, one must invoke the minimum principle for the temperature explicitly to avoid unphysical critical temperatures $\hat{T}_0$. As discussed in §2.3.1, upper bounds on $\overline{\langle wT \rangle}$ that take this principle into account can be found by solving (3.3.3). Numerically optimal solutions to (3.3.3) are presented in §3.3.1.

3.3.1 Numerically optimal bounds

Problem (3.3.3) was discretised into an SDP and solved with the high-precision solver SDPA-GMP [171] for $2.0 \times 10^5 \leq R \leq 3.4 \times 10^5$. The MATLAB toolbox SparseCoLO [54] was used to exploit sparsity in the SDPs. At each Rayleigh number, we employed the finite-element discretisation approach described in Appendix C on a Chebyshev mesh with at least 6000 piecewise-linear elements, increasing the resolution until the upper bounds changed by less than 1%. Achieving this at $R = 3.4 \times 10^5$ required approximately 12 200 elements. The numerical challenges associated with

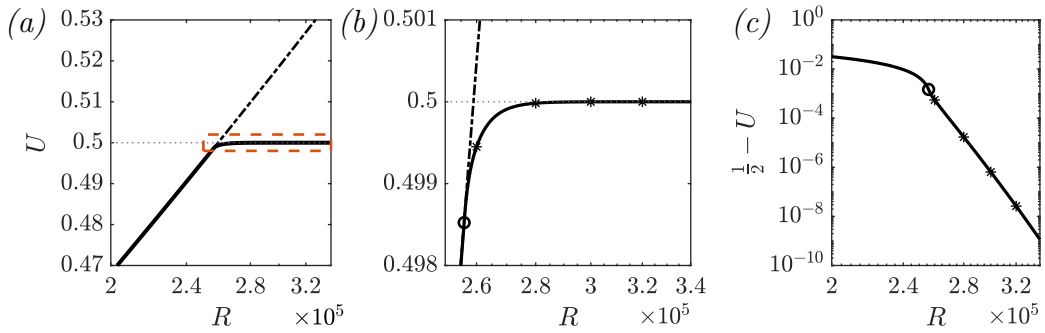

Figure 3.6: *(a)* Optimal bounds U on $\overline{\langle wT \rangle}$ computed by solving (3.3.3), which incorporates the minimum principle for temperature (—). Also plotted (-·-) are the bounds computed without the minimum principle ($\lambda(z) = -1$). *(b)* Detail of the region inside the red dashed box (---) in panel *(a)*. *(c)* Difference between our optimal bounds and the uniform bound $\overline{\langle wT \rangle} \leq 1/2$, shown in all panels as a dotted line (·····). In *(b)* and *(c)*, a circle at $R \approx 256\,269$ marks the point at which $\lambda(z)$ begins to vary from -1, while stars ($*$) mark the Rayleigh numbers at which τ are plotted in Figure 3.7.

setting up the SDPs accurately in double-precision using SparseCoLO on even finer meshes prevented us from considering a wider the range of Rayleigh numbers.

Figure 3.6 compares numerical upper bounds on the heat transfer obtained with (solid line) and without (dot-dashed line) the minimum principle for the temperature, that is, by optimising $\lambda(z)$ or by setting $\lambda(z) = -1$ in (3.3.3), respectively. The results for the latter case coincide with those described in §3.2.1 and are shown in Figure 3.2.

The choice $\lambda(z) = -1$ is optimal for $R < 256\,269$. For higher R, the numerical upper bounds on $\overline{\langle wT \rangle}$ with optimised $\lambda(z)$ are strictly better than those with $\lambda(z) = -1$ and, crucially, appear to approach the uniform bound $\frac{1}{2}$ from below as R is raised. Note that although the deviation from $\frac{1}{2}$ is small at the highest values of R that could be handled, it is much larger than the tolerance (10^{-25}) used by the multiple-precision SDP solver SDPA-GMP, giving us confidence that it is not a numerical artefact. Moreover, the deviation from $\frac{1}{2}$ of the numerical bounds, shown in Figure 3.6*(c)*, appears not to decay as a power law. If the optimal bound available within our bounding framework has the functional form $\frac{1}{2} - c_1 R^{-c_2}$, the range of Rayleigh numbers spanned by our computations is too small to accurately predict the exponent and the prefactor, in any case it is clear that the decay is much faster than predicted by the heuristic arguments in appendix B.

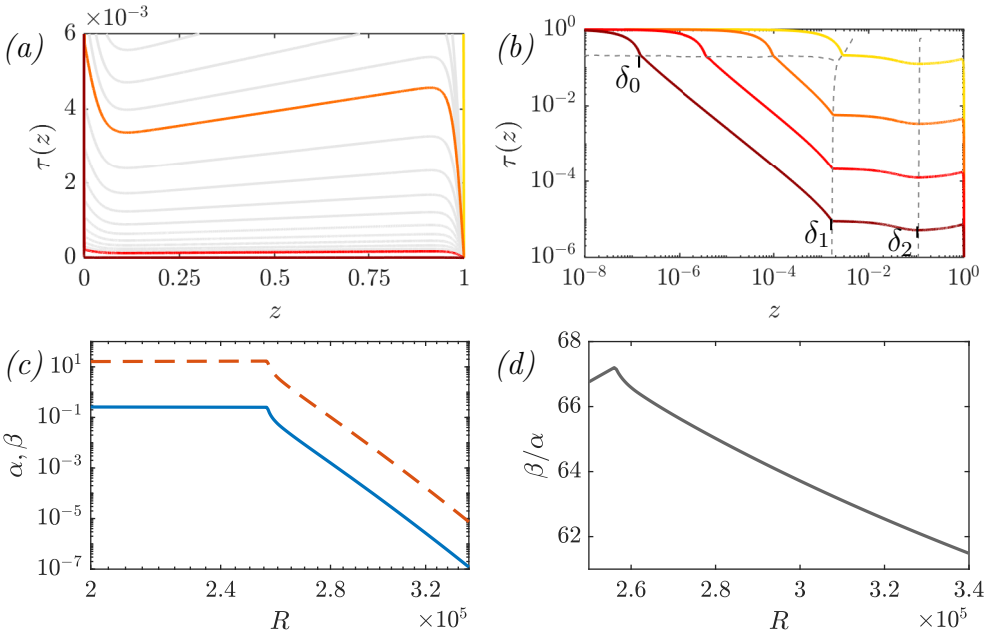

Figure 3.7: *(a)* Optimal $\tau(z)$ in the entire domain, plotted for $0 \leq \tau \leq 0.006$ for visualization purposes. At all Ra values, $\tau(0) = 1$. *(b)* Logarithmic plot of $\tau(z)$, highlighting the behaviour near $z = 0$. Coloured lines correspond to the Ra highlighted in Figure 3.6, for $R = 2.6 \times 10^5$ (—), 2.8×10^5 (—), 3.0×10^5 (—), 3.2×10^5 (—). Dashed lines (- - -) mark the boundaries of the sublayers $(0, \delta_0)$, (δ_0, δ_1) and (δ_1, δ_2), and the sublayer edges are labelled explicitly for $R = 3.2 \times 10^5$. *(c)* Variation with Ra of the optimal balance parameters α (—) and β (- - -) for (3.3.3). *(d)* Ratio of balance parameters, b/a, when the Lagrange multiplier is active.

Optimal profiles $\tau(z)$ for selected Rayleigh numbers are shown in Figures 3.7*(a,b)* and differ significantly from the corresponding profiles in Figure 3.2*(b)* obtained when the minimum principle for the temperature is disregarded. When the minimum principle is enforced, $\tau(z)$ appears to approach zero almost everywhere as R is raised, but always satisfies $\tau(0) = 1$. This leads to the formation of a very thin boundary layer near $z = 0$, which at high R consists of three distinct sublayers identified by two points, $z = \delta_0$ and $z = \delta_1$, at which $\tau(z)$ is not differentiable. These are indicated by gray dashed lines in Figure 3.7*(b)*. In the first sublayer, from $z = 0$ to $z = \delta_0$, τ is observed to vary linearly. The second sublayer, $\delta_0 < z < \delta_1$, is observed only for $R > 2.6 \times 10^5$ and we observe that $\tau \sim z^{-1}$ approximately. The third sublayer, from $z = \delta_1$ to the point $z = \delta_2$ at which $\tau(z)$ attains a local minimum, does not have a simple functional form. In the bulk, $\tau(z)$ increases approximately linearly with slope very close to α, and the condition $\tau(1) = 0$, which emerges as a result of the optimization, is attained through a small boundary layer of width ε near $z = 1$. We

choose the boundary of this layer as the point $z = 1 - \varepsilon$ at which $\tau(z)$ has a local maximum.

Figure 3.7*(c)* shows the variation of the balance parameters with R. Below $R = 256\,269$, both coincide with the values plotted in Figure 3.2*(c)*. At higher R, the minimum principle for the temperature becomes active and both balance parameters start to decay rapidly. It would be tempting to conjecture that $\alpha \sim \beta \sim R^{-p}$ for some power p but, given the small variation of β/α evident in Figure 3.7*(d)*, we cannot currently exclude that subtly different scaling exponents or higher-order corrections do not play an important role in obtaining an upper bound on $\overline{\langle wT \rangle}$ that approaches $\frac{1}{2}$ asymptotically from below.

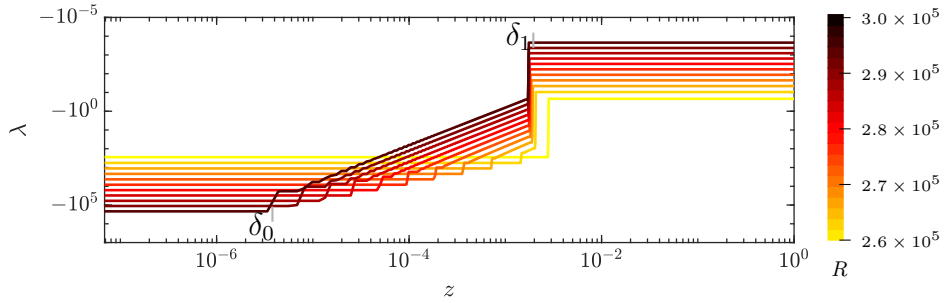

Figure 3.8: Variation of $\lambda(z)$ shown on a logarithmic scale to highlight the non-zero region of the Lagrange multiplier $q'(z)$, from $R = 2.6 - 3.0 \times 10^5$. The colorbar here applies for all τ, λ and $\hat{T}_0$. The edges of the boundary sublayers $(0, \delta_0)$ and (δ_0, δ_1) for the largest R value are explicitly labelled.

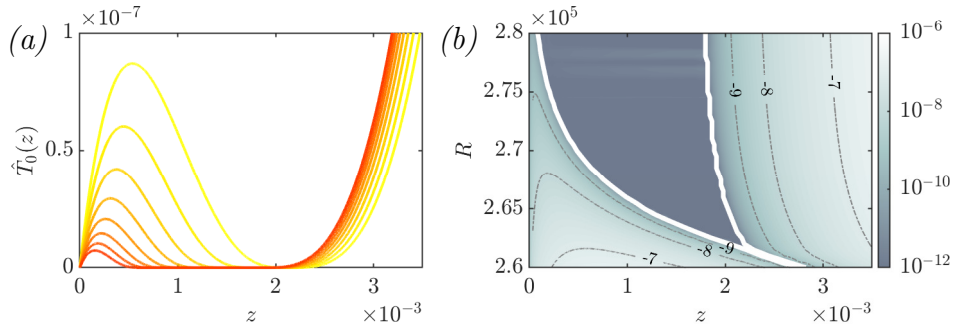

Figure 3.9: Variation with R of the critical temperature profiles, $\hat{T}_0$, plotted for $0 \leq z \leq 3.5 \times 10^{-3}$. *(a)* Plots of individual $\hat{T}_0$ from $R = 2.62 - 2.69 \times 10^5$. *(b)* Contour plot of $\hat{T}_0$ vs R. Solid white lines mark the boundary sublayer $\delta_0 \leq z \leq \delta_1$, within which $q' > 0$ and $\hat{T}_0 = 0$. Values of $\hat{T}_0$ below 10^{-12} are assumed to be numerical zeros.

Figure 3.8 shows the structure of $\lambda(z)$, whose (distributional) derivative represents the Lagrange multiplier enforcing the minimum principle. The multiplier, therefore,

is active in regions where $\lambda(z)$ is not constant. The choice $\lambda(z) = -1$ is optimal for $R \leq 256\,269$. At higher Rayleigh numbers, the multiplier becomes active between $z = \delta_0$ and $z = \delta_1$, which is what causes the second boundary sublayer in $\tau(z)$. In the immediate vicinity of the bottom boundary ($0 \leq z \leq \delta_0$), λ is constant and it appears that $\lambda(z) - \tau'(z) \approx \beta/2$ (cf. Figure 3.10*(c)*). Indeed, inspection of the cost function in (3.3.3) suggests that $\lambda(z) - \tau'(z) = \beta(1-z)/2$ should be optimal, but we could not identify the very small z-dependent correction in our numerical results. In the second sublayer ($\delta_0 \leq z \leq \delta_1$), where the Lagrange multiplier is active, $\lambda(z) \sim -z^{-2}$. Again, this is consistent with the minimization of the cost function in (3.3.3), as one expects $\lambda(z)$ to cancel the very large contribution of $\tau'(z)$ near the bottom boundary.

Further validation of our numerical results comes from inspection of the critical temperatures $\hat{T}_0(z)$, which can be recovered using (2.4.9) and are shown in Figure 3.9*(a,b)* for selected values of R. As expected, the critical temperatures are nonnegative for all z and vanish identically (up to small numerical tolerances) in the region $\delta_0 \leq z \leq \delta_1$, where $\lambda(z)$ is active. We note that, for a given Rayleigh number, this region is strictly larger than the range of z values for which the critical temperatures in Figure 3.3*(c)* are negative, indicating that the minimum principle alters the problem in a more subtle way than simply saturating the constraint $T \geq 0$.

To analyse the results further we define the diagnostic function

$$\chi(z) = \tau'(z) - \lambda(z)\,, \tag{3.3.4}$$

and rewrite (3.3.1) as

$$\overline{\langle wT \rangle} \leq \frac{1}{2} + \beta \left\langle \frac{1}{4}\left(z - \frac{1}{2} - \frac{\chi(z)}{\beta}\right)^2 - \frac{\tau(z)}{\beta} \right\rangle . \tag{3.3.5}$$

Panels *(a)*, *(c)* & *(d)* in Figure 3.10 suggest that $\chi(0)/\beta \to -\frac{1}{2}$ and $\chi(1)/\beta \to -\frac{3}{2}$ as $R \to \infty$. In fact, profiles $\chi(z)/\beta$ for different Rayleigh numbers collapse almost exactly

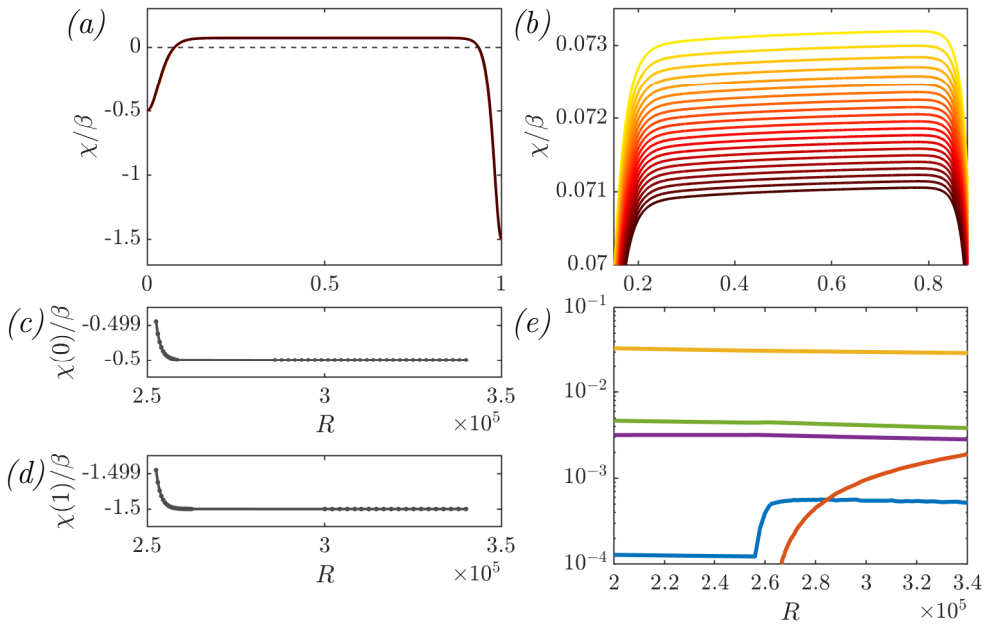

Figure 3.10: *(a)* Profiles $\chi(z)/b$ for $2.6 \times 10^5 \leq R \leq 3.0 \times 10^5$. *(b)* Detailed view of $\chi(z)/b$ in the bulk. *(c,d)* Variation of $\chi(0)/b$ and $\chi(1)/b$ with Ra. *(e)* Contributions to the integral of τ/b in the regions $(0, \delta_0)$ (—), (δ_0, δ_1) (—), (δ_1, δ_2) (—), $(\delta_2, 1-\varepsilon)$ (—) and $(1-\varepsilon, 1)$ (—), as a function of R.

throughout the layer, but subtle corrections are present; for instance, Figure 3.10*(b)* demonstrates that, in the bulk, the mean value of $\chi(z)/\beta$ decreases with R. It is also evident that $\chi(z)$ is not exactly constant throughout the bulk, but increases by approximately 10^{-4}. Since $\lambda(z)$ is constant in this region, we conclude that $\tau'(z)$ is not constant, but displays subtle and thus nontrivial variation.

Figure 3.10*(e)* illustrates the variation with R of contributions to the integral of $\tau(z)/\beta$ from regions $(0, \delta_0)$, (δ_0, δ_1), (δ_1, δ_2), $(\delta_2, 1-\varepsilon)$ and $(1-\varepsilon, 1)$. The largest contribution comes from the bulk $(\delta_2 \leq z \leq 1-\varepsilon)$, but it slowly decreases with R. The same is true of the contribution of the top boundary layer $(1-\varepsilon \leq z \leq 1)$ and the outermost boundary sublayer near $z = 0$ $(\delta_1 \leq z \leq \delta_2)$. Only in the first two boundary layers near $z = 0$ does the value of the integral increase with R, suggesting that the integral of $\tau(z)/\beta$ near the boundary layer may become the dominant term as $R \to \infty$. While the range of Rayleigh numbers covered by our computations is too small to confirm or disprove this conjecture, it is certain that the integral of

$\tau(z)/\beta$ must remain large enough to offset the positive term in (3.3.5) in order to obtain a bound on $\overline{\langle wT \rangle}$ smaller than 1/2.

Finally, Figures 3.8 and 3.10 suggest that, for sufficiently large R,

$$\lambda(z) = \begin{cases} \tau'(z) + \frac{\beta}{2}, & 0 \le z \le \delta_0, \\ -q_0 z^{-2}, & \delta_0 \le z \le \delta_1, \\ \tau'(1) + \frac{3\beta}{2}, & \delta_1 \le z \le 1, \end{cases} \tag{3.3.6}$$

for some positive constant q_0, and that $\alpha, \tau, q_0 \sim \beta$. The next section investigates whether such ansatz can lead to upper bounds on $\overline{\langle wT \rangle}$ that are strictly smaller than 1/2 at all Rayleigh numbers.

3.3.2 Analytical bound

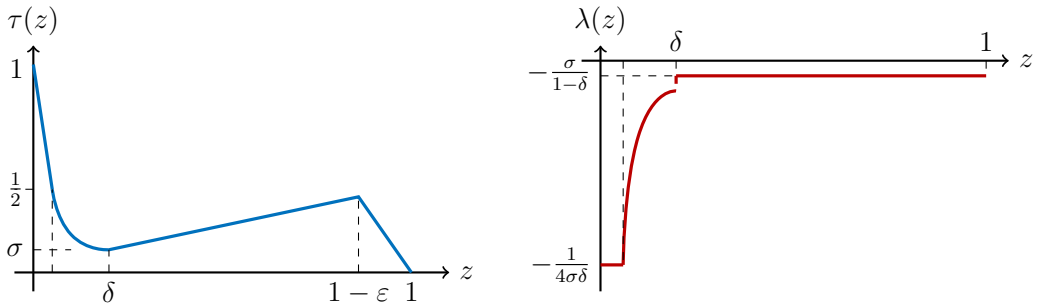

Figure 3.11: Sketch of the piecewise $\tau(z)$ and $\lambda(z)$ in (3.3.7) and (3.3.8).

In appendix E we present the general conditions under which standard analytical constructions (piecewise linear τ) that attempt to make our numerical results rigorous are guaranteed to fail. In the remainder of this section we demonstrate that a choice of $\tau(z), \alpha, \beta$ and $\lambda(z)$, inspired by the numerical optimisation can be used to prove Theorem 3.1.2.

We aim to choose the parameters to have the smallest bound on $\overline{\langle wT \rangle}$ while satisfying the spectral constraint in (3.2.6). This will require the use of a Hardy-type

inequality. The choice of profiles are

$$\tau(z) := \begin{cases} 1 - \dfrac{z}{4\sigma\delta}, & 0 \le z \le 2\sigma\delta, \\ \dfrac{\sigma\delta}{z}, & 2\sigma\delta \le z \le \delta, \\ \sigma + \alpha(z-\delta), & \delta \le z \le 1-\varepsilon, \\ (1-z)\dfrac{\sigma + \alpha(1-\varepsilon-\delta)}{\varepsilon}, & 1-\varepsilon \le z \le 1, \end{cases} \tag{3.3.7}$$

and

$$\lambda(z) := \begin{cases} -\dfrac{1}{4\sigma\delta}, & 0 \le z \le 2\sigma\delta, \\ -\dfrac{\sigma\delta}{z^2}, & 2\sigma\delta \le z \le \delta, \\ -\dfrac{\sigma}{1-\delta}, & \delta \le z \le 1. \end{cases} \tag{3.3.8}$$

Both piecewise functions $\tau(z)$ and $\lambda(z)$ are entirely determined by the bottom boundary layer width $\delta \in (0, \frac{1}{2})$, the top boundary layer width $\varepsilon \in (0, \frac{1}{2})$ and $\sigma \in (0, \frac{1}{2})$ the value of the profile at the inner sublayer at the bottom. The piecewise function $\tau(z)$ is constructed so as to have a bottom boundary layer divided into two parts, an inner sublayer where $\tau'(z)$ is a negative constant and an outer sublayer where $\tau'(z) \sim z^{-1}$. We set $\tau'(z) = \lambda(z)$ in the region of $[0, \delta]$ exactly so as to negate the otherwise $1/\delta$ the contribution from the positive $L2$ term in (3.3.1). The inverse-z scaling of $\tau(z)$ in the outer part of the lower boundary layer is one of the key ingredients in proving Theorem 3.1.2. The linear inner sublayer, instead, is used to satisfy the boundary condition $\tau(0) = 1$. In the bulk of the layer we have $\tau'([\delta, 1-\varepsilon]) = \alpha$, so the indefinite sign term is zero in $\tilde{\mathcal{S}}$ (3.2.6). Thus, we only need to control the indefinite sign term in the boundary layers.

Lemma 3.3.1. *Let $\tau(z)$ and $\lambda(z)$ be given by* (3.3.7) *and* (3.3.8)*. Suppose that $\delta, \varepsilon \leq \frac{1}{2}$, $\sigma, \alpha \leq 1$ and that*

$$\alpha = \sqrt{2\varepsilon}\,\sigma\delta \ln\left(\frac{1}{2\sigma}\right) - 2\sigma, \quad \textit{and} \tag{3.3.9a}$$

$$\beta = 6\sigma\delta \ln\left(\frac{1}{2\sigma}\right). \tag{3.3.9b}$$

Then,

$$U(\alpha, \beta, \delta, \varepsilon, \sigma) \leq \frac{1}{2} - \frac{\sigma\delta}{2} \ln\left(\frac{1}{2\sigma}\right). \tag{3.3.10}$$

Proof. We begin by estimating the first integral in (3.3.1) by using the AM-GM inequality, and τ and λ as given in (3.3.7) and (3.3.8). The assumptions $\delta \leq \frac{1}{2}$ and $\varepsilon \leq \frac{1}{2}$ imply $1 - \varepsilon - \delta \leq 1$ and $\frac{1}{1-\delta} \leq 2$ and the assumption $\sigma, \alpha < 1$ implies $\alpha + \sigma \leq \alpha + 2\sigma$, so

$$\begin{aligned}
\frac{1}{4\beta}\left\langle |\beta(z - \tfrac{1}{2}) - \tau'(z) + \lambda(z)|^2 \right\rangle &\leq \frac{\beta}{2}\left\langle |z - \tfrac{1}{2}|^2 \right\rangle + \frac{1}{2\beta}\left\langle |\tau'(z) - \lambda(z)|^2 \right\rangle \\
&= \frac{\beta}{24} + \frac{1}{2\beta}\int_\delta^1 |\tau'(z) - \lambda(z)|^2 \mathrm{d}z \\
&\leq \frac{\beta}{24} + \frac{(\alpha + 2\sigma)^2}{2\beta} + \frac{(\alpha + \sigma)^2}{2\beta\varepsilon} \qquad (3.3.11) \\
&\leq \frac{\beta}{24} + \frac{3(2\sigma + \alpha)^2}{4\beta\varepsilon}. \qquad (3.3.12)
\end{aligned}$$

Next we estimate from below the integral of $\tau(z)$,

$$\langle \tau(z) \rangle \geq \int_{2\sigma\delta}^{\delta} \tau(z)\,\mathrm{d}z = \sigma\delta \ln\left(\frac{1}{2\sigma}\right). \tag{3.3.13}$$

The inequality holds since $\tau(z) \geq 0$ on $[0, 1]$. Substituting (3.3.12) and (3.3.13) into (3.3.1) gives

$$U \leq \frac{1}{2} + \frac{\beta}{24} + \frac{3(2\sigma + \alpha)^2}{4\beta\varepsilon} - \sigma\delta \ln\left(\frac{1}{2\sigma}\right). \tag{3.3.14}$$

The result then follows from using (3.3.9). □

Next we turn to sufficient conditions that ensure the non-negativity of $\tilde{\mathcal{S}}$ in (3.2.6). For this we require a Hardy inequality for weighted integrals, the proof of which can be found in the appendix.

Lemma 3.3.2 (Hardy inequality)**.** *Let $f : [0,\infty) \to \mathbb{R}$ be a function such that $f, f' \in L^2(0,\infty)$ and such that $f(0) = 0$. Then, for any $\epsilon > 0$ and any $\nu \geq 0$,*

$$\int_0^\nu \frac{|f|^2}{(z+\epsilon)^2}\mathrm{d}z \leq 4\int_0^\nu |f'|^2\mathrm{d}z. \tag{3.3.15}$$

Lemma 3.3.3. *Let $\tau(z)$ be given by* (3.3.7) *and let $\alpha, \delta, \varepsilon, \sigma$ satisfy the conditions of Lemma 3.3.1. Suppose further that,*

$$\varepsilon = \frac{8}{\sigma+\alpha}\sqrt{\frac{\alpha\beta}{R}} \qquad \textit{and} \qquad \delta = \frac{2}{9\sigma}\sqrt{\frac{\alpha\beta}{R}}. \tag{3.3.16}$$

Then the spectral constraint $\tilde{\mathcal{S}} \geq 0$ in (3.2.6) *is satisfied.*

Proof. Initially we recall the simplified functional in (3.2.6), where $\hat{w}$ and $\hat{T}$ are subject to the boundary conditions (3.2.4). Substituting for $\tau(z)$ from (3.3.7) gives

$$\begin{aligned}\widetilde{\mathcal{S}}(\hat{w},\hat{T}) = \quad & \int_0^{2\sigma\delta} \frac{4\alpha}{R}|\hat{w}'|^2 + \beta|\hat{T}'|^2 - \left(\alpha + \frac{1}{4\sigma\delta}\right)\hat{w}\hat{T}\,\mathrm{d}z \\ & + \int_{2\sigma\delta}^{\delta} \frac{4\alpha}{R}|\hat{w}'|^2 + \beta|\hat{T}'|^2 - \left(\alpha + \frac{\sigma\delta}{z^2}\right)\hat{w}\hat{T}\,\mathrm{d}z \\ & + \int_{1-\varepsilon}^{1} \frac{4\alpha}{R}|\hat{w}'|^2 + \beta|\hat{T}'|^2 - \left(\frac{\sigma+\alpha(1-\delta)}{\varepsilon}\right)\hat{w}\hat{T}\,\mathrm{d}z. \end{aligned} \tag{3.3.17}$$

Since $\widetilde{\mathcal{S}}\{\hat{w},\hat{T}\} \geq \widetilde{\mathcal{S}}\{|\hat{w}|,|\hat{T}|\}$ with equality when w and T are nonnegative, we shall assume without loss of generality that $\hat{w}, \hat{T} \geq 0$. Then since $\alpha \leq 1$ by assumption, we estimate

$$\frac{9}{2}\frac{\sigma\delta}{(z+\sigma\delta)^2} \geq \begin{cases} \alpha + \dfrac{1}{4\sigma\delta}, & 0 \leq z \leq 2\sigma\delta, \\ \alpha + \dfrac{\sigma\delta}{z^2}, & 2\sigma\delta \leq z \leq \delta. \end{cases} \tag{3.3.18}$$

Using this estimate we can combine the first two integrals of (3.3.17) to conclude

$$\widetilde{\mathcal{S}}\{\hat{w},\hat{T}\} \geq \widetilde{\mathcal{S}}_B\{\hat{w},\hat{T}\} + \widetilde{\mathcal{S}}_T\{\hat{w},\hat{T}\}, \tag{3.3.19}$$

where

$$\widetilde{\mathcal{S}}_B\{\hat{w},\hat{T}\} := \int_0^\delta \frac{4\alpha}{R}|\hat{w}'|^2 + \beta|\hat{T}'|^2 - \frac{9}{2}\frac{\sigma\delta}{(z+\sigma\delta)^2}\hat{w}\hat{T}\,\mathrm{d}z, \tag{3.3.20a}$$

$$\widetilde{\mathcal{S}}_T\{\hat{w},\hat{T}\} := \int_{1-\varepsilon}^1 \frac{4\alpha}{R}|\hat{w}'|^2 + \beta|\hat{T}'|^2 - \frac{(\sigma+\alpha)}{\varepsilon}\hat{w}\hat{T}\,\mathrm{d}z. \tag{3.3.20b}$$

Next, we prove that $\widetilde{\mathcal{S}}_B\{\hat{w},\hat{T}\}$ and $\widetilde{\mathcal{S}}_T\{\hat{w},\hat{T}\}$ are individually nonnegative, thereby implying the nonnegativity of $\widetilde{\mathcal{S}}\{\hat{w},\hat{T}\}$.

First, we deal with $\widetilde{\mathcal{S}}_T\{\hat{w},\hat{T}\}$. Using the boundary conditions (3.2.4) along with the fundamental theorem of calculus and the Cauchy–Schwarz inequality gives,

$$|\hat{w}|^2 \leq (1-z)\int_{1-\varepsilon}^1 |\hat{w}'|^2\mathrm{d}z, \qquad |\hat{T}|^2 \leq (1-z)\int_{1-\varepsilon}^1 |\hat{T}'|^2\mathrm{d}z. \tag{3.3.21a,b}$$

Using (3.3.21a,b) in the expression (3.3.20b) gives

$$\widetilde{\mathcal{S}}_T\{\hat{w},\hat{T}\} \geq \int_{1-\varepsilon}^1 \frac{4\alpha}{R}|\hat{w}'|^2 + \beta|\hat{T}'|^2 - \frac{(\sigma+\alpha)}{\varepsilon}(1-z)\|\hat{w}'\|^2_{L^2(1-\varepsilon,1)}\|\hat{T}'\|^2_{L^2(1-\varepsilon,1)}\mathrm{d}z. \tag{3.3.22}$$

Integrating the final term gives a quadratic form in the $L^2(1-\varepsilon,1)$ norms of $\hat{w}'$ and $\hat{T}'$. As such it is non-negative when the discriminant is nonpositive, which gives,

$$\varepsilon \leq \frac{8}{\sigma+\alpha}\sqrt{\frac{\alpha\beta}{R}}. \tag{3.3.23}$$

Let ε be (3.3.16), then $\widetilde{\mathcal{S}}_T \geq 0$ as required.

The nonnegativity of $\widetilde{\mathcal{S}}_B$, instead, can be proven using the Hardy inequality given in Lemma 3.3.2. First, using Young's inequality

$$xy \leq \frac{h}{2}x^2 + \frac{1}{2h}y^2,$$

with a weight $h > 0$, we write

$$\widetilde{\mathcal{S}}_B\{\hat{w}, \hat{T}\} \geq \int_0^\delta \frac{4\alpha}{R}|\hat{w}'|^2 + \beta|\hat{T}'|^2 - \frac{9}{4}\frac{\sigma\delta h}{(z+\sigma\delta)^2}|\hat{w}|^2 - \frac{9}{4}\frac{\sigma\delta}{(z+\sigma\delta)^2 h}|\hat{T}|^2 \mathrm{d}z. \tag{3.3.24}$$

Then, we can apply Lemma 3.3.2 to estimate

$$\int_0^\delta \frac{|\hat{w}|^2}{(z+\sigma\delta)^2}\mathrm{d}z \leq 4\int_0^\delta |\hat{w}'|^2\mathrm{d}z, \qquad \int_0^\delta \frac{|\hat{T}|^2}{(z+\sigma\delta)^2}\mathrm{d}z \leq 4\int_0^\delta |\hat{T}'|^2\mathrm{d}z. \tag{3.3.24a,b}$$

Using (3.3.24*a,b*), (3.3.24), and choosing

$$h = 2\sqrt{\frac{\alpha}{\beta R}}, \tag{3.3.25}$$

we conclude that $\widetilde{\mathcal{S}}_B\{\hat{w}, \hat{T}\} \geq 0$ if

$$\sigma\delta \leq \frac{2}{9}\sqrt{\frac{2\alpha\beta}{R}}. \tag{3.3.26}$$

Let δ be given by (3.3.16) then $\widetilde{\mathcal{S}}_B \geq 0$. □

Proof of Theorem 3.1.2

Using the results of Lemma 3.3.1 and Lemma 3.3.3, we make the choices

$$\alpha = \sigma, \quad \delta = \varepsilon. \tag{3.3.26a,b}$$

The proof of the bound on $\overline{\langle wT \rangle}$ follows from algebraic manipulations to determine the relations between the parameters $(\alpha, \beta, \sigma, \delta, \varepsilon)$. Applying (3.3.26a,b) to (3.3.9a) and (3.3.9b), equating the two equations and rearranging we find that

$$\delta = 162 \frac{\alpha^2}{\beta^2}, \tag{3.3.27}$$

which can be combined with the choice of δ in (3.3.16) to give

$$\alpha = 3^{-\frac{12}{5}} \beta R^{-\frac{1}{5}}. \tag{3.3.28}$$

Using (3.3.28) in (3.3.27) and then both in (3.3.9b) gives

$$\alpha = \sigma = \frac{1}{2} \exp\left(-\frac{3^{\frac{11}{5}}}{4} R^{\frac{3}{5}} \right), \tag{3.3.29a}$$

$$\delta = \varepsilon = \frac{2}{3^{\frac{4}{5}}} R^{-\frac{2}{5}}, \tag{3.3.29b}$$

$$\beta = \frac{3^{\frac{12}{5}}}{2} R^{\frac{1}{5}} \exp\left(-\frac{3^{\frac{11}{5}}}{4} R^{\frac{3}{5}} \right). \tag{3.3.29c}$$

Then Theorem 3.1.2 follows by substituting (3.3.29a) and (3.3.29b) into (3.3.10) to obtain,

$$U \leq \frac{1}{2} - \frac{3^{\frac{7}{5}}}{8} R^{\frac{1}{5}} \exp\left(-\frac{3^{\frac{11}{5}}}{4} R^{\frac{3}{5}} \right). \tag{3.3.30}$$

The conditions on the parameters of $\delta, \varepsilon \leq \frac{1}{2}$ and $\sigma, \alpha \leq 1$ are satisfied for all $R > 4$.

Chapter 4

Insulating and perfectly conducting boundaries

What opposes unites, and the finest attunement
stems from things bearing in opposite directions,
and all things come about by strife.

Heraclitus of Ephesus

In this chapter we consider the setup where the lower boundary is a thermal insulator while the upper boundary is perfectly conducting (1.2.5d). Section 4.2 demonstrates a numerical optimisation and analytical bounds. Whereas §4.3 contains analytical bounds for when the minimum principle is utilised (Lemma 2.3.1). This analysis uses ideas in line with those presented in §3.3.2. The main result of this chapter is published [2].

Since the lower boundary is an insulator, there is no thermal boundary layer at $z = 0$. Physically this problem reduces to the dynamics to an unstably stratified upper thermal boundary layer shedding plumes that descend and mix the fluid. Unlike the isothermal boundaries considered in chapter 3, a mean conductive heat

flux exits and as such a Nusselt number can be defined as by (1.2.16) which is

$$Nu = \left(1 - 2\overline{\langle wT \rangle}\right)^{-1}. \tag{4.0.1}$$

As demonstrated in chapter 1 the uniform bounds for the problem when at least the upper boundary is kept at $T = 0$ is $0 \leq \overline{\langle wT \rangle} \leq \frac{1}{2}$. In terms of Nu these correspond to zero enhancement of heat flux due to convection, ($\overline{\langle wT \rangle} = 0, Nu = 1$), and 'pure' transport of heat due to convection alone, ($\overline{\langle wT \rangle} = \frac{1}{2}, Nu = \infty$).

4.1 Setup

The kinematic and thermal boundary conditions are

$$\boldsymbol{u}|_{z=\{0,1\}} = 0, \tag{4.1.1a}$$

$$\partial_z T|_{z=0} = T|_{z=1} = 0, \tag{4.1.1b}$$

and as a consequence $u \in \mathcal{U}_1$ and $T \in \mathcal{T}_2$ as defined in (2.1.2). The thermal boundary condition at the upper boundary ensures that the minimum principle, Lemma 2.3.1, holds for this problem. The governing equations admit the solution $\boldsymbol{u} = 0$, $p =$ constant and $T = -\frac{z^2}{2} + \frac{1}{2}$ at all R, representing the purely conductive state. This state is globally asymptotically stable irrespective of the horizontal periods L_x and L_y if $R < 2737.16$ [58] and linearly unstable if $R > 2772.27$ [123]. The range in R between the energy stability and linear stability limit is smaller as compared to isothermal boundaries considered in chapter 3 [58]. We are interested in bounds on $\overline{\langle wT \rangle}$ that hold for any $R \geq 2737.16$. We prove the following two theorems.

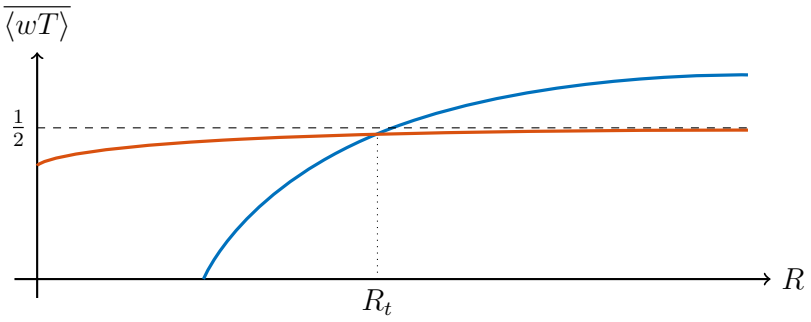

Figure 4.1: Representative plots of the three analytical bounds on $\overline{\langle wT \rangle}$, first the uniform in R upper bound of $\frac{1}{2}$ (---), then the bound proven in Theorem 4.1.1 (—) and finally the bound proven in Theorem 4.1.2 (—). R_t denotes the Rayleigh number above which Theorem 4.1.2 becomes the best provable bound on $\overline{\langle wT \rangle}$.

Theorem 4.1.1 (Isothermal top and insulating bottom)**.** *Supposing that* $\boldsymbol{u}$ *and* T *solve* (1.2.3) *subject to the boundary conditions* (4.1.1) *there exists a constant* $c > 0$ *such that for sufficiently large* $R > 0$*,*

$$\overline{\langle wT \rangle} \leq \frac{1}{2}\left(\frac{1}{2} + \frac{1}{\sqrt{3}}\right) - cR^{-\frac{1}{3}}. \tag{4.1.2}$$

Remark 4.1.1. It is shown in §4.2.2 that the theorem holds for $c \approx 0.4158$ for any $R > 111$.

Upper bounds on $\overline{\langle wT \rangle}$ imply the following bound on the Nusselt number.

Corollary 4.1.1. *For all sufficiently large* R

$$Nu \leq \left(\frac{1}{2} - \frac{1}{\sqrt{3}} + 2cR^{-\frac{1}{3}}\right)^{-1}. \tag{4.1.3}$$

The next result gives an upper bound on $\overline{\langle wT \rangle}$ that approaches $\frac{1}{2}$ asymptotically in R. Figure 4.1 shows with representative plots the two analytical bounds proven in this chapter. The results of Theorem 4.1.1 are 'better' at lower R, while for all $R > R_t$ Theorem 4.1.2 is the improved upper bound. The second main result of this chapter uses the minimum principle Lemma 2.3.1 and it will be demonstrated in §4.3 that this requires novel constructions of the background field and a Rellich-type inequality.

Theorem 4.1.2 (Isothermal top and insulating bottom enforcing $T \geq 0$)**.** *Suppose that* $\boldsymbol{u}$ *and* T *solve* (1.2.3) *subject to the boundary conditions* (4.1.1)*. Then there exists constants* $c_1, c_2 > 0$ *such that for sufficiently large* $R > 0$*,*

$$\overline{\langle wT \rangle} \leq \frac{1}{2} - c_1 R^{-\frac{1}{5}} \exp(-c_2 R^{\frac{3}{5}}). \tag{4.1.4}$$

Remark 4.1.2. It is shown in §4.3 that the theorem holds for $c_1 = 2^{\frac{1}{5}}$ and $c_2 = 2^{\frac{37}{5}} 3^{-2}$ for any $R > 1$.

Corollary 4.1.2. *For all sufficiently large* R

$$Nu \leq \frac{1}{2c_1} R^{\frac{1}{5}} \exp\left(c_2 R^{\frac{3}{5}}\right). \tag{4.1.5}$$

4.2 Optimal bounds at low R

It follows from the application of the background method as in §2.3 that the best bound on $\overline{\langle wT \rangle}$ is given by solving the optimisation problem in (2.3.16). The upper bound on $\overline{\langle wT \rangle}$ without imposing the minimum principle follows from setting $\lambda = -1$ in Proposition 2.4.1. The functional $\mathcal{S}$ is the same as in chapter 3 given by (3.2.1). The best upper bound U on $\overline{\langle wT \rangle}$ that can be proved with the approach in chapter 2 is

$$\overline{\langle wT \rangle} \leq \inf_{U, \tau(z), \alpha, \beta} \{U : \mathcal{S}\{\boldsymbol{u}, T\} \geq 0 \ \forall (\boldsymbol{u}, T) \in \mathbb{A}\}, \tag{4.2.1}$$

where $\mathbb{A} = \mathcal{U}_1 \times \mathcal{T}_2$ and the explicit expression for the upper bound given by (2.4.2). Since both $\boldsymbol{u} = (u, v, w)$ and T are horizontally periodic a Fourier decomposition is performed and the boundary conditions (4.1.1) become

$$\hat{w}_{\boldsymbol{k}}(0) = \hat{w}'_{\boldsymbol{k}}(0) = \hat{w}_{\boldsymbol{k}}(1) = \hat{w}'_{\boldsymbol{k}}(1) = 0, \tag{4.2.2a}$$

$$\hat{T}'_{\boldsymbol{k}}(0) = \hat{T}_{\boldsymbol{k}}(1) = 0. \tag{4.2.2b}$$

The optimisation problem can be stated as

$$\begin{aligned} \inf_{U,\tau(z),\alpha,\beta} \quad & U \\ \text{subject to} \quad & \mathcal{S}_{\boldsymbol{k}}\{\hat{w}_{\boldsymbol{k}}, \hat{T}_{\boldsymbol{k}}\} \geq 0 \quad \forall \hat{w}_{\boldsymbol{k}}, \hat{T}_{\boldsymbol{k}} : (4.2.2a,b), \quad \boldsymbol{k} \neq 0\,, \\ & \alpha, \beta > 0, \quad \tau(1) = 0, \end{aligned} \tag{4.2.3}$$

where

$$\overline{\langle wT \rangle} \leq U(\tau, \alpha, \beta) := \frac{1}{2} + \left\langle \frac{1}{4\beta} |\beta z - \tau'(z) - 1|^2 - \tau(z) \right\rangle, \tag{4.2.4}$$

and $\mathcal{S}_{\boldsymbol{k}}$ is defined by (2.4.6).

4.2.1 Numerically optimal bounds

The best bound on $\overline{\langle wT \rangle}$ can be approximated numerically at any fixed Raleigh number by discretising the problem of bounding (4.2.3) into an SDP [44, 46, 47, 140, 141]. As discussed in section §3.3.1 obtaining numerical bounds for non-negative temperature fields requires a piecewise-linear finite element approximation of the fields and tunable functions $(\hat{T}_0, \hat{T}_{\boldsymbol{k}}, \hat{w}_{\boldsymbol{k}}, \tau(z), \lambda(z))$ to enforce the condition on $\lambda(z)$ and sufficiently capture the steep boundary layers of $\tau(z)$. In this section we are not enforcing the minimum principle and as such do not, at least to the same extent, face the same problems in resolution of the $\tau(z)$. For this reason and due to its faster implementation we utilise the MATLAB package QUINOPT. This toolbox employs truncated Legendre series expansions to approximate $\tau(z)$ and the unknown temperature and velocity fields [51].

We set the horizontal periods $L_x = L_y = 2$, using a Legendre series up to sufficient terms until the change in the value of the bound U is below the tolerance level of 10^{-6}. Wavenumbers are checked up until the critical wavenumber k_c, where k_c is the largest k for which the infimum of $\mathcal{S}_{\boldsymbol{k}}$ is zero and can be calculated by the results of the following Lemma.

Lemma 4.2.1. *Fix R, α, β and $\tau(z)$ and let $f \in L^2(0,1)$. The inequality $\mathcal{S}_{\boldsymbol{k}}\{\hat{w}_{\boldsymbol{k}}, \hat{T}_{\boldsymbol{k}}\} \geq 0$ holds for all $\hat{w}_{\boldsymbol{k}}$ and $\hat{T}_{\boldsymbol{k}}$ if*

$$k^4 \geq \frac{R}{4\alpha\beta} \, \|f - \tau'(z)\|_\infty^2 \, . \tag{4.2.5}$$

Remark 4.2.1. Lemma 4.2.1 is stated in terms of a general f so as to be of use for other thermal boundary conditions (see chapter 7).

A stronger condition than the spectral constraint as given by (2.4.6) will be defined for computational ease and to prove bounds on $\overline{\langle wT \rangle}$ in this chapter. The simplified constraint when the boundary conditions are (4.1.1) is

$$\widetilde{\mathcal{S}}_{\boldsymbol{k}} := \left\langle \frac{\alpha}{Rk^2}|\hat{w}_{\boldsymbol{k}}''|^2 + \beta k^2 |\hat{T}_{\boldsymbol{k}}|^2 - (\alpha - \tau'(z))\hat{w}_{\boldsymbol{k}}\hat{T}_{\boldsymbol{k}} \right\rangle \geq 0 \quad \forall (\boldsymbol{u}, T) \in \mathbb{A}. \tag{4.2.6}$$

Note then that $\widetilde{\mathcal{S}}_{\boldsymbol{k}} \geq 0$ for all $\boldsymbol{k}$ is sufficient to enforce $\mathcal{S}_{\boldsymbol{k}} \geq 0$, where $\mathcal{S}_{\boldsymbol{k}}$ was originally defined in (2.4.6). We can now replace $\mathcal{S}_{\boldsymbol{k}}$ by $\widetilde{\mathcal{S}}_{\boldsymbol{k}}$ to obtain the problem

$$\begin{aligned} \inf_{U,\tau(z),\alpha,\beta} \quad & U \\ \text{subject to} \quad & \mathcal{S}_0\{\hat{T}_0\} \geq 0 \qquad \forall \hat{T}_0 : (4.2.2\text{b}), \\ & \widetilde{\mathcal{S}}_{\boldsymbol{k}}\{\hat{w}_{\boldsymbol{k}}, \hat{T}_{\boldsymbol{k}}\} \geq 0 \quad \forall \hat{w}_{\boldsymbol{k}}, \hat{T}_{\boldsymbol{k}} : (4.2.2a,b), \quad \boldsymbol{k} \neq 0 \, . \end{aligned} \tag{4.2.7}$$

The positive terms in the functional $\widetilde{\mathcal{S}}_{\boldsymbol{k}}$ are necessary to demonstrate the condition that $\widetilde{\mathcal{S}}_{\boldsymbol{k}} \geq 0$ analytically in §4.2.2 and §4.3. This can be understood intuitively from the boundary conditions. At $z = 0$ the boundary conditions (4.1.1) imply that $w \sim z^2$ while $T \sim c$, for some constant $c \in \mathbb{R}$. Then $\mathcal{S}_{\boldsymbol{k}}$ in (2.4.6) is approximately

$$\mathcal{S}_{\boldsymbol{k}} \sim \left\langle \frac{\alpha}{R\,k^2} \underbrace{c^2}_{|w''|^2} + \frac{\alpha}{R} \underbrace{z^2}_{|w'|^2} + \frac{\alpha k^2}{R} \underbrace{z^4}_{|w|^2} + \underbrace{0}_{|T'|^2} + \beta k^2 \underbrace{c^2}_{|T|^2} - (\alpha - \tau'(z)) \underbrace{cz^2}_{wT} \right\rangle ,$$

so that the positive $|T'|^2$ term no longer suffices to balance the sign-indefinite wT term of order cz^2. Given some balance of the parameters α, β and R only the $|T|^2$

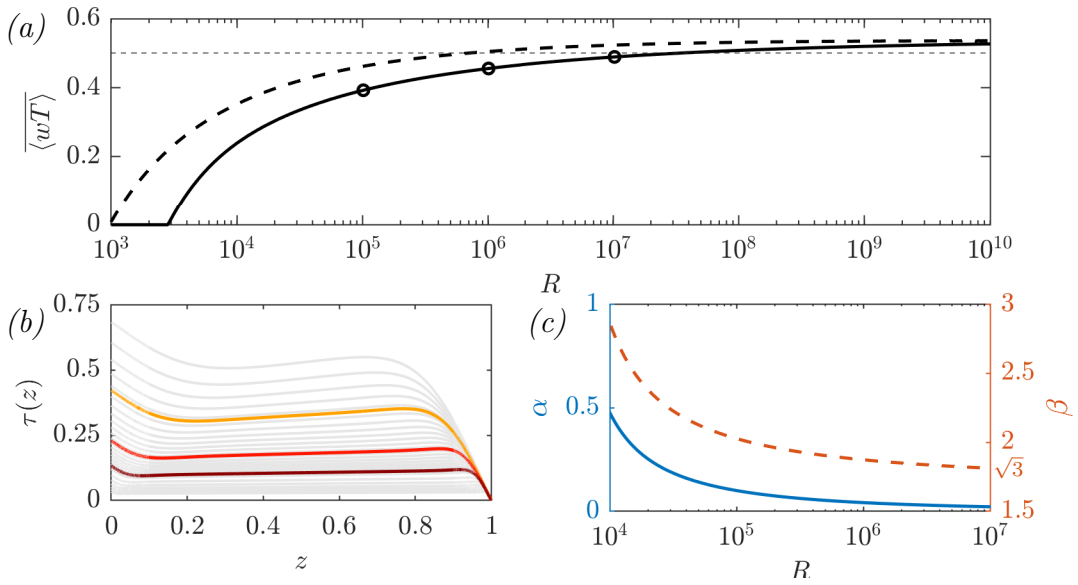

Figure 4.2: *(a)* Optimal bounds on $\overline{\langle wT \rangle}$ obtained by solving the wavenumber-dependent problem (2.4.12) with horizontal periods $L_x = L_y = 2$ (—) and the simplified problem (4.2.7)(- - -). The dashed horizontal line (- - -) is the uniform bound $\overline{\langle wT \rangle} \leq \frac{1}{2}$. Circles mark values of R at which optimal profiles $\tau(z)$ are plotted in panel *(b)*. *(b)* Optimal profiles $\tau(z)$ at $R = 10^5$ (—), 10^6 (—) and 10^7 (—). *(c)* Optimal balance parameters α (—, left axis) and β (- - -, right axis) as a function of R.

and $|w''|^2$ terms are of sufficient order in z, near the lower boundary, to ensure $\mathcal{S}_{\boldsymbol{k}} \geq 0$.

The numerical optimisation is carried out using both $\widetilde{\mathcal{S}}_{\boldsymbol{k}}$ and $\mathcal{S}_{\boldsymbol{k}}$. The bounds with both functionals are plotted in Figure 4.2*(a)*. While the original constraint provides the better numerical bound, the later will be used to obtain the analytical result in §4.2.2. So it is useful to observe numerically if any information is lost between the two cases. The optimal $\tau(z)$ are plotted in panel *(b)*, where the gradient at the lower boundary is -1, the balance parameters are shown in *(c)* where for increasing R, β tends to a constant of $\sqrt{3}$.

As was the case for isothermal boundary conditions let us analyse the mean temperature profiles $\hat{T}_0$. Due to the zero flux boundary condition at $z = 0$, the value of $\hat{T}_0(0)$ varies. For the conducting state this is $\frac{1}{2}$ and as the Rayleigh number increases $\hat{T}_0(0)$ decreases and in fact does so to a value below zero as displayed in Figure 4.3*(a)*. Looking closer at the behaviour of the temperature field, Figure 4.3*(b)*,

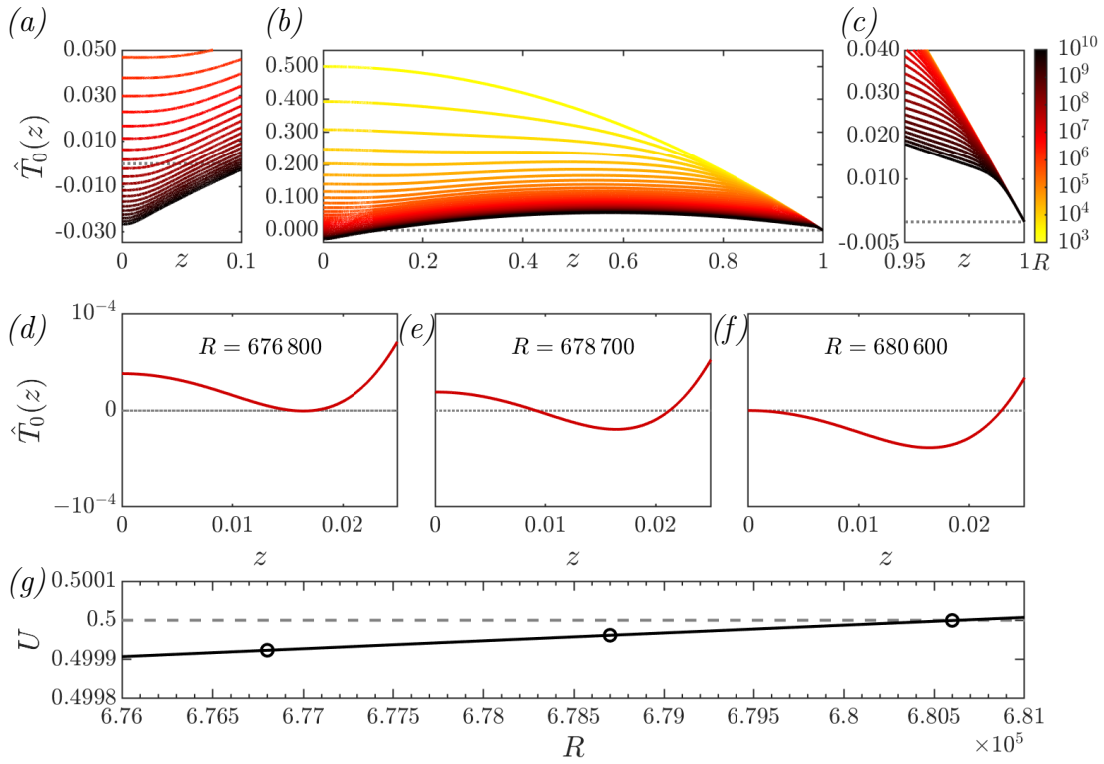

Figure 4.3: *Top*: Critical temperature $\hat{T}_0(z)$ recovered using (2.4.9). Colors indicate the Rayleigh number. Panels *(a)* and *(c)* show details of the boundary layers. *Middle*: Detailed view of $\hat{T}_0$ for $R = 676\,800$, $678\,700$, and $680\,600$. In *(d)*, $\hat{T}_0$ is nonnegative and has minimum of zero inside the layer. In *(e)*, $\hat{T}_0$ is initially positive but has a negative minimum. In *(f)*, $\hat{T}_0(0) = 0$ and there is no positive initial layer. *Bottom*: Upper bounds U on $\overline{\langle wT \rangle}$. Circles mark the values of Ra considered in *(d–f)* and $U = \frac{1}{2}$ at $R = 680\,600$.

as the Rayleigh number increases the value of $\hat{T}_0$ decreases in the bulk too, however the minimum of $\hat{T}_0$ occurs at a $z = \epsilon > 0$ (panels *(d)-(f)*). The minimum of $\hat{T}_0$ is first exactly equal to zero for $R = 676\,800$, for which the value of the bound $U < \frac{1}{2}$ *(g)*. Highlighted in *(e)* is the profile of $\hat{T}_0$ near the boundary where clearly for a range of z, $\hat{T}_0$ is negative and yet the value of U remains below $\frac{1}{2}$ as seen in *(g)*. When $U = \frac{1}{2}$ at $R = 680\,600$, we find that $\hat{T}_0(0) = 0$, and then for $R > 680\,600$ the bound on U exceeds $\frac{1}{2}$ and is suboptimal with respect to the known uniform upper bound $\overline{\langle wT \rangle} \leq \frac{1}{2}$. The behaviour of the optimising temperature fields near the lower boundary is similar to that of the isothermal case. Specifically the temperature field becomes negative for U below $\frac{1}{2}$. The question that arises is if enforcing the

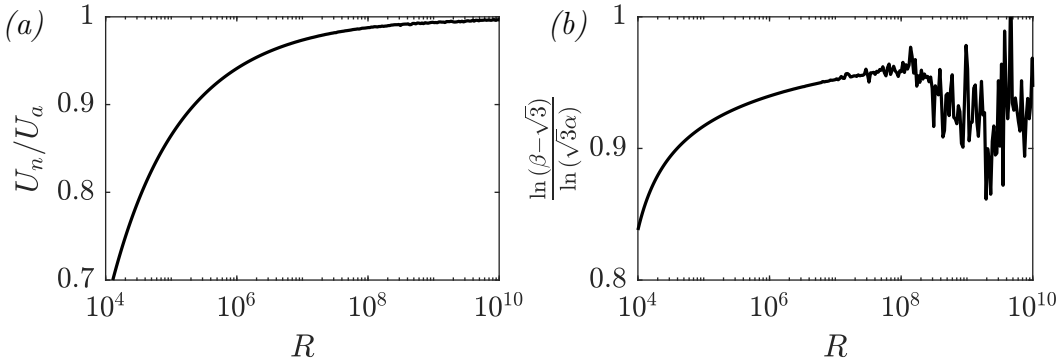

Figure 4.4: *(a)* Plot of a comparison of the numerically optimal bound obtained from solving (4.2.7) and the analytical bound of Theorem 4.1.1. *(b)* Plot comparing the optimal β and α given the relation (4.2.9) chosen for the analytical proof below.

non-negativity of the temperature field gives a bound U that asymptotes to $\frac{1}{2}$ from below as R increases.

In Figure 4.4 we compare the numerically optimal results obtained from solving (3.2.7) with the analytical results in §4.2.2. Panel *(a)* plots the ratio of the numerically optimal bound U and analytical result in Theorem 4.1.1. The agreement between the analytical and numerical bounds approaches 1 as R increases. Above the energy stability for the boundary conditions in this chapter the discrepancy is 0.7, while rapidly approaching 1 in R. In §4.2.2 a simple choice is made relating β and α in (4.2.9), panel *(b)* plots the corrected optimal parameters to see how valid the choice is. If (4.2.9) was exact then we would observe a perfect straight line at 1 for all R. This is not observed. While the value is above 0.85 and increases towards 1, numerical issues leave an inconclusive result for the largest R probed. The results in panel *(b)* indicate an alternative relation between α and β than (4.2.9). However, as will be discussed, such a choice would increase the algebraic complexity and it is not clear if alternative choices improve the analytic bound of Theorem 4.1.1.

As a final note, the bound obtained in this section appears at first glance to match, both in terms of asymptotic limit and R scaling, the one that is found in chapter 7 where the upper boundary has a fixed flux boundary condition. However, it is not apparent whether the two optimisation problems are identical, owing to the

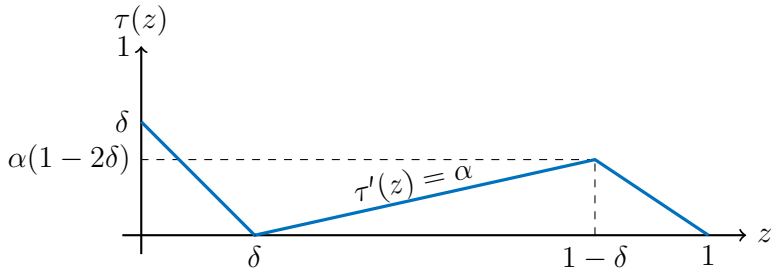

Figure 4.5: General piecewise-linear $\tau(z)$, parametrized by the boundary layer width δ and slopes of -1 near the lower boundary and α in the bulk.

lack of an answer to whether or not the analytical bounds are optimal within the framework of the boundary conditions in this chapter.

4.2.2 Analytical bound

The numerical results in §4.2.1 indicate that by optimising $\tau(z), \alpha, \beta$ we cannot improve the uniform bound $\overline{\langle wT \rangle} \leq \frac{1}{2}$ at arbitrarily large R, and that at best one has the upper bound $\overline{\langle wT \rangle} \lesssim 0.539$. Nevertheless it is possible to derive bounds analytically, that over a finite range of R improve the bound $\overline{\langle wT \rangle} \leq \frac{1}{2}$. This is achieved by considering piecewise-linear profiles $\tau(z)$ with two boundary layers of equal width, such as is sketched in Figure 4.5. The background field is chosen to be

$$\tau(z) := \begin{cases} \delta - z, & 0 \leq z \leq \delta, \\ \alpha(z-\delta), & \delta \leq z \leq 1-\delta, \\ \alpha\delta^{-1}(1-2\delta)(1-z), & 1-\delta \leq z \leq 1. \end{cases} \tag{4.2.8}$$

We also fix

$$\beta = \sqrt{3}(\alpha + 1). \tag{4.2.9}$$

The first preliminary result necessary to obtain Theorem 4.1.1, takes the chosen background profile (4.2.8) and gives an expression for the upper bound U in terms of the boundary layer variable δ.

Lemma 4.2.2. *Let $\tau(z)$ be given by (4.2.8) if $\alpha = \delta \leq \frac{1}{2}$. Then,*

$$U \leq \frac{1}{2}\left(\frac{1}{2} + \frac{1}{\sqrt{3}}\right) - \frac{9+2\sqrt{3}}{72}\delta\,. \tag{4.2.10}$$

Proof. Starting with the expression for the bound from (4.2.4), we evaluate two integrals given τ from (4.2.8). The integral of $\tau(z)$ is

$$\langle \tau \rangle = \frac{1}{2}\delta^2 + \frac{1}{2}\alpha(1-2\delta)(1-\delta). \tag{4.2.11}$$

The second integral is evaluated by expanding the squared term and substituting for β from (4.2.9) to get,

$$\begin{aligned}\frac{1}{4\beta}\left\langle |\beta z - \tau'(z) - 1|^2 \right\rangle &= \frac{\beta}{4}\left\langle z^2 \right\rangle - \frac{1}{2}\left\langle z(\tau'(z)+1) \right\rangle + \frac{1}{4\beta}\left\langle (\tau'(z)+1)^2 \right\rangle \\ &= \frac{\beta}{12} + \int_\delta^1 -\frac{1}{2}z(\tau'(z)+1) + \frac{1}{4\beta}(\tau'(z)+1)^2 \mathrm{d}z \\ &= \frac{3-\sqrt{3}}{24}(\alpha+1)(-1+\sqrt{3}+4\delta) \\ &\quad - \frac{1}{4}(2-\delta)(\delta - \alpha(1-2\delta)) + \frac{\sqrt{3}(\delta-\alpha(1-2\delta))^2}{12\delta(\alpha+1)}. \end{aligned} \tag{4.2.12}$$

Then using both (4.2.11) and (4.2.12) in (4.2.4) gives

$$\begin{aligned}U = \frac{1}{2} + \frac{3-\sqrt{3}}{24}(\alpha+1)(-1+\sqrt{3}+4\delta) - \frac{1}{4}(2-\delta)(\delta-\alpha(1-2\delta)) \\ + \frac{\sqrt{3}(\delta-\alpha(1-2\delta))^2}{12\delta(\alpha+1)} - \frac{1}{2}\delta^2 - \frac{1}{2}\alpha(1-2\delta)(1-\delta).\end{aligned} \tag{4.2.13}$$

The assumption that $\alpha = \delta \leq \frac{1}{2}$, implies the estimate $\frac{1}{1+\delta} \leq \frac{2}{3}$. The upper bound on U becomes

$$U \leq \frac{1}{4} + \frac{\sqrt{3}}{6} - \frac{1}{4}\delta + \frac{3-\sqrt{3}}{6}\delta^2 - \frac{9-4\sqrt{3}}{18}\delta^3. \tag{4.2.14}$$

Finally we estimate the higher order terms in δ given $\delta \leq \frac{1}{2}$ such that

$$\frac{3-\sqrt{3}}{6}\delta^2 - \frac{9-4\sqrt{3}}{18}\delta^3 \leq \frac{9-2\sqrt{3}}{72}\delta.$$

This gives the desired result. □

Next, it will be demonstrated that for a choice of $\delta = \delta(R)$ the spectral constraint $\widetilde{\mathcal{S}}_{\boldsymbol{k}} \geq 0$ is satisfied.

Lemma 4.2.3. *Let $\tau(z)$ be given by (4.2.8). Suppose that α, β and δ satisfy the conditions of Lemma 4.2.2. Further let*

$$\delta = \left(\frac{8\sqrt{3}}{R}\right)^{\frac{1}{3}}, \tag{4.2.15}$$

then the spectral constraint, $\widetilde{\mathcal{S}}_{\boldsymbol{k}} \geq 0$ with $\widetilde{\mathcal{S}}_{\boldsymbol{k}}$ given in (4.2.6), is satisfied for all $\boldsymbol{k} \geq 0$.

Proof. By definition $\tau'([\delta, 1-\delta]) = \alpha$. The sign-indefinite term in (4.2.6) becomes

$$\left\langle (\alpha - \tau'(z))\hat{w}_{\boldsymbol{k}}\hat{T}_{\boldsymbol{k}} \right\rangle = \int_{[0,\delta]\cup[1-\delta,1]} (\alpha - \tau'(z))\hat{w}_{\boldsymbol{k}}\hat{T}_{\boldsymbol{k}}\mathrm{d}z. \tag{4.2.16}$$

By use of the Cauchy-Schwarz inequality for any $\hat{w}_{\boldsymbol{k}} \in H^2(0,1)$ satisfying $\hat{w}_{\boldsymbol{k}}(0) = \hat{w}'_{\boldsymbol{k}}(0) = 0$, we have $\hat{w}'_{\boldsymbol{k}} \leq \sqrt{z}\ \|\hat{w}''_{\boldsymbol{k}}\|_2$ at the lower and $\hat{w}'_{\boldsymbol{k}} \leq \sqrt{1-z}\ \|\hat{w}''_{\boldsymbol{k}}\|_2$ at the upper boundary, which can be used to obtain the estimates

$$\hat{w}_{\boldsymbol{k}}(z) = \int_0^z \hat{w}'_{\boldsymbol{k}}(\eta)\mathrm{d}\eta \leq \tfrac{2}{3}z^{\frac{3}{2}}\|\hat{w}''_{\boldsymbol{k}}\|_2, \qquad z \in (0,1), \tag{4.2.17}$$

$$\hat{w}_{\boldsymbol{k}}(z) \leq \tfrac{2}{3}(1-z)^{\frac{3}{2}}\|\hat{w}''_{\boldsymbol{k}}\|_2, \qquad z \in (0,1). \tag{4.2.18}$$

Given $\delta \leq \frac{1}{2}$ the estimate $1 - 2\delta \leq 1$ holds. Using (4.2.17) and (4.2.18) with $\tau(z)$ given by (4.2.8) and the Cauchy-Schwarz inequality, the sign-indefinite term can be estimated to be

$$\begin{aligned}\int_{[0,\delta]\cup[1-\delta]} (\alpha - \tau'(z))\hat{w}_{\boldsymbol{k}}\hat{T}_{\boldsymbol{k}}\mathrm{d}z &\leq \left(\frac{2}{3}(\alpha+1)\int_0^\delta z^{\frac{3}{2}}|\hat{T}_{\boldsymbol{k}}|\mathrm{d}z \right.\\ &\quad \left. + \frac{2}{3}\alpha\delta^{-1}(1-\delta)\int_{1-\delta}^1 (1-z)^{\frac{3}{2}}|\hat{T}_{\boldsymbol{k}}|\mathrm{d}z\right)\|\hat{w}''_{\boldsymbol{k}}\|_2\\ &\leq \left(\tfrac{1}{3}\delta^2(\alpha+1) + \tfrac{1}{3}\delta\alpha\right)\|\hat{w}''_{\boldsymbol{k}}\|_2\|\hat{T}_{\boldsymbol{k}}\|_2. \end{aligned} \tag{4.2.19}$$

Then, $\widetilde{\mathcal{S}}_{\boldsymbol{k}}$ in (4.2.6) is estimated from below to get

$$\widetilde{\mathcal{S}}_{\boldsymbol{k}} \geq \frac{\alpha}{Rk^2}\|\hat{w}_{\boldsymbol{k}}''\|_2^2 + \beta k^2\|\hat{T}_{\boldsymbol{k}}\|_2^2 - \frac{\delta}{3}\left(\delta(\alpha+1)+\alpha\right)\|\hat{w}_{\boldsymbol{k}}''\|_2\|\hat{T}_{\boldsymbol{k}}\|_2. \tag{4.2.20}$$

The quadratic form is nonnegative under the following condition

$$\delta^2\left(\delta(\alpha+1)+\alpha\right)^2 \leq \frac{36\alpha\beta}{R}. \tag{4.2.21}$$

Given the definition of β from (4.2.9) and the assumption that $\alpha = \delta$ we further simplify to

$$\delta^3\frac{(\delta+2)^2}{(\delta+1)} \leq \frac{36\sqrt{3}}{R}, \tag{4.2.22}$$

Since $\delta \leq \frac{1}{2}$, the estimate $\frac{(\delta+2)^2}{\delta+1} \leq \frac{9}{2}$ holds and taking δ as (4.2.15), the required condition of $\widetilde{\mathcal{S}}_{\boldsymbol{k}} \geq 0$ holds. □

Proof of Theorem 4.1.1

The proof of the Theorem 4.1.1 follows from use of the results of Lemma 4.2.2 and Lemma 4.2.3. We obtain that

$$\overline{\langle wT\rangle} \leq \frac{1}{2}\left(\frac{1}{2}+\frac{1}{\sqrt{3}}\right) - \frac{9+2\sqrt{3}}{72}(8\sqrt{3})^{\frac{1}{3}}\,R^{-\frac{1}{3}}. \tag{4.2.23}$$

Lemma 4.2.2 holds for any $\delta \leq \frac{1}{2}$, given $\widetilde{\mathcal{S}}_{\boldsymbol{k}} \geq 0$. The latter condition of Lemma 4.2.3 holds whenever $\delta = \left(\frac{8\sqrt{3}}{R}\right)^{\frac{1}{3}} \leq \frac{1}{2}$ which is valid for $R \geq 111$.

Remark 4.2.2. The relation between α and β is influenced by the numerical results found in §4.2.1. The relation that $\delta = \alpha$ is one choice that gives a bound approaching $\frac{1}{2}\left(\frac{1}{2}+\frac{1}{\sqrt{3}}\right)$ from below in (4.2.13). The prefactor of the Rayleigh scaling can be improved either by choosing a smaller range of δ at the expense of a bound valid at larger R, or by choosing $\alpha = n\delta$ for $n < 1$. For simplicity we choose $n = 1$.

4.3 An analytical bound utilising the minimum principle

The upper bound derived in §4.2 can be improved by making use of the minimum principle from Lemma 2.3.1 which guarantees that temperature fields solving the Boussinesq equations (1.2.3) are nonnegative in the domain Ω at large time.

The major variation from the previous section is that we optimise over $\lambda(z)$ instead of fixing $\lambda = -1$. Similar to chapter 3 the key ingredients of the proof are; (i) a profile of $\tau(z)$ proportional to $1/z$ near the bottom boundary with multiple boundary layers; and (ii) the use of a Rellich inequality. The upper bound on $\overline{\langle wT \rangle}$ follows from Proposition 2.4.1, allowing $\lambda = \lambda(z)$ so that the optimisation problem is

$$\overline{\langle wT \rangle} \leq \inf_{U,\tau(z),\lambda(z)\alpha,\beta} \{U : \mathcal{S}\{\boldsymbol{u}, T\} \geq -\langle \lambda(z)\partial_z T - \lambda(0)\langle T(z=0)\rangle_h \rangle \ \ \forall (\boldsymbol{u}, T) \in \mathbb{A}\}, \tag{4.3.1}$$

where now $\mathbb{A} = \mathcal{U}_1 \times \mathcal{T}_2^+$ with the condition that

$$\lambda(0) = -1\,, \tag{4.3.2}$$

and where

$$U(\tau, \lambda, \alpha, \beta) := \frac{1}{2} + \left\langle \frac{1}{4\beta} |\beta z - \tau'(z) + \lambda(z)|^2 - \tau(z) \right\rangle. \tag{4.3.3}$$

To prove Theorem 4.1.2 we show that a choice of $\tau(z)$, α, β and $\lambda(z)$ can be made by a suitable adaptation of the method employed for the proof in §3.3.2. We

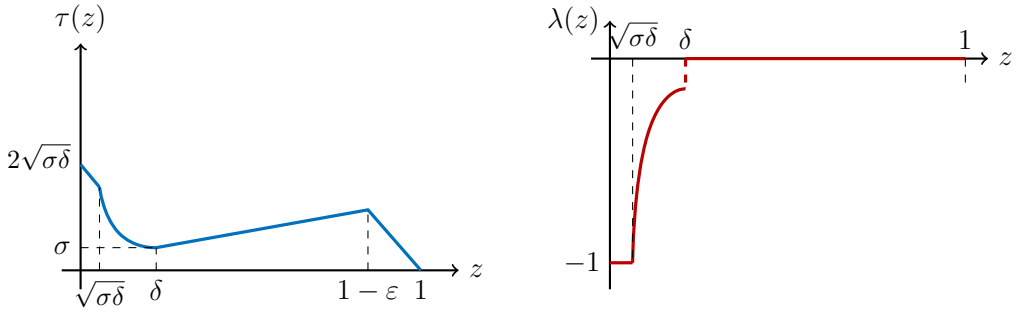

Figure 4.6: Sketch of the piecewise $\tau(z)$ and $\lambda(z)$ in (4.3.4) and (4.3.5).

start by choosing the functions $\tau(z)$ and $\lambda(z)$ to be

$$\tau(z) := \begin{cases} 2\sqrt{\sigma\delta} - z, & 0 \le z \le \sqrt{\sigma\delta}, \\ \dfrac{\sigma\delta}{z}, & \sqrt{\sigma\delta} \le z \le \delta, \\ \sigma + \alpha(z-\delta), & \delta \le z \le 1-\varepsilon, \\ (1-z)\dfrac{\sigma + \alpha(1-\varepsilon-\delta)}{\varepsilon}, & 1-\varepsilon \le z \le 1. \end{cases} \tag{4.3.4}$$

$$\lambda(z) := \begin{cases} -1, & 0 \le z \le \sqrt{\sigma\delta}, \\ -\dfrac{\sigma\delta}{z^2}, & \sqrt{\sigma\delta} \le z \le \delta, \\ 0, & \delta \le z \le 1. \end{cases} \tag{4.3.5}$$

These choices are sketched in Figure 4.6. The constants δ and ε indicate the size of the boundary layers at the lower and upper boundaries respectively. The difference between (4.3.4) and the function $\tau(z)$ used for the isothermal boundaries configuration (§3.3.2) is in the bottom boundary layer ($0 \le z \le \delta$). We require $\lambda(0) = -1$ and at the same time want $\lambda(z) - \tau'(z) = 0$ in the lower boundary so take the inner sublayer of $\tau(z)$ near the bottom boundary ($0 \le z \le \sqrt{\sigma\delta}$) to have slope equal to -1. The outer part of bottom boundary layer ($\sqrt{\sigma\delta} \le z \le \delta$) $\tau(z)$ behaves like z^{-1}. While at the edge of the bottom boundary layer ($z = \delta$), the value of $\tau(z)$ is σ.

Lemma 4.3.1. *Let $\tau(z)$ and $\lambda(z)$ be given by* (4.3.4) *and* (4.3.5) *respectively. Suppose that $\delta, \varepsilon \leq \frac{1}{2}$, $\sigma, \alpha < 1$, and*

$$\alpha = \frac{\sqrt{6}}{8}\sigma\delta\sqrt{\varepsilon}\,\ln\left(\frac{\delta}{\sigma}\right) - \sigma, \tag{4.3.6a}$$

$$\beta = \frac{3}{4}\sigma\delta\ln\left(\frac{\delta}{\sigma}\right). \tag{4.3.6b}$$

Then

$$U(\alpha, \beta, \delta, \varepsilon, \sigma) \leq \frac{1}{2} - \frac{\sigma\delta}{4}\ln\left(\frac{\delta}{\sigma}\right). \tag{4.3.7}$$

Proof. We begin by estimating the first integral in (4.3.3) by using the AMGM inequality and $\tau(z)$ and $\lambda(z)$ as given in (4.3.4) and (4.3.5). The assumptions $\delta, \varepsilon \leq \frac{1}{2}$ imply $1 - \varepsilon - \delta \leq 1$, so

$$\begin{aligned}
\frac{1}{4\beta}\left\langle|\beta z - \tau'(z) + \lambda(z)|^2\right\rangle &\leq \frac{\beta}{2}\left\langle z^2\right\rangle + \frac{1}{2\beta}\left\langle|\tau'(z) - \lambda(z)|^2\right\rangle \\
&= \frac{\beta}{6} + \frac{1}{2\beta}\int_\delta^1 |\tau'(z) - \lambda(z)|^2 \mathrm{d}z \\
&\leq \frac{\beta}{6} + \frac{\alpha^2}{2\beta} + \frac{(\sigma+\alpha)^2}{2\beta\varepsilon} \\
&\leq \frac{\beta}{6} + \frac{(\sigma+\alpha)^2}{\beta\varepsilon}.
\end{aligned} \tag{4.3.8}$$

Estimating the integral of $\tau(z)$ from below,

$$\langle\tau\rangle \geq \int_{\sqrt{\sigma\delta}}^{\delta} \tau(z)\mathrm{d}z = \frac{1}{2}\sigma\delta\ln\left(\frac{\delta}{\sigma}\right). \tag{4.3.9}$$

The inequality holds since $\tau(z) \geq 0$ on $[0, 1]$. Substituting (4.3.8) and (4.3.9) into (4.3.3) gives

$$U \leq \frac{1}{2} + \frac{\beta}{6} + \frac{(\sigma+\alpha)^2}{\beta\varepsilon} - \frac{1}{2}\sigma\delta\ln\left(\frac{\delta}{\sigma}\right). \tag{4.3.10}$$

The result then follows from using both of the relations in (4.3.6). □

Next we consider the sufficient conditions that ensure the satisfaction of (4.2.6). For this we require the following Rellich inequality for weighted integrals.

Lemma 4.3.2 (Rellich inequality)**.** *Let $f : [0,\infty) \to \mathbb{R}$ be a function satisfying $f, f', f'' \in L^2(0,\infty)$ and such that $f(0) = f'(0) = 0$. Then, for any $\epsilon > 0$ and any $\nu \geq 0$,*

$$\int_0^\nu \frac{|f|^2}{(z+\epsilon)^4}\mathrm{d}z \leq \frac{16}{9}\int_0^\nu |f''|^2\mathrm{d}z. \tag{4.3.11}$$

Lemma 4.3.3. *Let $\tau(z)$ be given by (4.3.4) and let $\alpha, \beta, \delta, \varepsilon, \sigma$ satisfy the conditions of Lemma 4.3.1. Suppose further that*

$$\varepsilon = \frac{6}{(\sigma+\alpha)}\sqrt{\frac{\alpha\beta}{R}}, \tag{4.3.12a}$$

$$\delta = \frac{3}{16\sigma}\sqrt{\frac{\alpha\beta}{R}}. \tag{4.3.12b}$$

Then the spectral constraint $\widetilde{\mathcal{S}}_{\boldsymbol{k}} \geq 0$ with $\widetilde{\mathcal{S}}_{\boldsymbol{k}}$ given by (4.2.6) is satisfied.

Proof. Initially we recall $\widetilde{\mathcal{S}}_{\boldsymbol{k}}$ from (4.2.6), given by $z-$dependent functions $\hat{w}_{\boldsymbol{k}}$ and $\hat{T}_{\boldsymbol{k}}$ satisfying the boundary conditions (4.2.2). Substituting for $\tau(z)$ gives

$$\begin{aligned}\widetilde{\mathcal{S}}_{\boldsymbol{k}} = &\int_0^{\sqrt{\sigma\delta}} \frac{\alpha}{Rk^2}|\hat{w}_{\boldsymbol{k}}''|^2 + \beta k^2|\hat{T}_{\boldsymbol{k}}|^2 - (\alpha+1)\,\hat{w}_{\boldsymbol{k}}\hat{T}_{\boldsymbol{k}}\,\mathrm{d}z \\ &+ \int_{\sqrt{\sigma\delta}}^{\delta} \frac{\alpha}{Rk^2}|\hat{w}_{\boldsymbol{k}}''|^2 + \beta k^2|\hat{T}_{\boldsymbol{k}}|^2 - \left(\alpha + \frac{\sigma\delta}{z^2}\right)\hat{w}_{\boldsymbol{k}}\hat{T}_{\boldsymbol{k}}\,\mathrm{d}z \\ &+ \int_{1-\varepsilon}^{1} \frac{\alpha}{Rk^2}|\hat{w}_{\boldsymbol{k}}''|^2 + \beta k^2|\hat{T}_{\boldsymbol{k}}|^2 - \left(\frac{\sigma+\alpha(1-\delta)}{\varepsilon}\right)\hat{w}_{\boldsymbol{k}}\hat{T}_{\boldsymbol{k}}\,\mathrm{d}z.\end{aligned} \tag{4.3.13}$$

Then given the assumption $\alpha \leq 1$ we can make the following estimates

$$8\frac{\sigma\delta}{(z+\sqrt{\sigma\delta})^2} \geq \begin{cases}\alpha+1, & 0 \leq z \leq \sqrt{\sigma\delta}, \\ \alpha + \dfrac{\sigma\delta}{z^2}, & \sqrt{\sigma\delta} \leq z \leq \delta.\end{cases} \tag{4.3.14}$$

By use of these estimates we can combine the first two integrals from (4.3.13) to conclude that

$$\widetilde{\mathcal{S}}_{\boldsymbol{k}}\{\hat{w}_{\boldsymbol{k}}, \hat{T}_{\boldsymbol{k}}\} \geq \widetilde{\mathcal{S}}_{\boldsymbol{k},B}\{\hat{w}_{\boldsymbol{k}}, \hat{T}_{\boldsymbol{k}}\} + \widetilde{\mathcal{S}}_{\boldsymbol{k},T}\{\hat{w}_{\boldsymbol{k}}, \hat{T}_{\boldsymbol{k}}\}, \tag{4.3.15}$$

where

$$\widetilde{\mathcal{S}}_{\boldsymbol{k},B}\{\hat{w}_{\boldsymbol{k}},\hat{T}_{\boldsymbol{k}}\} := \int_0^\delta \frac{\alpha}{Rk^2}|\hat{w}_{\boldsymbol{k}}''|^2 + \beta k^2|\hat{T}_{\boldsymbol{k}}|^2 - 8\frac{\sigma\delta}{(z+\sqrt{\sigma\delta})^2}\hat{w}_{\boldsymbol{k}}\hat{T}_{\boldsymbol{k}}\,\mathrm{d}z, \tag{4.3.16}$$

$$\widetilde{\mathcal{S}}_{\boldsymbol{k},T}\{\hat{w}_{\boldsymbol{k}},\hat{T}_{\boldsymbol{k}}\} := \int_{1-\varepsilon}^1 \frac{\alpha}{Rk^2}|\hat{w}_{\boldsymbol{k}}''|^2 + \beta k^2|\hat{T}_{\boldsymbol{k}}|^2 - \left(\frac{\sigma+\alpha}{\varepsilon}\right)\hat{w}_{\boldsymbol{k}}\hat{T}_{\boldsymbol{k}}\,\mathrm{d}z. \tag{4.3.17}$$

To show $\widetilde{\mathcal{S}}_{\boldsymbol{k}} \geq 0$ it is sufficient to demonstrate $\widetilde{\mathcal{S}}_{\boldsymbol{k},B}\{\hat{w}_{\boldsymbol{k}},\hat{T}_{\boldsymbol{k}}\}$ and $\widetilde{\mathcal{S}}_{\boldsymbol{k},T}\{\hat{w}_{\boldsymbol{k}},\hat{T}_{\boldsymbol{k}}\}$ are both individually nonnegative. Starting with $\widetilde{\mathcal{S}}_{\boldsymbol{k},T}$. Using the fundamental theorem of calculus, the boundary conditions (4.2.2) and the Cauchy-Schwarz inequality, we have that

$$|\hat{w}_{\boldsymbol{k}}(z)|^2 \leq \frac{4}{9}(1-z)^3\int_{1-\varepsilon}^1 |\hat{w}_{\boldsymbol{k}}''|^2\mathrm{d}z, \qquad z\in(1-\varepsilon,1). \tag{4.3.18}$$

Then, substituting (4.3.18) into (4.3.17), using the Cauchy-Scwharz inequality and evaluating the integral gives

$$\widetilde{\mathcal{S}}_{\boldsymbol{k},T} \geq \frac{\alpha}{Rk^2}\|\hat{w}_{\boldsymbol{k}}''\|^2_{L^2(1-\varepsilon,1)} + \beta k^2\|\hat{T}_{\boldsymbol{k}}\|^2_{L^2(1-\varepsilon,1)} - \frac{1}{3}\varepsilon(\sigma+\alpha)\|\hat{w}_{\boldsymbol{k}}''\|_{L^2(1-\varepsilon,1)}\|\hat{T}_{\boldsymbol{k}}\|_{L^2(1-\varepsilon,1)}. \tag{4.3.19}$$

The condition for the quadratic form to be nonnegative is

$$(\sigma+\alpha)\varepsilon \leq 6\sqrt{\frac{\alpha\beta}{R}}. \tag{4.3.20}$$

Let ε be given by (4.3.12a), then $\widetilde{\mathcal{S}}_{\boldsymbol{k},T} \geq 0$, as required.

The nonnegativity of $\widetilde{\mathcal{S}}_{\boldsymbol{k},B}$, instead, can be proven using the Rellich inequality stated in Lemma 4.3.2. First, using Young's inequality with a weight $h > 0$, estimating (4.3.16) from below gives

$$\widetilde{\mathcal{S}}_{\boldsymbol{k},B} \geq \int_0^\delta \frac{\alpha}{Rk^2}|\hat{w}_{\boldsymbol{k}}''|^2 + \beta k^2|\hat{T}_{\boldsymbol{k}}|^2 - \frac{4\sigma\delta h}{(z+\sqrt{\sigma\delta})^4}|\hat{w}_{\boldsymbol{k}}|^2 - \frac{4\sigma\delta}{h}|\hat{T}_{\boldsymbol{k}}|^2\mathrm{d}z. \tag{4.3.21}$$

Next, using the results from Lemma 4.3.2 gives the estimate

$$\int_0^\delta \frac{|\hat{w}|^2}{(z+\sqrt{\sigma\delta})^4}\mathrm{d}z \leq \frac{16}{9}\int_0^\delta |\hat{w}''|^2\mathrm{d}z. \tag{4.3.22}$$

Combining (4.3.22) and (4.3.21) and setting

$$h = \frac{3}{4k^2}\sqrt{\frac{\alpha}{\beta R}}, \tag{4.3.23}$$

we conclude that $\widetilde{\mathcal{S}}_{\boldsymbol{k},B}$ is nonnegative if

$$\sigma\delta \leq \frac{3}{16}\sqrt{\frac{\alpha\beta}{R}}. \tag{4.3.24}$$

Let δ be given by (4.3.12b), then $\widetilde{\mathcal{S}}_{\boldsymbol{k},B} \geq 0$ as required. □

Proof of Theorem 4.1.2

Using the results of Lemma 4.3.1 and Lemma 4.3.3, we make the choices

$$\sigma = \alpha, \qquad \delta = \varepsilon. \tag{4.3.24a,b}$$

The proof of the bound on $\overline{\langle wT\rangle}$ follow from algebraic manipulations to determine the relations between the parameters $(\alpha, \beta, \sigma, \delta, \varepsilon)$. Applying (4.3.24a,b) to (4.3.6a) and (4.3.6b), equating the two equations and rearranging gives that

$$\delta = 24\frac{\alpha^2}{\beta^2}, \tag{4.3.25}$$

which can be combined with δ in (4.3.12b) to give,

$$\alpha = 2^{-\frac{14}{5}}\beta R^{-\frac{1}{5}}. \tag{4.3.26}$$

Using (4.3.26) in (4.3.25) and then both in (4.3.6b) gives,

$$\alpha = \sigma = 2^{-\frac{13}{5}} 3 R^{-\frac{2}{5}} \exp\left(-\frac{2^{\frac{37}{5}}}{9} R^{\frac{3}{5}}\right), \tag{4.3.27a}$$

$$\delta = \varepsilon = 2^{-\frac{13}{5}} 3 R^{-\frac{2}{5}}, \tag{4.3.27b}$$

$$\beta = 2^{\frac{1}{5}} 3 R^{-\frac{1}{5}} \exp\left(-\frac{2^{\frac{37}{5}}}{9} R^{\frac{3}{5}}\right). \tag{4.3.27c}$$

Then Theorem 4.1.2 follows by substituting (4.3.27a) and (4.3.27b) into (4.3.7) to obtain

$$U \leq \frac{1}{2} - 2^{\frac{1}{5}} R^{-\frac{1}{5}} \exp\left(-\frac{2^{\frac{37}{5}}}{9} R^{\frac{3}{5}}\right). \tag{4.3.28}$$

The conditions on $\delta, \varepsilon, \sigma, \alpha$ are all satisfied for all $R > 1$.

Chapter 5

Infinite Prandtl number convection

Man cannot endure his own littleness unless

he can translate it into meaningfulness on the largest possible level.

Ernest Becker - The Denial of Death

In this chapter, we demonstrate that the scaling laws on $\overline{\langle wT \rangle}$ can approach $\frac{1}{2}$ with algebraic powers when the Prandtl number is infinite. The results presented appear in publication [3]. By infinite Pr we are considering the case of internally heated convection where the inertial and $\partial_t \boldsymbol{u}$ terms in the momentum equation (1.2.3b) are insignificant with respect to the Laplacian of velocity and buoyancy terms. As such the momentum equation describes a Stokes flow with forcing due to buoyancy. While the flows between infinite and finite Pr are different, the problems are closely enough related so that the quantity of interest is the mean vertical convective heat transport $\overline{\langle wT \rangle}$, akin to the $Pr < \infty$ case. In fact, for Rayleigh–Bénard convection this is a rigorously established fact [153, 154]. Unique to this chapter are two new features in the construction of the background fields $\tau(z)$: (i) $\tau(z)$ that have logarithmic or power law variation in the bulk of the domain and (ii) boundary layer widths of $\tau(z)$ that are not equal and thus scale differently with R. In contrast, the background fields in chapter 3 and chapter 4 had boundary layers of equal width.

5.1 Setup

The motion of the fluid is governed by the infinite Prandtl number Boussinessq equations

$$\nabla \cdot \boldsymbol{u} = 0\,, \tag{5.1.1a}$$

$$\nabla p = \Delta \boldsymbol{u} + R\,T\mathbf{e}_3\,, \tag{5.1.1b}$$

$$\partial_t T + \boldsymbol{u} \cdot \nabla T = \Delta T + 1. \tag{5.1.1c}$$

The flow is controlled by the same 'flux' Rayleigh number, R, defined in (1.2.4).

We consider two separate configurations that differ in the choice of thermal boundary condition at the bottom ($z = 0$) of the domain. The first configuration is identical to that considered in chapter 3, Figure 1.1*(a)*; the velocity satisfies no-slip conditions and boundaries are isothermal which can be taken as zero without loss of generality. The second configuration has the same boundary conditions as that considered in chapter 4, illustrated by Figure 1.1*(b)* where only the bottom plate is replaced by a perfect thermal insulator.

Theorem 5.1.1 (Isothermal case, $Pr = \infty$)**.** *Suppose that* $\boldsymbol{u} = (u, v, w)$ *and* T *solve* (5.1.1) *subject to the no-slip isothermal boundary conditions* (1.2.5c)*. There exists a constant* $c > 0$ *such that for sufficiently large* $R > 0$*,*

$$\overline{\langle wT \rangle} \leq \frac{1}{2} - c\,R^{-2}. \tag{5.1.2}$$

Remark 5.1.1. It is shown in §5.2.3 that Theorem 5.1.1 holds with $c = 216$ for any $R > 1892$.

Upper bounds on $\overline{\langle wT \rangle}$ imply bounds on the heat flux out of the top and bottom boundaries.

Corollary 5.1.1. *For sufficiently large R,*

$$\mathcal{F}_T \leq 1 - c\,R^{-2} \qquad \text{and} \qquad \mathcal{F}_B \geq c\,R^{-2}. \tag{5.1.3}$$

Similar results hold also for the case where the bottom boundary is perfectly insulating.

Theorem 5.1.2 (Insulating bottom, isothermal top, $Pr = \infty$)**.** *Suppose that $\boldsymbol{u} = (u, v, w)$ and T solve* (5.1.1) *subject to the boundary conditions* (1.2.5d)*. There exists a constant $c > 0$ such that for sufficiently large $R > 0$,*

$$\overline{\langle wT \rangle} \leq \frac{1}{2} - c\,R^{-4}. \tag{5.1.4}$$

Remark 5.1.2. It is shown in §5.3.3 that Theorem 5.1.2 holds with $c \approx 0.0107$ for all $R > 2961$.

Upper bounds on $\overline{\langle wT \rangle}$ can be transformed into an upper bound on Nu as defined in (1.2.16).

Corollary 5.1.2. *For sufficiently large R, $Nu \leq cR^4$.*

The proofs of Theorems 5.1.1 and 5.1.2 rely on two key ingredients. The first is a variational problem giving an upper bound on $\overline{\langle wT \rangle}$. To this end we need only to adapt the framework outlined in §2.3.1 by setting $\alpha = 0$. In contrast to chapter 3 and chapter 4 we only prove bounds that make use of the minimum principle.

The second key ingredient in the proofs are estimates of Hardy–Rellich type, obtained by observing that the reduced momentum equation (5.1.1b) determines the vertical velocity field as a function of the temperature field. Specifically, taking the vertical component of the double curl of (5.1.1b) gives

$$\Delta^2 w = -R\,\Delta_h T, \tag{5.1.5}$$

where $\Delta_h := \partial_x^2 + \partial_y^2$, is the horizontal Laplacian. Using the no-slip boundary conditions with the incompressibility condition (5.1.1a), the vertical velocity w satisfies

$$w|_{z=0} = \partial_z w|_{z=0} = w|_{z=1} = \partial_z w|_{z=1} = 0. \tag{5.1.6}$$

The vertical velocity can be viewed as slaved to the temperature field via (5.1.5). Equation (5.1.5) was exploited in Rayleigh–Bénard convection to obtain scaling laws on Nu that agreed with the classical scaling [35]. This was achieved by using (5.1.5) to derive inequalities of the Hardy–Rellich type (c.f. Lemma 5.2.4 below) that help the construction of a background field with a logarithmically-varying stable stratification in the bulk [35, 167]. Here, we use the same inequalities to construct (different) background fields suited to internally heated convection, which will enable us to bound $\overline{\langle wT \rangle}$ in the infinite Pr limit. In contrast with chapter 3 and chapter 4 the analysis carried out in this chapter does not pass into Fourier space. It turns out this is not necessary to obtain Theorem 5.1.1 and Theorem 5.1.2 such that for brevity of the argument and notation the results are presented without using a Fourier decomposition.

5.2 Bounds for isothermal boundaries

We first consider isothermal boundaries, where the top and bottom are held at zero temperature. Stated succinctly $(\boldsymbol{u}, T) \in \mathbb{A} = \mathcal{U}_1 \times \mathcal{T}_1^+$ as defined in (2.1.2). We first show that $\overline{\langle wT \rangle}$ can be bounded from above by constructing suitably constrained functions of the vertical coordinate z. Section 5.2.1 describes parametric ansätze for such functions, while §5.2.2 establishes auxiliary results that simplify the verification of the constraints and the evaluation of the bound. We then prove Theorem 5.1.1 in §5.2.3 by prescribing R-dependent values of the free parameters in our ansätze.

To bound $\overline{\langle wT \rangle}$ we take the quadratic auxiliary functional in (2.2.5) with the balance parameter α set to zero. The upper bound on $\overline{\langle wT \rangle}$ is given by (2.4.1),

parametrized by the balance parameter $\beta \in \mathbb{R}_+$ and the background field $\tau : [0,1] \to \mathbb{R}$ a piecewise-differentiable function with square-integrable derivative. We require $\tau(z)$ to satisfy

$$\tau(0) = 1, \qquad \tau(1) = 0. \tag{5.2.1}$$

The pair $(\beta, \tau(z))$ is said to satisfy the *spectral constraint* if

$$\left\langle \beta \left|\nabla T\right|^2 + \tau'(z) wT \right\rangle \geq 0, \tag{5.2.2}$$

where $T \in \mathcal{T}_1^+$ (2.1.3a) and $w = -R\Delta^{-2}\Delta_h T$ solves (5.1.5) with the boundary conditions (5.1.6). If the spectral constraint is satisfied, then it is possible to bound $\overline{\langle wT \rangle}$ from above in terms of τ, β, and the Lagrange multiplier $\lambda : [0,1] \to \mathbb{R}$.

Proposition 5.2.1 (Bounding framework, IH1)**.** *Suppose that the pair* $(\beta, \tau(z))$ *satisfies the spectral constraint and the boundary conditions in* (5.2.1)*. Further, let* $\lambda \in L^2(0,1)$ *be any nondecreasing function such that* $\langle \lambda(z) \rangle = -1$*. Then,*

$$\overline{\langle wT \rangle} \leq \frac{1}{2} + \left\langle \frac{1}{4\beta} \left| \tau'(z) - \lambda(z) - \beta\left(z - \frac{1}{2}\right)\right|^2 - \tau(z) \right\rangle =: U(\tau, \lambda, \beta).$$

Proof. The quadratic auxiliary functional used is

$$\mathcal{V}\{T\} = \left\langle \frac{\beta}{2} \left| T - \frac{\tau(z) + z - 1}{\beta} \right|^2 \right\rangle. \tag{5.2.3}$$

Then the same steps as in chapter 3 apply to give the estimate

$$\overline{\langle wT \rangle} \leq \tfrac{1}{2} + \sup_{\substack{T \in \mathcal{T}_1^+ \\ w = -R\Delta^{-2}\Delta_h T}} \left\langle -\beta \left|\nabla T\right|^2 - \tau'(z) wT + (\tau'(z) - \beta z)\partial_z T - \tau(z) \right\rangle. \tag{5.2.4}$$

This upper bound is finite if and only if the pair (β, τ) satisfies the spectral constraint of (5.2.2), in which case the supremum over T can be evaluated as before. The result

of the argument in §2.3.1 is that the bound in (5.2.4) is equivalent to

$$\overline{\langle wT\rangle} \leq \tfrac{1}{2} + \inf_{\substack{\lambda\in L^2(0,1)\\ \lambda \text{ nondecreasing}\\ \langle\lambda\rangle=-1}} \left\langle \tfrac{1}{4\beta}\left|\tau' - \lambda(z) - \beta\left(z-\tfrac{1}{2}\right)\right|^2 - \tau(z)\right\rangle. \tag{5.2.5}$$

The bound on $\overline{\langle wT\rangle}$ as presented in (5.2.5) follows from the fact that $\mathcal{S}_0$ in (2.4.5) is independent of α. Since we take α as zero, the proof follows identically by demonstrating the condition for which $\mathcal{S}_0 \geq 0$ as in §2.3.1 . □

Remark 5.2.1. The best upper bound on $\overline{\langle wT\rangle}$ provable with our approach is found upon minimizing the expression $U(\tau, \lambda(z), \beta(z))$ over all choices of $\tau(z)$, $\lambda(z)$ and β that satisfy the conditions of Proposition 5.2.1. This is hard to do analytically, but can be done computationally using a variety of numerical schemes (see Ref [41] and references therein). We leave such computations to future work and focus on proving Theorem 5.1.1 by constructing suboptimal $\tau(z)$, $\lambda(z)$ and β analytically.

Remark 5.2.2. The expression of U, conditions on $\tau(z)$ and $\lambda(z)$ are the same in this section as compared to bounding $\overline{\langle wT\rangle}$ at arbitrary Pr presented in §3.3. At this stage, having not chosen $\tau(z)$ or $\lambda(z)$, the key differences between the chapters is that: (i) $\alpha = 0$ in $\mathcal{S}_{\boldsymbol{k}}$ given by (2.4.6), so that the spectral constraint for the problem at infinite Pr is instead given by (5.2.2) (ii) there exists the relation (5.1.5) between w and T.

5.2.1 Ansätze

To prove the upper bound on $\overline{\langle wT\rangle}$, we seek $\beta > 0$, $\tau(z)$, and $\lambda(z)$ that satisfy the conditions of Proposition 5.2.1 and make the quantity $U(\beta, \tau, \lambda)$ as small as possible.

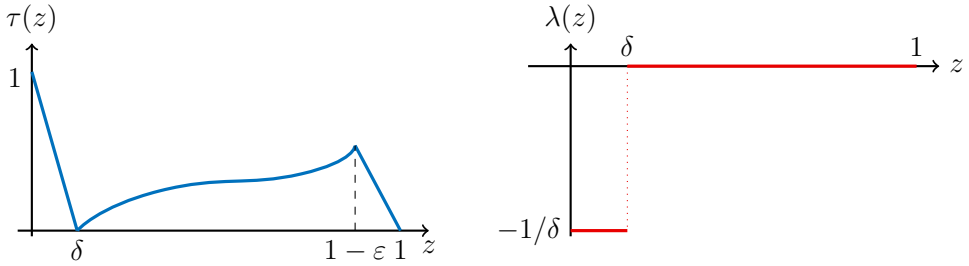

Figure 5.1: Sketches of the functions $\tau(z)$ in (5.2.6) and $\lambda(z)$ in (5.2.7) used to prove Theorem 5.1.1.

To simplify this task, we restrict τ to take the form

$$\tau(z) := \begin{cases} 1 - \dfrac{z}{\delta}, & 0 \le z \le \delta, \\ A \ln\left(\dfrac{z(1-\delta)}{\delta(1-z)}\right), & \delta \le z \le 1-\varepsilon, \\ A \ln\left(\dfrac{(1-\varepsilon)(1-\delta)}{\varepsilon\delta}\right)\left(\dfrac{1-z}{\varepsilon}\right), & 1-\varepsilon \le z \le 1. \end{cases} \tag{5.2.6}$$

and λ to be given by

$$\lambda(z) := \begin{cases} -\dfrac{1}{\delta}, & 0 \le z \le \delta, \\ 0, & \delta \le z \le 1. \end{cases} \tag{5.2.7}$$

These piecewise-defined functions, sketched in Figure 5.1, are fully specified by the bottom boundary layer width $\delta \in (0, \frac{1}{2})$, the top boundary layer width $\varepsilon \in (0, \frac{1}{2})$, and the parameter $A > 0$ that determines the amplitude of $\tau(z)$ in the bulk of the layer.

We also fix

$$\beta := \left\langle |\tau'(z) - \lambda(z)|^2 \right\rangle^{\frac{1}{2}} \left\langle |z - \tfrac{1}{2}|^2 \right\rangle^{-\frac{1}{2}} = 2\sqrt{3} \left\langle |\tau'(z) - \lambda(z)|^2 \right\rangle^{\frac{1}{2}}. \tag{5.2.8}$$

This choice is motivated by the desire to minimize the right-hand side of the inequality

$$\frac{1}{4\beta} \left\langle |\tau'(z) - \lambda(z) - \beta\left(z - \tfrac{1}{2}\right)|^2 \right\rangle \le \frac{\beta}{2} \left\langle |z - \tfrac{1}{2}|^2 \right\rangle + \frac{1}{2\beta} \left\langle |\tau'(z) - \lambda(z)|^2 \right\rangle, \tag{5.2.9}$$

which is used later in Lemma 5.2.2 by estimating from above the bound $U(\beta, \tau, \lambda)$ given the choices of $\tau(z)$ and $\lambda(z)$.

For any choice of the parameters δ, ε, and A, the function $\tau(z)$ satisfies the boundary conditions in (5.2.1), while $\lambda(z)$ is nondecreasing and satisfies the normalization condition $\langle\lambda(z)\rangle = -1$. To establish Theorem 5.1.1 using Proposition 5.2.1, we need to specify parameter values such that $U(\beta, \tau, \lambda) \leq \frac{1}{2} - O(R^{-2})$ while ensuring that the pair $(\beta, \tau(z))$ satisfies the spectral constraint. For the purposes of simplifying the algebra in what follows, we shall fix

$$A(\delta) = \frac{3\sqrt{15}}{20}\delta^{\frac{3}{2}} \tag{5.2.10}$$

from the outset. As explained in remark 5.2.5 below, this choice arises when insisting that the upper estimate on $U(\beta, \tau, \lambda)$ derived in Lemma 5.2.2 be strictly less than $\frac{1}{2}$ for values of δ and ε, at least when all other constraints on these parameters are ignored.

5.2.2 Preliminary estimates

We now derive a series of auxiliary results that make it simpler to specify the boundary layer widths δ and ε. The first result gives estimates on the value of β defined by (5.2.8).

Lemma 5.2.1 (Estimates on β)**.** *Let $\tau(z)$, $\lambda(z)$ and β be given by* (5.2.6)*,* (5.2.7)*, and* (5.2.8) *with A specified by* (5.2.10)*. Suppose that the boundary layer widths δ and ε satisfy*

$$\delta \leq \frac{1}{6}, \qquad \varepsilon \leq \frac{1}{3}, \qquad \delta \ln^2\left(\frac{1}{\delta^2}\right) \leq \varepsilon. \tag{5.2.11a,b,c}$$

Then,

$$\frac{9}{2\sqrt{5}}\delta \leq \beta \leq \frac{9}{2}\delta. \tag{5.2.12}$$

Remark 5.2.3. Condition (5.2.11c) is the key to proving the auxiliary results of this section. The other two restrictions, instead, are introduced to more easily keep track

of constants in our estimates, which is necessary to obtain an explicit prefactor for the $O(R^{-2})$ term. We have not attempted to optimize this prefactor.

Remark 5.2.4. Condition (5.2.11c) implies that $\delta \leq \varepsilon$. We will use this fact often in the proofs of this section.

Proof of Lemma 5.2.1. It suffices to estimate $\langle |\tau'(z) - \lambda(z)|^2 \rangle^{\frac{1}{2}}$ from above and below. For a lower bound, substitute our choices for $\tau(z)$ and $\lambda(z)$ to estimate

$$\left\langle |\tau'(z) - \lambda(z)|^2 \right\rangle = \int_\delta^1 |\tau'(z)|^2 \, \mathrm{d}z \geq \int_\delta^{1-\varepsilon} |\tau'(z)|^2 \, \mathrm{d}z = A^2 \int_\delta^{1-\varepsilon} \left| \frac{1}{z} + \frac{1}{1-z} \right|^2 \, \mathrm{d}z.$$

Expanding the square, dropping the nonnegative term $\frac{2}{z(1-z)}$, and recalling that $\varepsilon \leq \frac{1}{3}$ and $\delta \leq \frac{1}{6} < \frac{1}{3}$ by assumption, we can further estimate

$$\left\langle |\tau'(z) - \lambda(z)|^2 \right\rangle \geq A^2 \left(\int_\delta^{2/3} \frac{1}{z^2} \, \mathrm{d}z + \int_{1/3}^{2/3} \frac{1}{(1-z)^2} \, \mathrm{d}z \right) = \frac{A^2}{\delta}. \tag{5.2.13}$$

Taking the square root of both sides and substituting for the value of A from (5.2.10) gives $\langle |\tau'(z) - \lambda(z)|^2 \rangle^{1/2} \geq \frac{3\sqrt{15}}{20} \, \delta$, which combined with (5.2.8) proves the lower bound on β stated in (5.2.12).

For the upper bound on β, recall that condition (5.2.11c) implies $\delta \leq \varepsilon$, so $1 - \varepsilon \leq 1 - \delta \leq 1$. Then,

$$\begin{aligned} \frac{\langle |\tau'(z) - \lambda(z)|^2 \rangle}{A^2} &= \int_\delta^{1-\varepsilon} \left| \frac{1}{z} + \frac{1}{1-z} \right|^2 \, \mathrm{d}z + \frac{1}{\varepsilon} \ln^2 \left(\frac{(1-\varepsilon)(1-\delta)}{\varepsilon \delta} \right) \\ &\leq \int_\delta^{1-\delta} \left| \frac{1}{z} + \frac{1}{1-z} \right|^2 \, \mathrm{d}z + \frac{1}{\varepsilon} \ln^2 \left(\frac{1}{\delta^2} \right). \end{aligned}$$

Using the inequality $(a+b)^2 \leq 2a^2 + 2b^2$ we can further estimate

$$\begin{aligned} \frac{\langle |\tau'(z) - \lambda(z)|^2 \rangle}{A^2} &\leq 2 \left(\int_\delta^{1-\delta} \frac{1}{z^2} \, \mathrm{d}z + \int_\delta^{1-\delta} \frac{1}{(1-z)^2} \, \mathrm{d}z \right) + \frac{1}{\varepsilon} \ln^2 \left(\frac{1}{\delta^2} \right) \\ &= \frac{4}{\delta} \left(\frac{1-2\delta}{1-\delta} \right) + \frac{1}{\varepsilon} \ln^2 \left(\frac{1}{\delta^2} \right). \end{aligned}$$

Finally, we observe that $\frac{1-2\delta}{1-\delta} \leq 1$ for all $\delta \geq 0$ and apply (5.2.11c) to arrive at

$$\left\langle |\tau'(z) - \lambda(z)|^2 \right\rangle \leq \frac{5A^2}{\delta}. \tag{5.2.14}$$

Substituting our choice of A from (5.2.10) and taking a square root gives

$$\left\langle |\tau'(z) - \lambda(z)|^2 \right\rangle^{\frac{1}{2}} \leq \frac{3\sqrt{3}}{4}\,\delta, \tag{5.2.15}$$

which combined with (5.2.8) yields the upper bound on β in (5.2.12). □

Our second auxiliary result estimates the upper bound $U(\beta, \tau, \lambda)$ on $\overline{\langle wT \rangle}$ from Proposition 5.2.1 in terms of the bottom boundary layer width δ alone.

Lemma 5.2.2 (Estimates on $U(\beta, \tau, \lambda)$)**.** *Let $\tau(z)$, $\lambda(z)$ and β be given by* (5.2.6)*,* (5.2.7)*, and* (5.2.8) *with A specified by* (5.2.10)*. Suppose the boundary layer widths δ and ε satisfy the conditions of Lemma 5.2.1. Then,*

$$U(\beta, \tau, \lambda) \leq \frac{1}{2} - \frac{\delta}{8}. \tag{5.2.16}$$

Proof. Using inequality (5.2.9), the choice of β from (5.2.8), and the upper bound on $\langle |\tau'(z) - \lambda(z)|^2 \rangle$ from (5.2.14) yields

$$U(\beta, \tau, \lambda) \leq \frac{1}{2} + \frac{\sqrt{3}}{6}\left\langle |\tau'(z) - \lambda(z)|^2 \right\rangle^{\frac{1}{2}} - \langle \tau(z) \rangle \leq \frac{1}{2} + \frac{\sqrt{15}A}{6}\,\delta^{-\frac{1}{2}} - \langle \tau(z) \rangle\,.$$

Moreover, since we have chosen τ to be a non-negative function we can estimate $\langle \tau(z) \rangle = \int_0^1 \tau(z)\,\mathrm{d}z \geq \int_0^\delta \tau(z)\,\mathrm{d}z = \frac{1}{2}\delta$, to obtain

$$U(\beta, \tau, \lambda) \leq \frac{1}{2} + \frac{\sqrt{15}A}{6}\,\delta^{-\frac{1}{2}} - \frac{1}{2}\delta. \tag{5.2.17}$$

Substituting the choice of A from (5.2.10) into this inequality gives (5.2.16). □

Remark 5.2.5. The right-hand side of (5.2.17) is strictly smaller than $\frac{1}{2}$ only if $A \lesssim \delta^{3/2}$. It is this observation that dictates the choice of A in (5.2.10). For any fixed value of R, one should choose $A \sim \delta^{3/2}$ with a (possibly R-dependent) prefactor that optimises the balance between the positive and negative terms, subject to constraints on A, δ and all other parameters that ensure the spectral constraint is satisfied. To simplify the proof, however, we choose to fix this prefactor *a priori* irrespective of R.

The final auxiliary result gives sufficient conditions on δ and ε that ensure the spectral constraint (5.2.2) is satisfied.

Lemma 5.2.3 (Sufficient conditions for the spectral constraint)**.** *Let $\tau(z)$, $\lambda(z)$ and β be given by* (5.2.6), (5.2.7), *and* (5.2.8) *with A specified by* (5.2.10). *Suppose the boundary layer widths δ and ε satisfy the conditions of Lemma 5.2.1. Suppose further that*

$$\delta \leq (24\sqrt{3})^2\, R^{-2} \qquad \text{and} \qquad \varepsilon^3 \delta^{\frac{1}{2}}\, \ln^2\left(\frac{1}{\delta^2}\right) \leq 8\sqrt{3} R^{-1}. \tag{5.2.18a,b}$$

Then, the pair $(\beta, \tau(z))$ satisfies the spectral constraint (5.2.2).

The proof of this result relies on Hardy–Rellich inequalities [35], which extract a positive term from the *a priori* indefinite term $\langle \tau'(z) w T \rangle$.

Lemma 5.2.4 (Hardy–Rellich inequalities [35])**.** *Let $T, w : \Omega \to \mathbb{R}$ be horizontally periodic functions such that $\Delta^2 w = -R\Delta_h T$ subject to velocity boundary conditions* (5.1.6). *Then,*

$$\left\langle \frac{wT}{z} \right\rangle \geq \frac{4}{R} \left\langle \frac{w^2}{z^3} \right\rangle \qquad \text{and} \qquad \left\langle \frac{wT}{1-z} \right\rangle \geq \frac{4}{R} \left\langle \frac{w^2}{(1-z)^3} \right\rangle. \tag{5.2.19a,b}$$

Proof of Lemma 5.2.3. Let $\mathbb{1}_{(a,b)}$ denote the indicator function of the interval (a,b). Define the functions

$$f(z) := \left[\frac{1}{\delta} + \frac{A}{z(1-z)}\right] \mathbb{1}_{(0,\delta)}(z), \tag{5.2.20a}$$

$$g(z) := \left[\frac{1}{\varepsilon}\ln\left(\frac{(1-\varepsilon)(1-\delta)}{\varepsilon\delta}\right) + \frac{1}{z(1-z)}\right] \mathbb{1}_{(1-\varepsilon,1)}(z). \tag{5.2.20b}$$

Given the choice of τ from (5.2.6), we can rewrite the spectral constraint as

$$0 \leq \left\langle \beta|\nabla T|^2 + \tau'(z)wT \right\rangle = \mathcal{F}\{T\} + \mathcal{G}\{T\},$$

where

$$\mathcal{F}\{T\} := \frac{\beta}{2}\left\langle |\nabla T|^2 \right\rangle + A\left\langle \frac{wT}{z} \right\rangle - \left\langle f(z)wT \right\rangle, \tag{5.2.21a}$$

$$\mathcal{G}\{T\} := \frac{\beta}{2}\left\langle |\nabla T|^2 \right\rangle + A\left\langle \frac{wT}{1-z} \right\rangle - A\left\langle g(z)wT \right\rangle. \tag{5.2.21b}$$

Here, w is determined as a function of T by solving (5.1.5) subject to the boundary conditions in (5.1.6). We shall prove that $\mathcal{F}$ and $\mathcal{G}$ are individually non-negative.

First, let us consider $\mathcal{F}$. The Hardy–Rellich inequality (5.2.19a) gives

$$\mathcal{F}\{T\} \geq \frac{\beta}{2}\left\langle |\nabla T|^2 \right\rangle + \frac{4A}{R}\left\langle \frac{w^2}{z^3} \right\rangle - \left\langle f(z)wT \right\rangle. \tag{5.2.22}$$

Next, we estimate $\langle f(z)wT\rangle$. Since T vanishes at $z=0$ by virtue of the thermal boundary conditions in (1.2.5c), we can use the fundamental theorem of calculus and the Cauchy-Schwarz inequality to estimate $|T(\cdot,z)| \leq \sqrt{z}(\int_0^1 |\nabla T|^2 \mathrm{d}z)^{1/2}$. Squaring both sides and taking the horizontal average of which gives $\langle T^2\rangle_h \leq z\langle|\nabla T|^2\rangle$. Then, use of the Cauchy–Schwarz inequality, substitution for $\langle T^2\rangle_h$ and Youngs inequality

gives

$$\begin{aligned}\langle f(z)wT\rangle \leq \int_0^1 |f(z)|\,\langle |wT|\rangle_h \,\mathrm{d}z &\leq \int_0^1 |f(z)|\,\langle w^2\rangle_h^{1/2}\,\langle T^2\rangle_h^{1/2}\,\mathrm{d}z \\ &\leq \langle |\nabla T|^2\rangle^{\frac{1}{2}} \int_0^1 f(z) z^2 \left\langle \frac{w^2}{z^3}\right\rangle_h^{\frac{1}{2}} \mathrm{d}z \\ &\leq \langle |\nabla T|^2\rangle^{\frac{1}{2}}\,\langle f(z)^2 z^4\rangle^{\frac{1}{2}} \left\langle \frac{w^2}{z^3}\right\rangle^{\frac{1}{2}} \\ &\leq \frac{\beta}{2}\langle |\nabla T|^2\rangle + \frac{1}{2\beta}\langle f(z)^2 z^4\rangle \left\langle \frac{w^2}{z^3}\right\rangle.\end{aligned}$$

Upon using the lower bound on β from (5.2.12) to estimate the last term from above we obtain

$$\langle f(z)wT\rangle \leq \frac{\beta}{2}\langle |\nabla T|^2\rangle + \frac{\sqrt{5}}{9\delta}\langle f(z)^2 z^4\rangle \left\langle \frac{w^2}{z^3}\right\rangle. \tag{5.2.23}$$

This can be substituted into (5.2.22) along with the choice of A from (5.2.10) to find

$$\mathcal{F}\{T\} \geq \frac{\sqrt{5}}{9}\delta^{\frac{3}{2}}\left(\frac{27\sqrt{3}}{5R} - \frac{\langle f(z)^2 z^4\rangle}{\delta^{\frac{5}{2}}}\right)\left\langle \frac{w^2}{z^3}\right\rangle. \tag{5.2.24}$$

To conclude, we show that the term in parentheses is nonnegative when δ satisfies $\delta \leq \frac{1}{6}$ and (5.2.18a). To do this, we observe that the function $f(z)$ in (5.2.20a) is nonnegative function and that it is nonzero only if $z \leq \delta$. We can therefore bound it from above on the interval $(0,\delta)$ using the estimates $\frac{1}{1-z} \leq \frac{1}{1-\delta} \leq \frac{6}{5}$ and, consequently, obtain

$$\frac{\langle f(z)^2 z^4\rangle}{\delta^{\frac{5}{2}}} \leq \frac{1}{\delta^{\frac{5}{2}}}\int_0^\delta \left(\frac{1}{\delta} + \frac{6A}{5z}\right)^2 z^4\,\mathrm{d}z = \left(\frac{1}{5} + \frac{9\sqrt{15}}{100}\delta^{\frac{3}{2}} + \frac{81}{500}\delta^3\right)\delta^{\frac{1}{2}}.$$

Using the assumption that $\delta \leq \frac{1}{6}$ to estimate the expression in parentheses from its value at $\delta = \frac{1}{6}$, followed by an application of assumption (5.2.18a) to estimate the remaining $\delta^{\frac{1}{2}}$ term in terms of R we arrive at the desired inequality

$$\frac{\langle f(z)^2 z^4\rangle}{\delta^{\frac{5}{2}}} \leq \frac{9\delta^{\frac{1}{2}}}{40} \leq \frac{27\sqrt{3}}{5R}.$$

Analogous arguments show that $\mathcal{G}\{T\}$ is nonnegative. Using the Hardy–Rellich inequality (5.2.19b) we have

$$\mathcal{G}\{T\} \geq \frac{\beta}{2}\left\langle |\nabla T|^2 \right\rangle + \frac{4A}{R}\left\langle \frac{|w|^2}{(1-z)^3} \right\rangle - A\left\langle g(z) w T \right\rangle . \tag{5.2.25}$$

To estimate the last term, we use (in order) the inequality $\langle T^2 \rangle_h \leq (1-z)\left\langle |\nabla T|^2 \right\rangle$, the Cauchy–Schwarz inequality, and Young's inequality:

$$\begin{aligned}
\left\langle g(z) w T \right\rangle \leq \int_0^1 |g(z)| \left\langle |wT| \right\rangle_h \mathrm{d}z &\leq \int_0^1 |g(z)| \left\langle w^2 \right\rangle_h^{1/2} \left\langle T^2 \right\rangle_h^{1/2} \mathrm{d}z \\
&\leq \left\langle |\nabla T|^2 \right\rangle^{\frac{1}{2}} \int_0^1 g(z)(1-z)^2 \left\langle \frac{w^2}{(1-z)^3} \right\rangle_h^{\frac{1}{2}} \mathrm{d}z \\
&\leq \left\langle |\nabla T|^2 \right\rangle^{\frac{1}{2}} \left\langle g(z)^2 (1-z)^4 \right\rangle^{\frac{1}{2}} \left\langle \frac{w^2}{(1-z)^3} \right\rangle^{\frac{1}{2}} \\
&\leq \frac{\beta}{2A}\left\langle |\nabla T|^2 \right\rangle + \frac{A}{2\beta}\left\langle g(z)^2 (1-z)^4 \right\rangle \left\langle \frac{w^2}{(1-z)^3} \right\rangle .
\end{aligned}$$

Using the lower bound on β from (5.2.12) gives

$$\left\langle g(z) w T \right\rangle \leq \frac{\beta}{2A}\left\langle |\nabla T|^2 \right\rangle + \frac{\sqrt{5}A}{9\delta}\left\langle g(z)^2 (1-z)^4 \right\rangle \left\langle \frac{w^2}{(1-z)^3} \right\rangle , \tag{5.2.26}$$

which can be substituted into (5.2.25) along with the value of A from (5.2.10) to obtain

$$\mathcal{G}\{T\} \geq \frac{3\delta^{\frac{3}{2}}}{16\sqrt{5}}\left(\frac{16\sqrt{3}}{R} - \delta^{\frac{1}{2}}\left\langle g(z)^2 (1-z)^4 \right\rangle \right) \left\langle \frac{w^2}{(1-z)^3} \right\rangle . \tag{5.2.27}$$

To conclude the argument we show that the term in parentheses is non-negative. To demonstrate this, we first estimate $g(z)$ on the interval $(1-\varepsilon, 1)$ from above using the assumption that $\varepsilon \leq \frac{1}{3}$, so $\frac{2}{3} \leq z \leq 1$ and $\frac{1}{z(1-z)} \leq \frac{3}{2(1-z)}$. Thus,

$$g(z) \leq \frac{1}{\varepsilon}\ln\left(\frac{1}{\delta^2}\right) + \frac{3}{2(1-z)} \qquad \forall z \in (1-\varepsilon, 1).$$

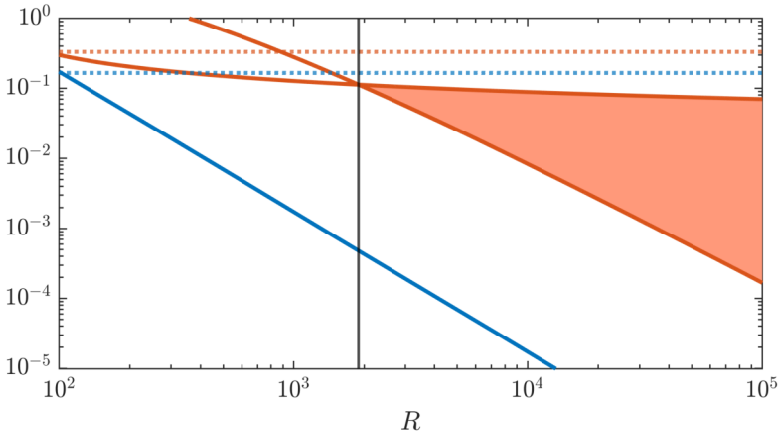

Figure 5.2: Variation with R of the allowed values for the bottom boundary layer width ε (shaded region), determined by condition (5.2.11c) in Lemma 5.2.1 and condition (5.2.18b) in Lemma 5.2.3 when the bottom boundary layer width δ (—) is chosen as in (5.2.28). Also shown are the uniform upper bounds $\delta \leq \frac{1}{6}$ (····) and $\varepsilon \leq \frac{1}{3}$ (····) imposed on these variables. A black vertical line marks the Rayleigh number $R_0 \simeq 1891.35$ above which all constraints on δ and ε are satisfied.

Then, we use the assumptions $\delta \leq \frac{1}{6}$ and $\delta \leq \varepsilon$ (cf. remark 5.2.4) to observe that $\ln\left(\frac{1}{\varepsilon\delta}\right) \leq \ln\left(\frac{1}{\delta^2}\right) \leq \ln^2\left(\frac{1}{\delta^2}\right)$ and $\frac{3}{4} \leq \frac{3}{4}\ln^2\left(\frac{1}{\delta^2}\right)$. Combining these estimates with the upper bound on g derived above gives

$$\begin{aligned}
\delta^{\frac{1}{2}}\left\langle g(z)^2(1-z)^4\right\rangle &\leq \delta^{\frac{1}{2}}\int_{1-\varepsilon}^{1}\left(\frac{1}{\varepsilon}\ln\left(\frac{1}{\delta^2}\right)+\frac{3}{2(1-z)}\right)^2(1-z)^4\,\mathrm{d}z \\
&= \delta^{\frac{1}{2}}\varepsilon^3\left(\frac{1}{5}\ln^2\left(\frac{1}{\delta^2}\right)+\frac{3}{4}\ln\left(\frac{1}{\delta^2}\right)+\frac{3}{4}\right) \\
&\leq 2\delta^{\frac{1}{2}}\varepsilon^3\ln^2\left(\frac{1}{\delta^2}\right) \\
\text{(by (5.2.18b))} \qquad &\leq \frac{16\sqrt{3}}{R},
\end{aligned}$$

as desired. This concludes the proof of Lemma 5.2.3. □

5.2.3 Proof of Theorem 5.1.1

It is now straightforward to prove the upper bound on $\overline{\langle wT\rangle}$ by specifying boundary layer widths δ and ε that satisfy the conditions of Lemmas 5.2.1, 5.2.2 and 5.2.3.

Since the estimate for the resulting upper bound obtained in Lemma 5.2.2 is minimized when δ is as large as possible, we choose the largest value consistent with

(5.2.18a),

$$\delta = (24\sqrt{3})^2 \, R^{-2}. \tag{5.2.28}$$

With this choice of δ, conditions (5.2.11c) and (5.2.18b) require ε to satisfy

$$\frac{27\,648}{R^2} \ln^2\left(\frac{R}{24\sqrt{3}}\right) \leq \varepsilon \leq \left(\frac{1}{48}\right)^{\frac{1}{3}} \ln^{-\frac{2}{3}}\left(\frac{R}{24\sqrt{3}}\right), \tag{5.2.29}$$

which is possible for $R > R_0 \simeq 1891.35$ (cf. Figure 5.2). For $R > R_0$, any choice of ε in this range is feasible. The optimal value could be determined at the expense of more complicated algebra either by optimizing the full bound $U(\beta, \tau, \lambda)$, or by deriving better ε-dependent estimates for it. However, we expect that any ε-dependent terms will contribute only higher-order corrections to the bound on $\overline{\langle wT \rangle}$.

To conclude the proof of Theorem 5.1.1, there remains to verify that the choice of δ is no larger than $\frac{1}{6}$ and that any ε satisfying (5.2.29) is no larger than $\frac{1}{3}$. It is easily checked that both conditions hold when $R \geq R_0$ (see Figure 5.2 for an illustration). For all such values of R, therefore, Lemma 5.2.2 and the choice of δ yield the upper bound $\overline{\langle wT \rangle} \leq U(\beta, \tau, \lambda) \leq \frac{1}{2} - cR^{-2}$ with $c = 216$.

5.3 Bounds for the insulating lower boundary

We now move on to studying the configuration where the top boundary is maintained at constant (zero) temperature and the bottom boundary is insulating. First we highlight the bound for $\overline{\langle wT \rangle}$ following steps similar to those used for the isothermal case (cf. §5.2). In §5.3.1 we present ansätze for $\tau(z)$ and $\lambda(z)$, with which we obtain crucial estimates in §5.3.2 , which give the bound in §5.3.3. Throughout this section we consider $T \in \mathcal{T}_2^+$ defined in (2.1.3a). Observe that this changes the set of temperature fields over which the spectral constraint in (5.2.2) is imposed.

Upper bounds on $\overline{\langle wT \rangle}$ for this configuration where derived in chapter 2, the variation in this chapter being that α is zero, leaving the positive constant β and the

piecewise-differentiable square-integrable function $\tau(z)$ as tunable parameters. Due to the boundary condition at $z = 0$ the $\tau(0)$ term drops from $\mathcal{S}_0$ in (2.4.5). We only need impose that

$$\tau(1) = 0. \tag{5.3.1}$$

These changes result in the following family of parametrized upper bounds on $\overline{\langle wT \rangle}$.

Proposition 5.3.1 (Bounding framework, IH3)**.** *Suppose that the pair* $(\beta, \tau(z))$ *satisfies the spectral constraint* (5.2.2) *and the boundary condition in* (5.3.1)*. Further, let* $\lambda \in L^2(0,1)$ *be a nondecreasing function such that* $\lambda(0) = -1$*. Then,*

$$\overline{\langle wT \rangle} \leq \frac{1}{2} + \left\langle \frac{1}{4\beta} \left| \tau'(z) - \lambda(z) - \beta z \right|^2 - \tau(z) \right\rangle =: U(\tau(z), \lambda(z), \beta).$$

Proof. As discussed in the proof of Proposition 5.2.1, the explicit bound on $\overline{\langle wT \rangle}$ is unchanged from the §2.3.1. Such that by use of the quadratic functional (5.2.3) subject to the boundary conditions (1.2.5d), an upper bound on $\overline{\langle wT \rangle}$ is given by

$$\overline{\langle wT \rangle} \leq \tfrac{1}{2} + \sup_{\substack{T \in \mathcal{T}_2^+ \\ w = -R\Delta^{-2}\Delta_h T}} \left\langle -b \left| \nabla T \right|^2 - \tau'(z) wT + (\tau(z) - \beta z + 1)\, \partial_z T - \tau(z) \right\rangle. \tag{5.3.2}$$

The supremum on the right-hand leads to the equivalent inequality

$$\overline{\langle wT \rangle} \leq \tfrac{1}{2} + \inf_{\substack{\lambda \in L^2(0,1) \\ \lambda \text{ nondecreasing} \\ \lambda \geq -1}} \left\langle \tfrac{1}{4\beta} \left| \tau'(z) - \lambda(z) - \beta z \right|^2 - \tau(z) \right\rangle, \tag{5.3.3}$$

as before. □

Remark 5.3.1. As was the case for isothermal boundaries and in §5.2, the bound on $\overline{\langle wT \rangle}$ is given by the same expression for the infinite Pr and arbitrary Pr cases, where only the spectral constraint (5.2.2) is altered.

5.3.1 Ansätze

The procedure for the proof of an upper bound on $\overline{\langle wT \rangle}$ is the same as that employed for isothermal boundaries. We construct $\beta > 0$, $\tau(z)$ and $\lambda(z)$ that satisfy the conditions of Proposition 5.3.1, while trying to minimize the corresponding bound $U(\beta, \tau, \lambda)$. Due to the Neumann boundary condition on T at $z = 0$, we can no longer employ the Poincaré estimates used in §5.2.2 to control the sign-indefinite term in the spectral constraint at the bottom boundary. Instead we modify $\tau(z)$ in $(\delta, \frac{1}{2})$ to increase slower than logarithmically in z and use results established in [167]. The function $\tau(z)$ is chosen to have the form

$$\tau(z) := \begin{cases} \delta - z, & 0 \le z \le \delta, \\ \dfrac{A}{1-\mu}\left(z^{1-\mu} - \delta^{1-\mu}\right) - A \ln\left(\dfrac{1-z}{1-\delta}\right), & \delta \le z \le 1-\varepsilon, \\ \dfrac{A\,B}{\varepsilon}\,(1-z)\,, & 1-\varepsilon \le z \le 1, \end{cases} \tag{5.3.4}$$

where

$$B = B(\varepsilon, \delta, \mu) := \frac{(1-\varepsilon)^{1-\mu} - \delta^{1-\mu}}{1-\mu} + \ln\left(\frac{1-\delta}{\varepsilon}\right). \tag{5.3.5}$$

On the other hand, the Lagrange multiplier $\lambda(z)$ is still chosen to be

$$\lambda(z) := \begin{cases} -1, & 0 \le z \le \delta, \\ 0, & \delta \le z \le 1. \end{cases} \tag{5.3.6}$$

These piecewise functions, sketched in Figure 5.3, are fully specified by the bottom and top boundary layer widths $\delta, \varepsilon \in (0, \frac{1}{2})$, the constant $A > 0$, and the exponent $\mu \in (0, 1)$ driving the behaviour of $\tau(z)$ in the bulk.

For β we take

$$\beta := \left\langle |\tau'(z) - \lambda(z)|^2 \right\rangle^{\frac{1}{2}} \left\langle z^2 \right\rangle^{-\frac{1}{2}} = \sqrt{3}\left\langle |\tau'(z) - \lambda(z)|^2 \right\rangle^{\frac{1}{2}}. \tag{5.3.7}$$

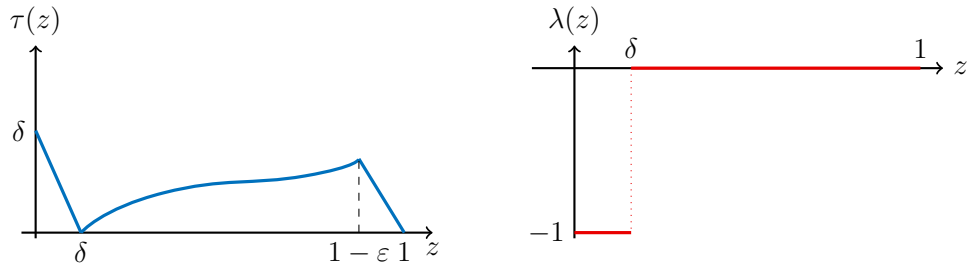

Figure 5.3: Sketch of the functions $\tau(z)$ (5.3.4) and $\lambda(z)$ in (5.3.6) used to prove Theorem 5.1.2.

This choice is motivated by minimizing the right hand side of the estimate

$$\begin{aligned}\frac{1}{4\beta}\left\langle|\tau'(z)-\lambda(z)-\beta z|^2\right\rangle &\leq \frac{\beta}{2}\left\langle z^2\right\rangle+\frac{1}{2\beta}\left\langle|\tau'(z)-\lambda(z)|^2\right\rangle \\ &= \frac{1}{\sqrt{3}}\left\langle|\tau'(z)-\lambda(z)|^2\right\rangle^{\frac{1}{2}}=\frac{\beta}{3},\end{aligned} \tag{5.3.8}$$

which is used in Lemma 5.3.2 below to estimate the value of the bound $U(\beta,\tau,\lambda)$ from above when $\tau(z)$ and $\lambda(z)$ are define by (5.3.4) and (5.3.6) respectively.

For any choice of the parameters δ, ε, A, and μ, the function $\tau(z)$ satisfies the boundary conditions in (5.3.1), while $\lambda(z)$ is nondecreasing and satisfies the condition $\lambda(0)=-1$. Thus, to establish Theorem 5.1.2 using Proposition 5.3.1 we need specify parameter values such that $U(\beta,\tau,\lambda)\leq\frac{1}{2}-O(R^{-4})$ while ensuring that $(\beta,\tau(z))$ satisfy the spectral constraint. For the purposes of simplifying the algebra in what follows, we shall fix

$$A(\delta,\mu)=\frac{2\sqrt{3}}{9}\sqrt{2\mu-1}\,\delta^{\mu+\frac{3}{2}} \tag{5.3.9}$$

from the outset. This choice arises when insisting that the upper estimate on $U(\beta,\tau,\lambda)$ derived in Lemma 5.3.2 below should be strictly less than $\frac{1}{2}$ for suitable choices of δ and ε, at least when all other constraints on these parameters are ignored.

5.3.2 Preliminary estimates

We now derive auxiliary results that simplify the choice of the exponent μ and of the boundary widths δ and ε. The first gives estimates on the value of β defined in (5.3.7).

Lemma 5.3.1 (Estimates on β)**.** *Let $\tau(z)$, $\lambda(z)$ and β be given by* (5.3.4), (5.3.6) *and* (5.3.7) *with A specified in* (5.3.9). *Suppose that $\mu \in (\frac{1}{2}, 1)$ and the boundary layer widths δ and ε satisfy*

$$\delta \leq \frac{1}{3}\left(\frac{1}{2}\right)^{\frac{1}{2\mu-1}}, \qquad \varepsilon \leq \frac{1}{3}, \qquad (2\mu-1)\,\delta^{2\mu-1}B(\varepsilon,\delta,\mu)^2 \leq \varepsilon, \qquad \text{(5.3.10a,b,c)}$$

where $B(\varepsilon,\delta,\mu)$ is defined by (5.3.5). *Then,*

$$\frac{\sqrt{2}}{3}\,\delta^2 \leq \beta \leq \frac{4}{3}\,\delta^2. \tag{5.3.11}$$

Remark 5.3.2. Condition (5.3.10a) and the bounds on μ imposed in Lemma 5.3.1 imply that $0 \leq \delta \leq \frac{1}{6}$. These uniform bounds will be used repeatedly in the following proofs.

Proof of Lemma 5.3.1. It suffices to estimate $\langle|\tau'(z)-\lambda(z)|^2\rangle^{\frac{1}{2}}$ from above and below. For a lower bound, we can substitute the choices of $\tau(z)$ and $\lambda(z)$ and then estimate

$$\left\langle|\tau'(z)-\lambda(z)|^2\right\rangle = \int_\delta^1 |\tau'(z)|^2\mathrm{d}z \geq \int_\delta^{1-\varepsilon} |\tau'(z)|^2\mathrm{d}z = A^2\int_\delta^{1-\varepsilon}\left|\frac{1}{z^\mu}+\frac{1}{1-z}\right|^2\mathrm{d}z.$$

Dropping the positive term $\frac{1}{1-z}$ from the integrand and integrating the rest gives

$$\left\langle|\tau'(z)-\lambda(z)|^2\right\rangle \geq A^2\left(\frac{\delta^{1-2\mu}-(1-\varepsilon)^{1-2\mu}}{2\mu-1}\right).$$

For every $\mu \in (\frac{1}{2}, 1)$, the second term inside the parentheses can be estimated upon observing that constraints (5.3.10a-b) imply

$$(1-\varepsilon)^{1-2\mu} \leq \left(\frac{2}{3}\right)^{1-2\mu} \leq \frac{1}{2^{2\mu}}\delta^{1-2\mu} \leq \frac{1}{2}\delta^{1-2\mu}. \tag{5.3.12}$$

Thus, we obtain

$$\left\langle |\tau'(z) - \lambda(z)|^2 \right\rangle \geq A^2 \frac{\frac{1}{2}\delta^{1-2\mu}}{2\mu - 1}. \tag{5.3.13}$$

Taking the square root of (5.3.13) and using (5.3.9) gives $\langle |\tau' - \lambda|^2 \rangle^{\frac{1}{2}} \geq \frac{\sqrt{6}}{9}\,\delta^2$, which combined with (5.3.7) proves the lower bound on β stated in (5.3.11).

To prove the upper bound on β, we start by using the inequality $(a+b)^2 \leq 2a^2+2b^2$, evaluating exactly the integral of $\tau'(z) - \lambda(z)$, and dropping the negative terms to get

$$\begin{aligned} \frac{\left\langle |\tau'(z) - \lambda(z)|^2 \right\rangle}{A^2} &= \int_\delta^{1-\varepsilon} \left| \frac{1}{z^\mu} + \frac{1}{1-z} \right|^2 \mathrm{d}z + \frac{B^2}{\varepsilon} \\ &\leq \int_\delta^{1-\varepsilon} \frac{2}{z^{2\mu}} + \frac{2}{(1-z)^2} \mathrm{d}z + \frac{B^2}{\varepsilon} \\ (\text{since } \mu > \tfrac{1}{2}) \quad &\leq \frac{2\delta^{1-2\mu}}{2\mu - 1} + \frac{2}{\varepsilon} + \frac{B^2}{\varepsilon}. \end{aligned} \tag{5.3.14}$$

Using assumption (5.3.10c), the second and final term in (5.3.14) can be estimated from above to arrive at

$$\frac{\left\langle |\tau'(z) - \lambda(z)|^2 \right\rangle}{A^2} \leq \frac{\delta^{1-2\mu}}{2\mu - 1}\left(2 + \frac{2}{B^2} + 1\right). \tag{5.3.15}$$

Next, we observe that for all $\varepsilon \in (0, \frac{1}{3})$, $\delta \in (0, \frac{1}{6})$, and $\mu \in (\frac{1}{2}, 1)$ we can estimate

$$B(\varepsilon, \delta, \mu) \geq B\left(\frac{1}{3}, \frac{1}{6}, \frac{1}{2}\right) = \frac{\sqrt{6}}{3} + \ln\left(\frac{5}{2}\right) > \sqrt{2},$$

so $B^{-2} \leq 1/2$. Using this estimate in (5.3.15), taking a square root, and substituting in the value of A given in (5.3.9) leads to the inequality $\langle |\tau'(z) - \lambda(z)|^2 \rangle^{1/2} \leq \frac{4\sqrt{3}}{9}\,\delta^2$.

Combining this with (5.3.7) yields the upper bound on β stated in (5.3.11) and concludes the proof of Lemma 5.3.1. □

The second auxiliary result of this section estimates the upper bound $U(\beta, \tau, \lambda)$ on $\overline{\langle wT \rangle}$ given by Proposition 5.3.1 using only the bottom boundary layer width δ.

Lemma 5.3.2 (Estimates on $U(\beta, \tau, \lambda)$)**.** *Let $\tau(z)$, $\lambda(z)$ and β be specified by* (5.3.4), (5.3.6) *and* (5.3.7) *with A given by* (5.3.9)*. Suppose μ and the boundary layer widths δ, ε satisfy the conditions of Lemma 5.3.1. Then,*

$$U(\beta, \tau, \lambda) \leq \frac{1}{2} - \frac{\delta^2}{18}. \tag{5.3.16}$$

Proof. Inequality (5.3.8) and the upper bound on β from (5.3.11) give

$$U(\beta, \tau, \lambda) \leq \frac{1}{2} + \frac{\beta}{3} - \langle \tau(z) \rangle \leq \frac{1}{2} + \frac{4}{9}\delta^2 - \langle \tau(z) \rangle \,. \tag{5.3.17}$$

The result follows upon observing that $\tau(z)$ is non-negative, so $\langle \tau(z) \rangle = \int_0^1 \tau(z) \mathrm{d}z \geq \int_0^\delta \tau(z) \mathrm{d}z = \frac{1}{2}\delta^2$. □

Remark 5.3.3. Recalling the definition of τ in (5.3.4) note that the right hand side of (5.3.17) can be strictly smaller than $\frac{1}{2}$ when δ^2 is small only if $A \lesssim \delta^{\mu+3/2}$. This observation dictates the choice of A in (5.3.9). For any fixed value of R, one should choose $A \sim \delta^{\mu+3/2}$ with a (possibly R-dependent) prefactor that optimises the balance between the positive and negative terms, subject to constraints on A, δ and all other parameters that ensure the spectral constraint is satisfied. To simplify the proof, however, we choose to fix this prefactor *a priori* irrespective of R.

The final auxiliary result gives the sufficient conditions on δ and ε that ensure the spectral constraint (5.2.2) is satisfied.

Lemma 5.3.3 (Sufficient conditions for spectral constraint)**.** *Let $\tau(z)$, $\lambda(z)$ and β be specified by* (5.3.4), (5.3.6) *and* (5.3.7) *with A given by* (5.3.9)*. Suppose that μ and the boundary layer widths satisfy the conditions of Lemma 5.3.1. Further, let*

$$h(\mu) = 2(2\mu - 1)(1 - \mu^2). \tag{5.3.18}$$

and suppose that

$$\delta \leq \varepsilon, \tag{5.3.19a}$$

$$\delta \leq h(\mu)\, R^{-2}, \tag{5.3.19b}$$

$$\frac{\sqrt{2\mu - 1}}{(1-\mu)^2}\, \delta^{\mu - \frac{1}{2}} \varepsilon^3 \ln^2\left(\delta^{-1}\right) \leq \frac{4}{3}\sqrt{6} R^{-1}. \tag{5.3.19c}$$

Then, the pair $(\beta, \tau(z))$ satisfies the spectral constraint (5.2.2)*.*

Unlike the analogous result obtained in §5.2.2, Lemma 5.3.3 cannot be proven using only the Hardy–Rellich inequalities stated in Lemma 5.2.4. The lack of a fixed boundary temperature at $z = 0$, makes it impossible to gain sufficient control on the contribution of the bottom boundary layer to the quadratic form in (5.2.2). This difficulty can be overcome using the following result, obtained as a particular case of a more general analysis by Whitehead and Wittenberg [[167], Eqs. (59) & (77)], which upon setting (in their notation) $\nu_1 = \frac{\mu}{2} - \nu_2$ and $\nu_2 = \frac{1}{2}\left(-1 + \sqrt{2(1-\mu^2)}\right)$.

Lemma 5.3.4 (Adapted from Ref. [167])**.** *Fix $\mu \in (\frac{1}{2}, 1)$ and $\zeta, R > 0$. Suppose $q(z) : [0,1] \to \mathbb{R}$, be a non-negative function, satisfying*

$$\left\langle q(z) z^{1+\mu/2} \right\rangle^2 \leq \frac{\zeta}{R} \frac{\sqrt{2}(3-\mu)(2+\mu)\sqrt{1-\mu^2}}{3+\mu}. \tag{5.3.20}$$

Then, for every w and T solving (5.1.5) *subject to the boundary conditions* (5.1.6)*,*

$$\left\langle \frac{1}{2}|\nabla T|^2 + \zeta \frac{wT}{z^\mu} - q(z) wT \right\rangle \geq 0. \tag{5.3.21}$$

We are now ready to prove Lemma 5.3.3.

Proof of Lemma 5.3.3. Let $\mathbb{1}_{(a,b)}$ denote the indicator function of the interval (a,b) and define the functions

$$f(z) := \left[1 + \frac{A(\delta,\mu)}{z^\mu} + \frac{A(\delta,\mu)}{1-z}\right] \mathbb{1}_{(0,\delta)}(z), \tag{5.3.22a}$$

$$g(z) := \left[\frac{B(\varepsilon,\delta,\mu)}{\varepsilon} + \frac{1}{z^\mu} + \frac{1}{1-z}\right] \mathbb{1}_{(1-\varepsilon,1)}(z). \tag{5.3.22b}$$

Given the choice of τ, we can rewrite the spectral constraint as

$$0 \leq \left\langle \beta|\nabla T|^2 + \tau' w T \right\rangle = \mathcal{F}\{T\} + \mathcal{G}\{T\},$$

where

$$\mathcal{F}\{T\} := \frac{\beta}{2}\left\langle |\nabla T|^2 \right\rangle + A\left\langle \frac{wT}{z^\mu} \right\rangle - \left\langle f(z)\, wT \right\rangle, \tag{5.3.23a}$$

$$\mathcal{G}\{T\} := \frac{\beta}{2}\left\langle |\nabla T|^2 \right\rangle + A\left\langle \frac{wT}{1-z} \right\rangle - A\left\langle g(z)\, wT \right\rangle. \tag{5.3.23b}$$

Observe that $\mathcal{F}\{T\}$ and $\mathcal{G}\{T\}$ are functionals of the temperature field only because w is determined as a function of T by solving (5.1.5) subject to the boundary conditions in (5.1.6). We shall prove that $\mathcal{F}\{T\}$ and $\mathcal{G}\{T\}$ are individually non-negative for all temperatures T from the space $\mathcal{T}_2^+$, which is sufficient for the spectral constraint to hold.

To prove that $\mathcal{F}\{T\} \geq 0$, we apply Lemma 5.3.4 with $q(z) = f(z)/\beta$ and $\zeta = A/\beta$, where f is given by (5.3.22a) and A given by (5.3.9). We therefore need to check that

$$\left\langle f(z) z^{1+\frac{\mu}{2}} \right\rangle^2 \leq \frac{\beta A}{R} \frac{\sqrt{2}(3-\mu)(2+\mu)\sqrt{1-\mu^2}}{3+\mu}. \tag{5.3.24}$$

To verify this inequality, we first bound from above the weighted integral on the left-hand side. By assumption we have $0 \leq z \leq \delta \leq \frac{1}{6}$ and $\mu \in (\frac{1}{2}, 1)$, from which we obtain $\frac{1}{1-z} \leq \frac{1}{z^\mu}$. Using this estimate and the definition of A from (5.3.9) we can

therefore estimate

$$\left\langle f(z)z^{1+\frac{\mu}{2}} \right\rangle \leq \int_0^\delta z^{1+\frac{\mu}{2}} + 2Az^{1-\frac{\mu}{2}} \mathrm{d}z = \left[\frac{2}{4+\mu} + \frac{8\sqrt{3}}{9} \frac{\sqrt{2\mu-1}}{(4-\mu)} \delta^{\frac{3}{2}} \right] \delta^{2+\frac{\mu}{2}}.$$

Using again that $0 \leq \delta \leq \frac{1}{6}$ and $\mu \in (\frac{1}{2}, 1)$, the bracketed expression can be bounded from above to obtain

$$\left\langle f(z)z^{1+\frac{\mu}{2}} \right\rangle \leq \left[\frac{4}{9} + \frac{8\sqrt{3}}{9} \cdot \frac{1}{3} \cdot \left(\frac{1}{6} \right)^{\frac{3}{2}} \right] \delta^{2+\frac{\mu}{2}} < \frac{1}{2} \delta^{2+\frac{\mu}{2}}. \tag{5.3.25}$$

Next, we bound from below the right-hand-side of (5.3.24). Using the lower bound on β from Lemma 5.3.1, the definition (5.3.9) of A, and the fact that $\mu \in (\frac{1}{2}, 1)$, we have

$$\begin{aligned} \frac{\beta A \sqrt{2}(3-\mu)(2+\mu)}{(3+\mu)} &\geq \frac{4\sqrt{3}}{27} \delta^{\mu+\frac{7}{2}} \sqrt{2\mu-1} \cdot \frac{(3-\mu)(2+\mu)}{(3+\mu)} \\ &\geq \frac{5}{9\sqrt{3}} \delta^{\mu+\frac{7}{2}} \sqrt{2\mu-1}. \end{aligned} \tag{5.3.26}$$

Combining (5.3.25) and (5.3.26), we conclude that (5.3.24) holds if

$$\delta^{\frac{1}{2}} \leq \frac{20}{9\sqrt{3}} \frac{\sqrt{(2\mu-1)(1-\mu^2)}}{R} \leq \sqrt{2} \frac{\sqrt{(2\mu-1)(1-\mu^2)}}{R},$$

which is true because δ satisfies (5.3.19a) by assumption. This proves that $\mathcal{F}\{T\} \geq 0$, as desired.

We now prove that $\mathcal{G}\{T\}$ is also nonnegative. This can be done following the same steps used in §5.2.2. The Hardy–Rellich inequality (5.2.19b) gives

$$\mathcal{G}\{T\} \geq \frac{\beta}{2} \left\langle |\nabla T|^2 \right\rangle + \frac{4A}{R} \left\langle \frac{w^2}{(1-z)^3} \right\rangle - A \left\langle g(z) w T \right\rangle. \tag{5.3.27}$$

To estimate the last term, as before we use the inequality $\langle T^2\rangle_h \le (1-z)\,\langle|\nabla T|^2\rangle$, the Cauchy–Schwarz inequality, and Young's inequality:

$$\langle g(z)wT\rangle \le \frac{\beta}{2A}\,\langle|\nabla T|^2\rangle + \frac{A}{2\beta}\,\langle g(z)^2(1-z)^4\rangle\left\langle\frac{w^2}{(1-z)^3}\right\rangle.$$

Using the lower bound on β from (5.3.11) gives

$$\langle g(z)wT\rangle \le \frac{\beta}{2A}\,\langle|\nabla T|^2\rangle + \frac{3\sqrt{2}\,A}{4\delta^2}\,\langle g(z)^2(1-z)^4\rangle\left\langle\frac{w^2}{(1-z)^3}\right\rangle,$$

which can be substituted into (5.3.27) along with the value of A from (5.3.9) to obtain

$$\mathcal{G}\{T\} \ge \frac{\sqrt{6(2\mu-1)}\,A}{6}\left(\frac{4\sqrt{6}}{\sqrt{2\mu-1}\,R} - \delta^{\mu-\frac{1}{2}}\,\langle g(z)^2(1-z)^4\rangle\right)\left\langle\frac{|w|^2}{(1-z)^3}\right\rangle. \tag{5.3.28}$$

To conclude the argument we need to show that term in the parentheses is non-negative. To demonstrate this, we first estimate from above the function $g(z)$ given in (5.3.22b) on the interval $(1-\varepsilon, 1)$. The assumption that $\delta \le \varepsilon$ implies that $1-\varepsilon \le 1-\delta \le 1$ and $\ln(\frac{1}{\varepsilon}) \le \ln(\frac{1}{\delta})$. Thus, for all $\delta \le \frac{1}{6}$ and $\mu \in (\frac{1}{2}, 1)$ the first term in $g(z)$ can be bounded as

$$\frac{B}{\varepsilon} \le \frac{1}{\varepsilon}\left(\frac{1}{1-\mu} + \ln\left(\frac{1}{\delta}\right)\right) \le \frac{2\ln\left(\frac{1}{\delta}\right)}{\varepsilon(1-\mu)}. \tag{5.3.29}$$

To estimate the other terms in $g(z)$, we observe that the assumptions $\varepsilon \le \frac{1}{3}$ and $\mu \in (\frac{1}{2}, 1)$ imply that $\frac{1}{z^\mu} \le \frac{1}{2(1-\mu)(1-z)}$ and $\frac{1}{1-z} \le \frac{1}{2(1-\mu)(1-z)}$. Consequently, we arrive at

$$g(z) \le \frac{2\ln\left(\frac{1}{\delta}\right)}{\varepsilon(1-\mu)} + \frac{1}{(1-\mu)(1-z)}. \tag{5.3.30}$$

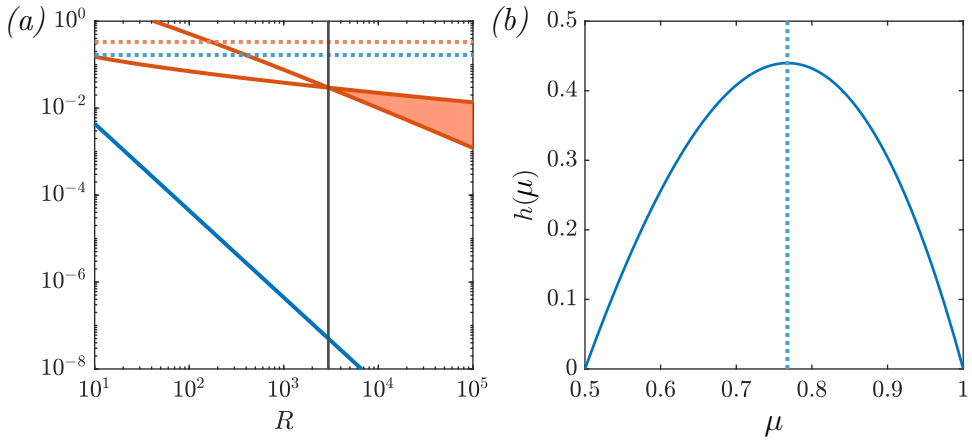

Figure 5.4: *(a)* Variation with $R$of the allowed values for the bottom boundary layer width δ (5.3.32) (—) and the feasible region of ε (5.3.34) (shaded region). Also shown are uniform upper bounds of $\delta \leq \frac{1}{6}$ (····), and $\varepsilon \leq \frac{1}{3}$ (····) imposed on the variables. A black vertical line marks the Rayleigh number, $R_0 \approx 2960.89$ above which all constraints on are satisfied. *(b)* Plot of the function $h(\mu)$ (5.3.18) (—). Shown also is the optimal $\mu^* = \frac{1+\sqrt{13}}{6}$ (····).

Finally, using (5.3.30) and evaluating the integral in the parentheses of (5.3.28) with the fact that $\ln(\frac{1}{\delta}) \leq \ln^2(\frac{1}{\delta})$ and $\frac{1}{3} \leq \frac{1}{3}\ln(\frac{1}{\delta})$ gives

$$\begin{aligned}
\delta^{\mu-\frac{1}{2}}\left\langle g(z)^2(1-z)^4\right\rangle &\leq \delta^{\mu-\frac{1}{2}}\int_{1-\varepsilon}^{1}\left(\frac{2\ln\left(\frac{1}{\delta}\right)}{\varepsilon(1-\mu)}+\frac{1}{(1-\mu)(1-z)}\right)^2(1-z)^4\,\mathrm{d}z \\
&= \frac{\delta^{\mu-\frac{1}{2}}\varepsilon^3}{(1-\mu)^2}\left[\frac{4}{5}\ln^2\left(\frac{1}{\delta}\right)+\ln\left(\frac{1}{\delta}\right)+\frac{1}{3}\right] \\
&\leq \frac{3\,\delta^{\mu-\frac{1}{2}}\varepsilon^3\ln^2\left(\frac{1}{\delta}\right)}{(1-\mu)^2} \\
\text{(by (5.3.19b))} \qquad &\leq \frac{4\sqrt{6}}{\sqrt{2\mu-1}\,R}. \qquad (5.3.31)
\end{aligned}$$

This concludes the proof of Lemma 5.3.3.

□

5.3.3 Proof of Theorem 5.1.2

To prove Theorem 5.1.2, we only need to specify R-dependent values for μ and for the boundary layer widths δ and ε that satisfy the conditions of Lemmas 5.3.1, 5.3.2 and 5.3.3.

Motivated by the desire to minimize the upper bound on $U(\beta, \tau, \lambda)$ stated in Lemma 5.3.2, we choose

$$\delta = h(\mu^*)R^{-2} \tag{5.3.32}$$

where $\mu^* = \frac{1+\sqrt{13}}{6}$ is the unique maximizer of $h(\mu)$ on the interval $(\frac{1}{2}, 1)$ (see Figure 5.4(b)). With these choices, conditions (5.3.10c) and (5.3.19b) require ε to satisfy

$$c_0 R^{-4\mu^*+2} B(\delta, \varepsilon, \mu^*)^2 \leq \varepsilon \leq c_2 R^{-\frac{2-2\mu^*}{3}} \ln^{-\frac{2}{3}}(\delta^{-1}), \tag{5.3.33}$$

where c_0, c_1 and c_2 are non-negative constants independent of R. Using the upper bound on B from (5.3.29), it suffices to find ε such that

$$\frac{4c_0}{(1-\mu^*)^2} R^{-4\mu^*+2} \ln^2\left(\frac{R^2}{h(\mu^*)}\right) \leq \varepsilon \leq c_2 R^{-\frac{2-2\mu^*}{3}} \ln^{-\frac{2}{3}}\left(\frac{R^2}{h(\mu^*)}\right). \tag{5.3.34}$$

Figure 5.4 shows that suitable values of ε exist when $R \geq R_0 \approx 2960.89$. One can also check that for all such values of $R$and any ε in the range given by §5.3.3 one has $\delta \leq \frac{1}{6}$, $\varepsilon \leq \frac{1}{3}$, and $\delta \leq \varepsilon$. We have therefore verified all conditions of Lemmas 5.3.1, 5.3.2 and 5.3.3.

To conclude the proof of Theorem 5.1.2, we simply substitute the choice of δ from (5.3.32) into Lemma 5.3.2 to find the upper bound $\overline{\langle wT \rangle} \leq U(\beta, \tau, \lambda) \leq \frac{1}{2} - cR^{-4}$, where $c = \frac{h^2(\mu^*)}{18} \simeq 0.0107$.

Remark 5.3.4. The top boundary layer width ε is not uniquely determined in the construction. Its optimal value could be obtained by considering more refined estimates on $U(\beta, \tau, \lambda)$ than Lemma 5.3.2, but we expect such estimates to provide only higher-order corrections to the eventual bound on $\overline{\langle wT \rangle}$.

Chapter 6

Free slip boundaries

Nice kabdan kaba boşaldım doldum,
Karıştım denize deniz ben oldum,
Damlanın içinde evreni buldum,
Yine benden bana getirdi beni.

.

From many containers I emptied and filled,
Mixed into the sea I became the sea instilled,
Within a droplet, found the universe distilled,
Brought again it has me, from me.

Ashik Daimi

In this section we look at an alteration to the idealised models considered thus far by changing the kinematic boundary conditions. While the expectation of no motion at the plate surface is physically reasonable in most flows, one scenario where this assumption can break down is for internally heated convection taking place within planets. Mantle convection is influenced by pressure and chemical variations, these are greatest at interfaces between different regions, like the mantle-liquid outer core boundary in the Earth. Then, since geophysical fluid phenomena occur at large scales, and consequently large R, convection can be said to be strong. For strong convection in rotating environments free slip boundary conditions can be considered

better models [96, 103]. The change in boundary conditions are also of interest from the purely mathematical investigation of bounds for a different flow of internally heated convection.

In the case of Rayleigh–Bénard convection, it has been proven that the bound on the Nusselt number, Nu, increases with a smaller power of the Rayleigh number for free slip boundaries than for no-slip [165]. This result was later extended to the case of the infinite Pr convection [166]. The upper bounds on Nu were later demonstrated to be optimal within the background method through numerical investigations [159]. Inspired by the analytical work at finite and infinite Pr for Rayleigh–Bénard convection, in this chapter, we apply a similar analysis to bounding $\overline{\langle wT \rangle}$ in internally heated convection subject to free-slip boundary conditions.

As highlighted in chapter 1, applications of the background method for internally heated convection have considered only the quantity $\overline{\langle T \rangle}$. Under free slip and isothermal boundaries it has been shown that $\overline{\langle T \rangle} \gtrsim R^{-\frac{5}{17}}$ holds for both finite and infinite Pr [166]. While no bounds on $\overline{\langle wT \rangle}$ for free slip existed prior to the work of this chapter, the linear and energy stability limits are known. For free slip and isothermal boundaries the flow is linearly unstable for $R > 16\,992.2$ while the static state is globally attracting only at $R < 10\,618.1$ [58]. Both values are, as expected, lower than that for no-slip isothermal boundaries (§3.1).

6.1 Setup

The kinematic and thermal boundary conditions are

$$w|_{z=\{0,1\}} = \partial_z u|_{z=\{0,1\}} = \partial_z v|_{z=\{0,1\}} = 0, \tag{6.1.1a}$$

$$T|_{z=\{0,1\}} = 0, \tag{6.1.1b}$$

such that the flow variables belong to the set $(\boldsymbol{u}, T) \in \mathbb{A} = \mathcal{U}_2 \times \mathcal{T}_1^+$, defined in (2.1.2). The results that follow are twofold, the first is valid for all Pr. While the second is obtained when the infinite Pr equations are considered (5.1.1).

A key variation in this chapter is the use of additional information through the inclusion of vorticity in the auxiliary functional. The vorticity is defined as $\boldsymbol{\omega} = \nabla \times \boldsymbol{u}$, such that, taking the curl of the momentum equation (1.2.3b) gives

$$\partial_t \boldsymbol{\omega} + \nabla \times (\boldsymbol{\omega} \times \boldsymbol{u}) = Pr \Delta \boldsymbol{\omega} + Pr R \left[\partial_y T, -\partial_x T, 0\right]. \tag{6.1.2}$$

The vorticity equation (6.1.2) can be simplified when in 2-d and take the scalar vorticity, defined as

$$\omega_y := \partial_x w - \partial_z u. \tag{6.1.3}$$

This scalar vorticity ω_y can be shown to satisfy

$$\partial_t \omega_y + \boldsymbol{u} \cdot \nabla \omega_y = Pr \Delta \omega_y + Pr\, R\, \partial_x T, \tag{6.1.4a}$$

$$\omega_y|_{z=\{0,1\}} = 0. \tag{6.1.4b}$$

In the infinite Pr case we can define a "pseudo-vorticity" [166] which plays a similar role to ω_y but in three dimensions.

Theorem 6.1.1 ($Pr < \infty$ free-slip, 2d)**.** *For $(\boldsymbol{u}, T)$ solving (1.2.3) subject to the free-slip isothermal boundary conditions (6.1.1), there exists a constant $c > 0$, such that for sufficiently large $R > 0$,*

$$\overline{\langle wT \rangle} \leq \frac{1}{2} - cR^{-\frac{40}{29}}.$$

Remark 6.1.1. It is shown in §6.2.1 that the theorem holds with $c \approx 0.6442$ for any $R > 66$.

Theorem 6.1.2 ($Pr = \infty$ free-slip, 3d)**.** *For* $(\boldsymbol{u}, T)$ *solve* (5.1.1) *subject to the free-slip isothermal boundary conditions* (6.1.1)*. There exists a constant* $c > 0$*, such that for sufficiently large* $R > 0$*,*

$$\overline{\langle wT \rangle} \leq \frac{1}{2} - cR^{-\frac{40}{29}} .$$

Remark 6.1.2. It is shown in §6.3.1 that the theorem holds with $c \approx 0.2946$ for any $R >$.

For the case of isothermal boundaries, the upper bounds on $\overline{\langle wT \rangle}$, for both finite and infinite Pr, translate into bounds on the flux out of the top and bottom.

Corollary 6.1.1. *For sufficiently large* R

$$\mathcal{F}_T \leq 1 - cR^{-\frac{40}{29}} \quad \textit{and} \quad \mathcal{F}_B \geq cR^{-\frac{40}{29}}. \tag{6.1.5}$$

6.2 Finite Prandtl number

To obtain a bound on $\overline{\langle wT \rangle}$ at arbitrary Pr, information from the vorticity field in two dimensions can be incorporated into the quadratic auxiliary functional (2.2.5). We include an enstrophy, more precisely an energy of the scalar vorticity term, within the functional along with its associated balance parameter $\gamma \in \mathbb{R}_+$. This gives

$$\mathcal{V}\{\boldsymbol{u}, \omega_y, T\} = \left\langle \frac{\alpha}{2RPr}|\boldsymbol{u}|^2 + \frac{\beta}{2}\left|T - \frac{\tau(z) + z - 1}{\beta}\right|^2 + \frac{\gamma}{2RPr}|\omega_y|^2 \right\rangle . \tag{6.2.1}$$

From the same symmetrisation arguments made in §2.5, the background field associated with ω_y is taken as zero.

Following the strategy outlined in §2.3.1 utilising the minimum principle, with the new auxiliary functional of (6.2.1), a bound can be obtained on $\overline{\langle wT \rangle}$. Using the boundary conditions (6.1.1), incompressibility, the identity $\langle |\nabla \boldsymbol{u}| \rangle = \langle |\omega_y|^2 \rangle$ and

integrating by parts, we obtain

$$\overline{\langle wT\rangle} \leq \inf_{\substack{U,\tau(z),\lambda(z)\\ \alpha,\beta,\gamma}} \{U : \mathcal{S}\{\boldsymbol{u}, T, \omega_y\} \geq 0 \ \forall (\boldsymbol{u}, T) \in \mathbb{A}\}, \tag{6.2.2}$$

where

$$\begin{aligned}\mathcal{S} := \Big\langle \frac{\alpha}{R}|\omega_y|^2 + \beta|\nabla T|^2 + \frac{\gamma}{R}|\nabla\omega_y|^2 - (\alpha - \tau'(z))wT - \gamma T\partial_x\omega_y \Big\rangle \\ + \langle(\beta z - \tau'(z) + \lambda)\partial_z T + \tau(z)\rangle - \frac{1}{2} + U,\end{aligned} \tag{6.2.3}$$

where $\lambda(z)$ is a non-decreasing function. The linear terms in (6.2.3) remain unchanged to the problem at no-slip boundaries from (3.2.1) and as such the explicit expression for the bound on $\overline{\langle wT\rangle}$ is the same and given by (2.4.1). However (6.2.3) contains additional quadratic terms such that in Fourier space we have

$$\begin{aligned}\mathcal{S}_{\boldsymbol{k}}\{\hat{w}_{\boldsymbol{k}}, \hat{T}_{\boldsymbol{k}}, \hat{\omega}_{y,\boldsymbol{k}}\} := \Big\langle \frac{\alpha + \gamma k^2}{R}|\hat{\omega}_{y,\boldsymbol{k}}|^2 + \frac{\gamma}{R}|\hat{\omega}'_{y,\boldsymbol{k}}|^2 + \beta|\hat{T}'_{\boldsymbol{k}}|^2 + \beta k^2|\hat{T}_{\boldsymbol{k}}|^2 \\ -(\alpha - \tau'(z))\mathrm{Re}\{\hat{w}_{\boldsymbol{k}}\hat{T}_{\boldsymbol{k}}\} - \gamma k\mathrm{Re}\{\hat{\omega}_{y,\boldsymbol{k}}\hat{T}_{\boldsymbol{k}}\}\Big\rangle.\end{aligned} \tag{6.2.4}$$

As before requiring that $\mathcal{S}_{\boldsymbol{k}} \geq 0$ is referred to as the spectral constraint.

A bound on $\overline{\langle wT\rangle}$ can be stated as the following optimisation problem, which we proceed to solve in §6.2.1, for a particular choice of balance parameters and and background profiles.

$$\begin{aligned}\inf_{\tau(z),\lambda(z),\alpha,\beta,\gamma} \quad & U := \frac{1}{2} + \left\langle \frac{1}{4\beta}|\beta(z - \tfrac{1}{2}) - \tau'(z) + \lambda(z)|^2 - \tau(z) \right\rangle \\ \text{subject to} \quad & \mathcal{S}_{\boldsymbol{k}}\{\hat{w}_{\boldsymbol{k}}, \hat{T}_{\boldsymbol{k}}, \hat{\omega}_{y,\boldsymbol{k}}\} \geq 0 \qquad \forall \hat{w}_{\boldsymbol{k}}, \hat{T}_{\boldsymbol{k}}, \hat{\omega}_{y,\boldsymbol{k}} : (6.1.1)(6.1.4\text{b}) \quad \boldsymbol{k} \neq 0, \\ & \lambda(z) \text{ nondecreasing and } \langle\lambda\rangle = -1.\end{aligned} \tag{6.2.5}$$

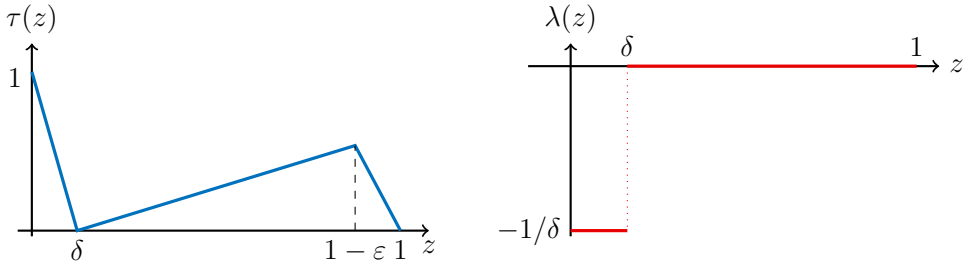

Figure 6.1: Sketches of functions $\tau(z)$ in (6.2.6) and $\lambda(z)$ in (6.2.7).

6.2.1 Analytical bound

To prove the bound in Theorem 6.1.1, we seek $\beta > 0$, $\tau(z)$ and $\lambda(z)$ that solve (6.2.5). In (6.2.4) it remains favourable to take $\tau'(z)$ as α in the bulk of the domain, such that the wT term is zero. The choice of profiles are

$$\tau(z) := \begin{cases} 1 - \dfrac{z}{\delta}, & 0 \le z \le \delta, \\ \alpha(z - \delta), & \delta \le z \le 1 - \varepsilon, \\ \alpha(1 - \delta - \varepsilon)\left(\dfrac{1 - z}{\varepsilon}\right), & 1 - \varepsilon \le z \le 1, \end{cases} \tag{6.2.6}$$

and

$$\lambda(z) := \begin{cases} -\dfrac{1}{\delta}, & 0 \le z \le \delta, \\ 0, & \delta \le z \le 1. \end{cases} \tag{6.2.7}$$

We also fix

$$\beta := \left\langle |\tau'(z) - \lambda(z)|^2 \right\rangle^{\frac{1}{2}} \left\langle |z - \tfrac{1}{2}|^2 \right\rangle^{-\frac{1}{2}} = 2\sqrt{3} \left\langle |\tau'(z) - \lambda(z)|^2 \right\rangle^{\frac{1}{2}}. \tag{6.2.8}$$

This choice minimizes the right hand side of the inequality

$$\frac{1}{4\beta} \left\langle |\beta(z - \tfrac{1}{2}) - \tau'(z) + \lambda(z)|^2 \right\rangle \le \frac{\beta}{2} \left\langle |z - \tfrac{1}{2}|^2 \right\rangle + \frac{1}{2\beta} \left\langle |\tau'(z) - \lambda(z)|^2 \right\rangle, \tag{6.2.9}$$

which will be used to estimate the bound.

Lemma 6.2.1. *Let $\tau(z)$, $\lambda(z)$ be given by* (6.2.6) *and* (6.2.7). *Let the boundary layers δ and ε satisfy*

$$\delta \leq \frac{1}{2}, \quad \varepsilon \leq \frac{1}{3}, \tag{6.2.9a,b}$$

and that

$$\alpha = \frac{2}{\sqrt{3}}\delta\varepsilon^{\frac{1}{2}}. \tag{6.2.10}$$

Then

$$\frac{2}{3}\delta \leq \beta \leq 4\delta. \tag{6.2.11}$$

Proof. We need to estimate $\langle|\tau'(z) - \lambda(z)|^2\rangle^{\frac{1}{2}}$ from above and below with β given by (6.2.8). For a lower bound, we substitute our choice of $\tau(z)$ and $\lambda(z)$ from (6.2.6) and (6.2.7), then the assumptions $\delta \leq \frac{1}{2}$ and $\varepsilon \leq \frac{1}{3}$ imply $1 - \varepsilon - \delta \geq \frac{1}{6}$, which gives

$$\left\langle|\tau'(z) - \lambda(z)|^2\right\rangle = \int_\delta^1 |\tau'(z)|^2 \mathrm{d}z \geq \int_{1-\varepsilon}^1 \frac{\alpha^2}{\varepsilon^2}(1 - \varepsilon - \delta)^2 \mathrm{d}z \geq \frac{1}{36}\frac{\alpha^2}{\varepsilon}. \tag{6.2.12}$$

Then, substituting into (6.2.8) and taking α as given by (6.2.10) we obtain

$$\beta = 2\sqrt{3}\left\langle|\tau'(z) - \lambda(z)|^2\right\rangle^{\frac{1}{2}} \geq 2\sqrt{3}\frac{\alpha}{\varepsilon^{\frac{1}{2}}} = \frac{2}{3}\delta. \tag{6.2.13}$$

For an upper bound, the assumptions of $\delta \leq \frac{1}{2}$ and $\varepsilon \leq \frac{1}{3}$ imply $1 - \varepsilon - \delta \leq 1$, then

$$\begin{aligned}\left\langle|\tau'(z) - \lambda(z)|^2\right\rangle &= \int_\delta^{1-\varepsilon} \alpha^2 \mathrm{d}z + \int_{1-\varepsilon}^1 \frac{\alpha^2}{\varepsilon^2}(1 - \varepsilon - \delta)^2 \mathrm{d}z = \alpha^2\varepsilon^{-1}(1 - \varepsilon - \delta)(1 - \delta) \\ &\leq \frac{\alpha^2}{\varepsilon}.\end{aligned} \tag{6.2.14}$$

Substituting into (6.2.8) with (6.2.10) for α gives

$$\beta \leq 2\sqrt{3}\frac{\alpha}{\varepsilon^{\frac{1}{2}}} = 4\delta. \tag{6.2.15}$$

□

The following auxiliary result estimates the upper bound U on $\overline{\langle wT \rangle}$ in terms of the bottom boundary layer width alone.

Lemma 6.2.2. *Let $\tau(z), \lambda(z)$ and α be given by* (6.2.6), (6.2.7) *and* (6.2.10). *Suppose that the conditions of Lemma 6.2.1 hold. Then*

$$U(\beta, \tau, \lambda) \leq \frac{1}{2} - \frac{\delta}{6}. \tag{6.2.16}$$

Proof. The explicit expression for U is given in (6.2.5). Since τ is a non-negative function we can estimate $\langle \tau(z) \rangle \geq \int_0^\delta \tau(z) \mathrm{d}z = \frac{1}{2}\delta$. Then, using (6.2.9), our choice of β in (6.2.8) and the upper bound on $\langle |\tau'(z) - \lambda(z)|^2 \rangle$ we get

$$U \leq \frac{1}{2} + \frac{\sqrt{3}}{6} \left\langle |\tau'(z) - \lambda(z)|^2 \right\rangle^{\frac{1}{2}} - \langle \tau(z) \rangle \leq \frac{1}{2} + \frac{\sqrt{3}}{6} \frac{\alpha}{\varepsilon^{\frac{1}{2}}} - \frac{1}{2}\delta. \tag{6.2.17}$$

Substitution for α from (6.2.10) gives the desired result. □

To demonstrate that the spectral condition is satisfied we require the following estimate, established in [165], relating the vertical velocity to the scalar vorticity in Fourier space.

Lemma 6.2.3. *Let $w_{\boldsymbol{k}}(z)$ and $\omega_{y,\boldsymbol{k}}(z)$ be functions zero at $z = 0$ and $z = 1$. Given the relation* (6.1.3) *and incompressibility $\nabla \cdot \boldsymbol{u} = 0$, it follows that*

$$|w_{\boldsymbol{k}}| \leq \frac{3^{\frac{3}{4}}}{2^{\frac{3}{2}}} k^{\frac{1}{2}} \min(z, 1-z) \|\omega_{y,\boldsymbol{k}}\|_2. \tag{6.2.18}$$

The following lemma states the choices of δ and ε made so as to satisfy the condition that $\mathcal{S}_{\boldsymbol{k}} \geq 0$ in (6.2.4).

Lemma 6.2.4. *Let $\tau(z), \lambda(z)$ be given by* (6.2.6) *and* (6.2.7) *and $\alpha < 1$ with δ and ε given by the conditions in Lemma 6.2.1 then suppose further that*

$$\delta = \frac{1}{3}\varepsilon^4, \tag{6.2.19a}$$

$$\gamma = \frac{9\sqrt{3}}{1250}R^2\varepsilon^{\frac{23}{2}}, \tag{6.2.19b}$$

$$\varepsilon = \left(\frac{2^{12}5^{16}}{3^{15}}\right)^{\frac{1}{29}} R^{-\frac{10}{29}}. \tag{6.2.19c}$$

Then the spectral constraint $\mathcal{S}_{\boldsymbol{k}} \geq 0$, for $\mathcal{S}_{\boldsymbol{k}}$ given by (6.2.4)*, is satisfied.*

Proof. The final term in (6.2.4) is estimated by use of the Cauchy-Schwarz and Young's inequalities with a nonnegative weight of 2β, to get

$$\gamma k \left\langle \mathrm{Re}\{i\hat{\omega}_{y,\boldsymbol{k}}\hat{T}_{\boldsymbol{k}}\} \right\rangle \leq \beta k^2 \left\langle |\hat{T}_{\boldsymbol{k}}|^2 \right\rangle + \frac{\gamma^2}{4\beta}\left\langle |\hat{\omega}_{y,\boldsymbol{k}}|^2 \right\rangle. \tag{6.2.20}$$

The $\mathcal{S}_{\boldsymbol{k}}$ estimated from below becomes

$$\mathcal{S}_{\boldsymbol{k}} \geq \left\langle \frac{\gamma}{R}|\hat{\omega}'_{y,\boldsymbol{k}}|^2 + \left(\frac{\alpha+\gamma k^2}{R} - \frac{\gamma^2}{4\beta}\right)|\hat{\omega}_{y,\boldsymbol{k}}|^2 + \beta|\hat{T}'_{\boldsymbol{k}}|^2 - (\alpha - \tau'(z))\mathrm{Re}\{\hat{w}_{\boldsymbol{k}}\hat{T}_{\boldsymbol{k}}\} \right\rangle, \tag{6.2.21}$$

where establishing that (6.2.21) is nonnegative is a sufficient condition to demonstrating that the spectral condition holds. Substituting for $\tau(z)$ and taking the modulus the wT term becomes

$$\left\langle (\alpha - \tau'(z))|\hat{w}_{\boldsymbol{k}}\hat{T}_{\boldsymbol{k}}| \right\rangle = \left(\alpha + \frac{1}{\delta}\right)\int_0^\delta |\hat{w}_{\boldsymbol{k}}\hat{T}_{\boldsymbol{k}}|\mathrm{d}z + \frac{\alpha}{\varepsilon}(1-\delta)\int_{1-\varepsilon}^1 |\hat{w}_{\boldsymbol{k}}\hat{T}_{\boldsymbol{k}}|\mathrm{d}z. \tag{6.2.22}$$

Consider first the integral at the lower boundary of $\hat{w}_{\boldsymbol{k}}\hat{T}_{\boldsymbol{k}}$. First, by assumption $\delta \leq \frac{1}{2}$ and $\varepsilon \leq \frac{1}{3}$ then (6.2.10) implies $\alpha = \frac{2}{\sqrt{3}}\delta\varepsilon^{\frac{1}{2}} \leq \frac{1}{\delta}$. Combining with the results of Lemma 6.2.3, the estimate $|T_{\boldsymbol{k}}| \leq \sqrt{z}\,\|T'_{\boldsymbol{k}}\|_2$, the estimate on β^{-1} from (6.2.11),

the Cauchy-Schwarz and Young's inequalities gives

$$\begin{aligned}\left(\alpha+\delta^{-1}\right)\int_0^{\delta}|\hat{w}_{\boldsymbol{k}}\hat{T}_{\boldsymbol{k}}|\mathrm{d}z &\leq \frac{3^{\frac{3}{4}}}{2^{\frac{1}{2}}5}k^{\frac{1}{2}}\delta^{\frac{5}{2}}\left(\alpha+\delta^{-1}\right)\|\hat{\omega}_{y,\boldsymbol{k}}\|_2\|\hat{T}'_{\boldsymbol{k}}\|_2\\ &\leq \frac{\beta}{2}\|\hat{T}'_{\boldsymbol{k}}\|_2^2+\frac{3^{3/2}}{100}\frac{k\delta^5}{\beta}\left(\alpha+\delta^{-1}\right)^2\|\hat{\omega}_{y,\boldsymbol{k}}\|_2^2\\ &\leq \frac{\beta}{2}\|\hat{T}'_{\boldsymbol{k}}\|_2^2+\frac{9\sqrt{3}}{50}k\delta^2\|\hat{\omega}_{y,\boldsymbol{k}}\|_2^2. \qquad (6.2.23)\end{aligned}$$

For the integral at the upper boundary we follow the same steps to obtain

$$\begin{aligned}\alpha\varepsilon^{-1}\left(1-\delta\right)\int_{1-\varepsilon}^{1}|\hat{w}_{\boldsymbol{k}}\hat{T}_{\boldsymbol{k}}|\mathrm{d}z &\leq \frac{3^{\frac{3}{4}}}{2^{\frac{1}{2}}5}k^{\frac{1}{2}}\alpha\varepsilon^{\frac{3}{2}}\|\hat{\omega}_{y,\boldsymbol{k}}\|_2\|\hat{T}'_{\boldsymbol{k}}\|_2\\ &\leq \frac{\beta}{2}\|\hat{T}'_{\boldsymbol{k}}\|_2^2+\frac{3\sqrt{3}}{50}k\delta\varepsilon^4\|\hat{\omega}_{y,\boldsymbol{k}}\|_2^2. \qquad (6.2.24)\end{aligned}$$

Substituting (6.2.10), (6.2.23) and (6.2.24) into the spectral constraint (6.2.4) gives

$$\mathcal{S}_{\boldsymbol{k}}\geq\frac{\gamma}{R}\|\hat{\omega}'_{y,\boldsymbol{k}}\|_2^2+\left(\frac{\frac{2}{\sqrt{3}}\delta\varepsilon^{1/2}+\gamma k^2}{R}-\frac{3\gamma^2}{8\delta}-\frac{9\sqrt{3}}{50}k\delta^2-\frac{3\sqrt{3}}{50}k\delta\varepsilon^4\right)\|\hat{\omega}_{y,\boldsymbol{k}}\|_2^2. \qquad (6.2.25)$$

The right hand side of which is non-negative if the term in parentheses is non-negative. Taking by assumption $\delta=\frac{1}{3}\varepsilon^4$ and that $\gamma=\frac{9\sqrt{3}}{1250}R^2\varepsilon^{\frac{23}{2}}$, the sufficient condition for the spectral constraint to hold is

$$\frac{2\sqrt{3}}{9}\frac{\varepsilon^{\frac{9}{2}}}{R}+\frac{9\sqrt{3}}{1250}\varepsilon^{\frac{23}{2}}Rk^2-\frac{3^7}{2^5 5^8}\varepsilon^{19}R^4-\frac{\sqrt{3}}{25}k\varepsilon^8\geq 0. \qquad (6.2.26)$$

The condition (6.2.26) is quadratic in k with a positive discriminant, and as such it is sufficient for the condition to hold for the minimising $k_m(R,\varepsilon)$. Minimising (6.2.26) with respect to k we find that

$$k_m=\frac{25}{9}\frac{1}{\varepsilon^{\frac{7}{2}}R}. \qquad (6.2.27)$$

Substituting (6.2.27) back into (6.2.26) and rearranging gives

$$\varepsilon \leq \left(\frac{2^8\,5^{16}}{3^{15}}\right)^{\frac{1}{29}} R^{-\frac{10}{29}}, \tag{6.2.28}$$

Then taking ε as (6.2.19c) yields the desired result. □

In Lemma 6.2.4 above we required relations between the variables $(\alpha, \beta, \gamma, \delta, \varepsilon)$. In terms of R the balance parameters are given as

$$\alpha = \frac{2}{3\sqrt{3}}\left(\frac{2^8 5^{16}}{3^{15}}\right)^{\frac{9}{58}} R^{-\frac{45}{29}}, \tag{6.2.29}$$

$$\beta = \frac{2}{9}\left(\frac{2^8 5^{16}}{3^{15}}\right)^{\frac{4}{29}} R^{-\frac{40}{29}}, \tag{6.2.30}$$

$$\gamma = \frac{9\sqrt{3}}{1250}\left(\frac{2^8 5^{16}}{3^{15}}\right)^{\frac{23}{58}} R^{-\frac{57}{29}}. \tag{6.2.31}$$

Proof of Theorem 6.1.1

The final proof of Theorem 6.1.1 then comes by the use of δ from Lemma 6.2.4 and Lemma 6.2.2 to obtain

$$\overline{\langle wT \rangle} \leq \frac{1}{2} - \frac{1}{18}\left(\frac{2^8\,5^{16}}{3^{15}}\right)^{\frac{4}{29}} R^{-\frac{40}{29}}. \tag{6.2.32}$$

6.3 Infinite Prandtl number

In the limit of infinite Prantl number the equations governing the dynamics and the resultant bounding problem is precisely the same as that presented in §5.2. The balance parameters for the kinetic energy of α and enstrophy γ in (6.2.1) are set to be identically zero. As discussed in chapter 5, at infinite Prandtl number the momentum equation can be written as

$$\Delta^2 w = -R\Delta_h T. \tag{6.3.1}$$

The bound on $\overline{\langle wT \rangle}$ is unchanged and given by (6.2.5), however with $\alpha = \gamma = 0$ the spectral constraint (6.2.4) becomes

$$\mathcal{S}_{\boldsymbol{k}} := \left\langle \beta|\hat{T}'_{\boldsymbol{k}}|^2 + \beta k^2|\hat{T}_{\boldsymbol{k}}|^2 + \tau'(z)\mathrm{Re}\{\hat{w}_{\boldsymbol{k}}\hat{T}_{\boldsymbol{k}}\} \right\rangle \geq 0, \quad \forall \hat{w}_{\boldsymbol{k}}\hat{T}_{\boldsymbol{k}} : (6.1.1). \tag{6.3.2}$$

6.3.1 Analytical bound

To prove the bound in Theorem 6.1.2, we seek $\beta > 0$, $\tau(z)$ and $\lambda(z)$ that satisfy the conditions of (6.2.5) and minimise U with $\mathcal{S}_{\boldsymbol{k}}$ given by (6.3.2). We take $\tau(z)$ and $\lambda(z)$ the same as in (6.2.6) and (6.2.7) and use both Lemma 6.2.1 and Lemma 6.2.2. To establish that the spectral constraint (6.3.2) is satisfied we require the following result, before which we introduce the pseudo-vorticity in Fourier space

$$\hat{\zeta}_{\boldsymbol{k}} := \frac{1}{k}\left(\partial_{zz} - k^2\right)\hat{w}_{\boldsymbol{k}} = \frac{1}{k}\mathcal{A}\hat{w}_{\boldsymbol{k}}, \tag{6.3.3}$$

where $\mathcal{A} = \partial_{zz} - k^2$. The pseudo-vorticity has boundary conditions

$$\hat{\zeta}_{\boldsymbol{k}}|_{z=\{0,1\}} = 0. \tag{6.3.4}$$

Lemma 6.3.1. *Taking* $(\boldsymbol{u}, T) \in \mathcal{U}_2 \times \mathcal{T}_1^+$, *where* $\boldsymbol{u}$ *and* T *satisfy* (6.3.1) *with boundary conditions* (6.1.1). *Let the pseudo-vorticity* $\hat{\zeta}_{\boldsymbol{k}}$ *be given by* (6.3.3). *Then*

$$k^2R^2\left\langle |\hat{T}_{\boldsymbol{k}}|^2 \right\rangle \geq k^4\left\langle |\hat{\zeta}_{\boldsymbol{k}}|^2 \right\rangle, \tag{6.3.5}$$

and

$$\left\langle |\hat{w}_{\boldsymbol{k}}\hat{T}_{\boldsymbol{k}}| \right\rangle = \frac{1}{R}\left\langle |\hat{\zeta}_{\boldsymbol{k}}|^2 \right\rangle. \tag{6.3.6}$$

Proof. Due to horizontal periodicity in Fourier space the equation linking $\hat{w}_{\boldsymbol{k}}$ and $\hat{T}_{\boldsymbol{k}}$ from (6.3.1) becomes

$$Rk^2\hat{T}_{\boldsymbol{k}} = \hat{w}''''_{\boldsymbol{k}} - 2k^2\hat{w}''_{\boldsymbol{k}} + k^4\hat{w}_{\boldsymbol{k}} = \mathcal{A}^2\hat{w}_{\boldsymbol{k}}. \tag{6.3.7}$$

Given the definition of the pseudo-vorticity from (6.3.3), substituting into (6.3.7) gives

$$kR\hat{T}_{\boldsymbol{k}} = \mathcal{A}\hat{\zeta}_{\boldsymbol{k}}. \tag{6.3.8}$$

Then if we square (6.3.8) and integrate over the domain, integrate by parts with use of the boundary conditions $\hat{\zeta}_{\boldsymbol{k}}(0) = \hat{\zeta}_{\boldsymbol{k}}(1) = 0$ gives

$$k^2R^2\left\langle|\hat{T}_{\boldsymbol{k}}|^2\right\rangle = \left\langle|\hat{\zeta}''_{\boldsymbol{k}}|^2 + 2k^2|\hat{\zeta}'_{\boldsymbol{k}}|^2 + k^4|\hat{\zeta}_{\boldsymbol{k}}|^2\right\rangle. \tag{6.3.9}$$

The first two terms on the right-hand side of (6.3.9) are positive and therefore the left hand side can be bounded from below, giving the desired result (6.3.5).

To demonstrate (6.3.6) we need only use (6.3.3) and (6.3.8), rearranging in terms of $\hat{w}_{\boldsymbol{k}}$ and $\hat{T}_{\boldsymbol{k}}$ such that substituting gives

$$\left\langle|\hat{w}_{\boldsymbol{k}}\hat{T}_{\boldsymbol{k}}|\right\rangle = \frac{1}{R}\left\langle|\hat{\zeta}_{\boldsymbol{k}}|^2\right\rangle.$$

□

The final result required to obtain Theorem 6.1.2 are the following conditions on the boundary layer variables of the background profiles to ensure the positivity of the spectral constraint (6.3.2).

Lemma 6.3.2. *Let $\tau(z)$ be given by* (6.2.6)*, and δ and ε satisfy the conditions of Lemma 6.2.1. Suppose further that*

$$\delta = \frac{1}{3}\varepsilon^4, \tag{6.3.10}$$

$$\varepsilon = \left(\frac{2^{24}5^{16}}{3^{23}}\right)^{\frac{1}{29}} R^{-\frac{10}{29}}. \tag{6.3.11}$$

Then, the spectral constraint (6.3.2) *is satisfied.*

Proof. The functional $\mathcal{S}_{\boldsymbol{k}}$ in Fourier space after use of (6.3.5) can be estimated from below,

$$\mathcal{S}_{\boldsymbol{k}} \geq \left\langle \beta|\hat{T}'_{\boldsymbol{k}}|^2 + \frac{\beta k^4}{R^2}|\hat{\zeta}_{\boldsymbol{k}}|^2 + \tau'(z)|\hat{w}_{\boldsymbol{k}}\hat{T}_{\boldsymbol{k}}| \right\rangle. \tag{6.3.12}$$

The sign indefinite term in $\mathcal{S}_{\boldsymbol{k}}$ is evaluated with $\tau(z)$ given by (6.2.6) and after rearranging we use (6.3.6) to get

$$\begin{aligned}
\left\langle \tau'(z)|\hat{w}_{\boldsymbol{k}}\hat{T}_{\boldsymbol{k}}| \right\rangle &= -\frac{1}{\delta}\int_0^{\delta} |\hat{w}_{\boldsymbol{k}}\hat{T}_{\boldsymbol{k}}|\mathrm{d}z + \frac{2}{\sqrt{3}}\delta\varepsilon^{\frac{1}{2}}\int_{\delta}^{1-\varepsilon} |\hat{w}_{\boldsymbol{k}}\hat{T}_{\boldsymbol{k}}|\mathrm{d}z \\
&\quad -\frac{2}{\sqrt{3}}\delta\varepsilon^{-\frac{1}{2}}(1-\varepsilon-\delta)\int_{1-\varepsilon}^{1} |\hat{w}_{\boldsymbol{k}}\hat{T}_{\boldsymbol{k}}|\mathrm{d}z \\
&\geq \frac{2}{\sqrt{3}}\frac{\delta\varepsilon^{\frac{1}{2}}}{R}\left\langle |\hat{\zeta}_{\boldsymbol{k}}|^2 \right\rangle - \left(\delta^{-1} + \frac{2}{\sqrt{3}}\delta\varepsilon^{\frac{1}{2}}\right)\int_0^{\delta} |\hat{w}_{\boldsymbol{k}}\hat{T}_{\boldsymbol{k}}|\mathrm{d}z \\
&\quad -\frac{2}{\sqrt{3}}\delta\varepsilon^{-\frac{1}{2}}(1-\delta)\int_{1-\varepsilon}^{1} |\hat{w}_{\boldsymbol{k}}\hat{T}_{\boldsymbol{k}}|\mathrm{d}z.
\end{aligned} \tag{6.3.13}$$

The integral at the lower boundary with (6.3.13), was previously estimated in (6.2.23) and follows through at infinite Pr where we only need to replace $\hat{\omega}_{y,k}$ in Lemma 6.2.3 with $\hat{\zeta}_k$. Likewise, the integral at the upper boundary has been estimated with (6.2.24). Using both (6.2.23) and (6.2.24) in (6.3.13) gives

$$\left\langle \tau'(z)|\hat{w}_{\boldsymbol{k}}\hat{T}_{\boldsymbol{k}}| \right\rangle \geq \left(\frac{2}{\sqrt{3}}\frac{\delta\varepsilon^{\frac{1}{2}}}{R} - \frac{9\sqrt{3}}{50}k\delta^2 - \frac{3\sqrt{3}}{50}k\delta\varepsilon^4\right)\left\langle |\hat{\zeta}_{\boldsymbol{k}}|^2 \right\rangle - \beta\left\langle |\hat{T}'_{\boldsymbol{k}}|^2 \right\rangle. \tag{6.3.14}$$

Substituting (6.3.14) into (6.3.12) and taking by assumption $\delta = \frac{1}{3}\varepsilon^4$ gives

$$\mathcal{S}_{\boldsymbol{k}} \geq \left(\frac{2}{9}\frac{\varepsilon^4 k^4}{R^2} + \frac{2\sqrt{3}}{9}\frac{\varepsilon^{\frac{9}{2}}}{R} - \frac{\sqrt{3}}{25}k\varepsilon^8\right)\left\langle |\hat{\zeta}_{\boldsymbol{k}}|^2 \right\rangle. \tag{6.3.15}$$

The sufficient condition to demonstrate $\mathcal{S}_{\boldsymbol{k}} \geq 0$ is to show that the parentheses in (6.3.15) is non-negative. In fact we need only demonstrate this for the minimising possible $k_m(R,\varepsilon)$. Minimising with respect to k, we find that

$$k_m = \left(\frac{9\sqrt{3}}{200}\right)^{\frac{1}{3}}\varepsilon^{\frac{4}{3}}R^{\frac{2}{3}}. \tag{6.3.16}$$

Substituting (6.3.16) back into (6.3.15) and rearranging gives the condition

$$\varepsilon \leq \left(\frac{2^{24}5^{16}}{3^{23}}\right)^{\frac{1}{29}} R^{-\frac{10}{29}}. \tag{6.3.17}$$

Taking ε as given by (6.3.11) gives the desired result. □

Having shown the relation of β to the boundary layer variables δ and ε in terms of R we have

$$\beta = \frac{192}{49}\left(\frac{2^{24}5^{16}}{3^{23}}\right)^{\frac{4}{29}} R^{-\frac{40}{29}}. \tag{6.3.18}$$

Proof of Theorem 6.1.2

The final proof of Theorem 6.1.2 follows by use of the results from Lemma 6.3.2 and Lemma 6.2.2, such that

$$\overline{\langle wT\rangle} \leq \frac{1}{2} - \frac{1}{18}\left(\frac{2^{24}5^{16}}{3^{23}}\right)^{\frac{1}{29}} R^{-\frac{40}{29}}. \tag{6.3.19}$$

Remark 6.3.1. The only balance parameter in the auxiliary functional for the $Pr = \infty$ case is that of β. However, the proof of Theorem 6.1.2 proceeds by taking an identical profile of $\tau(z)$ to the case of $Pr < \infty$ where α appears. The reason is as follows. Taking any piecewise linear $\tau(z)$ satisfying $\tau(0) = 1$ and $\tau(1) = 0$ with two boundary layers at the top and bottom, corresponds to choosing $\tau(z)$ with a gradient $n \geq 0$ in the bulk. However in (6.3.15), the crucial positive term of $\mathcal{O}(1)$ comes from choosing $n > 0$, otherwise for small k the parenthesis in (6.3.15) would not be positive since the only remaining positive term is $\mathcal{O}(k^4)$. Therefore, picking $n > 0$ is critical to satisfying the spectral constraint. It then turns out that optimising n gives exactly the α as chosen for the $Pr < \infty$ given in (6.2.10).

6.4 Discussion

With a change of the kinematic boundary conditions to free-slip, the upper bounds on heat transport have been demonstrated to be lower in both cases where $Pr < \infty$ and $Pr = \infty$ as compared to a flow between no-slip boundaries. The smaller exponent with R stems from the lack of vorticity production at the walls due to the boundary conditions and lack of vortex stretching by the flow. This makes the results arguably less physical for convection that is not asymptotically strong in R. Regardless we make a few remarks about the results established in this chapter and point to possible future directions for the research.

The two results of Theorem 6.1.1 and Theorem 6.1.2 exhibit the same scaling behaviour, however the proof valid at infinite Pr holds for three dimensions while that at arbitrary Pr is only true in two dimensions. For Rayleigh–Bénard convection, it has been demonstrated that by treating the governing equations valid for finite Pr as a perturbation of the infinite Pr system [155], a bound can be proven on the convective heat transport valid for large Rayleigh numbers in three dimensions and at all Pr [156]. However for Rayleigh–Bénard convection, such a proof relies on the use of a maximum principle for the temperature ($\|T\|_{L^\infty} \leq 1$), since this has not been proven for the problem in this chapter the proof does not follow through trivially. Nevertheless, it would be of interest to see if the ideas can be used to prove a bound on $\overline{\langle wT \rangle}$.

Considering Navier-slip boundary conditions is a means to interpolate between the no-slip and free-slip cases. This involves imposing Robin-type boundary conditions with a parameter referred to as the slip length which in different limits gives the different kinematic configurations. Bounds on heat transport under Navier-slip conditions have been proven for Rayleigh–Bénard convection [37]. Whether or not the same can be applied to $\overline{\langle wT \rangle}$ or $\overline{\langle T \rangle}$ in internally heated heated convection is an open question.

The background profiles $\tau(z)$ constructed in the proofs are piecewise linear. We demonstrated that constructions with multiply embedded boundary layers or logarithmic behaviour are critical to proving R-dependent bounds that are strictly less than $\frac{1}{2}$ in §3.3.2 & §5.2. Whether a similar approach and increasingly complicated profiles of $\tau(z)$ can be used to improve the bounds in Theorem 6.1.1 or Theorem 6.1.2, is an unanswered question, that may be elucidated through numerical optimisation. Furthermore, at arbitrary Pr and for $Pr = \infty$ we have proven bounds when the lower boundary is an insulator, yet we are as yet unable to do the same for free-slip boundaries. Seeking upper bounds with an insulating lower boundary and free-slip should be a future direction of research.

One key element in the proof of the free-slip theorems was the assumption that $\delta \neq \varepsilon$ in the constructions of $\tau(z)$. If instead we were to simplify the problem and set the boundary layer widths as equal then we would obtain $\overline{\langle wT \rangle} \leq \frac{1}{2} - cR^{-2}$, an identical result to Theorem 5.1.1. As such $\delta \neq \varepsilon$ is critical to our bound and specifically it was the case that $\delta = \varepsilon^4$. However, predictions from heuristic arguments of appendix B are that $\delta = \varepsilon^2$, for isothermal boundaries. It is anticipated that if a different background profile can be constructed where δ is not forced to be as small relative to ε, the upper bound on $\overline{\langle wT \rangle}$ could be improved. One way to probe if this is possible or not is to carry out a numerical optimisation of the problem with the SDP methods discussed throughout this thesis.

Chapter 7

Poorly conducting boundaries

Freedom is the truth of necessity.

G.W.F. Hegel - The Science of Logic

The results in this chapter appear in the publication [1]. Having proven bounds for internally heated convection where at least one of the boundaries is isothermal (chapter 3 & chapter 4), the major difficulty in bounding the heat transport was the subtle interplay between the lower and upper thermal boundary layers [2], and it was shown that the use of a minimum principle was necessary to obtain upper bounds on $\overline{\langle wT \rangle}$ which converge to $\frac{1}{2}$ from below asymptotically. If the thermal boundary condition at the top is replaced by a fixed flux condition the minimum principle can no longer be proven to hold, to the best of knowledge available at this time.

7.1 Setup

We are considering uniform internally heated convection with no-slip velocity boundary conditions and fixed-flux thermal boundary conditions

$$\boldsymbol{u}|_{z=\{0,1\}} = 0, \tag{7.1.1a}$$

$$\partial_z T|_{z=0} = 0, \quad \partial_z T|_{z=1} = -1, \tag{7.1.1b}$$

such that $(\boldsymbol{u}, T) \in \mathbb{A} = \mathcal{U}_1 \times \mathcal{T}_3$ as defined in (2.1.2).

We remove the subtleties associated with the lower boundary by considering a zero-flux condition as shown in Figure 1.1(c). The hypothesis behind this choice is that the resulting problem will be driven primarily by the properties of the unstably-stratified thermal boundary layer near the top boundary and, therefore, will bear a closer resemblance to Rayleigh–Bénard convection. To ensure that convection can reach a statistically stationary state we also replace the isothermal top boundary with a fixed-flux condition that matches the total generation of internal heat.

Within this flow configuration, our goal remains the same; to bound the convective heat flux $\overline{\langle wT \rangle}$. Consideration of the fluid's potential energy, which for the Boussinesq equations used here can be expressed as $(1 - z)T$, shows that

$$\overline{\langle wT \rangle} + \overline{\langle T|_{z=0} \rangle_h} - \overline{\langle T|_{z=1} \rangle_h} = \frac{1}{2}, \tag{7.1.2}$$

In (7.1.2), the input of potential energy ($\frac{1}{2}$) balances the reversible work, $\overline{\langle wT \rangle}$, done by the velocity field (equal to the average viscous dissipation) and the unknown rate $\overline{\langle T|_{z=0} \rangle_h} - \overline{\langle T|_{z=1} \rangle_h}$ at which the fluid's centre of mass would decrease due to conduction in the absence of fluid motion [71]. The sign of the conductive term $\overline{\langle T|_{z=0} \rangle_h} - \overline{\langle T|_{z=1} \rangle_h}$ is *a priori* unknown, but it can be shown [58] that

$$|\overline{\langle T|_{z=0} \rangle_h} - \overline{\langle T|_{z=1} \rangle_h}| \leq |\overline{\langle T \rangle} - \overline{\langle T|_{z=1} \rangle_h}|^{1/2}. \tag{7.1.3}$$

For sufficiently large Rayleigh numbers, this estimate can be combined with the bounds of [97] that

$$cR^{-1/3} < \overline{\langle T \rangle} - \overline{\langle T|_{z=1} \rangle_h} \leq \frac{1}{3}, \tag{7.1.4}$$

to find

$$\overline{\langle wT \rangle} \leq \frac{1}{2} + \frac{1}{\sqrt{3}}, \tag{7.1.5}$$

uniformly in R and Pr. However, assuming that $\langle T|_{z=0}\rangle_h$ and $\langle T\rangle$ scale similarly with the Rayleigh number, it was conjectured in [58] that the mean vertical heat transport should satisfy $\overline{\langle wT\rangle} \leq \frac{1}{2} - O(R^{-1/3})$. In this chapter while we are unable to prove such a bound instead it will be shown in Theorem 7.1.1 below, that upper bounds on $\overline{\langle wT\rangle}$ that approach $\frac{1}{2}(\frac{1}{2} + \frac{1}{\sqrt{3}}) > \frac{1}{2}$ from below are possible to obtain. Note that this improves the best known bound (7.1.5).

As the mean temperature $\langle T\rangle$ is conserved in time, we assume it vanishes without loss of generality. With this extra condition, the governing equations admit the solution $\boldsymbol{u} = 0$, $p =$ constant and $T = -\frac{z^2}{2} + \frac{1}{6}$ at all R, which represents a purely conductive state. This state is globally asymptotically stable irrespective of the horizontal periods L_x and L_y if $R < 1429.86$ and linearly unstable when $R > 1440$ for a sufficiently large horizontal period [57]. Convection is guaranteed above this Rayleigh number for at least one choice of the horizontal periods, but cannot be ruled out above the global stability threshold. We are therefore interested in bounds on $\overline{\langle wT\rangle}$ that hold for arbitrary $R \geq 1429.86$.

Theorem 7.1.1. *(Fixed flux uniform heating) Suppose that* $\boldsymbol{u}$ *and* T *solve* (1.2.3) *and satisfy the boundary conditions* (7.1.1)*. Then there exists a constant* $c > 0$ *such that for sufficiently large* $R > 0$*,*

$$\overline{\langle wT\rangle} \leq \frac{1}{2}\left(\frac{1}{2} + \frac{1}{\sqrt{3}}\right)\left(1 - cR^{-\frac{1}{3}}\right). \tag{7.1.6}$$

Remark 7.1.1. It is shown in §7.2.2 that the theorem holds for $c = 3.073$ for any $R > 591.51$.

Corollary 7.1.1. *For all sufficiently large* R*,*

$$Nu \leq \left[\frac{1}{2} - \frac{1}{\sqrt{3}} + c\left(\frac{1}{2} + \frac{1}{\sqrt{3}}\right)R^{-\frac{1}{3}}\right]^{-1}. \tag{7.1.7}$$

7.2 Optimal bounds with ϑ

To derive an upper bound on $\overline{\langle wT \rangle}$, it is convenient to lift the inhomogeneous boundary condition on the temperature with respect to the conductive profile by introducing the temperature perturbation

$$\vartheta(\boldsymbol{x}, t) = T(\boldsymbol{x}, t) + \frac{z^2}{2} - \frac{1}{6}. \tag{7.2.1}$$

The heat equation (1.2.3c) and boundary conditions (7.1.1b) can be used to show that ϑ satisfies

$$\partial_t \vartheta + \boldsymbol{u} \cdot \nabla \vartheta = \Delta \vartheta + zw, \tag{7.2.2a}$$

$$\partial_z \vartheta|_{z=0} = 0, \quad \partial_z \vartheta|_{z=1} = 0. \tag{7.2.2b}$$

Since we now work with homogeneous boundary conditions and the field ϑ the space on ϑ is well defined as

$$\mathcal{T}_3 = \Big\{ \vartheta \in H^1(\Omega) \;\Big|\; \vartheta \text{ is periodic in } x, y, \text{ (7.2.2b)} \Big\}. \tag{7.2.3}$$

Lemma 7.2.1. *Let w be the z-component of the divergence free field $\boldsymbol{u}$, with Dirichlet boundary conditions at $z = 0$ and $z = 1$. For any $f(z) : [0, 1] \to \mathbb{R}$*

$$\langle w f(z) \rangle = \int_0^1 \langle w(z) \rangle_h f(z) \, \mathrm{d}z = 0. \tag{7.2.4}$$

Proof. The vertical velocity, w, has no horizontal mean, given the no-slip boundary conditions (7.1.1) and incompressibility and as such the lemma follows trivially. □

Given (7.2.1) and Lemma 7.2.1 we conclude, in particular, that

$$\overline{\langle wT \rangle} = \overline{\langle w\vartheta \rangle}. \tag{7.2.5}$$

The rigorous upper bound on $\overline{\langle w\vartheta \rangle}$ is derived with the quadratic auxiliary functional (2.2.5) with T replaced by the temperature perturbations ϑ and as such the Lie derivative calculated over the equations where (7.2.2a) replaces (1.2.3c). Since it can be shown that $\mathcal{V}\{\boldsymbol{u}(t), \vartheta(t)\}$ remains uniformly bounded in time along solutions of (1.2.3b) and (7.2.2a) for any given initial velocity and temperature, employing the method outlined in (2.2), after integration by parts and the boundary conditions (7.2.2b), $\overline{\langle wT \rangle} \leq U$ if

$$\mathcal{S}\{\boldsymbol{u}, \vartheta\} := \left\langle \frac{\alpha}{R}|\nabla \boldsymbol{u}|^2 + \beta|\nabla\vartheta|^2 - (\alpha + 1 + \beta z - \varphi'(z))w\vartheta - \varphi'(z)\vartheta' + U \right\rangle \geq 0\,. \tag{7.2.6}$$

The major difference in $\mathcal{S}$ as compared to the previous two thermal boundary conditions (c.f. (2.2.9)) is a $\beta z w\vartheta$ term which consequently appears in the spectral constraint since it is quadratic.

Definition 7.2.1 (Spectral constraint)**.** The pair $(\alpha, \beta, \varphi(z))$ is said to satisfy the *spectral constraint* if

$$\left\langle \frac{\alpha}{R}\,|\nabla \boldsymbol{u}|^2 + \beta\,|\nabla\vartheta|^2 - (\alpha + 1 + \beta z - \varphi'(z))w\vartheta \right\rangle \geq 0,\ \forall (\boldsymbol{u}, \vartheta) \in \mathcal{U}_1 \times \mathcal{T}_3. \tag{7.2.7}$$

Lemma 7.2.2. *Suppose that $(\alpha, \beta, \varphi(z))$ satisfy the spectral constraint. Then,*

$$\overline{\langle wT \rangle} = \overline{\langle w\vartheta \rangle} \leq U(\beta, \varphi) := \left\langle \frac{\varphi'(z)^2}{4\beta} \right\rangle. \tag{7.2.8}$$

Proof. First take (7.2.6) and rewrite the functional $\mathcal{S}\{\boldsymbol{u}, \vartheta\}$ in Fourier space. Invoking the horizontal periodicity we expand the velocity and temperature fields using Fourier series,

$$\begin{bmatrix} \vartheta(x,y,z) \\ \boldsymbol{u}(x,y,z) \end{bmatrix} = \sum_{\boldsymbol{k}} \begin{bmatrix} \hat{\vartheta}_{\boldsymbol{k}}(z) \\ \hat{\boldsymbol{u}}_{\boldsymbol{k}}(z) \end{bmatrix} \mathrm{e}^{i(k_x x + k_y y)}\,. \tag{7.2.9}$$

The sum is over wavevectors $\boldsymbol{k} = (k_x, k_y)$ of magnitude $k = \sqrt{k_x^2 + k_y^2}$ that are compatible with the horizontal periods L_x and L_y. The (complex-valued) Fourier amplitudes $\hat{\vartheta}_{\boldsymbol{k}}$ and $\hat{\boldsymbol{u}}_{\boldsymbol{k}}$ satisfy

$$\hat{w}_{\boldsymbol{k}}(0) = \hat{w}'_{\boldsymbol{k}}(0) = \hat{w}_{\boldsymbol{k}}(1) = \hat{w}'_{\boldsymbol{k}}(1) = 0, \tag{7.2.10a}$$

$$\hat{\vartheta}'_{\boldsymbol{k}}(0) = \hat{\vartheta}'_{\boldsymbol{k}}(1) = 0. \tag{7.2.10b}$$

After substituting (7.2.9) into (7.2.6), the Fourier-transformed incompressibility condition $ik_x\hat{u}_{\boldsymbol{k}} + ik_y\hat{v}_{\boldsymbol{k}} + \hat{w}'_{\boldsymbol{k}} = 0$ can be combined with Young's inequality to estimate

$$\mathcal{S}\{\boldsymbol{u}, \vartheta\} \geq \mathcal{S}_0\{\hat{\vartheta}_0\} + \sum_{\boldsymbol{k}} \mathcal{S}_{\boldsymbol{k}}\{\hat{w}_{\boldsymbol{k}}, \hat{\vartheta}_{\boldsymbol{k}}\}, \tag{7.2.11}$$

where

$$\mathcal{S}_0\{\hat{\vartheta}_0\} := U + \int_0^1 \beta|\hat{\vartheta}'_0(z)|^2 - \varphi'(z)\hat{\vartheta}'_0(z)\,\mathrm{d}z\,, \tag{7.2.12a}$$

and

$$\mathcal{S}_{\boldsymbol{k}}\{\hat{w}_{\boldsymbol{k}}, \hat{\vartheta}_{\boldsymbol{k}}\} := \int_0^1 \frac{\alpha}{R}\left(\frac{|\hat{w}''_{\boldsymbol{k}}(z)|^2}{k^2} + 2|\hat{w}'_{\boldsymbol{k}}(z)|^2 + k^2|\hat{w}_{\boldsymbol{k}}(z)|^2\right) + \beta|\hat{\vartheta}'_{\boldsymbol{k}}(z)|^2 + \beta k^2|\hat{\vartheta}_{\boldsymbol{k}}(z)|^2 - [\alpha + 1 + \beta z - \varphi'(z)]\hat{w}_{\boldsymbol{k}}(z)^*\hat{\vartheta}_{\boldsymbol{k}}(z)\,\mathrm{d}z\,. \tag{7.2.12b}$$

Standard arguments (see e.g.,[2]) show that the right-hand side of (7.2.11) is nonnegative if and only if each summand is nonnegative, and that to check these conditions one can assume that $\hat{w}_{\boldsymbol{k}}$ and $\hat{\vartheta}_{\boldsymbol{k}}$ are real valued functions. If $\mathcal{S}_{\boldsymbol{k}} \geq 0$ this implies the spectral constraint is satisfied. The bound can then be obtained from necessary condition that gives $\mathcal{S}_0 \geq 0$. We continue by observing that

$$\mathcal{S}_0 = \int_0^1 \beta\left(\hat{\vartheta}'_0(z) - \frac{\varphi'(z)}{2\beta}\right)^2 - \frac{\varphi'(z)^2}{4\beta} + U\,\mathrm{d}z \geq U - \int_0^1 \frac{\varphi'(z)^2}{4\beta}\,\mathrm{d}z, \tag{7.2.13}$$

so the constraint $\mathcal{S}_0 \geq 0$ is satisfied if we choose

$$U = \int_0^1 \frac{\varphi'(z)^2}{4\beta}\,\mathrm{d}z. \tag{7.2.14}$$

□

Remark 7.2.1. Setting $\hat{\vartheta}_0'(z) = \frac{1}{2\beta}\varphi'(z)$ except for infinitesimally thin boundary layers near $z = 0$ and 1, where $\hat{\vartheta}_0' = 0$ to satisfy (7.2.10b), reveals that this choice is optimal.

7.2.1 Numerically optimal bounds

In the proof of Lemma 7.2.2, the functional (7.2.6) is estimated from below by two functionals $\mathcal{S}_0$ and $\sum_{\boldsymbol{k}} \mathcal{S}_{\boldsymbol{k}}$. The best bound on $\overline{\langle w\vartheta\rangle}$ is then found upon solving the optimisation problem

$$\begin{aligned}\inf_{U,\varphi'(z),\alpha,\beta} \big\{U :\quad & \mathcal{S}_0\{\hat{\vartheta}_0\} \geq 0 \quad \forall\, \hat{\vartheta}_0 : (7.2.10\mathrm{b}),\\ & \mathcal{S}_{\boldsymbol{k}}\{\hat{w}_{\boldsymbol{k}}, \hat{\vartheta}_{\boldsymbol{k}}\} \geq 0 \quad \forall\, \hat{w}_{\boldsymbol{k}}, \hat{\vartheta}_{\boldsymbol{k}} : (7.2.10a,b),\ \forall \boldsymbol{k} \neq 0\big\}.\end{aligned} \tag{7.2.15}$$

Additionally we consider $\varphi'(z)$, rather than $\varphi(z)$, as the optimization variable because only the former appears in the problem.

We start by solving (7.2.15) numerically to guide the analysis, by using the MATLAB toolbox QUINOPT [49]. This toolbox employs truncated Legendre series expansions for the tunable function $\varphi(z)$ and for the unknown fields $\hat{\vartheta}_0$, $\hat{\vartheta}_{\boldsymbol{k}}$ and $\hat{w}_{\boldsymbol{k}}$ in order to discretise the convex variational problem (7.2.15) into a numerically tractable semidefinite program (SDP) [44, 46, 47, 140, 141]. Numerically optimal solutions to (7.2.15) were obtained for $10^3 \leq R \leq 10^9$ in a two-dimensional domain with horizontal period $L_x = 2$. The number of terms in the Legendre series expansion used by QUINOPT was increased until the optimal upper bound changed by less than 1%, and an iterative procedure (see e.g., [47]) was employed to check the spectral

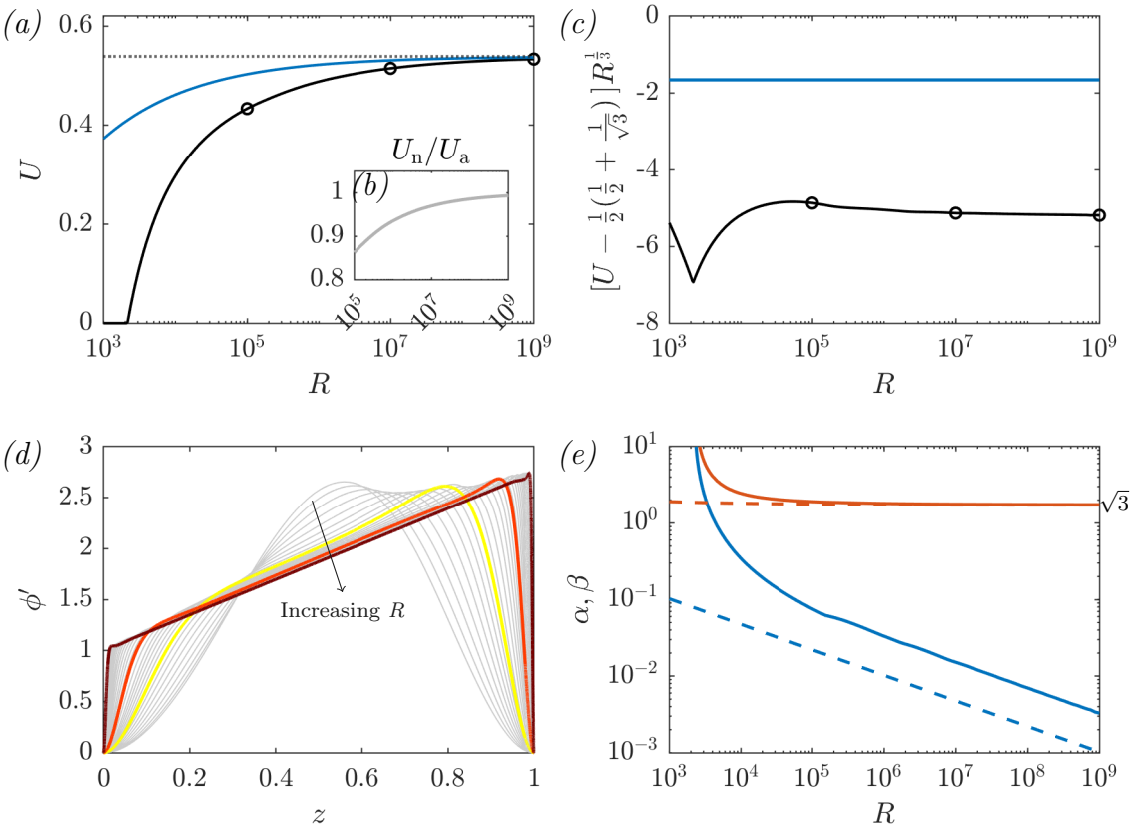

Figure 7.1: *Panel (a)*: Numerically optimal bounds U_n computed with QUINOPT(—), compared to the analytical bound U_a (7.2.36) (—) and the improved uniform upper bound $\frac{1}{2}(\frac{1}{2}+\frac{1}{\sqrt{3}})$ (·····). Insert *(b)* shows the ratio of the two R-dependent bounds. *Panel (c)*: Analytical (—) and numerical (—) corrections to the uniform bound $\frac{1}{2}(\frac{1}{2}+\frac{1}{\sqrt{3}})$, compensated by $R^{\frac{1}{3}}$. *Panel (d)*: Numerically optimal profiles φ' for $10^3 \leq R \leq 10^9$ (—). Highlighted profiles for $R = 10^5$ (—), $R = 10^7$ (—) and $R = 10^9$ (—) correspond to the circles in panels *(a)* and *(c)*. *Panel (e)*: Balance parameters α (— optimal; - - - analytical) and β (— optimal; - - - analytical).

constraints $\mathcal{S}_{\boldsymbol{k}} \geq 0$ up to the cut-off wavenumber

$$k_c := \left(\frac{R}{4\alpha\beta}\right)^{\frac{1}{4}} \|\alpha + 1 + \beta z - \varphi'(z)\|_\infty^{\frac{1}{2}}\,. \tag{7.2.16}$$

This value is derived using Lemma 4.2.1, recalling that it is true that $\mathcal{S}_{\boldsymbol{k}} \geq 0$ for any $k \geq k_c$.

The numerically optimal bounds on $\overline{\langle w\vartheta \rangle}$ are compared to the analytical bound Theorem 7.1.1 in Figure 7.1*(a)*. The former are zero until $R_E = 2\,147$, which differs from the energy stability limit reported by [57] due to the choice of horizontal period

made in our numerical implementation. Insert *(b)* reveals that the optimal and analytic bounds appear to tend to the same asymptotic value as $R \to \infty$ and, as evidenced by panel *(c)*, seem to do so at the same rate. This strongly suggests that the only possible improvement to our analytical bound is the magnitude of the $O(R^{-\frac{1}{3}})$ correction.

Figures 7.1*(d)* and 7.1*(e)* show the optimal profiles of $\varphi'(z)$ and the optimal balance parameters α, β in the range of R spanned by our computations. For large R, the optimal $\varphi'(z)$ are approximately piecewise linear, corroborating our analytical choice in (7.2.20), and the optimal balance parameters behave like the analytical ones (plotted with dashed lines). The main differences between the optimal and analytical $\varphi'(z)$ profiles are oscillations near the edge of the boundary layers and the fact that the two boundary layers of the optimal $\varphi'(z)$ have different widths. This suggests that a better prefactor for the $O(R^{-\frac{1}{3}})$ term in our analytical bound could be obtained, at the expense of more complicated algebra, by considering boundary layers of different size.

7.2.2 Analytical bound

The numerically optimal results indicate two key points, first that the uniform upper bound on $\overline{\langle wT \rangle}$ is exactly half that known previously from [58]. Secondly that the R correction to the uniform bound scales as $R^{\frac{1}{3}}$. We proceed to demonstrate the results observed in the numerical optimisation.

Theorem 7.2.1. *(Uniform upper bound) Suppose that* $\boldsymbol{u}$ *and* T *solve* (1.2.3) *subject to boundary conditions* (7.1.1)*. Then for all* R *and* Pr*,*

$$0 \leq \overline{\langle wT \rangle} \leq \frac{1}{2}\left(\frac{1}{2} + \frac{1}{\sqrt{3}}\right). \tag{7.2.17}$$

Proof. We use the results of Lemma 7.2.2 and seek α and β and a function $\varphi(z)$ that minimize the right-hand side of (7.2.8) whilst satisfying the spectral constraint

(7.2.7). The simplest way to ensure this is to set $\varphi'(z) = \alpha + 1 + \beta z$, because then the sign-indefinite term in (7.2.6) vanishes giving $\mathcal{S} \geq 0$. The bound for this choice then reads

$$\overline{\langle wT \rangle} \leq U = \frac{1}{12}\left[\beta + 3(\alpha+1) + \frac{(\alpha+1)^2}{\beta}\right]. \tag{7.2.18}$$

Then minimising with respect to β we find that $\beta = \sqrt{3}(\alpha+1)$, minimising for α the optimal choice is $\alpha = 0$. Substituting for the minimising α and β in (7.2.18) gives $U = \frac{1}{2}\left(\frac{1}{2} + \frac{1}{\sqrt{3}}\right)$. □

Theorem 7.2.1 halves the previous uniform bound [58]. An even better result that depends explicitly on the Rayleigh number can be obtained by letting $\varphi'(z)$ develop boundary layers of width δ near $z = 0$ and 1. Specifically, we still fix

$$\beta = \sqrt{3}(\alpha+1), \tag{7.2.19}$$

but this time take

$$\varphi'(z) = (\alpha+1)\xi(z), \qquad \xi(z) = \begin{cases} \left(\frac{1}{\delta} + \sqrt{3}\right) z, & 0 \leq z \leq \delta, \\ 1 + \sqrt{3}\, z, & \delta \leq z \leq 1-\delta, \\ \left(\frac{1+\sqrt{3}}{\delta} - \sqrt{3}\right)(1-z), & 1-\delta \leq z \leq 1. \end{cases} \tag{7.2.20}$$

At first glance (7.2.8) suggests setting $\varphi'(z) = 0$ throughout the boundary layers, to minimise U, given that we require $\varphi'(z)$ to satisfy a value in the bulk from $\mathcal{S}_{\boldsymbol{k}} \geq 0$. However it is the case that a linear variation makes the spectral constraint easier to satisfy and results in a smaller bound on $\overline{\langle wT \rangle}$.

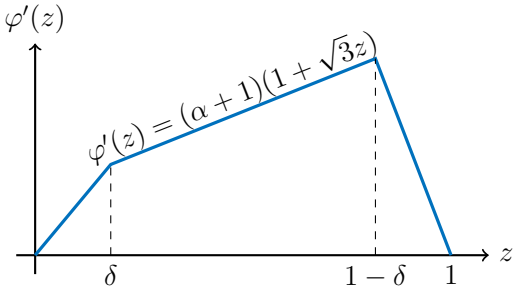

Figure 7.2: Sketch of the piecewise-linear $\varphi'(z)$ in (7.2.20).

The following result derives necessary conditions for $\mathcal{S}_{\boldsymbol{k}} \geq 0$ where $\mathcal{S}_{\boldsymbol{k}}$ is defined in (7.2.12b).

Lemma 7.2.3. *Let β and $\varphi'(z)$ be given by (7.2.19) and (7.2.20) and that $\delta \leq \frac{1}{3}$, then*

1. *The upper bound can be estimated as*

$$U \leq \frac{1}{2}\left(\frac{1}{2} + \frac{1}{\sqrt{3}} - U_0\delta\right)(\alpha+1), \tag{7.2.21}$$

   where $U_0 = \frac{4+3\sqrt{3}}{6}$.

2. *Suppose that*

$$\delta = d_0\left(\frac{\alpha}{(\alpha+1)R}\right)^{\frac{1}{4}}, \tag{7.2.22}$$

   where $d_0 = [540(7\sqrt{3}-12)]^{\frac{1}{4}}$. For $\mathcal{S}_{\boldsymbol{k}}$ given by (7.2.12b) the spectral constraint, $\mathcal{S}_{\boldsymbol{k}} \geq 0$, is satisfied.

Proof. To prove *1.*, substitute β given by (7.2.19) into $\varphi'(z)$ defined in (7.2.20) then both into U as given by (7.2.8). Computing the integral gives

$$\begin{aligned}\overline{\langle wT\rangle} \leq U =& \frac{1}{2}\left(\frac{1}{2} + \frac{1}{\sqrt{3}} - \frac{6+5\sqrt{3}}{9}\,\delta + \frac{\sqrt{3}}{6}\delta^2\right)(\alpha+1)\\ =& \frac{1}{2}\left(\frac{1}{2} + \frac{1}{\sqrt{3}} - U_0\delta\right)(\alpha+1),\end{aligned} \tag{7.2.23a}$$

where we have defined

$$U_0 \leq \frac{1}{9}(6+5\sqrt{3}) - \frac{\sqrt{3}}{6}\delta. \tag{7.2.24}$$

However, since by assumption $\delta \leq \frac{1}{3}$ we can fix $U_0 = \frac{4+3\sqrt{3}}{6}$, which yields (7.2.21) as desired.

To prove *2.*, given $\varphi'(z)$ from (7.2.20) and β in (7.2.19) the spectral constraint (7.2.7) can be written using the indicator function $\mathbb{1}_{(a,b)}$ on the interval (a,b) as

$$\left\langle \frac{\alpha}{R}|\nabla \boldsymbol{u}|^2 + \sqrt{3}(\alpha+1)|\nabla\vartheta|^2 - f(z)\mathbb{1}_{(0,\delta)}(z)w\vartheta - f(z)\mathbb{1}_{(1-\delta,1)}(z)w\vartheta \right\rangle \geq 0, \tag{7.2.25}$$

where

$$f(z) := (\alpha+1)\left[1+\sqrt{3}z - \xi(z)\right]. \tag{7.2.26}$$

By virtue of the boundary conditions on $\hat{w}_{\boldsymbol{k}}$ in (7.2.10a), with the fundamental theorem of calculus and the Cauchy-Scwharz inequality we have that

$$|\hat{w}_{\boldsymbol{k}}| = \left| \int_0^z \partial_{\tilde{z}} \hat{w}_{\boldsymbol{k}} \, \mathrm{d}\tilde{z} \right| \leq \sqrt{z}\|\hat{w}'_{\boldsymbol{k}}\|_2. \tag{7.2.27}$$

Since the same estimate can be constructed for $\hat{w}'_{\boldsymbol{k}}$ in terms of $\hat{w}''_{\boldsymbol{k}}$, we can write

$$|\hat{w}_{\boldsymbol{k}}| \leq \int_0^z \sqrt{\tilde{z}} \left(\int_0^1 |\hat{w}''_{\boldsymbol{k}}|^2 \mathrm{d}z \right)^{\frac{1}{2}} \mathrm{d}\tilde{z} = \frac{2}{3} z^{\frac{3}{2}} \|\hat{w}''_{\boldsymbol{k}}\|_2. \tag{7.2.28}$$

To show the spectral constraint (7.2.7) holds, we pass to Fourier space as illustrated in the proof of Lemma 7.2.2. Thus taking (7.2.12b), (7.2.19) and (7.2.20) we can drop the explicitly positive terms in $\hat{w}'_{\boldsymbol{k}}$, $\hat{w}_{\boldsymbol{k}}$ and $\hat{\vartheta}'_{\boldsymbol{k}}$ and consider the following

$$\mathcal{S}_{\boldsymbol{k}} \geq \frac{\alpha k^2}{R}\|\hat{w}''_{\boldsymbol{k}}\|_2^2 + \sqrt{3}(\alpha+1)k^2\|\hat{\vartheta}_{\boldsymbol{k}}\|_2^2 - \int_{[0,\delta]\cup[1-\delta,1]} f(z)\hat{w}_{\boldsymbol{k}}\hat{\vartheta}_{\boldsymbol{k}} \, \mathrm{d}z, \tag{7.2.29}$$

Using (7.2.28) (noting that the $\hat{w}_{\boldsymbol{k}}$ and $\hat{\vartheta}_{\boldsymbol{k}}$ are functions of z only), $\xi(z)$ and the Cauchy-Schwarz inequality the sign-indefinite term at the lower boundary can be estimated as

$$\begin{aligned}\left|\int_0^\delta [1+\sqrt{3}z-\xi(z)]\hat{w}_{\boldsymbol{k}}\hat{\vartheta}_{\boldsymbol{k}}\,\mathrm{d}z\right| &\le \frac{2}{3}\int_0^\delta \left[1-\frac{z}{\delta}\right] z^{\frac{3}{2}}|\hat{\vartheta}_{\boldsymbol{k}}|\,\mathrm{d}z\|\hat{w}''_{\boldsymbol{k}}\|_2 \\ &\le \frac{2}{3}\left(\int_0^\delta \left[1-\frac{z}{\delta}\right]^2 z^3\mathrm{d}z\right)^{\frac{1}{2}} \|\hat{w}''_{\boldsymbol{k}}\|_2\|\hat{\vartheta}_{\boldsymbol{k}}\|_2 \\ &= \frac{\delta^2}{3\sqrt{15}}\|\hat{w}''_{\boldsymbol{k}}\|_2\|\hat{\vartheta}_{\boldsymbol{k}}\|_2. \end{aligned} \tag{7.2.30}$$

Similarly near $z=1$ we have

$$\begin{aligned}\left|\int_{1-\delta}^1 [1+\sqrt{3}z-\xi(z)]\hat{w}_{\boldsymbol{k}}\hat{\vartheta}_{\boldsymbol{k}}\,\mathrm{d}z\right| &\le \frac{2(1+\sqrt{3})}{3}\int_{1-\delta}^1 \left[1-\frac{1-z}{\delta}\right](1-z)^{\frac{3}{2}}|\hat{\vartheta}_{\boldsymbol{k}}|\mathrm{d}z\|\hat{w}''_{\boldsymbol{k}}\|_2 \\ &\le \frac{1+\sqrt{3}}{3\sqrt{15}}\,\delta^2\|\hat{w}''_{\boldsymbol{k}}\|_2\|\hat{\vartheta}_{\boldsymbol{k}}\|_2\,. \end{aligned} \tag{7.2.31}$$

Substituting both (7.2.30) and (7.2.31) into (7.2.29) gives

$$\mathcal{S}_{\boldsymbol{k}} \ge \frac{\alpha}{Rk^2}\|\hat{w}''_{\boldsymbol{k}}\|_2^2 + \sqrt{3}(\alpha+1)k^2\|\hat{\vartheta}_{\boldsymbol{k}}\|_2^2 - \frac{2+\sqrt{3}}{3\sqrt{15}}(\alpha+1)\delta^2\|\hat{w}''_{\boldsymbol{k}}\|_2\|\hat{\vartheta}_{\boldsymbol{k}}\|_2 \ge 0. \tag{7.2.32}$$

The right hand side of the last inequality is a homogeneous quadratic form, $mx^2 + ny^2 - lxy$, and is nonnegative if its discriminant is nonpositive ie $l^2-4mn \ge 0$, which gives the condition

$$\delta \le d_0\left(\frac{\alpha}{(\alpha+1)R}\right)^{\frac{1}{4}}. \tag{7.2.33}$$

It is then clear that taking the choice of δ from (7.2.22) satisfies the spectral constraint, where $d_0 = [540(7\sqrt{3}-12)]^{\frac{1}{4}}$. □

Proof of Theorem 7.1.1

The upper bound follows from using the results of Lemma 7.2.3. First, we substitute δ from (7.2.22) into (7.2.21) and since $\alpha > 0$ we get that

$$\begin{aligned} U &\leq \frac{1}{2}\left(\frac{1}{2}+\frac{1}{\sqrt{3}}\right)(\alpha+1) - \frac{1}{2}U_0\, d_0\, \alpha^{\frac{1}{4}}(\alpha+1)^{\frac{3}{4}} R^{-\frac{1}{4}} \\ &\leq \frac{1}{2}\left(\frac{1}{2}+\frac{1}{\sqrt{3}}\right)(\alpha+1) - \frac{1}{2}U_0\, d_0\, \alpha^{\frac{1}{4}} R^{-\frac{1}{4}}. \end{aligned} \tag{7.2.34}$$

This bound can be optimised analytically over α by solving the equation $\partial U/\partial\alpha = 0$, which gives

$$\alpha = a_0 R^{-\frac{1}{3}}, \tag{7.2.35}$$

with $a_0 = \left[\frac{1}{2}U_0 d_0\,(-3+2\sqrt{3})\right]^{\frac{4}{3}}$. Finally, substituting α back into the bound in (7.2.34), gives after rearranging the upper bound

$$\overline{\langle wT\rangle} \leq \frac{1}{2}\left(\frac{1}{2}+\frac{1}{\sqrt{3}}\right)\left(1 - 3a_0\, R^{-\frac{1}{3}}\right). \tag{7.2.36}$$

Remark 7.2.2. One finds that when α is given by (7.2.35) the corresponding value of δ in (7.2.22) is less than $\frac{1}{3}$ for any $R \geq 591.51$, which is the regime where our bound is of interest. The result implies that $\delta = O(R^{-\frac{1}{3}})$, which correlates with "classical" scaling arguments proposed in Rayleigh–Bénard convection [131].

Remark 7.2.3. The result of Theorem 7.1.1 gives a lower bound on the mean temperature difference between the bottom and top boundaries, $\overline{\langle \delta T\rangle_h}$. Specifically it is implied that

$$\overline{\langle \delta T\rangle_h} \geq \frac{1}{2}\left(\frac{1}{2}-\frac{1}{\sqrt{3}}\right) - cR^{-\frac{1}{3}}. \tag{7.2.37}$$

This bound is negative when $R \geq 78\,390$, so conduction downwards from the top to the bottom cannot be ruled out in this regime.

Chapter 8

Future outlook: non-uniform heating

The struggle itself towards the heights is enough to fill a man's heart.

One must imagine Sisyphus happy.

Albert Camus - The Myth of Sisyphus

In this final chapter we consider turbulent convection driven by non-uniform heating/cooling, a direction for future work that generalises much of the studies conducted in this thesis. The ideas presented specifically generalise the configuration studied in chapter 7. Convection driven by a uniform heat source is an idealisation of internally heated convection as observed in nature. Referring back to the example of mantle convection first discussed in chapter 1, the distribution of radioactive isotopes is not uniform within the Earth. Planetary formation creates a bias to the distribution of isotopes. Additionally, due to an increase in pressure with depth from the planets surface, a higher concentration of radiogenic material is predicted closer to the surface [5, 103, 127]. Use of a specific non-uniform heating profile would apply to only one problem of choice. Instead this chapter considers a wide class of profiles, and examines the effect of varying heating on the resulting convective and conductive heat transport as given by the background method.

Non-uniform heating/cooling has attracted significant interest in recent years [7, 76, 101, 130, 143]. Varying the region of heating can allow for an investigation

of different regimes of heat transport due to turbulent convection. Numerical and experimental investigations [76, 94] demonstrate that heat transport can be enhanced if the heating is modified from near the lower boundary to being distributed within the bulk of the domain. Having a non-uniform heat source could be arranged (and viewed) as interpolating between boundary driven Rayleigh-Bénard and internally heated convection. However, the exact nature of such an interpolation of the underlying PDEs remains unclear.

As with uniform internal heating, previous studies for non-uniform heating have focused on the quantity $\overline{\langle T \rangle}$. Nevertheless it is interesting to investigate if bounds on $\overline{\langle wT \rangle}$ for the poorly conducting boundaries in chapter 7 can be improved. The seemingly non-physical result proven for poorly conducting boundaries was that for large R, conduction of heat from the top boundary to the bottom cannot be ruled out. Hence it is of interest to ask if one can demonstrate $\overline{\langle T|_{z=0} \rangle_h} - \overline{\langle T|_{z=1} \rangle_h} \geq 0$, by means of a non-uniform heating/cooling profile. The discussion in this chapter presents ideas for a bound on $\overline{\langle wT \rangle}$ and is intended to describe the future work possible through the generalisation to non-uniform heating/cooling.

8.1 Setup

For non-uniform heating the only alteration necessary to the equations governing internally heated convection in (1.2.3), is to the temperature equation (1.2.3c) which becomes

$$\partial_t T + \boldsymbol{u} \cdot \nabla T = \Delta T + H(z), \tag{8.1.1}$$

where $H(z)$ is assumed to be a z-dependent function representing the heating or cooling. Notice that if we wanted to increase the generality of the argument we could consider non-uniform heating which varies in all three spatial directions $H(\boldsymbol{x})$. The discussion of this chapter is restricted to horizontally periodic heating/cooling. The dimensional heating is $H = H_0 H(z)$, where H_0 has units of energy per unit volume

and time. The Rayleigh number as defined in (1.2.4) remains unchanged. It will be convenient to introduce the function,

$$\eta(z) := \int_0^z H(z)\mathrm{d}z, \tag{8.1.2}$$

which is a measure of the potential energy in the system. In this section we take the boundary conditions to be

$$\boldsymbol{u}|_{z=\{0,1\}} = 0, \tag{8.1.3a}$$

$$\partial_z T|_{z=0} = 0, \quad \partial_z T|_{z=1} = -\eta(1). \tag{8.1.3b}$$

Taking $\eta = z$ reduces the problem to that discussed in chapter 7.

Given the definition (8.1.2) and boundary conditions (8.1.3) we can evaluate the energy balance of the system by taking $\overline{\langle z \cdot (8.1.1)\rangle}$ and integrate by parts to obtain

$$\begin{aligned}\overline{\langle wT\rangle} + \overline{\langle T|_{z=0}\rangle_h} - \overline{\langle T|_{z=1}\rangle_h} &= -\overline{\langle \partial_z T|_{z=1}\rangle_h} - \langle z\, H(z)\rangle \\ &= \langle\eta\rangle - \eta(1) - \overline{\langle \partial_z T|_{z=1}\rangle_h} \\ &= \langle\eta\rangle\,. \end{aligned} \tag{8.1.4}$$

The left hand side of (8.1.4) is the sum of the mean heat flux due to convection and conduction. For a statistically stationary state to be achieved we could make the following two choices for the thermal boundary condition at the top. The two possible scenarios are

1. mean one heating/cooling in the domain, $\eta(1) = 1$.

2. mean zero heating/cooling in the domain, $\eta(1) = 0$.

As demonstrated in chapter 1 a Nusselt number can be defined in terms of the ratio of overall heat transport to mean conductive heat transport. In terms of $\eta(z)$,

for non-uniform heating this becomes

$$Nu = \frac{\overline{\langle \delta T \rangle_h} + \overline{\langle wT \rangle}}{\overline{\langle \delta T \rangle_h}} = \frac{\langle \eta(z) \rangle}{\langle \eta(z) \rangle - \overline{\langle wT \rangle}} \,. \tag{8.1.5}$$

In case 1. where $\eta(1) = 1$ the boundary conditions are inhomogeneous and as was done in chapter 7 we can write the temperature field in terms of perturbations and the conductive profile,

$$T(\boldsymbol{x}, t) = \vartheta(\boldsymbol{x}, t) + T_c(z). \tag{8.1.6}$$

It follows that the mean vertical convective heat transport holds the relation, $\overline{\langle wT \rangle} = \overline{\langle w\vartheta \rangle}$. The steady conductive temperature profile can be found after taking $\boldsymbol{u} = 0$ and $T(\boldsymbol{x}, t) = T(\boldsymbol{x})$ in (8.1.1). Given horizontal periodicity and the insulating lower boundary condition we obtain that

$$T_c' = -\eta(z). \tag{8.1.7}$$

Writing (8.1.1) in terms of ϑ gives

$$\partial_t \vartheta + \boldsymbol{u} \cdot \nabla \vartheta = \Delta \vartheta + w\, \eta(z), \tag{8.1.8}$$

where ϑ has boundary conditions

$$\vartheta'|_{z=\{0,1\}} = 0 \,. \tag{8.1.9}$$

8.2 Bounds on heat transport

Following the auxiliary functional methodology initially outlined in chapter 2 and chapter 7 when working with ϑ, a minimization problem for an upper bound on $\overline{\langle w\vartheta \rangle}$ can be constructed. We are concerned with upper bounds given the energy balance

relation of (8.1.4). From the background method the upper bound on $\overline{\langle w\vartheta\rangle} \leq U$ is given by minimising U, provided

$$\mathcal{S} := \Big\langle \frac{\alpha}{R}|\nabla \boldsymbol{u}|^2 + \beta|\nabla\vartheta|^2 - (\alpha + 1 + \beta\eta(z) - \varphi')\, w\vartheta - \varphi'(z)\vartheta' + U \Big\rangle \geq 0 \qquad \forall (\boldsymbol{u},\vartheta) \in \mathcal{U}_1 \times \mathcal{T}_3, \quad (8.2.1)$$

subject to the boundary conditions (8.1.3a) and (8.1.9). Exploiting horizontal periodicity we carry out a Fourier mode decomposition of the constraint $\mathcal{S} \geq 0$ and following an argument analogous to that used in §7.2 arrive at the conditions

$$\mathcal{S}_0 := \big\langle \beta|\vartheta'|^2 - \varphi'(z)\vartheta' + U \big\rangle \geq 0, \quad (8.2.2)$$

$$\mathcal{S}_{\boldsymbol{k}} := \Big\langle \frac{\alpha}{R}\Big(\frac{|w_{\boldsymbol{k}}''|^2}{k^2} + 2|w_{\boldsymbol{k}}'|^2 + k^2|w_{\boldsymbol{k}}|^2\Big) + \beta|\vartheta_{\boldsymbol{k}}'|^2 + \beta k^2|\vartheta_{\boldsymbol{k}}|^2 - (\alpha + 1 + \beta\,\eta(z) - \varphi'(z))\,\mathrm{Re}\{w_{\boldsymbol{k}}\vartheta_{\boldsymbol{k}}^*\}\Big\rangle \geq 0 \quad \forall \boldsymbol{k} \neq 0. \quad (8.2.3)$$

Using (8.2.2) and an argument analogous to Lemma 7.2.2, then provided the parameters α, β, φ are such that (8.2.3) holds for all $(\boldsymbol{u},\vartheta) \in \mathcal{U}_1 \times \mathcal{T}_3$, the optimal value of U is given by

$$U = \Big\langle \frac{\varphi'(z)^2}{4\beta} \Big\rangle. \quad (8.2.4)$$

8.2.1 Uniform upper bound

Recall that if the upper boundary is isothermal it is the case that $\overline{\langle wT\rangle} \leq \frac{1}{2}$, while in chapter 7 we established that $\overline{\langle wT\rangle} \leq \frac{1}{2}\left(\frac{1}{2} + \frac{1}{\sqrt{3}}\right)$. In this setting, with non-uniform heating given by $H(z)$, we first investigate the uniform in R and Pr upper bound on $\overline{\langle wT\rangle}$, which we denote U_0.

As with Theorem 7.2.1 we make the choices, $\alpha = 0$ and $\varphi'(z) = 1 + \beta\eta(z)$ which guarantees that $\mathcal{S}_{\boldsymbol{k}} \geq 0$ for all $\boldsymbol{k} \neq 0$. Then the choice of background profile in (8.2.4)

gives

$$U_0 = \left\langle \frac{(1+\beta\eta(z))^2}{4\beta} \right\rangle = \frac{1}{4\beta} + \left\langle \frac{\eta(z)}{2} + \frac{\beta\eta^2(z)}{4} \right\rangle, \tag{8.2.5}$$

which is optimised with the choice

$$\beta = \frac{1}{\langle \eta(z)^2 \rangle^{\frac{1}{2}}}, \tag{8.2.6}$$

such that

$$U_0 = \frac{1}{2} \langle \eta(z)^2 \rangle^{\frac{1}{2}} + \frac{1}{2} \langle \eta(z) \rangle . \tag{8.2.7}$$

Given the definition of Nu in (8.1.5), we can substitute the uniform bound U_0 which gives

$$Nu \leq \frac{2 \langle \eta(z) \rangle}{\langle \eta(z) \rangle - \langle \eta(z)^2 \rangle^{\frac{1}{2}}}. \tag{8.2.8}$$

From the physics of turbulent convection, as R increases the heat transport due to convection over conduction increases. In the asymptotic limit of $R = \infty$ where $U = U_0$, the expectation is that $Nu = \infty$, which can only occur provided the denominator of (8.2.8) be zero. For convenience we define

$$\sigma := \langle \eta(z) \rangle - \langle \eta(z)^2 \rangle^{\frac{1}{2}} . \tag{8.2.9}$$

Therefore the uniform in R and Pr upper bound on $\overline{\langle w\vartheta \rangle}$ and Nu are given by (8.2.7) and (8.2.8) respectively.

The condition that $\sigma = 0$ is equivalent to equating the right hand side of the energy balance relation from (8.1.4) to U_0 in (8.2.7). The implication of which is that the energy injected into the system due to internal heating is equivalent to the uniform upper bound on mean convective heat transport given by the background method. A final alternative way of stating this condition is that if $\sigma = 0$ then $\overline{\langle \delta T \rangle_h} := \overline{\langle T|_{z=0} \rangle_h} - \overline{\langle T|_{z=1} \rangle_h} \geq 0$. In uniform internal heating where $\eta(z) = z$ it follows that $\sigma = \frac{1}{2} - \frac{1}{\sqrt{3}} < 0$ and $\overline{\langle \delta T \rangle_h} = \frac{1}{2}\left(\frac{1}{2} - \frac{1}{\sqrt{3}}\right) < 0$ (chapter 7). The question

that arises is if there is a non-uniform heating or cooling profile for either $\eta(1) = 1$ or $\eta(1) = 0$ where $\sigma = 0$.

Further to the condition of $\sigma = 0$ the upper bounding framework for $\overline{\langle w\vartheta \rangle}$ can yield R dependent bounds. With a non-trivial selection of $\varphi'(z)$ an expression of the bound U can be obtained in terms of $\eta(z)$ which yields R-dependent conditions for $\mathcal{S}_{\boldsymbol{k}} \geq 0$. As shown throughout this thesis and in particular in chapter 7, the non-negativity of $\mathcal{S}_{\boldsymbol{k}}$ is determined by a particular condition on the boundary layer widths of $\varphi'(z)$ with respect to R. We next present a choice of background profile, building on the analogous problem with uniform internal heating in chapter 7, and investigate the condition $\mathcal{S}_{\boldsymbol{k}} \geq 0$

8.3 Choice of background profile

The Rayleigh number scaling for any bound on $\overline{\langle w\vartheta \rangle}$ is given by constructing a $\varphi'(z)$ with nonzero boundary layers. In chapter 7 we realised that in the limit $R = \infty$, $\alpha = 0$ and $\beta = \frac{1}{\langle \eta^2 \rangle^{\frac{1}{2}}}$ where uniform internal heating was equivalent to the choice $\eta = z$. Also we were able to establish from the numerical results in §7.2.1 that for uniform heating and $R < \infty$ a particular relation exists between α and β. In analogy to the $H(z) = 1$ case, we choose

$$\beta = \frac{\alpha + 1}{\langle \eta(z)^2 \rangle^{\frac{1}{2}}}, \tag{8.3.1}$$

and the background profile is taken to be,

$$\varphi' = (\alpha + 1) \begin{cases} \left(1 + \dfrac{\eta(\delta)}{\langle |\eta|^2 \rangle^{\frac{1}{2}}}\right) \dfrac{z}{\delta}, & 0 \leq z \leq \delta, \\ 1 + \dfrac{\eta(z)}{\langle |\eta|^2 \rangle^{\frac{1}{2}}}, & \delta \leq z \leq 1 - \delta, \\ \left(1 + \dfrac{\eta(1-\delta)}{\langle |\eta|^2 \rangle^{\frac{1}{2}}}\right) \dfrac{(1-z)}{\delta}, & 1 - \delta \leq z \leq 1. \end{cases} \tag{8.3.2}$$

The value in the bulk of φ' is necessitated by the sign-indefinite term in the condition $\mathcal{S}_{\boldsymbol{k}} \geq 0$. The behaviour in the boundary layers is chosen such that the profile is continuous at δ and $1-\delta$ given that $\varphi'(0) = \varphi'(1) = 0$.

From the boundary conditions on w in (8.1.3), the use of the fundamental theorem of calculus and the Cauchy-Schwarz inequality we have that

$$\hat{w}_{\boldsymbol{k}} \leq \frac{2}{3} z^{\frac{3}{2}} \|\hat{w}''_{\boldsymbol{k}}\|_2. \tag{8.3.3}$$

The $\hat{w}_{\boldsymbol{k}}\hat{T}_{\boldsymbol{k}}$ term in (8.2.3) integrated from 0 to δ can be estimated after substitution for $\varphi'(z)$, β, $\hat{w}_{\boldsymbol{k}}$ and with an additional use of Cauchy-Schwarz to obtain

$$\begin{aligned}
&\int_0^\delta (\alpha + 1 + \beta\eta(z) - \varphi'(z))|\hat{w}_{\boldsymbol{k}}\hat{\vartheta}_{\boldsymbol{k}}|\mathrm{d}z \\
&\quad \leq \int_0^\delta \frac{2}{3}(\alpha+1)\left[1 + \frac{\eta(z)}{\langle|\eta|^2\rangle^{\frac{1}{2}}} - \left(1 + \frac{\eta(\delta)}{\langle|\eta|^2\rangle^{\frac{1}{2}}}\right)\frac{z}{\delta}\right] z^{\frac{3}{2}}\hat{\vartheta}_{\boldsymbol{k}}\mathrm{d}z \|\hat{w}''_{\boldsymbol{k}}\|_2 \\
&\quad \leq \frac{2}{3}(\alpha+1) \underbrace{\left(\int_0^\delta \left[1 + \frac{\eta}{\langle|\eta|^2\rangle^{\frac{1}{2}}} - \left(1 + \frac{\eta(\delta)}{\langle|\eta|^2\rangle^{\frac{1}{2}}}\right)\frac{z}{\delta}\right]^2 z^3 \mathrm{d}z\right)^{\frac{1}{2}}}_{\Psi_0} \|\hat{w}''_{\boldsymbol{k}}\|_2 \|\hat{\vartheta}_{\boldsymbol{k}}\|_2.
\end{aligned} \tag{8.3.4}$$

The integral Ψ_0 once evaluated for a particular profile $H(z)$ gives a $\delta = \delta(R)$ to satisfy the condition $\mathcal{S}_{\boldsymbol{k}} \geq 0$. While Ψ_0 is evaluated for $[0, \delta]$, at the upper boundary in the range $[1-\delta, 1]$ the integral of the sign-indefinite term is nearly identical and we shall denote it as Ψ_1 where $\eta(\delta)$ is replaced with $\eta(1-\delta)$ and z with $1-z$. Substituting (8.3.4) into (8.2.3) gives

$$\mathcal{S}_{\boldsymbol{k}} \geq \frac{\alpha}{Rk^2}\|\hat{w}''_{\boldsymbol{k}}\|_2^2 + \beta k^2 \|\hat{\vartheta}_{\boldsymbol{k}}\|_2^2 - \frac{2}{3}(\alpha+1)(\Psi_0 + \Psi_1)\|\hat{w}''_{\boldsymbol{k}}\|_2 \|\hat{\vartheta}_{\boldsymbol{k}}\|_2. \tag{8.3.5}$$

The homogeneous quadratic form is non-negative given it has a nonpositive discriminant, which yields that

$$\Psi_0 + \Psi_1 \leq \sqrt{\frac{9\alpha}{R(\alpha+1)\left\langle \eta^2 \right\rangle^{\frac{1}{2}}}}\,. \tag{8.3.6}$$

The condition (8.3.6) may appear odd, due to the fact that the heating distribution $\eta(z)$ appears both on the left and right-hand side. However, as will be demonstrated for $H(z)$ in §8.4, and in fact for all $\eta(z) \in L^2(\Omega)$, then up to constants $\Psi_i \lesssim \delta^2$ for $i \in \{1,2\}$. This was the case for $H(z) = 1$ as demonstrated in §7.2.2. This implies the following inequality (up to constants)

$$\delta \lesssim \left(\frac{9\alpha}{R(\alpha+1)\left\langle \eta^2 \right\rangle^{\frac{1}{2}}}\right)^{\frac{1}{4}}. \tag{8.3.7}$$

Finally, having looked at the condition of $\mathcal{S}_{\boldsymbol{k}} \geq 0$, we next consider the upper bound U. Substituting for β from (8.3.1) and $\varphi'(z)$ given by (8.3.2) in U (8.2.4) gives

$$\begin{aligned} U = \frac{\delta}{12}\left\langle |\eta(z)|^2 \right\rangle^{\frac{1}{2}}(\alpha+1)\left[\left(1+\frac{\eta(\delta)}{\left\langle |\eta(z)|^2\right\rangle^{\frac{1}{2}}}\right)^2 + \left(1+\frac{\eta(1-\delta)}{\left\langle |\eta(z)|^2\right\rangle^{\frac{1}{2}}}\right)^2\right] \\ + \frac{1}{4}(\alpha+1)\left\langle |\eta(z)|^2 \right\rangle^{\frac{1}{2}} \int_{\delta}^{1-\delta}\left(1+\frac{\eta(z)}{\left\langle |\eta(z)|^2\right\rangle^{\frac{1}{2}}}\right)^2 \mathrm{d}z\,. \end{aligned} \tag{8.3.8}$$

In the expression (8.3.8), the first term is positive and order δ. For a bound of the form $U \leq U_0(\eta) - c(\eta)R^{-\frac{1}{3}}$, both the uniform upper bound (U_0) and negative δ contribution would have to come from the second term in (8.3.8). Based on this reasoning the bound on $\overline{\langle w\vartheta \rangle}$ can be estimated to be of the form

$$U \leq \frac{1}{4}(\alpha+1)\left\langle |\eta(z)|^2 \right\rangle^{\frac{1}{2}}\left[\int_{\delta}^{1-\delta}\left(1+\frac{\eta(z)}{\left\langle |\eta(z)|^2\right\rangle^{\frac{1}{2}}}\right)^2 \mathrm{d}z + \frac{2}{3}\delta\right] + \mathcal{O}(\delta^2). \tag{8.3.9}$$

The ideas and expressions presented depend directly on the choice of heating distribution $\eta(z)$. We will next propose three different heating profiles of interest to gain an understanding of the behaviour of σ and the upper bound U. While we do not obtain a clear and definitive result the test profiles provide insight into the effect of non-uniform heating or cooling on σ, U_0 and $\overline{\langle \delta T \rangle_h}$.

8.4 Non-uniform heating and cooling profiles

For the two possible cases of $\eta(1) = 0$ or $\eta(1) = 1$, we now examine test profiles and calculate σ in (8.2.9) to see if the condition $\sigma = 0$ can be satisfied. The uniform upper bound for each heating profile can be found by calculating U_0 given by (8.2.7). Whether or not a R correction to a uniform upper bound exists is not currently known and left to future work. Initially we propose two possible heating and cooling profiles that have mean one internal heating i.e. $\eta(1) = 1$. These profiles, in the appropriate limit for the parameters that define them, become equivalent to uniform internal heating. Following this we take a brief look at a profile with net zero heating and cooling i.e. $\eta(1) = 0$.

8.4.1 Mean one internal heating: $\eta(1) = 1$

Starting with the case of mean one heating within the domain, the boundary condition at the top from (8.1.3), is unit outwards heat flux. We consider two different families of $H(z)$.

Smooth heating localised at the bottom

The first family of profiles we consider are smooth profiles parameterised by $n \in \mathbb{R}_+$. The heating profile choice is

$$H(n, z) = (n + 1)(1 - z)^n \quad \forall n \geq 0. \tag{8.4.1}$$

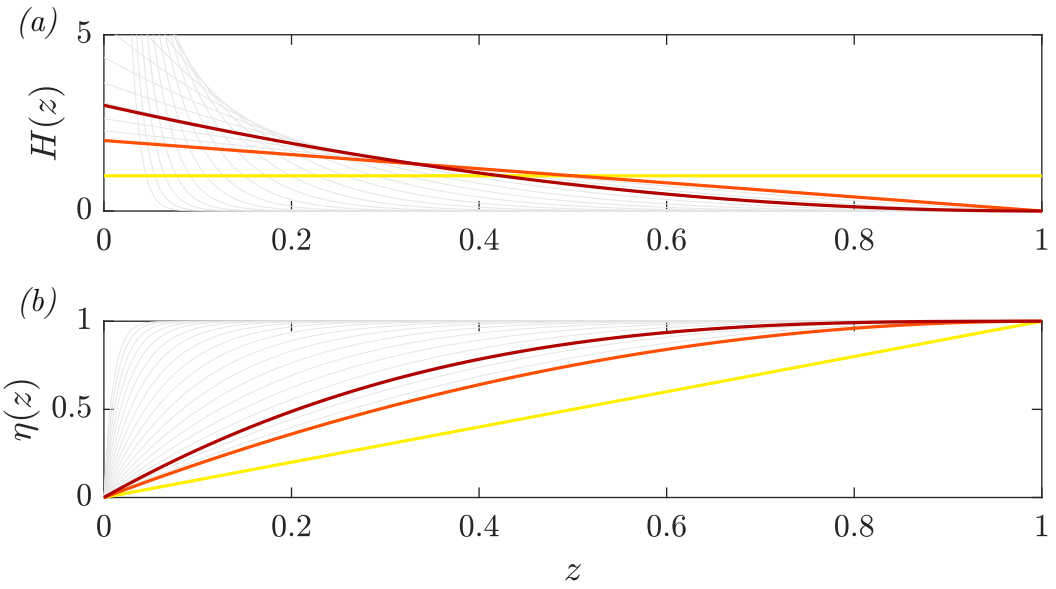

Figure 8.1: *(a)* Plots of the heating profiles $H(z)$ given by (8.4.1) and *(b)* plots of the heating distributions $\eta(z)$ given in (8.4.2) for $n \in [1, 100]$ (—) with $n = 0$ (—), $n = 1$ (—) and $n = 2$ (—) highlighted

The corresponding $\eta(z)$ can be found using (8.1.2), from which we obtain

$$\eta(n, z) = 1 - (1 - z)^{n+1}. \tag{8.4.2}$$

In Figure 8.1 we plot example profiles of $H(z)$ and $\eta(z)$, where the cases of $n = 0$ (—), $n = 1$ (—) and $n = 2$ (—), are highlighted while higher n are plotted in grey up to $n = 100$. As n increases the heating profile is a polynomial of increasing order with the heating becoming further localised to the lower boundary. At $n = \infty$ the heating profile becomes a Dirac delta distribution at zero. Whereas for $n = 0$ the heating is profile is that of uniform internal heating. Evaluating σ as defined in (8.2.9) gives

$$\sigma = \frac{n+1}{n+2} - \left[\frac{2n^2 + 4n + 2}{(n+2)(2n+3)}\right]^{\frac{1}{2}}. \tag{8.4.3}$$

Therefore, only when $n = \infty$ and the heating profile is a Dirac delta is the condition $\sigma = 0$ satisfied. Stated in other words for the right hand side of the energy balance relation (8.1.4) to match the uniform upper bound given by the background method the heating is taken to be a Dirac delta distribution. As n increases we also notice

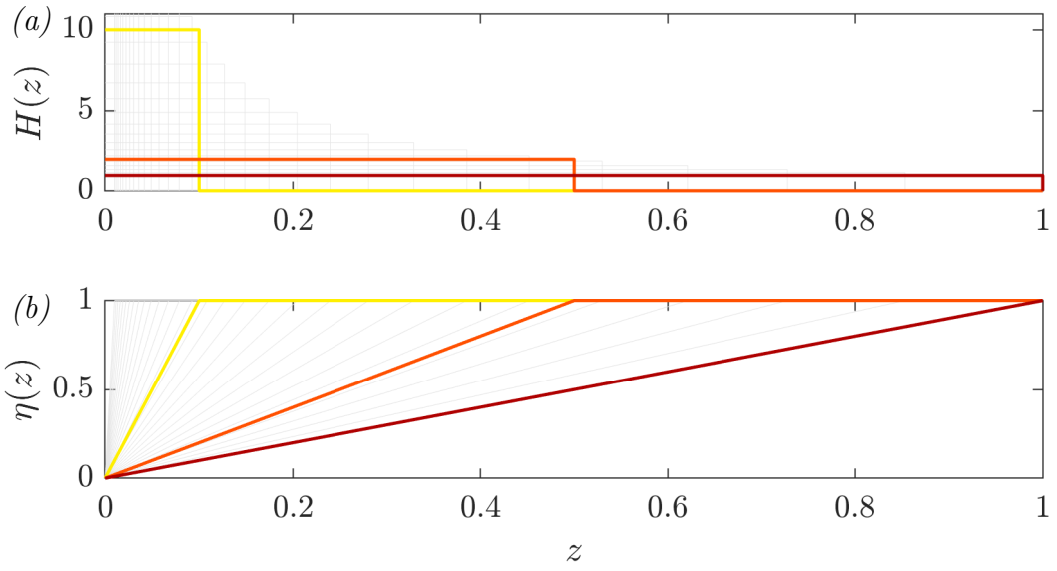

Figure 8.2: *(a)* Plots of piecewise heating profiles $H(z)$ given by (8.4.4) and *(b)* plots of the heating distribution $\eta(z)$ given in (8.4.5) with $p = 1$ for $h \in [0.01, 1]$ (—) with $h = 1$ (—), $h = 0.5$ (—) and $n = 0.1$ (—) highlighted.

that $\langle \eta \rangle$ tends to one. The energy injected into the system given by the right hand side of (8.1.4) is given exactly by $\langle \eta \rangle$. Thus as n goes from 0 to ∞, $\langle \eta \rangle$ goes from $\frac{1}{2}$ to 1.

Piecewise constant heating and cooling

Consider discontinuous $H(z)$ parameterised by $h \in (0, 1)$ and $p \geq 1$ as

$$H(p, h, z) = \begin{cases} \dfrac{p}{h}, & 0 \leq z \leq h, \\ \dfrac{1-p}{1-h}, & h \leq z \leq 1, \end{cases} \tag{8.4.4}$$

where h is region over which heat is added to the system while p quantifies the cooling. The corresponding $\eta(z)$ is

$$\eta(p, h, z) = \begin{cases} \dfrac{p}{h} z, & 0 \leq z \leq h, \\ \dfrac{1-p}{1-h}(z-h) + p, & h \leq z \leq 1. \end{cases} \tag{8.4.5}$$

In Figure 8.2 we plot example profiles of (8.4.4) and (8.4.5) taking $p = 1$ which corresponds to profiles with no cooling and constant heating in a region $(0, h)$, where smaller h results in larger heating in a smaller region localised near the lower boundary. While for $p > 1$, there is cooling in some region $z \in (h, 1)$, but the mean heating and cooling is one. Evaluating σ as defined in (8.2.9) gives

$$\sigma = \frac{1}{2}(1 + p - h) - \frac{1}{\sqrt{3}}\left[(1 - h)(1 + p) + p^2\right]^{\frac{1}{2}}. \tag{8.4.6}$$

If $p = h = 1$ the heating is uniform, as in chapter 7, where $\sigma < 0$. If $p = 1$ (no cooling in the domain) then only if $h = 0$ do we obtain $\sigma = 0$. As can be seen in Figure 8.2*(b)* as h decreases $\langle\eta\rangle$ tends towards one.

8.4.2 Mean zero heating/cooling: $\eta(1) = 0$

The final non-uniform heating profile considering is one where there is net zero heating/cooling in the domain due to the choice $\eta(1) = 0$. For $n \in 2\mathbb{N} - 1$ we consider the following profile

$$H(n, z) = (1 - 2z)^n. \tag{8.4.7}$$

The corresponding $\eta(z)$ to (8.4.7) is given by

$$\eta(n, z) = \frac{1 - (1 - 2z)^{n+1}}{2(n + 1)}, \tag{8.4.8}$$

from which evaluating σ in (8.2.9) gives

$$\sigma = \frac{1}{2(n + 2)} - \frac{1}{\sqrt{2(n + 2)(2n + 3)}}. \tag{8.4.9}$$

As would be expected from physical arguments in this case the limiting behaviour of σ and $\langle\eta\rangle$ can be said to be the opposite to that of the profiles (8.4.1) and (8.4.4). Taking $n = \infty$ in (8.4.9) gives $\sigma = 0$ however then $\langle\eta\rangle \to 0$. In this scenario the

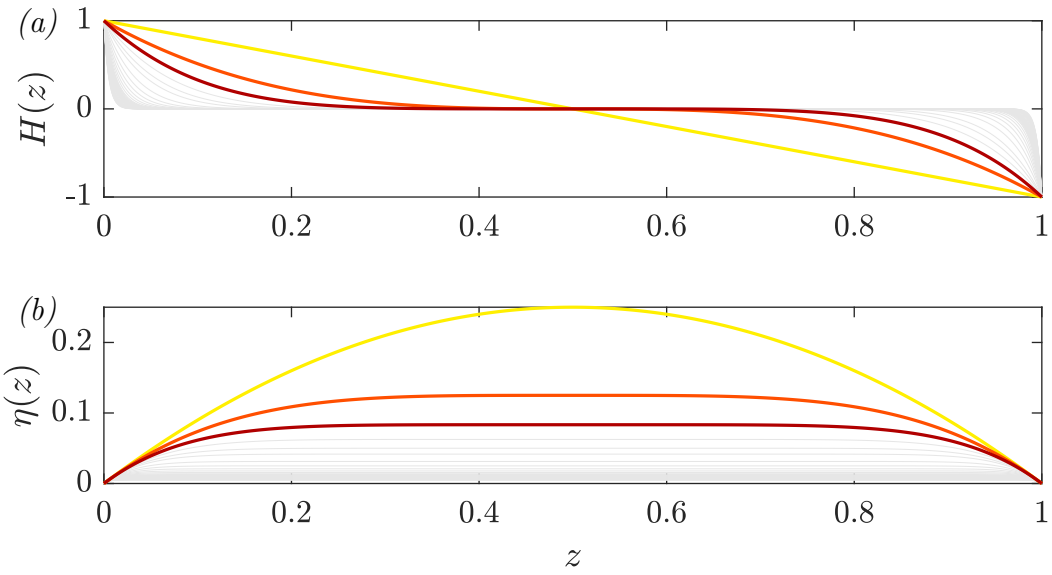

Figure 8.3: *(a)* Plots of smooth heating and cooling profiles $H(z)$ given by (8.4.7) and *(b)* plots of the heating distribution $\eta(z)$ given by (8.4.8) for $n \in \mathbb{N}_{[1,101]}$ (—) with $n = 1$ (—), $n = 3$ (—) and $n = 5$ (—) highlighted.

upper bound on $\overline{\langle wT \rangle}$ is somewhat more difficult to interpret. Since for n increasing, U_0 as given in (8.2.7) goes to zero. For a fluid that is contained in an insulating box with no net heating or cooling, the mean vertical convective heat transport may not be the best diagnostic quantity to further understand the turbulence.

8.5 Discussion

The discussion in this chapter indicates that for $\eta(1) = 1$ or $\eta(1) = 0$, taking a family of non-uniform heating profiles gives the uniform upper bound U_0 defined in (8.2.7) that can match the energy balance of the system (8.1.4), only in the case where the heating converges to a Dirac delta distribution. This occurs in the limiting case of the test profiles of $n \to \infty$ for (8.4.1) and $h \to 0$ for (8.4.4). However, the key question is if there exists a R correction to the uniform upper bound U_0 as the heating profiles become closer to a Dirac delta. This question is left to future work and requires evaluating Ψ_0 in (8.3.4) given the heating profiles (8.4.1), (8.4.4) and (8.4.7). Stated another way, is there a limit that can be taken for tunable non-uniform heating or

cooling profiles where one can obtain a bound on the Nusselt number from (8.2.8) of the form $Nu \lesssim R^{\frac{1}{3}}$.

For example, if we were to consider any non-uniform heating profile, after evaluating Ψ_0 from (8.3.4) we get

$$\overline{\langle wT \rangle} \leq \underbrace{\frac{1}{2}\left[\langle \eta(z)^2 \rangle^{\frac{1}{2}} + \langle \eta(z) \rangle\right]}_{U_0} - f(n, R). \tag{8.5.1}$$

The unanswered question in this case is whether $f(n, R)$ is finite, nonzero and positive in its arguments. Likewise for any other non-uniform heating/cooling profile a similar $f(parameters)$ can be determined by evaluating Ψ_0 and determining the δ necessary to ensure that $\mathcal{S}_{\boldsymbol{k}} \geq 0$ stated in (8.2.1).

The case of net zero heating/cooling has previously seen investigation with the so called *optimal wall-to-wall transport method* [130, 143]. The optimal wall-to-wall transport method allows for both upper and lower bound to be formulated. The quantity of interest in these studies was $\overline{\langle T \rangle}$, so an application of the method to $\overline{\langle wT \rangle}$ has not been carried out, but warranted since there are key physical differences between $\overline{\langle T \rangle}$ and $\overline{\langle wT \rangle}$. As mentioned at the beginning of the chapter, one could further generalise the problem and investigate non-uniform heating by considering $H = H(x, z)$ or $H(x, y, z)$. This exact generalisation has been carried out in the bounding of $\overline{\langle T \rangle}$ with the optimal wall-to-wall transport method. In fact in previous studies [130, 143] not only was the horizontal periodicity relaxed, so too were restrictions on the domain geometry. However within the application of the background method from §8.2 we invoke periodicity to simplify the analysis, and without this would need to take an alternative approach. It is anticipated that such an analysis is still possible, albeit using different estimates and techniques.

As hinted at with the three choices of non-uniform heating/cooling profiles (8.4.1), (8.4.4) and (8.4.7), many choices can be made for the profile $H(z)$. One approach to future investigations could be taking physically realistic profiles based on the problem

being investigated. The simulations carried out for internally heated convection usually are motivated by examples such as the mantle, the Venusian atmosphere or the interior of stars. All three of these scenarios will involve a non-uniform heating profile, which have an exponentially decaying structure. From the perspective of the analysis this need not change much of the approach but it could constitute a research direction that is of more interest from the perspective of the physics. However, the ideas sketched out in this chapter are general so as to capture all possible $H(z)$.

One final direction that could be of interest is to consider non-uniform heating where the heating profile evolves with time. The idea is to replace $H(\boldsymbol{x})$ with $H(\boldsymbol{x}, t)$. Then, H evolves according to another advection-diffusion equation of

$$\partial_t H + \boldsymbol{u} \cdot \nabla H = \Delta H. \tag{8.5.2}$$

Consequently H behaves as a passive scalar which appears in the temperature equation releasing heat in proportion to the concentration of H. The motivation for this comes from double-diffusive convection, where in addition to T a second scalar C evolves in the fluid, usually intended to represent the salinity. The proposed internal heating system in dimensional units would be governed by the following set of equations

$$\hat{\nabla} \cdot \hat{\boldsymbol{u}} = 0, \tag{8.5.3a}$$

$$\hat{\partial}_t \hat{\boldsymbol{u}} + \hat{\boldsymbol{u}} \cdot \hat{\nabla} \hat{\boldsymbol{u}} + \hat{\nabla} \hat{p} = \nu \hat{\Delta} \hat{\boldsymbol{u}} + g(\alpha_T \hat{T} - \alpha_H \hat{H}) \mathbf{e}_3, \tag{8.5.3b}$$

$$\hat{\partial}_t \hat{T} + \hat{\boldsymbol{u}} \cdot \hat{\nabla} \hat{T} = \kappa_T \hat{\Delta} \hat{T} + \Lambda \hat{H}, \tag{8.5.3c}$$

$$\hat{\partial}_t \hat{H} + \hat{\boldsymbol{u}} \cdot \hat{\nabla} \hat{H} = \kappa_H \hat{\Delta} \hat{H}, \tag{8.5.3d}$$

where Λ is the rate of heat release. This system represents a different flow but can be viewed as a generalisation to the internally heated convection studied in this thesis. The internal heating would no longer come from an *a priori* prescribed function but

instead be given by a field that diffuses and is advected by the flow. The boundary conditions need to be chosen such that the flow can become unstable and that H evolves and drives convection through heat input into the fluid. With locations of higher concentration of H injecting a higher relative quantity of heat into the fluid. This model has recently been studied in numerical simulations, where the authors highlight the rich complexity of the phenomena that can occur [38].

Chapter 9

Conclusions

When we can't think for ourselves, we can always quote !

Ludwig Wittgenstein

Obtaining rigorous scaling laws on the emergent properties of turbulence remains a fruitful research avenue in the analysis of fluid flows. Internally heated (IH) convection has demonstrated itself to be one such flow. A combination of numerical optimisation, novel choices in the optimisation parameters, and estimates from analysis are used to tackle IH convection. The ultimate behaviour of the mean vertical convective heat transport $\overline{\langle wT \rangle}$ was and remains largely unknown. This thesis proves rigorous upper bounds on $\overline{\langle wT \rangle}$ for a fluid between two parallel plates. The scaling of $\overline{\langle wT \rangle}$ with the Rayleigh number, R, is investigated for three different thermal and two different kinematic boundary conditions. The results are obtained by a modern application of the background field method. Numerical optimisation is employed to guide the mathematical proofs.

The two possible kinematic boundary conditions are no-slip and free-slip. For the thermal boundary conditions, if the boundaries are perfect thermal conductors then the temperature is assumed to be the same and constant at the top and bottom, and taken to be zero. Alternatively, the lower boundary can be considered a thermal insulator. The third and final configuration corresponds to a thermal insulator at the

bottom and a poor thermal conductor at the upper boundary. When the boundaries are isothermal and held at the same temperature, $\overline{\langle wT \rangle}$ quantifies the flux of heat leaving the upper and lower boundaries. A standard Nusselt number cannot be defined in this case as the mean conductive heat flux is zero. If on the other hand, the lower boundary is a thermal insulator then $\overline{\langle wT \rangle}$ quantifies the enhancement of vertical heat transport due to convection over conduction. Here, the Nusselt number can be well defined.

The upper bounds on $\overline{\langle wT \rangle}$, presented in Table 1.2, use the background field method formulated in terms of auxiliary functions. A major advantage of the approach is its flexibility to incorporate additional information into the optimisation problem. In this thesis, we use the information in the minimum principle on the temperature field. This states that when at the very least a boundary is isothermal, the temperature is non-negative in the domain. For uniform IH convection not only is the minimum principle useful but it is crucial to proving a bound on $\overline{\langle wT \rangle}$ which is better than the upper bound $\overline{\langle wT \rangle} \leq \frac{1}{2}$ for arbitrarily large R. A Lagrange multiplier is used to enforce the minimum principle.

The general idea of the background field method is that upper bounds can be obtained provided a quadratic integral is positive semidefinite. The most important decision variable to construct is the background field. In most analytic constructions piecewise linear background profiles are sufficient to capture the asymptotic behaviour of turbulence as demonstrated for Rayleigh–Bénard (RB) convection (see Table 1.1). When instead numerical optimisation is performed the optimal coefficients can be determined for a range of parameter values. Surprisingly, we demonstrated that for IH convection between isothermal and no-slip boundaries, standard piecewise linear constructions of background temperature fields, $\tau(z)$, are insufficient to prove bounds on $\overline{\langle wT \rangle}$ that do not become suboptimal at finite R (outlined in appendix E). Guided by numerical optimisation §3.3.1 we found that by a $\tau(z)$ with sub-layers at the bottom boundary one of which varies as z^{-1}, it can be proven that $\overline{\langle wT \rangle} \to \frac{1}{2}$ from

below as $R \to \infty$. One discovery in the problems was that the Lagrange multiplier enforcing the minimum principle is 'activated' at a particular R above the energy stability limit. As illustrated in Figure 3.1 and Figure 4.1 there are two R dependent upper bounds for each thermal configuration where the upper boundary is isothermal, ones without (Theorem 3.1.1 and Theorem 4.1.1) and the others with (Theorem 3.1.2 and Theorem 4.1.2) the minimum principle being utilised. Each upper bound is better for a particular range of R. The specific value of the cross over from one bound to the other can be calculated but will ultimately depend on the constants c which could be fine tuned. Instead, the scaling of the bounds in both regimes is of more interest.

Numerical optimisation utilising a minimum principle was carried out only in the case of isothermal boundaries. The same strategy could have been used for the configuration in chapter 4 of an insulating bottom and isothermal top. Nevertheless, based on preliminary calculations at low R values, it was anticipated that the finer discretisation and high level of precision required would increase the computational difficulty. While the semidefinite programming (SDP) carried out in numerical work has many benefits, a common problem is that SDPs do not scale well with size, even after a chordal decomposition to speed up the process. On reflection of the numerical optimisation in §3.3.1 the range of R spanned is small and could have been further increased. The results demonstrate that the bound U on heat transport approached $\frac{1}{2}$ faster than any sensible power law that could be fit to the data, which is why no fit was suggested. The numerically optimal $\tau(z)$ exhibits a bottom boundary layer with three sub-layers and yet the analytic constructions only have two, but appear to capture the behaviour of the bound. It is worth repeating that the analytical constructions exactly match the optimal profiles in the two inner layers per the ansatz (3.3.6).

In addition to novel $\tau(z)$, (compared to standard applications of the background method) the proofs of the bounds in Theorem 3.1.2 and Theorem 4.1.2 require the

use of weighted Hardy and Rellich inequalities to satisfy the constraints within the optimisation problem. In the studies of RB convection the use of inequalities of Hardy–Rellich type had previously been used to prove bounds on the Nusselt number which scales with the so-called 'classical' scaling. However, this was only necessary when working in the limit $Pr = \infty$. Using the same Hardy–Rellich inequality and $\tau(z)$ that is logarithmic in the bulk of the fluid layer, we also prove bounds in the infinite Pr limit for IH convection. In contrast to RB convection at infinite Pr, the scaling laws on heat transport for IH convection do not have any logarithmic terms and are instead a pure power law as established in Theorem 5.1.1 and Theorem 5.1.2. These results are qualitatively different from those established for $Pr < \infty$. Another difference is that the boundary layer widths of the $\tau(z)$ vary independently of each other, whereas in RB convection and IH convection for $Pr < \infty$ the boundary layer widths are taken to be equal. At $Pr = \infty$, when the lower boundary is an insulator with a perfectly conducting upper boundary, we require a result established in [167] where $\tau(z)$ has a power law variation in the bulk of the form $z^{1-\mu}$ for $\mu \in (0, 1)$. Once more by using $\tau(z)$ with different boundary layer widths a pure power law scaling is established. Additionally, in contrast to RB convection and the work in [167], the exponent μ can be taken to be independent of R.

One feature of the upper bound on $\overline{\langle wT \rangle}$ for RB convection is that the provable bounds on the Nusselt number, $Nu = 1 + \overline{\langle wT \rangle}$, are the same irrespective of the thermal boundary conditions. As far as is currently known, $Ra^{\frac{1}{2}}$ for $Pr < \infty$, $Ra^{\frac{1}{3}}$ for $Pr = \infty$ and $Ra^{\frac{5}{12}}$ for free-slip boundaries, where Ra is the Rayleigh number for RB convection. In contrast the results in Table 1.2 demonstrate that the upper bounds on $\overline{\langle wT \rangle}$ for IH convection differ when the thermal boundary conditions change. The only case where we do not know if changing thermal boundary conditions yield bounds with a different scaling is the case of free-slip, where only isothermal boundaries were considered. Another distinction between the bounds for the two types of convection is that heat transport is the lowest in the infinite Pr limit for RB

convection. In this thesis, we find that instead, the provable bound for heat transport in IH convection is lowest for free-slip boundaries, irrespective of the regime of Pr (Theorem 6.1.1 and Theorem 6.1.2).

Poorly conducting thermal boundaries were studied in chapter 7 and are distinct from the two other thermal boundary configurations due to a lack of a provable minimum principle on the temperature field. From the perspective of physics, we would expect the temperature difference between the bottom and top boundaries, $\overline{\langle \delta T \rangle_h}$, to be positive. Yet, our upper bound on $\overline{\langle wT \rangle}$ in Theorem 7.1.1 cannot rule out the possibility of $\overline{\langle \delta T \rangle_h} < 0$, beyond a particular R. Specifically with Theorem 7.1.1 equation (7.1.2) implies that $\overline{\langle \delta T \rangle_h} \geq \frac{1}{2}\left(\frac{1}{2} - \frac{1}{\sqrt{3}}\right) + R^{-\frac{1}{3}}$, which is negative for $R \geq 78\,390$. We were nevertheless able to halve the best known uniform upper bound $\overline{\langle wT \rangle} \leq \frac{1}{2} + \frac{1}{\sqrt{3}}$ from [58] with Theorem 7.2.1. The $R^{-\frac{1}{3}}$ scaling of the bound appears to be optimal within the bounding framework as seen from the numerical optimisation attained in §7.2.1.

In addition to highlighting the largely unexplored problem of IH convection, this thesis has highlighted the value of computation in proving bounds. Numerical optimisation is carried out with semidefinite programming. Semidefinite programs are well studied convex optimisation problems, with many algorithms available in the literature. The ease of use and availability of solvers, the guarantee of a single optimal solution for convex optimisation problems and the relatively simple and fast computations make semidefinite programs a desirable tool for determining optimal scaling. Our aim in this work has not been to improve the tools of numerical optimisation for the proof of bounds. All the same, it does present numerical results that demonstrate the applicability of semidefinite programming to fluid dynamics. In particular, the finite element discretisation used in chapter 3 and explained in appendix C provides a positive demonstration of convex optimisation in the analysis of turbulence and chaotic systems.

9.1 Outlook

The scaling laws established in this thesis for IH convection are entirely novel and yet foster many questions. The first is whether or not the upper bounds in Table 1.2 are sharp. If the bounds on $\overline{\langle wT \rangle}$ are not sharp then one can ask how they compare with any other investigation on $\overline{\langle wT \rangle}$ be it through simulations or experiments. Even before searching through the literature, it seems reasonable to conduct an eye test on the R-dependent results. First, in the cases where a minimum principle is utilised, we have bounds that approach $\frac{1}{2}$ as $R \to \infty$, however for no-slip boundary conditions at $Pr < \infty$ the bound approaches $\frac{1}{2}$ exponentially fast in R. It seems unlikely that the only possible flows which satisfy the governing PDEs are those that saturate this exponential bound. Intriguingly, it has been conjectured in previous works on IH convection that $\overline{\langle wT \rangle} \leq \frac{1}{2} - cR^{-\frac{1}{3}}$ [58], for some $c \in \mathbb{R}$. The scaling laws proven in this thesis are far from an exponent of $\frac{1}{3}$. Further still the upper bounds proven in this thesis are not equivalent to those predicted from phenomenological arguments [23, 152] and heuristics as discussed in appendix B.

The known simulations and experiments leave much to be decided. In Figure 3.2 we plot results from experiments and simulations compared with numerically optimal bounds. While the nature of turbulence is qualitatively different from two to three dimensions, the simulations from [62] suggest that $\overline{\langle wT \rangle}$ decreases for $R \gtrsim 10^9$. Regardless of the possibility of $\overline{\langle wT \rangle}$ decreasing for large R, the scaling is qualitatively different from the rigorous laws proven in this thesis. The one case where simulations are entirely lacking is the case of $Pr = \infty$. If this gap in the research is addressed, we could compare our pure power laws in chapter 5 and chapter 6.

While the table of results (Table 1.2) provides a summary of the research carried out, one question that it naturally gives rise to is about the clear gaps where rigorous bounds are not as yet known. Specifically, the first case to solve is that of free-slip boundaries with an insulating lower and isothermal upper boundary. Preliminary

investigations indicate that a direct application of the proofs in chapter 6 does not yield an upper bound that asymptotes to $\frac{1}{2}$ as R increases. The key variation is in the boundary condition at $z = 0$ and the loss of a Poincaré inequality. In §4.3 this difficulty was overcome by using the additional boundary condition on w, whereas in §5.3 the background profile is altered in the bulk to have a power law variation. Considering the alterations made at no-slip when the boundary is insulating may guide future analysis for free-slip boundaries. The other major result missing is in the configuration with poorly conducting boundaries. A minimum principle is not available but at this point, the nature of the optimal upper bounds remains unknown. However, the Hardy–Rellich and vorticity inequalities used in the other setups should also translate to the analysis of poorly conducting boundaries. Completing the missing results should be the basis of future work, be it through analysis or computation.

There are several ways to determine if the bounds are sharp. In particular, it may be possible to compute exact steady solutions to IH convection while optimising the aspect ratio to maximise heat transport. A similar approach when applied to RB convection indicates that the Nusselt number scales by the 'classical' scaling regime of $Ra^{\frac{1}{3}}$ [161, 162]. Alternatively, as mentioned in chapter 8 the optimal wall-to-wall method could be used to determine both upper and lower bounds on $\overline{\langle wT \rangle}$. Application of the method has recently indicated that for RB convection in 3D both upper and lower bounds can be proven that transport heat in the 'ultimate' scaling regime of $Ra^{\frac{1}{2}}$ [87]. The premise of the method is to enforce the advection-diffusion equation entirely as opposed to only energy balances, as in the background field approach. Then, one constructs velocity fields that optimise heat transport. While applied to IH the quantity studied so far has only been $\overline{\langle T \rangle}$ [130, 143], although, the application to $\overline{\langle wT \rangle}$ should be relatively straightforward given preliminary investigations. A final approach to determine whether the bounds

are sharp could be in the search of unstable periodic orbits. This approach finds extremal solutions to the governing equations [91].

Finally, we should highlight the two unpublished chapters in this thesis. Specifically that of free-slip boundaries in chapter 6 and non-uniform heating or cooling from chapter 8. As discussed in their respective chapters, there are many questions to answer. For free-slip boundaries the exponents of the bounds warrant further investigations to rule out the possibility of alternative $\tau(z)$ that could improve the upper bounds. While for non-uniform heating or cooling, the profiles need to be evaluated to assess if upper bounds can be proven where the maximum energy injected into the system matches the upper bound obtained with the background method. For non-uniform heating this would be a means to demonstrate that by varying the heating/cooling the temperature difference between the boundaries is provably positive. As a concluding note, several interesting variations on uniform IH convection can be briefly mentioned, like convection in a rotating domain, IH convection in a porous medium and IH convection of a conducting fluid subject to a magnetic field. Bounds have been proven for RB convection under rotation and in a porous medium but not for magnetoconvection. As such, there remains a plethora of scenarios of IH convection to be explored which ultimately will enrich our understanding of turbulent convection. The hope being that in pursuit of answers, novel mathematical ideas and numerical schemes can be developed that enhance the study of all things fluid dynamics.

Bibliography

[1] Arslan, A., Fantuzzi, G., Craske, J., and Wynn, A. Bounds for internally heated convection with fixed boundary heat flux. *Journal of Fluid Mechanics 992* (2021), R1.

[2] Arslan, A., Fantuzzi, G., Craske, J., and Wynn, A. Bounds on heat transport for convection driven by internal heating. *Journal of Fluid Mechanics 919* (2021), A15.

[3] Arslan, A., Fantuzzi, G., Craske, J., and Wynn, A. Rigorous scaling laws for internally heated convection at infinite prandtl number. *arXiv:2205.03175 [physics.flu-dyn]* (2022).

[4] Balmforth, N. J., Ghadge, S. A., Kettapun, A., and Mandre, S. D. Bounds on double-diffusive convection. *Journal of Fluid Mechanics 569* (2006), 29–50.

[5] Bercovici, D. Mantle convection. *Encyclopedia of Solid Earth Geophysics Springer* (2011).

[6] Bergholz, R. Natural convection of a heat generating fluid in a closed cavity. *Journal of Heat Transfer* (1980), 242–247.

[7] Bouillaut, V., Lepot, S., Aumaître, S., and Gallet, B. Transition to the ultimate regime in a radiatively driven convection experiment. *Journal of Fluid Mechanics 861* (2019).

[8] Boyd, S., and Vandenberghe, L. *Convex Optimization*. Cambridge University Press, 2004.

[9] Busse, F. H. On Howard's upper bound for heat transport by turbulent convection. *Journal of Fluid Mechanics 37*, 3 (1969), 457–477.

[10] Busse, F. H. Bounds for turbulent shear flow. *Journal of Fluid Mechanics 41*, 1 (1970), 219–240.

[11] Busse, F. H. Patterns of convection in spherical shells. *Journal of Fluid Mechanics 72*, 1 (1975), 67–85.

[12] Busse, F. H., and Riahi, N. Patterns of convection in spherical shells. part 2. *Journal of Fluid Mechanics 123* (1982), 283–301.

[13] Chandrasekhar, S. *Hydrodynamic and hydromagnetic stability*. Courier Corporation, 2013.

[14] Chernyshenko, S. I. Relationship between the methods of bounding time averages. *Philosophical Transactions of the Royal Society A 380*, 1 (2022), 20210044.

[15] Chernyshenko, S. I., Goulart, P. J., Huang, D., and Papachristodoulou, A. Polynomial sum of squares in fluid dynamics: a review with a look ahead. *Philosophical Transactions of the Royal Society A 372*, 2020 (2014), 20130350.

[16] Cheung, F. B., and Chawla, T. Complex heat transfer processes in heat-generating horizontal fluid layers. *Annual Review of Heat Transfer 1* (1987).

[17] Christopher, T. W., and Llewellyn Smith, S. G. Bounding temperature dissipation in time-modulated Rayleigh–Bénard convection. *Physical Review Fluids 6*, 5 (2021), 1–9.

[18] Constantin, P. Geometric statistics in turbulence. *SIAM Review. 36*, 1 (1994), 73–98.

[19] Constantin, P., and Doering, C. R. Variational bounds in dissipative systems. *Physica D: Nonlinear Phenomena 82*, 3 (1995), 221–228.

[20] Constantin, P., and Doering, C. R. Variational bounds on energy dissipation in incompressible flows. II. Channel flow. *Physical Review E 51*, 4 (1995), 3192–3198.

[21] Constantin, P., and Doering, C. R. Heat transfer in convective turbulence. *Nonlinearity 9*, 4 (1996), 1049–1060.

[22] Constantin, P., and Doering, C. R. Infinite Prandtl number convection. *Journal of Statistical Physics Phys. 94*, 1-2 (1999), 159–172.

[23] Creyssels, M. Model for thermal convection with uniform volumetric energy sources. *Journal of Fluid Mechanics 919* (2021), A13.

[24] Davidson, P. A. *Turbulence in rotating, stratified and electrically conducting fluids.* Cambridge University Press, 2013.

[25] Debler, W. R. *The onset of laminar natural convection in a fluid with homogenously distributed heat sources.* PhD thesis, University of Michigan, 1959.

[26] Ding, Z., and Kerswell, R. R. Exhausting the background approach for bounding the heat transport in Rayleigh–Bénard convection. *Journal of Fluid Mechanics 889* (2020), A33(1–33).

[27] Ding, Z., and Marensi, E. Upper bound on angular momentum transport in Taylor–Couette flow. *Physical Review E 100* (2019), 063109.

[28] Doering, C. R., and Constantin, P. Energy dissipation in shear driven turbulence. *Physical Review Letters 69*, 11 (1992), 1648–1651.

[29] Doering, C. R., and Constantin, P. Variational bounds on energy dissipation in incompressible flows: Shear flow. *Physical Review E 49*, 5 (1994), 4087–4099.

[30] Doering, C. R., and Constantin, P. Variational bounds on energy dissipation in incompressible flows. III. Convection. *Physical Review E 53*, 6 (1996), 5957–5981.

[31] Doering, C. R., and Constantin, P. Bounds for heat transport in a porous layer. *Journal of Fluid Mechanics 376* (1998), 263–296.

[32] Doering, C. R., and Constantin, P. On upper bounds for infinite Prandtl number convection with or without rotation. *Journal of Mathematical Physics 42*, 2 (2001), 784–795.

[33] Doering, C. R., and Gibbon, J. D. *Applied analysis of the Navier-Stokes equations.* Cambridge university press, 1995.

[34] Doering, C. R., and Hyman, J. M. Energy stability bounds on convective heat transport: Numerical study. *Physical Review E 55*, 6 (1997), 7775–7778.

[35] Doering, C. R., Otto, F., and Reznikoff, M. G. Bounds on vertical heat transport for infinite Prandtl number Rayleigh–Bénard convection. *Journal of Fluid*

Mechanics 560 (2006), 229–241.

[36] Doering, C. R., Spiegel, E. A., and Worthing, R. A. Energy dissipation in a shear layer with suction. *Physics of Fluids 12*, 8 (2000), 1955–1968.

[37] Drivas, T. D., Nguyen, H. Q., and Nobili, C. Bounds on heat flux for Rayleigh-Bénard convection between Navier-slip fixed temperature boundaries. *Philosophical Transactions of the Royal Society A 380*, 1 (2022), 20210044.

[38] Du, Y., Zhang, M., and Yang, Y. Two-component convection flow driven by a heat-releasing concentration field. *Journal of Fluid Mechanics 929* (2021), A35.

[39] Emara, A. A., and Kulacki, F. A. A numerical investigation of thermal convection in a heat-generating fluid layer. *Journal of Heat Transfer 102*, 3 (1980), 531–537.

[40] Fantuzzi, G. Bounds for Rayleigh–Bénard convection between free-slip boundaries with an imposed heat flux. *Journal of Fluid Mechanics 837* (2018), R5.

[41] Fantuzzi, G., Arslan, A., and Wynn, A. The background method: Theory and computations. *Philosophical Transactions of the Royal Society A 380*, 1 (2022), 20210038.

[42] Fantuzzi, G., Goluskin, D., Huang, D., and Chernyshenko, S. I. Bounds for deterministic and stochastic dynamical systems using sum-of-squares optimization. *SIAM Journal on Applied Dynamical Systems 15*, 4 (2016), 1962–1988.

[43] Fantuzzi, G., Nobili, C., and Wynn, A. New bounds on the vertical heat transport for Bénard–Marangoni convection at infinite Prandtl number. *Journal of Fluid Mechanics 885* (2020), R4(1—-12).

[44] Fantuzzi, G., Pershin, A., and Wynn, A. Bounds on heat transfer for Bénard–Marangoni convection at infinite Prandtl number. *Journal of Fluid Mechanics 837* (2018), 562–596.

[45] Fantuzzi, G., and Wynn, A. Construction of an optimal background profile for the Kuramoto–Sivashinsky equation using semidefinite programming. *Physics Letters A 379*, 1-2 (2015), 23–32.

[46] Fantuzzi, G., and Wynn, A. Construction of an optimal background profile for the Kuramoto–Sivashinsky equation using semidefinite programming. *Physics Letters A 379*, 1-2 (2015), 23–32.

[47] Fantuzzi, G., and Wynn, A. Optimal bounds with semidefinite programming: An application to stress-driven shear flows. *Physical Review E 93*, 4 (2016), 043308.

[48] Fantuzzi, G., and Wynn, A. Semidefinite relaxation of a class of quadratic integral inequalities. In *Proceedings of 55th IEEE Conference on Decision and Control* (2016), vol. 2, IEEE, pp. 6192–6197.

[49] Fantuzzi, G., and Wynn, A. Exact energy stability of Bénard-Marangoni convection at infinite Prandtl number. *Journal of Fluid Mechanics 822* (2017), R1.

[50] Fantuzzi, G., Wynn, A., Goulart, P. J., and Papachristodoulou, A. Optimization with affine homogeneous quadratic integral inequality constraints. *IEEE Transactions on Automatic Control 62*, 12 (2017), 6221–6236.

[51] Fantuzzi, G., Wynn, A., Goulart, P. J., and Papachristodoulou, A. QUINOPT, version 2.2. https://github.com/aeroimperial-optimization/QUINOPT, 2017.

[52] Foias, C., Manley, O., and Temam, R. Attractors for the Bénard problem: existence and physical bounds on their fractal dimension. *Nonlinear Analysis 11*, 8 (1987), 939–967.

[53] Fujisawa, K., Fukuda, M., Kobayashi, K., Kojima, M., Nakata, K., Nakata, M., and Yamashita, M. SDPA (SemiDefinite Programming Algorithm) and SDPA-GMP User's Manual – Version 7.1.1. Tech. rep., Department of Mathematical and Computing Sciences, Tokyo Institute of Technology, Tokyo, Japan, 2008.

[54] Fujisawa, K., Kim, S., Kojima, M., Okamoto, Y., and Yamashita, M. User's Manual for SparseCoLO: Conversion Methods for SPARSE COnic-form Linear Optimization Problems. Tech. rep., Department of Mathematical and Computing Sciences, Tokyo Institute of Technology, Tokyo, Japan, 2009.

[55] Fukuda, M., Kojima, M., Murota, K., and Nakata, K. Exploiting sparsity in semidefinite programming via matrix completion I: General Framework. *SIAM*

Journal on Optimization 11, 3 (2000), 647–674.

[56] Gallet, B., Doering, C. R., and Spiegel, E. A. Destabilizing Taylor-Couette flow with suction. *Physics of Fluids 22*, 3 (2010), 034105.

[57] Goluskin, D. Internally heated convection beneath a poor conductor. *Journal of Fluid Mechanics 771* (2015), 36–56.

[58] Goluskin, D. *Internally heated convection and Rayleigh–Bénard convection*. Springer Briefs in Applied Sciences and Technologies. Springer, Cham, 2016.

[59] Goluskin, D., and Doering, C. R. Bounds for convection between rough boundaries. *Journal of Fluid Mechanics 804* (2016), 370–386.

[60] Goluskin, D., and Fantuzzi, G. Bounds on mean energy in the Kuramoto–Sivashinsky equation computed using semidefinite programming. *Nonlinearity 32*, 5 (2019), 1705–1730.

[61] Goluskin, D., and Spiegel, E. A. Convection driven by internal heating. *Physics Letters A 377*, 1-2 (2012), 83–92.

[62] Goluskin, D., and Spiegel, E. A. Convection driven by internal heating. *Physics Letters A 377*, 1-2 (2012), 83–92.

[63] Goluskin, D., and van der Poel, E. P. Penetrative internally heated convection in two and three dimensions. *Journal of Fluid Mechanics 791* (2016).

[64] Grossmann, S., and Lohse, D. Scaling in thermal convection: a unifying theory. *Journal of Fluid Mechanics 407* (2000), 27–56.

[65] Hagstrom, G. I., and Doering, C. R. Bounds on heat transport in Bénard–Marangoni convection. *Physical Review E 81*, 4 (2010), 047301.

[66] Hagstrom, G. I., and Doering, C. R. Bounds on surface stress-driven shear flow. *J. Nonlinear Sci. 24*, 1 (2014), 185–199.

[67] Hopf, E. Über die anfangswertaufgabe für die hydrodynamischen grundgleichungen. erhard schmidt zu seinem 75. geburtstag gewidmet. *Mathematische Nachrichten 4* (1950), 213–231.

[68] Howard, L. N. Note on a paper of John W. Miles. *Journal of Fluid Mechanics 10*, 4 (1961), 509–512.

[69] Howard, L. N. Heat transport by turbulent convection. *Journal of Fluid Mechanics 17*, 3 (1963), 405–432.

[70] Howard, L. N. Bounds on flow quantities. *Annual Review of Fluid Mechanics 4*, 1 (1972), 473–494.

[71] Hughes, G. O., Gayen, B., and Griffiths, R. W. Available potential energy in Rayleigh–Bénard convection. *Journal of Fluid Mechanics 729* (2013), R3.

[72] Ierley, G. R., Kerswell, R. R., and Plasting, S. C. Infinite-Prandtl-number convection. Part 2. A singular limit of upper bound theory. *Journal of Fluid Mechanics 560* (2006), 159–227.

[73] Ingersoll, A. P., and Porco, C. C. Solar heating and internal heat flow on jupiter. *Icarus 35*, 1 (1978), 27–43.

[74] Jahn, M., and Reineke, H.-H. Free convection heat transfer with internal heat sources, calculations and measurements. In *Proceedings of the 5th International Heat Transfer Conference* (1974), pp. 74–78.

[75] Kakac, S., Aung, W. M., and Viskanta, R. Natural convection: fundamentals and applications. *Washington, DC, Hemisphere Publishing Corp., 1985, 1191 p.* (1985).

[76] Kazemi, S., Ostilla-Mónico, R., and Goluskin, D. Transition between boundary-limited scaling and mixing-length scaling of turbulent transport in internally heated convection. *Physical Review Letters 129* (Jul 2022), 024501.

[77] Kerswell, R. R. Upper bounds on the energy dissipation in turbulent precession. *Journal of Fluid Mechanics 321* (1996), 335–370.

[78] Kerswell, R. R. Variational bounds on shear-driven turbulence and turbulent Boussinesq convection. *Physica D: Nonlinear Phenomena 100*, 3–4 (1997), 355–376.

[79] Kerswell, R. R. Unification of variational principles for turbulent shear flows: the background method of Doering–Constantin and the mean-fluctuation formulation of

Howard–Busse. *Physica D: Nonlinear Phenomena 121*, 1-2 (1998), 175–192.

[80] Kerswell, R. R. Variational principle for the Navier–Stokes equations. *Physical Review E 59*, 5 (1999), 5482–5494.

[81] Kerswell, R. R. New results in the variational approach to turbulent Boussinesq convection. *Physics of Fluids 13*, 1 (2001), 192–209.

[82] Kerswell, R. R. Upper bounds on general dissipation functionals in turbulent shear flows: revisiting the 'efficiency' functional. *Journal of Fluid Mechanics 461* (2002), 239–275.

[83] Kondratenko, P., Nikolski, D., and Strizhov, V. Free-convective heat transfer in fluids with non-uniform volumetric heat generation. *International journal of heat and mass transfer 51*, 7-8 (2008), 1590–1595.

[84] Kulacki, F. A., and Goldstein, R. J. Thermal convection in a horizontal fluid layer with uniform volumetric energy sources. *Journal of Fluid Mechanics 55*, 2 (1972), 271–287.

[85] Kulacki, F. A., and Goldstein, R. J. Thermal convection in a horizontal fluid layer with uniform volumetric energy sources. *Journal of Fluid Mechanics 55*, 2 (1972), 271–287.

[86] Kumar, A. Pressure-driven flows in helical pipes: Bounds on flow rate and friction factor. *Journal of Fluid Mechanics 904* (2020), A5.

[87] Kumar, A. Three dimensional branching pipe flows for optimal scalar transport between walls . *arxiv:2205.03367 [math.AP]* (2022).

[88] Kumar, A. Geometrical dependence of optimal bounds in taylor–couette flow. *Journal of Fluid Mechanics 948* (2022), A11.

[89] Kumar, A., Arslan, A., Fantuzzi, G., Craske, J., and Wynn, A. Analytical bounds on the heat transport in internally heated convection. *Journal of Fluid Mechanics 938* (2022), A26.

[90] Kumar, A., and Garaud, P. Bound on the drag coefficient for a flat plate in a uniform flow. *Journal of Fluid Mechanics 900* (2020), A6(1–24).

[91] Lakshmi, M. V., Fantuzzi, G., Fernández-Caballero, J., Hwang, Y., and Chernyshenko, S. I. Finding extremal periodic orbits with polynomial optimisation, with application to a nine-mode model of shear flow. *SIAM Journal on Applied Dynamical Systems 19*, 2 (2020), 763–787.

[92] Lee, H., Wen, B., and Doering, C. R. Improved upper bounds on the energy dissipation rate for shear flow with injection and suction. *Physics of Fluids 31*, 8 (2019), 085102.

[93] Lee, S. D., Lee, J. K., and Suh, K. Y. Boundary condition dependent natural convection in a rectangular pool with internal heat sources. *Journal of Heat Transfer 129*, 5 (2007), 679–682.

[94] Lepot, S., Aumaître, S., and Gallet, B. Radiative heating achieves the ultimate regime of thermal convection. *Proceedings of the National Academy of Sciences of the U.S.A. 115*, 36 (2018), 8937–8941.

[95] Leray, J. Sur le mouvement d'un liquide visqueux emplissant l'espace. *Acta Mathematica 63*, none (1934), 193 – 248.

[96] Limare, A., Jaupart, C., Kaminski, E., Fourel, L., and Farnetani, C. G. Convection in an internally heated stratified heterogeneous reservoir. *Journal of Fluid Mechanics 870* (2019), 67–105.

[97] Lu, L., Doering, C. R., and Busse, F. H. Bounds on convection driven by internal heating. *Journal of Mathematical Physics 45*, 7 (2004), 2967–2986.

[98] Malkus, W. V. R. The heat transport and spectrum of thermal turbulence. *Proceedings of the Royal Society A 225*, 1161 (1954), 196–212.

[99] Marchioro, C. Remark on the energy dissipation in shear driven turbulence. *Physica D: Nonlinear Phenomena 74*, 3–4 (1994), 395–398.

[100] Miles, J. W. On the stability of heterogeneous shear flows. *Journal of Fluid Mechanics 10*, 4 (1961), 496–508.

[101] Miquel, B., Lepot, S., Bouillaut, V., and Gallet, B. Convection driven by internal heat sources and sinks: Heat transport beyond the mixing-length or "ultimate" scaling regime. *Physical Review Fluids 4*, 12 (2019), 121501.

[102] Mosek ApS. *The MOSEK optimization toolbox for MATLAB. Version 9.1.* Mosek ApS, 2020. https://docs.mosek.com/9.1/toolbox/index.html.

[103] Mulyukova, E., and Bercovici, D. Mantle convection in terrestrial planets. *Oxford Research Encyclopedia of Planetery Sciences* (2020).

[104] Nakata, K., Fujisawa, K., Fukuda, M., Kojima, M., and Murota, K. Exploiting sparsity in semidefinite programming via matrix completion II: implementation and numerical results. *Mathematical Programming B 95*, 2 (2003), 303–327.

[105] Nemirovski, A. Advances in convex optimization: Conic programming. In *International Conference of Mathematics* (2006), vol. 1, pp. 413–444.

[106] Nesterov, Y., and Nemirovskii, A. *Interior-Point Polynomial Algorithms in Convex Programming*. Society for Industrial and Applied Mathematics, 1994.

[107] Nicodemus, R., Grossmann, S., and Holthaus, M. Improved variational principle for bounds on energy dissipation in turbulent shear flow. *Physica D: Nonlinear Phenomena: Nonlin. Phen. 101*, 1-2 (1997), 178–190.

[108] Nicodemus, R., Grossmann, S., and Holthaus, M. Variational bound on energy dissipation in plane Couette flow. *Physical Review E 56*, 6 (1997), 6774–6786.

[109] Nicodemus, R., Grossmann, S., and Holthaus, M. The background flow method. Part 1. Constructive approach to bounds on energy dissipation. *Journal of Fluid Mechanics 363* (1998), 281–300.

[110] Nicodemus, R., Grossmann, S., and Holthaus, M. The background flow method. Part 2. Asymptotic theory of dissipation bounds. *Journal of Fluid Mechanics 363* (1998), 301–323.

[111] Nobili, C. The role of boundary conditions in scaling laws for turbulent heat transport. *Mathematics in Engineering 5*, 1 (2023), 1–41.

[112] Nobili, C., and Otto, F. Limitations of the background field method applied to Rayleigh–Bénard convection. *Journal of Mathematical Physics 58*, 9 (2017), 093102.

[113] O'Donoghue, B., Chu, E., Parikh, N., and Boyd, S. Conic optimization via operator splitting and homogeneous self-dual embedding. *Journal of Optimization*

Theory and Applications 169, 3 (2016), 1–27.

[114] Otero, J., Dontcheva, L. A., Johnston, H., Worthing, R. A., Kurganov, A., Petrova, G., and Doering, C. R. High-Rayleigh-number convection in a fluid-saturated porous layer. *Journal of Fluid Mechanics 500* (2004), 263–281.

[115] Otero, J., Wittenberg, R. W., Worthing, R. A., and Doering, C. R. Bounds on Rayleigh–Bénard convection with an imposed heat flux. *Journal of Fluid Mechanics 473* (2002), 191–199.

[116] Otto, F., and Seis, C. Rayleigh–Bénard convection: Improved bounds on the Nusselt number. *Journal of Mathematical Physics 52*, 8 (2011), 083702.

[117] Pachev, B., Whitehead, J. P., Fantuzzi, G., and Grooms, I. Rigorous bounds on the heat transport of rotating convection with Ekman pumping. *Journal of Mathematical Physics 61*, 2 (2020), 023101.

[118] Peckover, R. S., and Hutchinson, I. H. Convective rolls driven by internal heat sources. *Physics of Fluids 17*, 7 (1974), 1369–1371.

[119] Plasting, S. C., and Ierley, G. R. Infinite-Prandtl-number convection. Part 1. Conservative bounds. *Journal of Fluid Mechanics 542*, 2005 (2005), 343–363.

[120] Plasting, S. C., and Kerswell, R. R. Improved upper bound on the energy dissipation rate in plane Couette flow: the full solution to Busse's problem and the Constantin-Doering-Hopf problem with one-dimensional background field. *Journal of Fluid Mechanics 477* (2003), 363–379.

[121] Priestley, C. H. B. Vertical heat transfer from impressed temperature fluctuations. *Australian Journal of Physics 7*, 1 (1954), 202–209.

[122] Riahi, N. Nonlinear convection in a horizontal layer with an internal heat source. *Journal of the Physical Society of Japan 53*, 12 (1984), 4169–4178.

[123] Roberts, P. Convection in a self-gravitating fluid sphere. *Mathematika 12*, 2 (1965), 128–137.

[124] Roberts, P. Convection in horizontal layers with internal heat generation. theory. *Journal of Fluid Mechanics 30*, 1 (1967), 33–49.

[125] Roberts, P. H. On the thermal instability of a rotating-fluid sphere containing heat sources. *Philosophical Transactions of the Royal Society of London A 263*, 1136 (1968), 93–117.

[126] Rosa, R. M. S., and Temam, R. M. Optimal minimax bounds for time and ensemble averages of dissipative infinite-dimensional systems with applications to the incompressible Navier–Stokes equations. *Pure and Applied Functional Analysis 7*, 1 (2022), 327–355.

[127] Schubert, G., Turcotte, D. L., and Olson, P. *Mantle convection in the Earth and planets*. Cambridge University Press, 2001.

[128] Seis, C. Scaling bounds on dissipation in turbulent flows. *Journal of Fluid Mechanics 777* (2015), 591–603.

[129] Siggers, J. H., Kerswell, R. R., and Balmforth, N. J. Bounds on horizontal convection. *Journal of Fluid Mechanics 517* (2004), 55–70.

[130] Song, B., Fantuzzi, G., and Tobasco, I. Bounds on heat transfer by incompressible flows between balanced sources and sinks. *Physica D: Nonlinear Phenomena* (2022), 133591.

[131] Spiegel, E. A. A generalization of the mixing-length theory of turbulent convection. *The Astrophysical Journal 138* (1963), 216.

[132] Spiegel, E. A., and Veronis, G. On the boussinesq approximation for a compressible fluid. *The Astrophysical Journal 131* (1960), 442.

[133] Stanley, S. Chapter 6 - magnetic field generation in planets. In *Encyclopedia of the Solar System*, T. Spohn, D. Breuer, and T. V. Johnson, Eds., third edition ed. Elsevier, Boston, 2014, pp. 121–136.

[134] Steinberner, U., and Reineke, H.-H. Turbulent buoyancy convection heat transfer with internal heat sources. In *International Heat Transfer Conference* (1978), Begel House Inc.

[135] Straughan, B. Continuous dependence on the heat source and non-linear stability for convection with internal heat generation. *Mathematical Methods in the Applied Sciences 13*, 5 (1990), 373–383.

[136] Straus, J. M. Penetrative convection in a layer of fluid heated from within. *The Astrophysical Journal 209* (1976), 179–189.

[137] Tang, W., Caulfield, C.-C. P., and Young, W. R. Bounds on dissipation in stress-driven flow. *Journal of Fluid Mechanics 510* (2004), 333–352.

[138] Tasaka, Y., and Takeda, Y. Effects of heat source distribution on natural convection induced by internal heating. *International Journal of Heat and Mass Transfer 48*, 6 (2005), 1164–1174.

[139] Thirlby, R. Convection in an internally heated layer. *Journal of Fluid Mechanics 44*, 4 (1970), 673–693.

[140] Tilgner, A. Bounds on poloidal kinetic energy in plane layer convection. *Physical Review Fluids 2*, 12 (2017), 123502.

[141] Tilgner, A. Time evolution equation for advective heat transport as a constraint for optimal bounds in Rayleigh-Bénard convection. *Physical Review Fluids 4*, 1 (2019), 1–11.

[142] Tilgner, A. A rigorous bound on the scaling of dissipation with velocity amplitude in flow past a sphere. *Journal of Fluid Mechanics 916* (2021), 1–10.

[143] Tobasco, I. Optimal cooling of an internally heated disc. *Philosophical Transactions of the Royal Society A 310*, 1 (2022), 20210040.

[144] Tobasco, I., Goluskin, D., and Doering, C. R. Optimal bounds and extremal trajectories for time averages in nonlinear dynamical systems. *Physics Letters A 382*, 6 (2018), 382–386.

[145] Tritton, D. J. Internally heated convection in the atmosphere of venus and in the laboratory. *Nature 257*, 5522 (1975), 110–112.

[146] Tritton, D. J., and Zarraga, M. N. Convection in horizontal layers with internal heat generation. experiments. *Journal of Fluid Mechanics 30*, 1 (1967), 21–31.

[147] Tveitereid, M. Thermal convection in a horizontal fluid layer with internal heat sources. *International Journal of Heat and Mass Transfer 21*, 3 (1978), 335–339.

[148] Vallis, G. K. Geophysical fluid dynamics: whence, whither and why? *Proceedings of the Royal Society A 472*, 2192 (2016), 20160140.

[149] Vandenberghe, L., and Andersen, M. S. Chordal graphs and semidefinite optimization. *Foundations and Trends in Optimisation 1*, 4 (2015), 241–433.

[150] Vandenberghe, L., and Boyd, S. Semidefinite Programming. *SIAM Review. 38*, 1 (1996), 49–95.

[151] Waki, H., Nakata, M., and Muramatsu, M. Strange behaviors of interior-point methods for solving semidefinite programming problems in polynomial optimization. *Computational Optimization and Applications 53*, 3 (2012), 823–844.

[152] Wang, Q., Lohse, D., and Shishkina, O. Scaling in internally heated convection: a unifying theory. *Geophysical Research Letters 47* (2020), e2020GL091198.

[153] Wang, X. Infinite prandtl number limit of rayleigh-bénard convection. *Communications on Pure and Applied Mathematics 57*, 10 (2004), 1265–1282.

[154] Wang, X. Asymptotic behavior of the global attractors to the Boussinesq system for Rayleigh-Bénard convection at large Prandtl number. *Communications on Pure and Applied Mathematics 60*, 9 (2007), 1293–1318.

[155] Wang, X. Bound on vertical heat transport at large prandtl number. *Physica D: Nonlinear Phenomena 237*, 6 (2008), 854–858.

[156] Wang, X., and Whitehead, J. P. A bound on the vertical transport of heat in the 'ultimate' state of slippery convection at large prandtl numbers. *Journal of Fluid Mechanics 729* (2013), 103–122.

[157] Wen, B., and Chini, G. P. Inclined porous medium convection at large Rayleigh number. *Journal of Fluid Mechanics 837* (2018), 670–702.

[158] Wen, B., Chini, G. P., Dianati, N., and Doering, C. R. Computational approaches to aspect-ratio-dependent upper bounds and heat flux in porous medium convection. *Physics Letters A 377*, 41 (dec 2013), 2931–2938.

[159] Wen, B., Chini, G. P., Kerswell, R. R., and Doering, C. R. Time-stepping approach for solving upper-bound problems: Application to two-dimensional Rayleigh–

Bénard convection. *Physical Review E 92*, 4 (2015), 043012.

[160] Wen, B., Dianati, N., Lunasin, E., Chini, G. P., and Doering, C. R. New upper bounds and reduced dynamical modeling for Rayleigh–Bénard convection in a fluid saturated porous layer. *Communications in Nonlinear Science and Numerical Simulations 17*, 5 (2012), 2191–2199.

[161] Wen, B., Goluskin, D., and Doering, C. R. Steady rayleigh–bénard convection between no-slip boundaries. *Journal of Fluid Mechanics 933* (2022), R4.

[162] Wen, B., Goluskin, D., Leduc, M., Chini, G. P., and Doering, C. R. Steady Rayleigh-Bénard convection between stress-free boundaries. *Journal of Fluid Mechanics 905* (2020), R4(1–13).

[163] Wen, Z., Goldfarb, D., and Yin, W. Alternating direction augmented Lagrangian methods for semidefinite programming. *Mathematical Programming Computation 2*, 3-4 (2010), 203–230.

[164] Whitehead, J. P., and Doering, C. R. Internal heating driven convection at infinite Prandtl number. *Journal of Mathematical Physics 52*, 9 (2011), 093101.

[165] Whitehead, J. P., and Doering, C. R. Ultimate state of two-dimensional Rayleigh–Bénard convection between free-slip fixed-temperature boundaries. *Physical Review Letters 106*, 24 (2011), 244501.

[166] Whitehead, J. P., and Doering, C. R. Rigid bounds on heat transport by a fluid between slippery boundaries. *Journal of Fluid Mechanics 707* (2012), 241–259.

[167] Whitehead, J. P., and Wittenberg, R. W. A rigorous bound on the vertical transport of heat in Rayleigh–Bénard convection at infinite Prandtl number with mixed thermal boundary conditions. *Journal of Mathematical Physics 55*, 9 (2014), 093104.

[168] Wittenberg, R. W. Bounds on Rayleigh–Bénard convection with imperfectly conducting plates. *Journal of Fluid Mechanics 665* (2010), 158–198.

[169] Wittenberg, R. W., and Gao, J. Conservative bounds on Rayleigh–Bénard convection with mixed thermal boundary conditions. *The European Physical Journal B 76*, 4 (2010), 565–580.

[170] Wörner, M., Schmidt, M., and Grötzbach, G. Direct numerical simulation of turbulence in an internally heated convective fluid layer and implications for statistical modelling. *Journal of Hydraulic Research 35*, 6 (1997), 773–797.

[171] Yamashita, M., Fujisawa, K., Fukuda, M., Kobayashi, K., Nakata, K., and Nakata, M. Latest developments in the sdpa family for solving large-scale sdps. In *Handbook on semidefinite, conic and polynomial optimization*. Springer, 2012, pp. 687–713.

[172] Yan, X. On limits to convective heat transport at infinite Prandtl number with or without rotation. *Journal of Mathematical Physics 45*, 7 (2004), 2718–2743.

[173] Zheng, Y., Fantuzzi, G., and Papachristodoulou, A. Chordal and factor-width decompositions for scalable semidefinite and polynomial optimization. *arXiv:2107.02379 [math.OC]* (2021).

[174] Zheng, Y., Fantuzzi, G., Papachristodoulou, A., Goulart, P. J., and Wynn, A. Chordal decomposition in operator-splitting methods for sparse semidefinite programs. *Mathematical Programming 180* (2020), 489–532.

Appendix A

Miscellaneous Proofs

A.1 Proof of Lemma 2.3.2

First, we prove that λ is nondecreasing if $\mathcal{B}_q$ is a positive functional. Fix any $z_1, z_2 \in (0,1)$ with $z_1 < z_2$ and choose $\varepsilon > 0$ small enough that $0 < z_1 - \varepsilon$ and $z_2 + \varepsilon < 1$. Consider a temperature profile $T_\varepsilon(\boldsymbol{x}) = T_\varepsilon(z)$ that varies only in z and satisfies

$$\partial_z T_\varepsilon := \begin{cases} \varepsilon^{-1} & z_1 - \varepsilon \leq z \leq z_1 + \varepsilon, \\ -\varepsilon^{-1} & z_2 - \varepsilon \leq z \leq z_2 + \varepsilon, \\ 0 & \text{otherwise.} \end{cases}$$

Clearly, $T_\varepsilon \in \mathcal{T}$ and is nonnegative, so the positivity of $\mathcal{B}_q$ yields

$$0 \leq \mathcal{L}_q\{T_\varepsilon\} = -\langle \lambda(z)\partial_z T_\varepsilon \rangle = \frac{1}{\varepsilon}\int_{z_2-\varepsilon}^{z_2+\varepsilon} \lambda(z)\mathrm{d}z - \frac{1}{\varepsilon}\int_{z_1-\varepsilon}^{z_1+\varepsilon} \lambda(z)\mathrm{d}z. \tag{A.1.1}$$

Letting $\varepsilon \to 0$ using Lebesgue's differentiation theorem and rearranging yields $\lambda(z_1) \leq \lambda(z_2)$, which implies that λ is nondecreasing since z_1 and z_2 are arbitrary.

To prove the reverse statement, suppose that λ is nondecreasing but that $\mathcal{B}_q$ is not positive. This means that there exist a constant $c > 0$ and a temperature field $T_0 \in \mathcal{T}$, nonnegative on the domain Ω, such that $\mathcal{B}_q(T_0) \leq -c$. By a standard

approximation argument, we may also assume that $\lambda(z)$ is smooth on $[0,1]$. Then, integration by parts using the boundary conditions on T_0 yields

$$\langle \lambda'(z) T \rangle = \mathcal{B}_q(T_0) \leq -c.$$

This is a contradiction because the left-hand side is a nonnegative quantity, as $\lambda'(z) \geq 0$ (λ is nondecreasing) and $T_0(\boldsymbol{x}) \geq 0$ on Ω by assumption.

A.2 Proof of Lemma 3.3.2

Set $f(z) = g(z)\sqrt{z+\epsilon}$ where $g(z)$ satisfies $g(0) = 0$ and estimate

$$\begin{aligned} |f'|^2 &= (z+\epsilon)|g'|^2 + \left(\frac{1}{2}g^2\right)' + \frac{1}{4}(z+\epsilon)^{-1}|g|^2 \\ &= (z+\epsilon)|g'|^2 + \left(\frac{1}{2}g^2\right)' + \frac{1}{4}(z+\epsilon)^{-2}|f|^2 \\ &\geq \left(\frac{1}{2}g^2\right)' + \frac{1}{4}(z+\epsilon)^{-2}|f|^2. \end{aligned} \tag{A.2.1}$$

Upon integrating this inequality in z from 0 to ν and using the boundary condition $g(0) = 0$, we find

$$\begin{aligned} \int_0^\nu |f'(z)|^2 \,\mathrm{d}z &\geq \frac{1}{2}g(\nu)^2 + \frac{1}{4}\int_0^\nu (z+\epsilon)^{-2}|f(z)|^2 \,\mathrm{d}z \\ &\geq \frac{1}{4}\int_0^\nu (z+\epsilon)^{-2}|f(z)|^2 \,\mathrm{d}z, \end{aligned} \tag{A.2.2}$$

which is the desired inequality.

A.3 Proof of Lemma 4.2.1

Estimating the sign-indefinite term in $\mathcal{S}_{\boldsymbol{k}}$, using the Hölder and Cauchy–Schwarz inequalities yields

$$\left\langle \left| (f - \tau'(z)) \hat{w}_{\boldsymbol{k}} \hat{T}_{\boldsymbol{k}} \right| \right\rangle \leq \|f - \tau'(z)\|_\infty \left\langle |\hat{w}_{\boldsymbol{k}}|^2 \right\rangle^{\frac{1}{2}} \left\langle |\hat{T}_{\boldsymbol{k}}|^2 \right\rangle^{\frac{1}{2}}. \tag{A.3.1}$$

Consequently,

$$\mathcal{S}_{\boldsymbol{k}} \geq \frac{\alpha k^2}{R} \left\langle |\hat{w}_{\boldsymbol{k}}|^2 \right\rangle - \|f - \tau'(z)\|_\infty \left\langle |\hat{w}_{\boldsymbol{k}}|^2 \right\rangle^{\frac{1}{2}} \left\langle |\hat{T}_{\boldsymbol{k}}|^2 \right\rangle^{\frac{1}{2}} + \beta k^2 \left\langle |\hat{T}_{\boldsymbol{k}}|^2 \right\rangle. \tag{A.3.2}$$

The right-hand side is a homogeneous quadratic form in $\langle |\hat{w}_{\boldsymbol{k}}|^2 \rangle^{\frac{1}{2}}$ and $\left\langle |\hat{T}_{\boldsymbol{k}}|^2 \right\rangle^{\frac{1}{2}}$ and is nonnegative for any choice of $\hat{w}_{\boldsymbol{k}}$ and $\hat{T}_{\boldsymbol{k}}$ if and only if (4.2.5) holds.

A.4 Proof of Lemma 4.3.2

Write $f'(z) = \sqrt{z+\epsilon}g(z)$ and $f(z) = (z+\epsilon)^{3/2}h(z)$ for suitable functions g and h satisfying $g(0) = 0 = h(0)$. Then,

$$\begin{aligned} |f''|^2 &= (z+\epsilon)|g'|^2 + \frac{g^2}{4(z+\epsilon)} + \left(\frac{1}{2}g^2\right)' \\ &= (z+\epsilon)|g'|^2 + \frac{|f'|^2}{4(z+\epsilon)^2} + \left(\frac{1}{2}g^2\right)' \\ &\geq \frac{|f'|^2}{4(z+\epsilon)^2} + \left(\frac{1}{2}g^2\right)' \end{aligned} \tag{A.4.1a}$$

and

$$\begin{aligned} |f'|^2 &= (z+\epsilon)^3|h'|^2 + \frac{9}{4}(z+\epsilon)h^2 + (z+\epsilon)^2\left(\frac{3}{2}h^2\right)' \\ &= (z+\epsilon)^3|h'|^2 + \frac{9}{4}\frac{|f|^2}{(z+\epsilon)^2} + (z+\epsilon)^2\left(\frac{3}{2}h^2\right)' \\ &\geq \frac{9}{4}\frac{|f|^2}{(z+\epsilon)^2} + (z+\epsilon)^2\left(\frac{3}{2}h^2\right)' \end{aligned} \tag{A.4.1b}$$

Combining (A.4.1b) and (A.4.1a) and then integrating in z from 0 to ν yields

$$\begin{aligned} \int_0^\nu |f''|^2 \mathrm{d}z &\geq \int_0^\nu \frac{9|f|^2}{16(z+\epsilon)^4} + \left(\frac{3}{8}h^2\right)' + \left(\frac{1}{2}g^2\right)' \mathrm{d}z \\ &= \int_0^\nu \frac{9|f|^2}{16(z+\epsilon)^4}\,\mathrm{d}z + \frac{3}{8}h(\nu)^2 + \frac{1}{2}g(\nu)^2 \\ &\geq \int_0^\nu \frac{9|f|^2}{16(z+\epsilon)^4}\mathrm{d}z, \end{aligned} \tag{A.4.2}$$

which completes the proof.

Appendix B

Heuristic scaling arguments

Phenomenological predictions for the variation of $\overline{\langle wT \rangle}$ with the Rayleigh number under isothermal boundaries can be derived by coupling the total heat budget through the layer with scaling assumptions for characteristic length scales δ_T and ε_T of the lower and upper thermal boundary layers, respectively. These length scales can be defined such that $\overline{\langle T \rangle}/\delta_T = \mathcal{F}_B$ and $\overline{\langle T \rangle}/\varepsilon_T = \mathcal{F}_T$. Averaging (1.2.3c) over space and infinite time indicates that δ_T and ε_T satisfy

$$\frac{\overline{\langle T \rangle}}{\delta_T} + \frac{\overline{\langle T \rangle}}{\varepsilon_T} = 1, \tag{B.0.1}$$

while the second identity in (3.0.1) yields

$$\overline{\langle wT \rangle} = \frac{1}{2} - \frac{\overline{\langle T \rangle}}{\delta_T}. \tag{B.0.2}$$

For the sake of definiteness, assume that the mean temperature and δ_T decay as power laws in R, that is, $\overline{\langle T \rangle} = R^{-\alpha_0}/\sigma_0$ and $\delta_T = R^{-\alpha_1}/\sigma_1$ with $\alpha_0, \alpha_1 \geq 0$. If $\overline{\langle wT \rangle}$ approaches a constant as R is raised, then $\overline{\langle T \rangle} \leq O(\delta_T)$ and $\alpha_1 \leq \alpha_0$, the inequality being strict if $\overline{\langle wT \rangle} \to 1/2$. Moreover, (B.0.1) implies that

$$\frac{1}{\varepsilon_T} = \sigma_0 R^{\alpha_0} - \sigma_1 R^{\alpha_1}. \tag{B.0.3}$$

The scalings behind internally heated convection with the isothermal boundary conditions (3.1.1) are therefore necessarily subtle, because the leading scaling of ε_T (hence, of $\overline{\langle T \rangle}$) and the correction implied by δ_T both play a crucial role. Any heuristic argument therefore needs to distinguish between the physics associated with the unstably stratified flow near the upper boundary from the (very different) stably stratified flow near the lower boundary. In particular, one must determine whether $\overline{\langle T \rangle}$ reduces at the same rate as δ_T, meaning that $\overline{\langle wT \rangle}$ tends to a constant value in the range $[0, 1/2)$ determined by the relative magnitude of the prefactors σ_0 and σ_1, or slightly faster, implying that $\overline{\langle wT \rangle}$ approaches $1/2$ as the Rayleigh number is raised.

As noted by [164], one way to derive a scaling for ε_T is to assume that the upper boundary layer maintains a state of marginal stability [98, 121]. In this case, ε_T adjusts itself such that the local Rayleigh number R_{ε_T}, based on the average temperature and depth of the upper boundary layer, remains constant. Expressing R_{ε_T} in terms of R to leading order, we conclude that

$$R_{\varepsilon_T} = \overline{\langle T \rangle} \varepsilon_T^3 R \sim \sigma_0^4 R^{1-4\alpha_0}\,, \tag{B.0.4}$$

should be independent of R, which implies that $\alpha_0 = 1/4$, as noted by [62, Table 2] and consistent with the scalings [see regimes III_∞ and IV_u] [152]. Alternatively, if one uses an argument based on balancing a characteristic free-fall velocity $\sqrt{PrR\overline{\langle T \rangle}}$ with the velocity scale $1/\varepsilon_T$ implied by diffusion at the wall [131], then to leading order

$$\varepsilon_T \sqrt{PrR\overline{\langle T \rangle}} \sim \sigma_0^{\frac{3}{2}} Pr^{\frac{1}{2}} R^{1-3\alpha_0}, \tag{B.0.5}$$

is independent of R, implying that $\alpha_0 = 1/3$. In either case ($\alpha_0 = 1/4$ or $\alpha_0 = 1/3$), the resulting scaling corresponds to the first term in the asymptotic expansion of ε_T and does not provide any information about the correction due to δ_T, which is crucial to determine the asymptotic behaviour of $\overline{\langle T \rangle}$.

The simplest argument relating to δ_T, although not necessarily the most faithful, comes from assuming that in some vicinity of the lower boundary there is a balance between heating and diffusion because the flow is stably stratified. In terms of the dimensionless variables used here, heating over δ_T is proportional to δ_T and diffusion is equal to $\overline{\langle T \rangle}/\delta_T$, which implies that $\delta_T^2 \sim \overline{\langle T \rangle}$. This requires $\alpha_1 = \alpha_0/2$, leading to $\alpha_1 = 1/8$ or $\alpha_1 = 1/6$ for scaling of ε_T based on [98] or [131], respectively, and therefore to $\overline{\langle wT \rangle} = 1/2 - \sigma_1 R^{-\frac{1}{8}}/\sigma_0$ or $\overline{\langle wT \rangle} = 1/2 - \sigma_1 R^{-\frac{1}{6}}/\sigma_0$. Assuming that $\max(\overline{T})$ scales in the same way as $\overline{\langle T \rangle}$, meaning that the average temperature is approximately uniform away from boundaries, the possibility that $\delta_T^2 \sim \overline{\langle T \rangle}$ (so $\alpha_1 = \alpha_0/2$) is in reasonably good agreement with data from experiments and simulations [58, table 3.2].

An alternative argument might consider a Richardson number Ri at the lower boundary layer to quantify the destablising effects of turbulence relative to the stabilising effects of the density stratification. In terms of dimensionless quantities, the density stratification is $\overline{\langle T \rangle}/\delta_T$ and we assume that the destabilising shear across the lower boundary scales according to $\sqrt{\overline{\langle T \rangle}}/\delta_T$. Together, these scales imply that $Ri \sim \delta_T$. This is significant because, if the flow tends towards a state of marginal stability, then $Ri = 1/4$ according to the Miles–Howard criterion for steady, laminar, parallel and inviscid shear flow [68, 100]. We would therefore conclude that either $\overline{\langle wT \rangle} = 1/2 - \sigma_1 R^{-\frac{1}{4}}/\sigma_0$ or $\overline{\langle wT \rangle} = 1/2 - \sigma_1 R^{-\frac{1}{3}}/\sigma_0$, corresponding to [98] or [131] respectively. The latter scaling would be consistent with the conjectured bound for insulating lower boundary conditions, but, unlike the scaling argument outlined in the previous paragraph, is far from the wide range of scaling possibilities that have been inferred from experiments and simulations [58]. Indeed, available data is too scattered to provide conclusive information about the asymptotic behaviour of $\overline{\langle T \rangle}$, highlighting the need for further experiments and simulations in addition to the rigorous bounds pursued here.

Appendix C

Computational methodology

The optimisation problems (2.4.12) and (3.3.3) can be discretised into SDPs following a general strategy, and then solved using efficient algorithms for convex optimisation. This "discretise-then-optimise" approach preserves the linearity of the original infinite-dimensional problems and enables one to readily impose additional constraints, such as the inequalities on $\tau(0)$, $\tau(1)$ and the monotonicity constraint on λ, that are not easy to enforce following "optimise-then-discretise" strategies based on the numerical solution of the Euler–Lagrange equations for (2.4.12) and (3.3.3).

The discretisation process starts by approximating the tunable functions τ, λ and the unknown fields $\hat{T}_0$, $\hat{T}_{\boldsymbol{k}}$ and $\hat{w}_{\boldsymbol{k}}$ using a finite set of basis functions $\{\Phi_1(z), \ldots, \Phi_n(z)\}$, e.g.,

$$\tau(z) = \sum_{i=1}^{n} A_i \Phi_i(z). \tag{C.0.1}$$

Here we use a single set of basis functions for simplicity, but different fields could be approximated using different bases to improve accuracy or allow for varying degrees of smoothness. Note that while the functions τ and λ are arbitrary, so we are free to choose such a finite-dimensional representation without much loss of generality, assuming the same for the test functions $\hat{T}_0$, $\hat{T}_{\boldsymbol{k}}$ and $\hat{w}_{\boldsymbol{k}}$ represents a relaxation of the constraints in (2.4.12) and (3.3.3). Strictly speaking, therefore, our numerical results

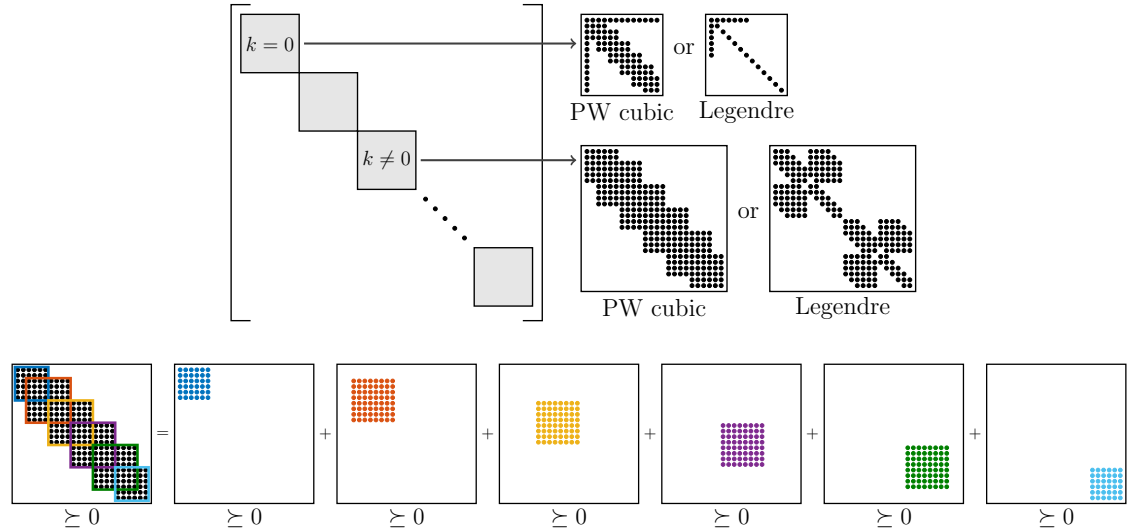

Figure C.1: *Top:* Structure of the LMI for a two-dimensional version of the internally heated convection problem in chapter 2. The basis functions are products of sinusoidal functions with wavenumber k in the horizontal direction, and either Legendre polynomials or piecewise (PW) cubic basis functions with compact support in the vertical direction. *Bottom:* Chordal decomposition of a block with nonzero wavenumber k for the PW cubic case.

are not rigorous upper bounds on the vertical heat flux, but we expect convergence as $n \to \infty$.

Substituting expansions such as (C.0.1) into the inequalities on $\mathcal{S}_0$ and $\tilde{\mathcal{S}}$ in (2.4.12) and (3.3.3) reduces them to quadratic polynomial inequalities, where the independent variables are the (unknown) expansion coefficients of $\hat{T}_0$, $\hat{T}_{\boldsymbol{k}}$ and $\hat{w}_{\boldsymbol{k}}$, and the coefficients depend linearly on the optimisation variables—the scalars U, α, β and the expansion coefficients of τ and λ. These quadratic polynomial inequalities are equivalent to positive semidefinitess constraints on matrices that depend linearly on the polynomial coefficients, and hence on the optimisation variables. These are referred to as linear matrix inequalities (LMIs). Moreover, the inequalities $\tau(0) \leq 1$, $\tau(1) \leq 0$ and the monotonicity constraint on $\lambda(z)$ in (3.3.3) can be projected onto the expansion basis to obtain a set of linear constraints on the expansions coefficients of τ and λ. The discrete problems are therefore SDPs [8] and can be solved with a variety of algorithms [see, e.g., 105].

A crucial observation is that the choice of basis functions strongly influences the structure of the linear matrix inequality (LMI) constraints and, therefore, its com-

putational complexity. For instance, Figure C.1 illustrates different LMI structures obtained when a version of the internally heated problem chapter 2, is discretized using sinusoidal functions with wavenumber k in the horizontal direction and either Legendre polynomials or compactly-supported piecewise-cubic functions in the vertical direction. The block-diagonal structure corresponds to the decoupling of different wavenumbers, and the positive semidefiniteness of each block can be imposed separately to obtain an SDP with multiple smaller LMIs. This is convenient because SDPs of this type can currently be solved more efficiently than SDPs with a single large LMI.

The structure of each block can be exploited in a similar way using *chordal decomposition* techniques for SDPs [55, 104, 149, 173, 174], which decompose sparse LMIs into smaller ones by considering their dense principal submatrices (see the bottom panel in Figure C.1). This requires introducing additional optimization variables to account for the overlap between dense submatrices, but, if these are small and do not overlap significantly, then the added cost is negligible compared to the savings associated by the reduction in LMI dimension.

To tackle (2.4.12) and (3.3.3), we used a finite-element approximation similar to that considered by [44]. The reason for this choice is twofold. First, a piecewise-linear finite-element representation for λ enables us to impose exactly the monotonicity constraint, which is key to enforcing the minimum principle on the temperature as discussed in §3.3. Second, the optimal τ and λ have steep boundary layers near the bottom boundary that cannot be approximated accurately at a reasonable computational cost using global polynomial expansions (e.g. Legendre series). Finite-element bases, instead, lead to SDPs with *chordal sparsity* [55] that can be solved extremely efficiently. For our particular problem, however, we also found that finite-element bases lead to SDPs with worse numerical conditioning than those obtained with other bases, such as Legendre polynomials. Accurate solution, therefore, required the multiple-precision solver SDPA-GMP [53, 151]. Despite this issue, which we do not

expect to be generic, the enhanced sparsity of the finite-element approach resulted in significant efficiency gains compared to accurate Legendre series expansions.

As a final note to discretise (7.2.15), we used global polynomial expansions in the Legendre basis as implemented in the MATLAB toolbox QUINOPT [49, 51], which result in SDPs with good numerical conditioning that can be solved to high accuracy with the solver MOSEK [102].

Appendix D

Comparison of the spectral constraints

We provide further computational evidence that replacing the constraint $\mathcal{S}_{\boldsymbol{k}} \geq 0$ in (2.4.6) with the stronger constraint $\tilde{\mathcal{S}} \geq 0$ in (3.2.6) does not affect the qualitative behaviour of the optimal bounds on $\overline{\langle wT \rangle}$. The simplified optimization problem (3.2.7) was solved using the finite-element expansion approach described in appendix C. For simplicity, instead, the wavenumber-dependent problem (2.4.12) was solved using the general-purpose toolbox QUINOPT [49], which implements Legendre series expansions. The critical wavenumbers were determined with the help of the following result.

The result from Lemma 4.2.1 guarantees that, when implementing (2.4.12) numerically, it suffices to consider wavenumbers with

$$k < \left(\frac{R}{4\alpha\beta}\right)^{\frac{1}{4}} \|\alpha - \tau'(z)\|_{\infty}^{\frac{1}{2}}. \tag{D.0.1}$$

While the right-hand side of this inequality is unknown a priori, as it depends on the optimisation variables α, β and $\tau(z)$, in practice one can simply solve (2.4.12) using all wavevectors with k smaller than an arbitrarily chosen value. Then, one checks whether $\mathcal{S}_{\boldsymbol{k}}$ is indeed nonnegative for all k satisfying (D.0.1), and repeats the computation with a larger set of wavevectors if these checks fail.

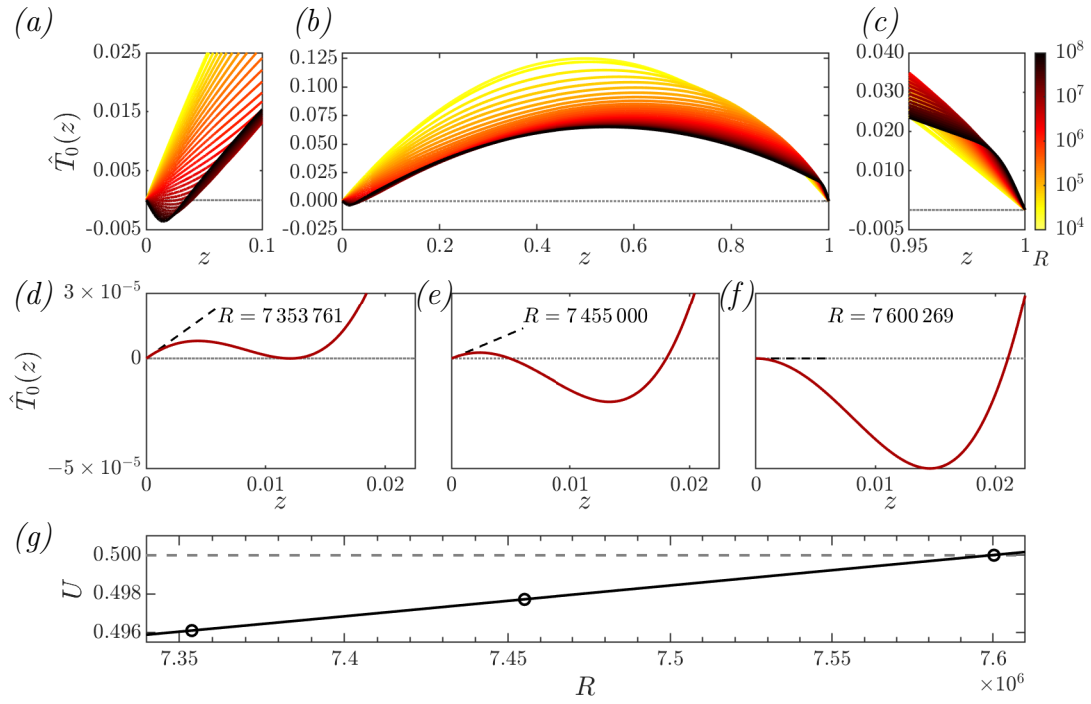

Figure D.1: *Top*: Critical temperature $\hat{T}_0(z)$ recovered using (2.4.9) when the spectral constraint is given by $\mathcal{S}_{\boldsymbol{k}} > 0$. Colors indicate the Rayleigh number. Panels *(a)* and *(c)* show details of the boundary layers. *Middle*: Detailed view of $\hat{T}_0$ for $R = 7\,353\,761$, $7\,455\,000$, and $7\,600\,269$. Dashed lines (**- - -**) are tangent to $\hat{T}_0$ at $z = 0$. In *(d)*, $\hat{T}_0$ is nonnegative and has minimum of zero inside the layer. In *(e)*, $\hat{T}_0$ is initially positive but has a negative minimum. In *(f)*, $\hat{T}_0'(0) = 0$ and there is no positive initial layer. *Bottom*: Upper bounds U on $\overline{\langle wT \rangle}$. Circles mark the values of Ra considered in *(d–f)* and $U = 1/2$ at $R = 7\,600\,269$.

Upper bounds obtained by solving the full problem (2.4.12) and the simplified problem (3.2.7) are shown in Figure 3.2. As expected, using the simplified spectral constraint yields worse bounds at a fixed Rayleigh number. While the full spectral constraint yields bounds that are zero up for all R up to the energy stability threshold, which depends on the choice of horizontal periods L_x and L_y, the simplified functional $\tilde{\mathcal{S}}$ is insensitive to these values and gives a conservative estimate for the nonlinear stability threshold. Nevertheless, both sets of result display the same qualitative increase as R is raised. This is further demonstrated in Figures D.1, where the critical temperature fields and bound U is computed with $\tilde{\mathcal{S}}$, which can be compared to Figure 3.3. Panels *(d)-(f)* demonstrate that the same behaviour in $\hat{T}_0$ near the lower boundary occurs for $\tilde{\mathcal{S}}$ in addition to $\mathcal{S}_{\boldsymbol{k}}$, while panel *(g)* displays the value of the bound for each corresponding critical temperature.

In particular, the upper bound reaches $1/2$ exactly when the critical temperature $\hat{T}_0$, which minimizes the functional $\mathcal{S}_0$, has zero gradient at $z = 0$, as can be observed in Figures D.1*(f)* & *(g)*. Shown in panels *(a)*-*(c)* are the critical temperature fields, $\hat{T}_0$, for $10^4 \leq R \leq 10^8$. In the middle row of the figure, going from left to right, observe first that for $R > 7\,353\,761$ the critical temperature is negative in the domain. Then panel *(e)* shows a value of R at which $\hat{T}_0$ is positive in a small region very close to the wall but clearly violates the minimum principle further away. In *(f)*, where $R = 7\,600\,269$, for our choice of $L_x = L_y = 2$, the numerically optimal bound equals $\frac{1}{2}$, at which point we have $\hat{T}_0'(0) = 0$. These results for the $\boldsymbol{k}$-dependent spectral constraint qualitatively match the results for the simplified spectral constraint (3.2.6) presented Figure 3.3.

These observations confirm that strengthening the spectral constraints using the wavevector-independent functional $\tilde{\mathcal{S}}$ only affects the computational results §3.2.1 quantitatively, but preserves the overall qualitative behaviour.

Appendix E

Shortcomings of standard background method

In the case of perfectly conducting boundaries discussed in chapter 3. The numerical optimisation from §3.3.1 suggests that the upper bound on $\overline{\langle wT \rangle}$ obtained from the optimization problem (3.3.3) approaches $\frac{1}{2}$ asymptotically from below as $R \to \infty$. To confirm this observation with a proof requires, for every $R \geq 1$, construction of feasible decision variables $\alpha, \beta, \tau(z), \lambda(z)$ whose corresponding cost is strictly less than $\frac{1}{2}$. This section discusses the challenges presented by this goal. Specifically, we show that no construction is possible if one tries to mimic key properties of the numerically optimal decision variables presented in §3.3.1 and, at the same time, enforces the spectral constraint using estimates typically used in successful applications of the background method. The proposition in this section illustrates the necessity of new estimates employed in the proof in addition to the construction of novel background profiles, not previously utilised in similar convection problems. These novel ingredients are later demonstrated in §3.3.2.

To aid the discussion, the following definition introduces three subsets $\mathcal{X}, \mathcal{Y}$ and $\mathcal{Z}$ of decision variables that capture some of the properties observed from our numerical study.

Definition E.0.1. Let $0 < \delta < 1 - \varepsilon < 1$ and $h > 0$ and $R \geq 1$. Decision variables $(\alpha, \beta, \tau(z), \lambda(z))$ are said to belong to:

1. The set $\mathcal{X}\{\delta, \varepsilon\}$ if the following conditions hold:
   (a) The balance parameters satisfy $0 < \alpha \leq \beta$;
   (b) $\tau \in C^1[0,1]$ with boundary conditions $0 \leq \tau(0) \leq 1$ and $\tau(1) = 0$;
   (c) The derivative of τ satisfies $\tau'|_{[0,\delta]} \leq 0$, $\tau'|_{[\delta,1-\varepsilon]} \geq 0$, and $\|\tau'\|_{L^\infty(1-\varepsilon,1)} \leq 2\beta$.
2. The set $\mathcal{Y}\{h\}$ if both $\tau'(z)$ and $\lambda(z)$ are constant on the interval $(\frac{1}{2} - h, \frac{1}{2} + h)$.
3. The set $\mathcal{Z}\{\delta, \varepsilon, R\}$ if

$$\delta^2 \|\alpha - \tau'\|_{L^\infty(0,\delta)} + \varepsilon^2 \|\alpha - \tau'\|_{L^\infty(1-\varepsilon,1)} \leq 8\sqrt{\frac{2\alpha\beta}{R}}.$$

The set $\mathcal{X}\{\delta, \varepsilon\}$ contains profiles τ which possess an initial (and potentially severe) boundary layer in an interval $[0, \delta]$, then increase in a bulk region $[\delta, 1 - \varepsilon]$, before approaching $\tau(1) = 0$ in an upper boundary layer contained in the interval $[1 - \varepsilon, 1]$ and in which τ' is controlled by the balance parameter β, as seen in previous results. Optimal decision variables $(\alpha, \beta, \tau(z), \lambda(z))$ obtained in §3.3.1 appear, with compelling evidence, to belong to a set of the form $\mathcal{X}\{\delta, \varepsilon\}$ with the exception of the differentiability condition $\tau \in C^1[0,1]$. Indeed, the optimal profiles τ appear to be piecewise differentiable, losing differentiability at two points corresponding to the boundaries of non-constant behaviour of the multiplier $\lambda(z)$ observed in figure 3.8. However, since no higher derivatives of τ appear in the optimization problem (3.3.3), adding the constraint $(\alpha, \beta, \tau(z), \lambda(z)) \in \mathcal{X}$ to (3.3.3) will not change its optimal cost.

The set $\mathcal{Y}\{h\}$ contains decision variables for which τ' and λ are constant in some interval centred at $\frac{1}{2}$. Figures 3.8 and 3.10 reveal that this is not the case for the

numerically optimal τ, so the use of $\mathcal{Y}\{h\}$ corresponds to a proof which ignores subtle variations from a purely linear profile away from the boundaries. Without further assumptions (say, restriction to fluids with infinite Prandtl number), it is not clear how such variations can be exploited in analytical constructions.

The set $\mathcal{Z}\{\delta, \varepsilon, R\}$ relates to a choice of profiles τ and balance parameters α, β for which the constraint $\mathcal{S}_{\boldsymbol{k}} \geq 0$ can be proven to hold for a given R. In particular, if $\alpha, \beta, \tau(z)$ satisfy (3.2.6) and it is the case that $\tau'|_{[\delta, 1-\varepsilon]} = \alpha$, then the argument implies that $\tilde{\mathcal{S}} \geq 0$. Specifically, $\mathcal{Z}\{\delta, \varepsilon, R\}$ provides sufficient control of the severity of the boundary layers of τ for the spectral constraint to be provably satisfied. While crude, estimates of this form in conjunction with constant $\tau'(z)$ in a bulk region $\delta \leq z \leq 1 - \varepsilon$ are employed for almost all analytical constructions of background fields.

We now return to the original question of attempting to upper-bound $\overline{\langle wT \rangle}$ via an analytical construction of feasible decision variables $(\alpha, \beta, \tau(z), \lambda(z))$ for (3.3.3). It is not unreasonable, based upon the above evidence, to propose R-dependent balance parameters $\alpha = \alpha_R, \beta = \beta_R$, boundary layer widths $\delta = \delta_R, \varepsilon = \varepsilon_R$ and profiles τ_R, λ_R which satisfy

$$(a_R, b_R, \tau_R(z), \lambda_R(z)) \in \mathcal{X}\{\delta_R, \varepsilon_R\} \cap \mathcal{Y}\{h\} \cap \mathcal{Z}\{\delta_R, \varepsilon_R, R\}, \qquad R \geq 1,$$

for some $h > 0$. The following result shows that, for such a construction, there is a hard lower bound on the optimal cost achievable using (3.3.3).

Proposition E.0.1. *Let* $0 < \delta < 1 - \varepsilon < 1$ *and* $h > 0, R \geq 1$. *Suppose that*

$$(\alpha, \beta, \tau(z), \lambda(z)) \in \mathcal{X}\{\delta, \varepsilon\} \cap \mathcal{Y}\{h\} \cap \mathcal{Z}\{\delta, \varepsilon, R\}. \tag{E.0.1}$$

Then

$$\left\langle \frac{1}{4\beta} \left| \beta(z - \tfrac{1}{2}) - \tau'(z) + \lambda(z) \right|^2 - \tau \right\rangle \geq \frac{\beta}{6} \left(h^3 - 24 \cdot \frac{1 + 2\sqrt{2}}{R^{\frac{1}{4}}} \right).$$

From the proof, the consequence of Proposition E.0.1 is the following. If one constructs feasible decision variables for the optimization problem (3.3.3) which satisfy (E.0.1), then the best achievable bound U for which $\overline{\langle wT \rangle} \leq U$ must satisfy

$$U \geq \frac{1}{2} + \frac{\beta}{6} \left(h^3 - 24 \cdot \frac{1 + 2\sqrt{2}}{R^{\frac{1}{4}}} \right).$$

Hence, using such a construction with the assumption that τ' and λ are constant in a bulk region $(\frac{1}{2} - h, \frac{1}{2} + h)$, it is not possible to prove that $\overline{\langle wT \rangle} < \frac{1}{2}$ at arbitrarily high Rayleigh number.

Consequently, one must ask what conditions should be dropped if a rigorous bound $\overline{\langle wT \rangle} < \frac{1}{2}, R \geq 1$, is to be found. The numerical evidence presented in §3.3.1 suggests that the optimal decision variables do belong to $\mathcal{X}$. Consequently, either $\mathcal{Y}$ or $\mathcal{Z}$ must be dropped. Figure 3.8 indicates that optimal multipliers $\lambda(z)$ are constant outside a lower boundary layer. Hence, dropping $\mathcal{Y}$ corresponds to choosing a profile with non-constant $\tau'(z)$ in the bulk; the cost function of (3.3.3) and Figure 3.10*(b)* suggests that a quadratic ansatz for $\tau(z)$ may be beneficial. Dropping $\mathcal{Z}$ corresponds to requiring more sophisticated analysis of the spectral constraint. Using these insights will be the focus of future research.

Proof. It is assumed that $(a, b, \tau, q) \in \mathcal{X}\{\delta, \varepsilon\} \cap \mathcal{Y}\{h\} \cap \mathcal{Z}\{\delta, \varepsilon, R\}$. The first step is to bound $\langle \tau(z) \rangle$ from above. To do this, we work back from $z = 1$, using the assumptions to estimate τ.

Let $1-\varepsilon \le z \le 1$. Since $\tau \in C^1[0,1]$ and $\tau(1)=0$, the mean value theorem implies that there exist $z_\varepsilon \in (1-\varepsilon, 1)$ such that

$$-\tau'(z_c) = \frac{\tau(z)}{1-z} \ge \frac{\tau(z)}{\varepsilon}.$$

Since $(\alpha, \beta, \tau(z))$ satisfy (3.2.6), it follows that

$$\begin{aligned}
\varepsilon^4 \|\alpha - \tau'\|^2_{L^\infty(1-\varepsilon,1)} \le \frac{128\alpha\,\beta}{R} &\implies \varepsilon^4 \left(\alpha + \frac{\tau(z)}{\varepsilon}\right)^2 \le 128\frac{\alpha\,\beta}{R} \\
&\implies \varepsilon^4 \left(\frac{\alpha}{\beta}\right)^2 + \left(\frac{\alpha}{\beta}\right)\left(\frac{2\varepsilon^3\tau(z)}{\beta} - \frac{128}{R}\right) + \left(\frac{\varepsilon\tau(z)}{\beta}\right)^2 \le 0 \\
&\implies \left(\frac{2\varepsilon^3\tau(z)}{\beta} - \frac{128}{R}\right)^2 \ge 4\varepsilon^4 \left(\frac{\varepsilon\tau(z)}{\beta}\right)^2 \\
&\implies \frac{\tau(z)\varepsilon^3}{\beta} \le \frac{32}{R} \qquad \text{(E.0.2a)}
\end{aligned}$$

Next, since $\tau(1)=0$, the assumption that $\|\tau'\|_{L^\infty(1-\varepsilon,1)} \le 2\beta$ gives $|\tau(z)| \le \varepsilon\|\tau'\|_{L^\infty(1-\varepsilon,1)} \le 2\beta\varepsilon$, which in turn implies

$$\varepsilon \ge \frac{1}{2\beta}\tau(z). \qquad \text{(E.0.3)}$$

Since $1-\varepsilon < z < 1$ was arbitrary in the above argument, it follows from (E.0.2a) and (E.0.3) and the fact that $\tau'(z) \ge 0$ for all $z \in [\delta, 1-\varepsilon]$ that

$$\|\tau\|_{L^\infty(\delta,1)} \le \|\tau\|_{L^\infty(1-\varepsilon,1)} \le 4\beta R^{-\frac{1}{4}}. \qquad \text{(E.0.4)}$$

We now estimate τ in the lower boundary layer $[0,\delta]$. The mean value theorem implies that there exists z_δ such that

$$\tau'(z_\delta) = \frac{\tau(\delta) - \tau(0)}{\delta}.$$

Since $(\alpha, \beta, \tau(z))$ satisfy (3.2.6), using the above equation and the assumption that $0 < \alpha \leq \beta$, it then follows that

$$\begin{aligned}
\delta^4 \|\alpha - \tau'\|^2_{L^\infty(0,\delta)} \leq 128 \cdot \frac{\alpha\,\beta}{R} \quad &\Longrightarrow \quad \delta^4 \left|\alpha + \left(\frac{\tau(0) - \tau(\delta)}{\delta}\right)\right|^2 \leq 128 \cdot \frac{\alpha\,\beta}{R} \\
&\Longrightarrow \quad \delta^2 |\alpha\delta + \tau(0) - \tau(\delta)|^2 \leq 128 \cdot \frac{\beta^2}{R} \\
&\Longrightarrow \quad \frac{\delta}{\beta}\tau(0) \leq \frac{8\sqrt{2}}{R^{\frac{1}{2}}} + \frac{\delta\tau(\delta)}{\beta} \\
\text{(by (E.0.4))} \quad &\Longrightarrow \quad \frac{\delta}{\beta}\tau(0) \leq \frac{8\sqrt{2}}{R^{\frac{1}{2}}} + \frac{4\delta}{R^{\frac{1}{4}}} \qquad \text{(E.0.5)}
\end{aligned}$$

Using (E.0.4), (E.0.5), the assumption that $\tau'(z) \leq 0$ on $[0, \delta]$ and $R \geq 1$ gives

$$\frac{1}{\beta}\langle \tau(z) \rangle \leq \frac{\delta}{\beta}\tau(0) + \frac{(1-\delta)}{\beta}\|\tau\|_{L^\infty(\delta,1)} \leq \frac{8\sqrt{2}+4}{R^{\frac{1}{4}}} \qquad \text{(E.0.6)}$$

Next we consider the L^2 component of the cost function. Using the assumption that τ', λ are constant in an interval $(1/2 - h, 1/2 + h)$,

$$\begin{aligned}
\frac{1}{4\beta}\left\langle \left|\tau' - \lambda - \beta(z - 1/2)\right|^2 \right\rangle \quad &\geq \quad \frac{1}{4\beta}\int_{\frac{1}{2}-h}^{\frac{1}{2}+h} \left[\tau' - \lambda - \beta(z - 1/2)\right]^2 \,\mathrm{d}z \\
&\geq \quad \frac{\beta}{4}\int_{\frac{1}{2}-h}^{\frac{1}{2}+h} (z - 1/2)^2 \,\mathrm{d}z \\
&= \quad \frac{\beta h^3}{6}. \qquad \text{(E.0.7)}
\end{aligned}$$

Combining the above estimate with (E.0.6) gives the stated result

$$\left\langle \frac{1}{4\beta}\left|\tau' - \lambda - \beta(z - 1/2)\right|^2 - \tau(z) \right\rangle \geq \frac{\beta}{6}\left(h^3 - 24 \cdot \frac{1 + 2\sqrt{2}}{R^{\frac{1}{4}}}\right).$$

□